Identification of Biofilm-associated Proteins *in vitro* and in the Plasma of Patients with Biofilm-related Implant Disease

Md. Arifur Rahman

B. Pharm, M. Pharm (Research)

A thesis submitted in fulfillment of the requirements for the degree of

Doctor of Philosophy

Department of Biomedical Science, Faculty of Medicine and Health Sciences

Macquarie University, Sydney, Australia

Supervisor: A/Prof. Karen Vickery

Associate supervisors: Prof. Mark S. Baker

Dr. Honghua Hu

May 2019

Dedicated to

My Entire Ancestors

and

Future Generations

Table of Contents

Table of Contents ii

Abstract x

Declaration of Originality xii

Publications and Communications xiii

Manuscripts in preparation xiii

Conference presentations xiii

Poster presentations xiii

Oral presentations xiv

Awards arising during candidature xiv

Acknowledgements xv

List of Figures xvii

List of Tables xxiv

List of Symbols and Abbreviations xxvi

Thesis Structure and Chapter Outline 1

Chapter 1: Literature Review 3

1.1. Healthcare-associated infections 3

1.2. Bacterial biofilms and its associated health infections 7

1.2.1 Bacterial biofilms 7

1.3. Biofilm infections associated with implantable medical devices 15

1.4. Biofilm on hospital surfaces 21

1.5. *Staphylococcus aureus* and biofilms 22

1.5.1. *Staphylococcus aureus* 22

1.5.2. *Staphylococcus aureus* pathogenicity and pathogenic determinants 23

1.5.3. *Staphylococcus aureus* biofilms 24
1.6. *Staphylococcus aureus* biofilm regulation 25
1.6.1. Agr quorum-sensing system 26
1.6.2. SarA (Staphylococcal accessory regulator) 29
1.6.3. Sigma B regulation 29
1.7. Bacterial biofilm proteomics 31
1.7.1. *Staphylococcus aureus* proteomics 32
1.8. Transcriptomics of bacterial biofilms 33
1.9. Human proteomics 34
1.10. MS-based proteomics and bioinformatics 35
1.10.1. MS-based proteomics workflow 35
1.10.2. Processing of samples 36
1.10.3. MS instrumentation and peptide fragmentation 39
1.10.4. MS data processing for protein identification 41
1.10.5. Protein quantification 42
1.10.6. Tandem mass tag (TMT) liquid chromatography MS/MS 43
1.10.7. Gene Ontology (GO) and enrichment analysis 48
1.10.8. Subcellular localisation 49
1.10.9. Pathway analysis 49
1.10.10. Protein-protein interaction network analysis 50
1.11. Aims and scope of the PhD project 52
Project hypotheses 52
Project objectives 52
Chapter 2: Materials and Methods 54

2.1. Microorganism and culture conditions 54
2.1.1. *S. aureus* planktonic growth conditions 54
2.1.2. Bacterial colony forming units (CFU) counting 54
2.1.3. Biofilm growth conditions 54
2.1.4. 3-day wet biofilm (3dwb) 55
2.1.5. 12-day wet biofilm (12dwb) 56
2.1.6. 12-day dry surface biofilm (DSB) 56
2.2. Protein extraction, fractionation and processing for MS/MS analysis 57
2.2.1. Protein extraction from 24 hour planktonic culture 57
2.2.2. Extraction of biofilm proteins 57
2.2.3. Determination of protein concentration 58
2.2.4. Protein reduction, alkylation, and digestion 59
2.2.5. TMT labeling and high pH fractionation 61
2.2.6. Nanoflow liquid chromatography electrospray ionisation tandem mass spectrometry (Nanoflow LC-ESI-MS/MS) 62
2.2.7. Database search, statistical analysis, and bioinformatics 64
2.3. Validation of biofilm proteomics results by quantitative reverse-transcription PCR 65
2.3.1. Planktonic and biofilms culture conditions 67
2.3.2. RNA extraction from planktonic cultures 67
2.3.3. RNA extraction from biofilms 67
2.3.4. Reverse transcription 68
2.3.5. Primers 68
2.3.6. Quantitative real-time PCR 69
2.3.7. Relative quantification of gene expression 70
2.4. Depletion of human plasma protein and processing for MS/MS analysis 70

2.4.1. Patients and ethics 70
2.4.2. Collection and processing of human plasma samples 71
2.4.3. Depletion of human plasma proteins 72
2.4.4. Protein reduction, alkylation, and digestion 72
2.4.5. TMT labeling and high pH fractionation 73
2.4.6. Nanoflow LC-ESI-MS/MS using Q Exactive 76
2.4.7. Database search, statistical analysis, and bioinformatics 76
Chapter 3: Comparison of the proteome of *Staphylococcus aureus* planktonic culture and 3-day biofilm reveals potential role of key proteins in biofilm 78
Abstract 79
Background 79
Methods 79
Results 79
Conclusions 80
Introduction 80
Materials and Methods 82
Microorganism and culture conditions 83
Sample Processing 83
Nanoflow LC-ESI-MS/MS 83
Nanoflow LC-ESI-MS/MS using Orbitrap Elite 84
Nanoflow LC-ESI-MS/MS using Q Exactive 84
Database search, statistical analysis, and bioinformatics 84
Correlation of TMT data with real-time qPCR results 85
Results 85
TMT identification 85

GO analysis and annotation of DRSPs 132
KEGG pathway analysis of DRSPs 133
Protein–protein interaction analysis of DRSPs 136
Correlation of TMT data with real-time qPCR results 138
Discussion 138
Conclusions 146
Chapter 4: Proteome of *Staphylococcus aureus* biofilm changes significantly with age 147
Abstract 148
Introduction 148
Materials and Methods 150
Microorganism and culture conditions 152
Sample Processing 152
Nanoflow LC-ESI-MS/MS 152
Nanoflow LC-ESI-MS/MS using Orbitrap Elite 153
Nanoflow LC-ESI-MS/MS using Q Exactive 153
Database search, statistical analysis, and bioinformatics 153
Validation of TMT data with qPCR results 154
Results 154
TMT identification of differentially regulated proteins 154
GO analysis and annotation of differentially regulated proteins 156
Significant differentially regulated proteins and pathway analysis in the 3dwb 160
Significantly upregulated proteins and pathway analysis in the 12dwb 167
Significantly downregulated proteins and pathway analysis in the 3dwb 172
Significantly downregulated proteins and pathway analysis in the 12dwb 179

Differentially regulated proteins common to both 3dwb and 12dwb 182
Protein-protein interaction (PPI) analysis 182
Validation of TMT data with real-time qPCR 184
Discussion 185
Conclusions 193
Chapter 5: One step forward with dry surface biofilm: TMT-based quantitative proteomic analysis reveals proteomic shifts between traditional hydrated biofilm and Dry surface biofilms from *Staphylococcus aureus* 194
Abstract 195
Introduction 196
Materials and Methods 197
Microorganism and culture conditions 197
Sample processing 198
Nanoflow LC-ESI-MS/MS 200
Nanoflow LC-ESI-MS/MS using Orbitrap Elite 200
Nanoflow LC-ESI-MS/MS using Q Exactive 200
Database search, statistical analysis, and bioinformatics 201
Validation of TMT data with qPCR results 201
Results and Discussion 202
TMT identification of differentially regulated proteins in the wet and DSB 202
Energy metabolism associated proteins are significantly upregulated in the wet 204
Sugar transporter and cell-wall synthesis proteins are highly abundant in the DSB 205
Fatty acid pathway could be a novel target for DSB 214
Ribosomal and ABC transporter proteins revealed decreased abundance in the wet 219
Significantly downregulated Proteins in the DSB 223

Significant differentially expressed stress response proteins in the wet and DSB 224
Validation of TMT data with qPCR results 225
Conclusions 227
Chapter 6: Breast implant capsular contracture reveals changes in the regulation of low-abundance plasma proteins 228
Abstract 229
Introduction 229
Materials and Methods 231
Patients and ethics 233
Collection and processing of human plasma samples 233
Depletion of human plasma proteins 233
Sample Processing for TMT labeling and high pH fractionation 233
Nanoflow LC-ESI-MS/MS using Q Exactive 234
Database search, statistical analysis, and bioinformatics 234
Results 235
TMT identification 235
GO analysis of the identified proteins 242
KEGG pathway analysis of the identified proteins 244
Protein-protein interaction analysis of the identified proteins 245
Discussion 247
Conclusions 252
Chapter 7: General Discussion 253
References 264
Appendices 338
Appendix 1. Human ethics approval 339

Appendix 3. Validation of selected genes from *S. aureus* proteomic results using qPCR..346

Appendix 4. Functional classification of the significantly upregulated common proteins between 3dwb and 12dwb compared with planktonic culture 347

Appendix 5. Functional classification of the significantly downregulated common proteins between 3dwb and 12dwb compared with planktonic culture 352

Appendix 6. Functional classification of the significantly upregulated common proteins between 12dwb and DSB compared with planktonic culture.....362

Appendix 7. Functional classification of the significantly downregulated common proteins between 12dwb and DSB compared with planktonic culture.....369

Appendix 8. Copyright permission for figures.....380

Abstract

Despite the rapid advancement in implantable medical devices (IMD) and surgical techniques, the problem of IMD-associated infections has increased from 2% to 40%, depending on the type of IMDs. It is estimated that approximately 65 to 85% of all hospital-acquired infections are associated with biofilms, this represents a serious challenge. *Staphylococcus aureus* and coagulase-negative staphylococci account for about 80% of medical device-related diseases. Infections associated with biofilms are enormously problematic to eliminate due to their elevated tolerance against the host immune defence system and antimicrobials. There is currently no effective technique for early identification of biofilms. In addition, recent findings of biofilms on dry hospital surfaces emphasise the failures in current cleaning practices and disinfection, and the difficulty in removing these dry surface biofilms (DSB). DSB have been shown to be principally composed of protein. Therefore, we compared the proteomes of *S. aureus* during planktonic, hydrated (wet) biofilms and DSB *in vitro*. *In vivo*, we compared the plasma proteome (following depletion of high-abundant proteins) of healthy patients with those of patients with biofilm-related breast implant capsular contracture (CC). The proteomes were determined using high-resolution Tandem Mass Tag (TMT)-based mass spectrometry.

In the *in vitro* proteomics study, we identified 1636 non-redundant total biofilm extractomes from *S. aureus*. Among the significant upregulated proteins in 3-day wet biofilm (wet) compared to planktonic, we identified proteins associated with ABC transporters, biosynthesis of amino acids, response to stress, a biofilm dispersing extracellular enzyme hysA; whereas virulence factors, energy metabolism and chitinase, an extracellular enzyme responsible for preventing initial attachment of biofilm formation, were significantly downregulated. HysA in conjunction with chitinase may play an important role in the elimination and/or prevention of biofilm development.

In comparison with 3-day wet and 12-day wet biofilm, we observed a significant range of quantitative proteomic shifts in different stages of biofilms. Further pathway analysis showed that the major alterations in biofilm formation results from the changes in the level of metabolic

activity in different growth mode of biofilms. Therefore, changes in metabolic activity could be a significant factor of *S. aureus* biofilm maturation and persistence.

In the novel DSB proteomics study, proteins significantly upregulated in DSB were involved in energy metabolism and peptidoglycan biosynthesis pathway such as ptaA, murC and murB. These three proteins are all linked with peptidoglycan biosynthesis pathway and are responsible for cell wall formation and may play a role in biofilm formation and persistence of DSB on dry surfaces.

In the *in vivo* plasma proteomics study, we have seen clear differences in plasma proteome of biofilm-related breast implant CC patients in comparison to healthy controls. These novel findings promote further research to verify outcomes in large groups of patients and various clinical backgrounds.

In summary, the current pioneering study could potentially prove useful in designing vaccines, anti-biofilm agents, diagnostic biomarker(s), and much needed antimicrobial therapies for biofilm-related diseases, as well as advanced, targeted disinfectants and detergents to remove biofilms from dry environments.

Declaration of Originality

I hereby declare that the work presented in this thesis has not been submitted for a higher degree to any other university or institution. To the best of my knowledge, this submission contains no material previously published or written by another person, except where due reference is stated otherwise. Any contribution made to the research by others is explicitly acknowledged.

Md. Arifur Rahman

Department of Biomedical Sciences

Faculty of Medicine and Health Sciences

Macquarie University

Publications and Communications

Manuscripts in preparation

- Comparison of the proteome of *Staphylococcus aureus* planktonic culture and 3-day biofilm reveals potential role of key proteins in biofilm.
- Proteome of *Staphylococcus aureus* biofilm changes significantly with age
- One step forward with dry surface biofilm: TMT-based quantitative proteomic analysis reveals proteomic shifts between traditional hydrated biofilm and DSB from *Staphylococcus aureus*

Conference presentations

Poster presentations

- One Step Forward with Dry Surface Biofilm: TMT-Based Quantitative Mass Spectrometry of *Staphylococcus aureus* Reveals Novel Regulators of Biofilm Formation. The 8th American Society for Microbiology (ASM) Conference on Biofilms, Washington DC, USA from 7 October to 11 October 2018.
- Comparative Proteomic Profiling Reveals New Insight between Different Growth Phase of Biofilm Extractomes from *Staphylococcus aureus* Using TMT-based Quantitative MS. 17th Human Proteome Organization World Congress, Orlando, Florida, USA from 29 September to 4 October 2018.
- TMT-based Quantitative Mass Spectrometry Reveals Proteomic Shifts between Traditional Hydrated Biofilm and DSB from *Staphylococcus aureus*: One Step Forward with Dry Surface Biofilm (DSB). 9th AOHUPO Conference (which is held as part of MSP2018): Conference on Mass Spectrometry and Proteomics, Hotel Hankyu Expo Park, Osaka, Japan, 15 May to 18 May 2018.

- Comparative Proteomic analysis using TMT-based MS Reveals New Insight between Different Growth Phase of Biofilms from *S. aureus*. The Australasian Proteomics Society (APS) - 2018: 23rd Annual Lorne Proteomics Symposium, Cumberland Lorne Resort, Lorne, Victoria, Australia, 1 to 4 February 2018.
- Proteomic Analysis of *Staphylococcus aureus* Planktonic and Hydrated Biofilms using TMT-based Mass Spectrometry. HUPO 2017: 16th Human Proteome Organization World Congress, The Convention Centre Dublin (The CCD), Dublin, Ireland, 17 to 21 September 2017.

Oral presentations

TMT-based Quantitative Mass Spectrometry Reveals Proteomic Shifts between Traditional Hydrated Biofilm and DSB from *Staphylococcus aureus*: One Step Forward with Dry Surface Biofilm (DSB). 9th AOHUPO Conference (which is held as part of MSP2018): Conference on Mass Spectrometry and Proteomics, Hotel Hankyu Expo Park, Osaka, Japan, 15 May to 18 May 2018.

Awards arising during candidature

- Travel stipend from the United States Human Proteome Organisation (HUPO) to support attendance at HUPO, Orlando, Florida, USA, 29 September to 4 October 2018.
- Macquarie University Postgraduate Research Fund (PGRF) Award.
- Beijing Genomics Institute-Asia Oceania HUPO and Australasian Proteomics Society-Asia Oceania HUPO Travel Fellowship Awards to present my work as an invited speaker as oral presentation at the 9th AOHUPO Conference, Osaka, Japan, 15 May to 18 May 2018.
- Finalist for NSW Australian Society for Microbiology (ASM) Student Travel Award 2018.
- International Macquarie University Research Excellence Scholarship (iMQRES) holder.

Acknowledgements

In the Name of Allah, the Most Gracious and Most Merciful.

He who does not thank people does not thank Allah.

My PhD is a great opportunity and I am really pleased to express my sincere gratitude to those who made my candidature and thesis possible.

First and foremost, I would like to thank from the inner core of my heart my respected supervisor A/Prof. Karen Vickery for giving me such an incredible opportunity to do my PhD study under her supervision, and for her inspiration, excellent guidance, understanding and all her help throughout my study. Karen, you provided the best learning environment, sound advice, good teaching, and many good ideas. This thesis would not have been possible without your patience and constant encouragement. I feel proud and would like to express my deepest gratitude to one of the most wise and open-hearted people that I have ever met in my life.

Next, I convey my greatest regards and gratitude to Dr. Honghua Hu for assisting me in my research. Her support, encouragement and active co-operation in all respect were great contributors to the completion of my work.

I would like to express my grateful thanks from the bottom of my heart to my Co-supervisor Prof. Mark S. Baker and his team members for their valuable comments, guidance and critical suggestions to make this thesis better.

I express my deep regards and heartfelt gratitude to all respected personnel from Australian Proteomic Analysis Facility (APAF) for providing great collaboration to complete the majority of my PhD research. Especially, I would like to thank Dr Ardeshir Amirkhani, Dr. Alamgir Khan, Prof. Mark Molloy, Dr. Xiaomin Song, Dr. Dana Pascovici and Dr. Karthik S Kamath for their major help with proteomic experiments, analysis, valuable ideas, constructive criticism and kind co-operation.

Further, I would also like to thank Macquarie University, the Faculty of Medicine and Health Sciences, for their support and help, especially Ms. Viviana Bong, Ms. Laura Newey, Ms. Louise Marr and Ms. Lucy Lu. It was a joy for me to work with such dedicated and talented staff.

Special thanks from every corner of my heart to my lab members, Dr. Khalid Aljohani, Dr. Maria Mempin, Dr. Durdana Chowdhury, Dr. Dayane De Melo Costa, Dr. Shamaila Tahir, Farhana Parvin, and Fatemah Sadeghpour Heravi for helping me get through the difficult times, their constant support, valuable suggestions, help and friendly environment to work and learn. In particular, 3 biofilms were grown to optimise protein extraction, 12 biofilms were produced for proteomic analysis and 4 biofilms were grown for proteomics qRT-PCR validation. I would not have been able to grow these biofilms without the initial help of Dr. Durdana Chowdhury, who showed me how to grow biofilm and helped me grow my first biofilm. I am also highly thankful to Farhana Parvin for her kind assistance in growing biofilms and occasional media change when I was unavailable for my biofilm proteomics validation work using qRT-PCR.

Finally, I would like to thank Almighty 'ALLAH' for his miraculous blessings on me to carry on with my endeavours.

Last but not least, I wish to thank my sweet parents and all my family members who have always supported me spiritually and prayed for my success. Their sacrifice and mental support strengthen my research motif, which is embedded in my heart.

Thanks again to all.

Md. Arifur Rahman

List of Figures

Figure 1.1: Scheme showing the phases of the formation of *S. aureus* biofilm; modified from [109]. (A) Individual planktonic bacterial cells adhere to a biotic or abiotic surface (B) Further continue to grow cells and multiply and ultimately develop microcolonies leading to the deposition of biofilm matrix (C) Exodus, premature detachment of a biofilm subpopulation. (D) Continue to produce excessive EPS matrix components results in the formation of a matured biofilm (E) Final step, biofilm cell detachment/disassembly occur and return to a planktonic mode of growth. 12

Figure 1.2: *S. aureus* colonisation sites in the human body. Modified from web site: https://www.coloringsky.com/human-body-coloring-pages-for-kids/. 23

Figure 1.3: Schematic representation of the regulatory network of *S. aureus* biofilm development based on PIA dependent/independent. Biofilm development based on PIA, the icaADBC gene cluster play a central role to initiate the expression of PIA by downregulating the activity of icaR and tcaR. The regulation of icaR gene can be controlled by upregulating the activity of Spx and downregulating the activity of Rbf genes. SrrAB gene plays a vital role in triggering the expression of icaADBC during oxygen deficient conditions. In contrast, PIA independent biofilm development is controlled via the proteins associated with cell-wall and attachment. Modified from [83]. 26

Figure 1.4: Schematic representation of the networks in the formation of biofilm regulation. The agr quorum-sensing system triggers the expression of surface proteins (e.g., proteases) of Staphopain by downregulating the activity of Rot (toxin repressor). On the Staphylococcal surface and in the biofilm matrix, these proteases then degrade proteins. SaeRS induces nuclease enzyme production that breaks eDNA in the biofilm matrix. SigB downregulates agr expression whereas it has been demonstrated that SarA directly enhances agr expression. Adapted from [109]. 28

Figure (1.5): An overview of TMT-labeling based MS analysis. 38

Figure 2.1: Centre for disease control (CDC) bioreactor. The CDC biofilm reactor comprises of eight (8) polypropylene coupon holders (rods) and each rod can hold three removable polycarbonate coupons (1.27cm diameter and 0.3cm thick) suspended from a polyethylene ported lid. The lid with rods and removable coupons is equipped in a 1 litre glass vessel with sidearm discharge port. During all liquid phases (batch phases) of biofilm development, mixing and shear were provided by baffle rotation generated by a magnetic stir plate. 55

Figure 2.2: An example of BCA protein assay standard curve generated. 59

Figure 2.3: Experimental workflow for TMT labeling and analysis. *S. aureus* strain cultivated in TSB to grow a planktonic culture pooled from biological triplicates, and biofilms (3-day, 12-day, and DSB) in biological triplicates. The Centres for Disease Control biofilm reactor was used to grow biofilms. Proteins were extracted from the 9 replicates of 3 biofilm conditions, and a pooled control from planktonic culture was generated from equal aliquots of protein from the control triplicates. Proteolytically digested peptides were labeled with TMT 10-plex reagents and subjected to high pH RP-HPLC fractionation followed by LC−MS/MS analysis. TMT-10-plex experimental design adapted from Samantha et al., (2016) [336]. 60

USA) stage tips. To make the stage tip, 3 layers of SDB-RPS disks were cut and stacked using a 16-G Hamilton syringe needle into bottom of a 200µl pipette tip. Each stage tip was placed onto a 1.5ml Eppendorf tube. Each sample was added to the stage tip and centrifuged 1000xg for 5 minutes. Stage tip containing samples were washed twice with 0.2% TFA and centrifuged at 1000xg for 5 minutes. Samples were eluted with 100µl of elution buffer containing 5% ammonium hydroxide (Sigma-Aldrich) in 80% acetonitrile (ACN; Acros Organics, USA) and centrifuged at 1000xg for 5 minutes. Samples were vacuum dried (miVac, Genevac Ltd, England) and stored at -20°C until further processing. 61

Figure 2.4: Experimental workflow for RNA extraction and qPCR analysis. *S. aureus* strain cultivated in TSB to grow a planktonic culture, and biofilms (3-day, 12-day, and DSB). The Centres for Disease Control biofilm reactor was used to grow biofilms. Each growth condition was conducted in two biological replicates (BR) and two technical replicates (TR). RNA was extracted and subjected to ezDNase treatment to remove genomic DNA and cDNA synthesis followed by qPCR analysis of selected genes. 66

Figure 2.5: Experimental workflow for plasma depletion, TMT labeling and analysis. Plasma from each patient (10 healthy control, 10 CC) was processed for the depletion of high-abundant proteins using MARS-14 to improve depth of detection in plasma samples. Proteolytically digested peptides were labeled with TMT 10-plex reagents and subjected to high pH RP-HPLC fractionation followed by LC−MS/MS analysis. 75

Figure 3.1: Experimental workflow for the analysis of *S. aureus* planktonic and biofilm proteome using TMT labeling based MS. *S. aureus* strain cultivated in TSB to grow a planktonic culture pooled from biological triplicates, and 3-day biofilm in biological triplicates. The Centres for Disease Control biofilm reactor was used to grow biofilms. Proteolytically digested peptides were labeled with TMT 10-plex reagents and subjected to high pH RP-HPLC fractionation followed by LC−MS/MS analysis. 82

Figure 3.2: Classification of the DRSPs of *S. aureus* biofilm using Gene Ontology based on their functional annotations. (A) GO Protein Classes. We performed GO functional annotation for significant differentially regulated proteins of 3dwb in comparison to planktonic. In this analysis we considered only proteins dysregulated >2 fold and $p<0.05$. 132

Figure 3.3: The DRSPs of *S. aureus* biofilm showed functional diversity using KEGG pathway analysis. (A) major pathways involved in significantly upregulated proteins; (B) major pathways involved in significantly downregulated proteins. Number scale represents; number of proteins identified in specific pathways. 135

Figure 3.4: The network of DRSPs of *S. aureus* biofilm was analysed by STRING software (v.10.0). High-confidence interactions (≥0.7) and omitted nodes that are not connected in the network in STRING software were selected for this study. 137

Figure 3.5: This figure showing structural component of hyaluronic acid (HA) and breaking point. HA comprises of repeating disaccharides units of N-acetyl-D-glucosamine and D-glucuronic acid, and the units are linked by repeating glycosidic bonds beta-1,4 and beta-1,3. . 142

Figure 3.6: Pathway demonstration showing significantly upregulated proteins (red colour encoded genes) involved in amino sugar and nucleotide sugar metabolism and linked with peptidoglycan biosynthesis in 3dwb. 144

Figure 4.1: Experimental workflow for the analysis of *S. aureus* planktonic and two different growth stage of biofilm proteome using TMT labeling based MS. *S. aureus* strain cultivated in TSB to grow a planktonic culture pooled from biological triplicates, and biofilms (3-day and 12-day) in biological triplicates. The Centres for Disease Control biofilm reactor was used to grow biofilms. Proteolytically digested peptides were labeled with TMT 10-plex reagents and subjected to high pH RP-HPLC fractionation followed by LC−MS/MS analysis. 151

Figure 4.2: The volcano plot shows the distribution of the differential protein expression profile of (A) 3dwb compared to planktonic and; (B) 12dwb compared to planktonic. Y-axis in the form of −log 10 represents p-value; greater numerical value is associated with lower p-value and greater legitimacy. X-axis represents fold change (log_2) of the differentially regulated proteins are represented by blue lines. The two vertical blue lines represent fold changes of -1.5 and +1.5. Therefore, the dots above red line in the positive side are significantly (<0.05) upregulated proteins, and the dots in the negative side represent the significantly (<0.05) downregulated proteins..... 156

Figure 4.3: Venn diagram shows the dispersion of common and significant differential proteins in the 3dwb and 12dwb. Pathway analysis performed using KEGG. 156

Figure 4.4: Classification of the significant differentially regulated proteins of 3dwb and 12dwb based on their functional annotations using Gene Ontology. In this analysis we considered only proteins dysregulated >2 fold and p<0.05. (A) GO Molecular Function for 3dwb; (B) GO Molecular Function for 12dwb..... 158

Figure 4.5: Classification of the significant differentially regulated proteins of 3dwb and 12dwb based on their functional annotations using Gene Ontology. (A) GO Biological Processes for 3dwb; (B) GO Biological Processes for 12dwb. 159

Figure 4.6: Significant differentially regulated proteins involved in central metabolism in 3dwb. Red names denote encoded genes with increased abundance while blue names denote encoded genes with decreased expression..... 161

Figure 4.7. The protein-protein interaction network as analysed by STRING software with high confidence (0.700) and omitted nodes those are not connected to the network. Red arrows

represent upregulation and blue arrows represent downregulation. The map of the significantly upregulated and downregulated proteins from (A) 3dwb and (B) 12dwb show high interactions, which indicates that the proteins are biologically linked, at least partly, as a group. 184

Figure 4.8: Linking pathway demonstration of phosphotransferase (PTS), galactose metabolism, and peptidoglycan biosynthesis in 12dwb. Bacterial biofilm can uptake sugars by specific sugar transport systems (e.g. PTS) and non-PTS system (e.g. galactose metabolism). LacAE involved in the metabolism of sugar molecules via fructose 6-phosphate which is also linked with glycolysis and synthesis of cell-wall components. In addition, peptidoglycan biosynthesis proteins (e.g. femX) is also directly linked with cell-wall formation. EII: Enzyme II; Red names denote encoded genes with increased abundance in 12dwb. 187

Figure 4.9: (A) General view of the selected part of the peptidoglycan biosynthesis pathway; (B) Selected part of the structure of *S. aureus* peptidoglycan which is linked with the potential role of femX significantly identified in 12dwb; modified from [521]. FemX from *S. aureus* play vital role in the transfer of Gly_1 to the ϵ-NH_2 group of Lys from glycyl-tRNA. Further chain elongation process initiated by the help of femA and femB which is ultimately ended up of the terminal Gly_5. Gly_5 is cross-linked to the second last D-Ala residue and this step regulated by transpeptidase reaction, and inactivated by both β-lactams and vancomycin. V denotes vancomycin which is binds to the terminal D-Ala-D-Ala. 188

Figure 4.10. Novel regulators of *S. aureus* biofilm formation in (A) 3-day biofilm, and (B) 12-day biofilm identified from TMT-based analysis. 191

Figure 5.1: Experimental workflow for the analysis of *S. aureus* planktonic, wet, and DSB proteome using TMT labeling based MS. *S. aureus* strain cultivated in TSB to grow a planktonic culture pooled from biological triplicates, and biofilms (12-day and DSB) in biological triplicates. The Centres for Disease Control biofilm reactor was used to grow biofilms. Proteolytically digested peptides were labeled with TMT 10-plex reagents and subjected to high pH RP-HPLC fractionation followed by LC−MS/MS analysis. 199

Figure 5.2: The volcano plot shows the distribution of the differential protein expression profile of (A) wet compared to planktonic; (B) DSB compared to planktonic. Y-axis in the form of −log

10 represents p-value; greater numerical value is associated with lower p-value and greater legitimacy. X-axis represents fold change (log_2) of the differentially regulated proteins are represented by blue lines. The two vertical blue lines represent fold changes of -1.5 and +1.5. Therefore, the dots above red line in the positive side are significantly (<0.05) upregulated proteins, and the dots in the negative side represent the significantly (<0.05) downregulated proteins.....203

Figure 5.3: Venn diagram shows the dispersion of common and significant differential proteins in the wet and DSB. Pathway analysis was performed using KEGG. 204

Figure 5.5. (A) Selected part of the peptidoglycan biosynthesis pathway and link with amino sugar metabolism; (B) Novel regulators of *S. aureus* biofilm formation in the DSB identified from TMT-based analysis.....213

Figure 5.6: Selected part of type II fatty acid synthesis pathway for bacteria and the significant role of FabI in the last step of the elongation cycle in the synthesis of fatty acids. Modified from KEGG mapping online tool (https://www.genome.jp/kegg/). 215

Figure 6.1: Experimental workflow for plasma depletion, TMT labeling and analysis. In this study, we utilized 2xTMT 10-plex reagents. In set 1, 10 samples (C1 to D5) were combined together, subjected to high pH fractionation followed by LC-MS/MS analysis. In set 2, another 10 samples (C6 to D10) were combined together, subjected to high pH fractionation followed by LC-MS/MS analysis. Database search was also performed separately on these two sets. The two sets were combined for analysis using TMTprePro R package. 232

Figure 6.2: Box plots of the average level of log2 protein for each sample.....236

Figure 6.3: Heatmap analysis of the significantly changed proteins. Rows denote proteins and columns denote different samples. Each cell's colour represents a shift in protein expression; red indicates increased and blue indicates decreased relative to the healthy controls. In this study, we performed two set of TMT-based analysis and combined the two sets for analysis by TMT-PrePro R package. 237

Figure 6.4A: Classification of the significantly identified proteins based on their functional annotations in the cellular component category using GO. 242

Figure 6.4B: Classification of the significantly identified proteins based on their functional annotations in the biological processes category using GO. 243

Figure 6.5: PPI network analysis of the significantly differentially regulated proteins in the disease group in comparison with the healthy group using IPA. Interactions between two proteins are indicated with grey lines. Red nodes, denotes upregulated protein and green nodes, denotes downregulated protein. 246

Figure 7.1: A proposed hypothetical model based on the synthesis of the significant proteomic data generated in this study observed between different stages of biofilms. 259

List of Tables

Table 1.2: List of major biofilm dispersal proteins adapted from [322]. 30

Table 1.3: List of commonly used database searching tools, subcellular localisation, pathway analysis, and PPI analysis tools, and others. 45

Table 2.1: Culture conditions for the formation of 12dwb from *S. aureus*. 56

Table 2.2: Culture conditions for the formation of DSB from *S. aureus*. 57

Preparation of diluted albumin (BSA) standards 58

Measurement of protein concentration 59

Table 2.3: Pooled 20 fractions after high pH RP-HPLC. 62

Table 2.4: Primer sequences used in this study 69

Table 2.5: Details of selected patients used in this study. 71

Table 2.6: Pooled 17 fractions after high pH RP-HPLC. 74

Table 3.2: List of the significantly upregulated proteins in *S. aureus* biofilm in comparison to planktonic culture (fold change >2, p <0.05).. 88

Table 3.3: List of the significantly downregulated proteins in *S. aureus* biofilm in comparison to planktonic culture (fold change >-2, p <0.05).. 101

Table 3.4: List of the significantly differentially expressed virulence factor proteins identified by VFDB in *S. aureus* biofilm in comparison to planktonic culture (fold change >2, p <0.05). 128

Table 3.5: Relative correlation of selected qPCR gene expression data to TMT protein expression data in 3dwb in comparison to planktonic culture. 138

Table 4.2: Functional classification of the significantly upregulated proteins in 3dwb in comparison to 12dwb and planktonic (fold change >2, p<0.05). 163

Table 4.3: Functional classification of the significantly upregulated proteins in 12dwb in comparison to 3dwb and planktonic (fold change >2, p <0.05). 168

Table 4.4: Functional classification of the significantly downregulated proteins in 3dwb in comparison to 12dwb and planktonic (fold change >2, p <0.05). 173

Table 4.5: Functional classification of the significantly downregulated proteins in 12dwb in comparison to 3dwb and planktonic (fold change >2, p <0.05). 180

Table 4.6: Relative correlation of the selected qPCR gene expression data to TMT protein expression data (significant and common) in 3dwb and 12dwb compared with planktonic. 185

Table 5.2: Functional classification of the significantly upregulated proteins in 12-day wet biofilm in comparison to DSB and planktonic (fold change >2, p<0.05). 207

Table 5.3: Functional classification of the significantly upregulated proteins in DSB in comparison to 12-day wet biofilm and planktonic (fold change >2, p<0.05). 216

Table 5.4: Functional classification of the significantly downregulated proteins in 12-day wet biofilm in comparison to DSB and planktonic (fold change >2, p<0.05). 220

Table 5.5: Functional classification of the significantly downregulated proteins in DSB in comparison to 12-day wet biofilm and planktonic (fold change >2, p<0.05). 223

Table 5.6: Relative correlation of selected qPCR gene expression data to TMT protein expression data (significant and common) in 12dwb and DSB compared with planktonic. 226

Table 6.2: Functional classification of the significantly differentially expressed proteins in the disease group compared with the control group (p < 0.05). 238

Table 6.3: List of bacterial proteins found in this study. 241

List of Symbols and Abbreviations

Aap	Accumulation-associated protein
ABC	ATP-binding cassette family
%	Percent
°	Degree
°C	degrees Celsius
2D	two-dimensional
3D	three-dimensional
ACN	Acetonitrile
agr	accessory gene regulator
AGs	Aminoglycosides
AIPs	autoinducing peptides
AMD	Acid Mine Drainage
ATCC	American Type Culture Collection
Atl	Autolysins
Bap	Biofilm-associated proteins
BCA	Bicinchonic acid
BSA	Bovine serum albumin
BSIs	Bloodstream Infections
CAUTIs	Catheter Associated Urinary Tract Infections

CC	Capsular contracture
CDC	Centres for Disease Control
CFU	Colony forming units
CHIPS	extracellular capsular polysaccharides, chemotaxis inhibitory proteins
CID	collision-induced dissociation
CLABSIs	Central Line Associated Bloodstream Infections
cm	Centimeter
cm2	square centimeter
coa	Coagulase
CoNS	Coagulase Negative Staphylococci
CRP	C-reactive protein
CSF	Cerebral spinal fluid
DMSO	Dimethyl sulfoxide
DSB	Dry Surface Biofilm
DTT	Dithiothreitol
e.g.	for example
Eap	Extracellular adherence proteins
Ecb	Extracellular complement-binding proteins
eDNA	extracellular DNA
EDTA	Ethylenediamine-N, N'-tetraacetic acid
Efb	extracellular fibrinogen-binding proteins

EPS	Extracellular Polymeric Substances
ESBL	Extended Spectrum Beta Lactamase
ESI	electrospray ionization
ESR	Erythrocyte Sedimentation Rate
ETD	electron transfer dissociation
FA	Formic acid
FDR	false detection rate
FLIPr	formyl peptide receptor-like-1 inhibitory proteins
FnBPs	Fibronectin Binding Proteins
FT-ICR	Fourier transform ion cyclotron resonance
FWHM	Full Width at Half Maximum
GO	Gene ontology
HAIs	Healthcare associated Infections
HBA	Horse blood agar
HCD	higher-energy collision dissociation
hla	alpha-hemolysin
HPD	Human Pathway Database
HPLC	High-performance liquid chromatography
i.e.	that is
IAA	Iodoacetamide
IAIs	Implant-Associated Infections

ica	intercellular adhesin
isaA	immunodominant staphylococcal antigen A
KEGG	Kyoto Encyclopedia of Genes and Genomes
LC	Liquid-chromatography
LC-MS	liquid chromatography-mass spectrometry
MARS-14	Multiple affinity removal systems
MATE	Multidrug and toxic compound extrusion family
MF	Major Facilitator superfamily
mL	Millilitre
mm	Milimetre
mM	Millimolar
MMR	Mismatch repair system
MRSA	Methicillin Resistant *Staphylococcus aureus*
MS	mass spectrometry
MSCRAMMs	microbial surface component recognising adhesive matrix molecules
MSSA	Methicillin Sensitive *Staphylococcus aureus*
MWCO	Molecular weight cut off
nano-UPLC	nano ultra-high pressure liquid chromatography
NHPA	National Health Performance Authority
NTC	No template control
PA	Pathway analysis

PBS	Phosphate buffered saline
PIA	Polysaccharide Intercellular Adhesin
PNAG	Poly-N-acetylglucosamine
PPI	Protein-protein interaction
PPM	Parts Per Million
PSMs	phenol-soluble modulins
PTSAgs	pyrogenic toxin superantigens
QACs	Quaternary Ammonium Compounds
qPCR	Quantitative real-time PCR
RND	Resistance Nodulation Division family
Rot	Repressor of Toxin
RP-HPLC	Reverse phase-high pressure liquid chromatography
rpm	Revolutions per minute
Rt	retention time
SAK	staphylokinases
sarA	staphylococcal accessory regulator
SCIN	staphylococcal complement inhibitors
SCV	Small Colony Variant
SDB-RPS	Styrene Divinylbenzene-Reversed Phase Sulfonate
Sdr	Serine-aspartate-repeat family
Ses	staphylococcal enterotoxins

SMR	Small Multidrug Resistance family
SpA	Staphylococcal protein A
ssaA	staphylococcal secretory antigen A
SSIs	Surgical Site Infections
T2SS	Type II Secretion Systems
T4SS	Type IV secretion systems
TA	Teichoic Acid
TEAB	Triethylammonium bicarbonate
TFA	Trifluoroacetic acid
TGF-β1	Transforming Growth Factor Beta-1
TMT	Tandem Mass Tags
TOF	Time of flight
TSB	Tryptone soya broth
UTIs	Urinary Tract Infections
v/v	Volume per volume
VAP	Ventilator Associated Pneumonia
VFDB	Virulence Factors of Pathogenic Bacteria Database
X	Times
β-ME	Beta-mercaptoethanol
μg	Microgram
μL	Microlitre

μM	Micromolar
μm	Micrometer
σB	sigma factor B

Thesis Structure and Chapter Outline

This thesis is presented as a literature review, materials and methods section plus a series of chapters formatted for publication. This outline has resulted in some repetition in introduction and methods in each chapter, however, the results and implications for bacterial survival, diagnostic and biofilm removal potentials are found within each potential manuscript.

Chapter 1 summarises the literature relevant to the thesis beginning with the role of bacterial biofilms in healthcare-associated infections and infections associated with implantable medical devices. In addition, given the recent discovery of 'dry surface biofilm' (DSB) on hospital surfaces, this chapter also highlights their importance in increased disease transmission and the failure of current cleaning/disinfectant protocols as a result. The next part of the chapter summarises the background of *Staphylococcus aureus* biofilm and pathogenic factors related to human infection and reviews the current literature on *S. aureus* from a proteomics perspective. The final part of the chapter includes the literature on the advancement of proteomic technologies, particularly Tandem Mass Tag (TMT)-based mass spectrometry (MS) and the advantages of its application in bacterial biofilm proteomics as well as in human plasma proteomics.

Chapter 2 describes the materials and methods performed for the studies presented in Chapter 3 to 6.

Chapter 3 presents a comprehensive proteomic reference map between *S. aureus* planktonic and early stage biofilm. To our knowledge, this is the first study to use TMT coupled with tandem MS to examine the proteomics of *S. aureus* biofilm. The upregulated and downregulated proteins for the two lifestyles examined are presented. Further analysis of the identified potential marker proteins was also conducted.

Chapter 4 investigated the protein expression profile of *S. aureus* biofilm at two times points – early biofilm (3-days) and late biofilm (12-days) development. The protein profile signatures across the different growth stages of biofilms and their effects on metabolic processes,

biosynthetic processes, transport systems and stress response are reported. Further analysis of the identified potential marker proteins was also performed.

Chapter 5 provides a novel approach to better understand DSB biology by comparing the proteome of wet and DSB from *S. aureus*. The upregulated and downregulated proteins for wet and DSB are presented. Further investigations into the significantly differentially expressed marker proteins are reported. The role of the upregulated proteins in biofilm formation and persistence on dry surfaces are also discussed.

Chapter 6 employed plasma proteome profiling to assess biofilm-related breast implant capsular contracture (CC). This chapter provides an overview of the advantages of high-throughput, quantitative analysis using TMT-based MS proteomics of plasma following depletion of high-abundance plasma proteins. The changes in plasma protein expression profiles in plasma collected from CC patients and from healthy control patients are presented. The potential of this study to better understand the underlying mechanisms involved in CC development are also discussed.

Chapter 7 discusses the major finding from Chapters 3 to 6 and highlights conclusions, significance and future directions.

Chapter 1: Literature Review

Over 99% of all micro-organisms present on earth prefer to live in biofilms [1]. Biofilms are particularly problematic in healthcare settings, in which *Staphylococcus aureus* and coagulase-negative staphylococci comprise approximately 65% of infections associated with medical devices [2-8]. Infections induced by *S. aureus* associated with biofilms often lead to significantly increased morbidity and mortality, increased duration of hospitalisation, and has resulted in a significant increase in expenses associated with *S. aureus* infections [9, 10]. This review outlines the different types of healthcare-associated infections (HAIs), incidences accompanying with HAIs, biofilm infections related with implantable medical devices and its impact on human health. This review will also discuss *S. aureus* biofilms from a proteomic perspective, its regulatory mechanisms as well as the mechanisms of biofilm resistance and tolerance.

Biofilm-related infections are tremendously problematic to eliminate because of their high tolerance against antimicrobials and host immune defenses, indicating altered metabolic profile when compared to their planktonic counterpart. Biofilms are also problematic on hospital surfaces, with the recent discovery termed as dry surface biofilm (DSB). This review will discuss the importance of DSB in terms of increased transmission of disease from healthcare settings and the failing of current cleaning and disinfectant protocols, which warrant further investigations to know the deeper biology of the formation of complex DSB.

In recent times, we have experienced rapid advancement in the proteomic technologies from gel-based mass spectrometry (MS) analysis to high-resolution labeling based (e.g. TMT) MS and the development of protein databases. Therefore, this review will discuss the MS based analysis techniques especially with TMT, database searches, associated bioinformatics, and its applications in bacterial biofilm proteomics as well as human proteomics, which is the main subject of this thesis.

1.1. Healthcare-associated infections

HAIs are those infections obtained by patients during medical treatment [11]. The infections develop in hospital or other healthcare environment and initially seem 48 hours/more afterward

hospitalisation or in between 30 days subsequently receiving healthcare [12]. Adverse drug events, HAIs and surgical complications are the three most prevalent kinds of adverse events affecting hospitalised patients [13-17]. According to the United States Center for Disease Control and Prevention, about 1.7 million hospitalised patients obtain HAIs each year as being addressed for other health problems, resulting in over 98,000 deaths (1 in 17) directly attributed to HAIs [12]. According to the European Centre for Disease Prevention and Control, in 2011 to 2012 the prevalence of HAIs in Europe was 6%, which equates to approximately 4,100,000 patients developing a HAI each year [18]. In Australia, an estimated 6% of patients develop a HAI [19] with around 200,000 HAIs occurring per year [20]. These figures highlight the prevalence of HAI and why they are the most common complication affecting hospital patients. A very recent systematic review of the peer-reviewed literature reported that 83,096 HAIs per year occurred in Australian hospitals from 2010 to 2016, however, this number did not include HAIs due to pneumonia, gastroenterological or general bloodstream infections. The authors concluded that their estimates only represented 40 to 50% of HAIs. A recent USA based study reported that 6% of patients had HAIs with the uppermost 75.8% obtaining surgical site infections (SSIs), urinary tract infections (UTIs), pneumonia, and bloodstream infections, with *Staphylococcus aureus* being the most commonly isolated microorganism [12, 21]. HAIs result in unnecessary adverse clinical consequences, extra costs to healthcare and personal costs to the patients. Many HAIs are associated with the use of prostheses and implants such as central line-associated bloodstream infections (CLABSIs) and catheter-associated UTIs [22, 23].

HAIs are divided into the following categories which include SSIs, bloodstream infection (BSIs), catheter-associated urinary tract infections (CAUTIs), and Ventilator-associated pneumonia (VAP), among others.

Surgical site infections (SSIs)

The type of surgery determines the percentage of patients developing SSIs, which can range from anywhere between 2% and 36%. [24-27]. For example, the incidence of SSIs after gastrectomy or hepatectomy is reported to be 11.3%, while after colorectal surgery it is 15.5%, but after pancreaticoduodenectomy it is as high as 36.9% [28]. In contrast, SSIs developed in only 79 out of 3,096 patients (2.55%) following orthopedic surgery [29]. The duration of hospital stay in SSI

patients can increase between 4 and 32 days in comparison to patients without post-operative infections [30-32]. Australian surgical mortality audit (2012-2016) found that 20% of surgical patients that died had an HAI [33]. In these patients, HAI had increased risk of post-operative complications (51% versus 30.3%), increased re-operations (22.6% versus 10.9%) and increased unplanned admittance to an intensive care unit (29.3% versus 14.8%). The microorganisms usually involved in these SSIs include *S. aureus*, coagulase-negative *Staphylococci*, *E. coli*, and *Enterococcus* spp. [34]. *S. aureus* has been recognised as a significant cause of HAIs for more than 100 years [35].

Bloodstream infections (BSIs)

BSIs are a foremost threat to the safety of patients and result in significant burdens to healthcare systems. A very recent study reported that the occurrence of catheter-related BSIs as 3.93 per 1,000 central-catheter days [36]. In the late 1990s, the basic mortality rate for patients with healthcare-associated (HA) BSIs was as high as 30% [37, 38], which decreased to around 15% by 2013 [39].

Escherichia coli, *S. aureus,* and *Streptococcus pneumoniae* have been reported to be the three most common organisms isolated from bloodstream infections, which occur at approximately 35, 25 and 10 per 100,000 population, respectively [40]. HABSIs are associated with extended hospital stays, with an additional 10 days for BSIs associated with the central line [41] and 12-days for BSIs caused by *S. aureus* [41]. Central line-associated (CLA) BSIs also significantly increase morbidity, mortality and healthcare costs, and these have been addressed with great attention [42, 43]. As a result, in 2009, there were 25,000 fewer CLA BSIs in US hospital ICUs compared in 2001, a 58% decrease, with approximately 6,000 lives saved which indicated that a projected economic savings of US$ 414 million in likely extra healthcare expenses, even though the expenses of bringing down these infections are still high [12, 44].

Catheter-associated urinary tract infections (CAUTIs)

Globally, CAUTIs are the most commonly faced HAIs and a leading cause of microbial infections, comprising about 40% of HAIs, with important morbidity and mortality consequences and considerable economic expenses [12, 24, 45-48]. In the US, CAUTI is the most frequently

described HAI with more than 550,000 cases per year [49]. CAUTIs can results in several health associated problems such as severe septicaemia due to bladder stones and mild catheter encrustation, endotoxic shock, and pyelonephritis [45, 50]. The rate of CAUTIs has been estimated at approximately 5% per day and is caused by bacteria or yeasts, including both Gram-positive and Gram-negative bacteria [12, 46, 51, 52]. Even catheters removed from patients without a history of UTI often are contaminated with pathogens. Studies by Chatterjee *et al.* (2014) reported that 130 of 150 catheters removed from patients without a history of UTIs had pathogens on the catheter and in the concomitant urine samples [5]. They found the most common microorganisms included both Gram-positive and Gram-negative bacteria such as *S. aureus*, *Staphylococcus epidermidis*, *P. aeruginosa*, *E. coli* etc. [5]. Previous studies has shown higher infection risks are associated with patients who have long-term catheters and other urinary tract diseases than those without [12, 52]. A non-concurrent cohort study conducted for 4 sequential years in Australian healthcare-associated urinary tract infection found that patients had an additional 4 days of hospitalisation [12, 53].

Ventilator associated pneumonia (VAP)

VAP is the second most common HAI in ICUs around the world [54, 55] and the leading cause of death from HAIs in critically ill patients [56]. This type of pneumonia develops from 9% to 27% of patients with assisted ventilation and patients who develop VAP having higher mortality (ranging from 24% to 76%), longer hospital stays (up to an extra 7 days), higher antibiotic usage and more costly treatment (by approximately US$40,000) when compared to those without VAP [57-62].

Multiple studies have reported that *S. aureus*, *P. aeruginosa*, *Enterobacteriaceae*, *Haemophilus influenza*, and streptococci are the most frequent pathogens isolated in VAP [63-66]. In particular, bacteria causing late VAP are generally multidrug-resistant bacteria which include: (i) methicillin-resistant *S. aureus* (MRSA), (ii) *Acinetobacter*, (iii) *P. aeruginosa*, and (iv) extended-spectrum beta-lactamase producing bacteria (ESBL) [39, 67].

1.2. Bacterial biofilms and its associated health infections

1.2.1 Bacterial biofilms

Bacterial growth in a liquid culture medium is commonly referred to as the planktonic mode of growth which is the most generally utilised technique for studies of bacterial growth. The general agreement, though, is that most species of bacteria have the capacity to develop in the state of biofilm [68].

In the 1600s, Anton Van Leeuwenhoek was the first to notice the presence of aggregates of microorganisms attached to his tooth scrapings of his own dental plaque [69]. While in the 1940s, studies showed that bacterial growth increased in the presence of a surface and grew more on surfaces than in the surrounding medium [70, 71]. However, it was not until the late 1970s that the concept of a "biofilm" was described by Costerton [72]. Since then, with an increased understanding of biofilms, several definitions have been proposed [73-77]. The following is the most widely accepted definition by Donlan and Costerton (2002):

"A biofilm is a microbially derived sessile community characterised by cells that are irreversibly attached to a substratum or interface or to each other, embedded in a matrix of extracellular polymeric substances that they have produced, and with an altered phenotype with respect to growth rate and gene transcription", Donlan and Costerton [78].

Biofilms are the prevalent microbial way of life in natural habitats because of their protective nature, permitting their existence under harsh ambient temperature circumstances (e.g., thermal waters, glaciers), humidity (e.g., deserts, rainforests) and acidity (e.g., sulphuric pools and geysers) [79].

Biofilms grow on almost any kind of natural or industrial surface. In industry, they cause contamination of water and food, metal surface erosion and equipment obstruction [80, 81]. Biofilms are also prominent in medical surroundings, where they occur in up to 75% of human microbial infections based on the US National Institute of Health [82] and of these, biofilms are projected to account for or involve 80% [83, 84]. For example, *Staphylococcus* spp have been associated with numerous infections related to medical devices including sutures, mechanical heart valves and orthopaedic prosthesis (Table 1.1). By using the biofilm mode of growth,

indwelling bacteria have enhanced environmental protection that provides greater defense against a broad range of antibiotics, enables infections to persist and promotes selection for antibiotic resistant genes [85, 86].

Table 1.1: Variety of human infections caused by biofilms [87].

Infection or disease	Commonly involved bacterial species
Dental caries	Acidogenic Gram-positive cocci
Periodontitis	Gram-negative anaerobic oral bacteria
Otitis media	Non-typeable *Haemophilus influenza*
Chronic tonsillitis	Various species
Cystic fibrosis pneumonia	*P. aeruginosa*, *Burkholderia cepacia*
Endocarditis	Viridans group streptococci, staphylococci
Necrotizing fasciitis	Group A streptococci
Musculoskeletal infections	Gram-positive cocci
Osteomyelitis	Various species
Biliary tract infection	Enteric bacteria
Infectious kidney stones	Gram-negative rods
Bacterial prostatitis	*E. coli* and other Gram-negative bacteria
Infections related to medical devices	
Contact lens	*P. aeruginosa*, Gram-positive cocci
Sutures	Staphylococci
Ventilation-associated pneumonia	Gram-negative rods
Mechanical heart valves	Staphylococci
Vascular grafts	Gram-positive cocci
Arteriovenous shunts	Staphylococci
Endovascular catheter infections	Staphylococci
Cerebral spinal fluid-shunts	Staphylococci
Peritoneal dialysis (CAPD) peritonitis	Various species
Urinary catheter infections	*E. coli,* Gram-negative rods
IUDs	*Actinomyces israelii* and others
Penile prostheses	Staphylococci
Orthopaedic prosthesis	Staphylococci

1.2.1.1. Bacterial biofilm composition

Bacterial live within biofilms are covered by a self-produced matrix of extracellular polymeric substances (EPS) matrix (Flemming and Wingender, 2010). Although it varies from species to species, the EPS components include: protein (>2%), polysaccharides (1–2%), DNA molecules (<1%), RNA (<1%), other constituents such as minerals and ions, and up to 97% of water [88, 89]. These components of EPS play a pivotal role in biofilms by providing mechanical stability and mediating attachment to surfaces to form a cohesive, three-dimensional polymer network interconnecting and immobilising biofilms transiently [89-91].

In *Staphylococcus* biofilms, proteins such as fibronectin-binding proteins (FnBPs) and biofilm-associated proteins (Bap), polysaccharide intercellular adhesin (PIA), extracellular DNA (eDNA), and teichoic acids have been shown to be components of EPS matrix [92-95]. Each component's contribution to the formation of biofilms differs between staphylococcal strains.

Polysaccharide intercellular adhesin (PIA) is thought to be a principal extracellular component (80–85%) and is mainly composed of β-1,6-linked N-acetylglucosamine residues. *In vitro*, PIA is generated from UDP-N-acetylglucosamine through intercellular adhesin (ica) locus products [96]. In some strains of *S. aureus* biofilm development is dependent upon the ica locus [icaR (regulatory) and icaADBC (biosynthetic) genes] [97], however, ica-independent mechanisms have been shown to be sufficient for biofilm formation in some strains, *S. aureus* and in coagulase-negative staphylococci [98]. Studies by Houston *et al.* (2011) demonstrated that fibronectin-binding proteins (FnBPs) can mediate *S. aureus* biofilm development via a vital role by the major autolysin (Atl), agr, and sigB regulation [99]. However, accumulation-associated protein (Aap) play significant role in PIA-independent biofilm formation in *S. epidermidis* [100, 101]. Biofilm-associated protein (Bap) plays a significant position among the adhesive proteins involved in the formation of biofilms, which has been shown to be crucial for both initial attachment and intercellular accumulation during the growth of *S. aureus* biofilm. The Bap gene is also found in *Staphylococcus* spp. including *S. chromogenes, S. epidermidis*, *S. xylosus*, *S. hyicus*, *S. simulans* and several other staphylococcal species [102].

1.2.1.2. Bacterial biofilm formation

Biofilm formation differs between different bacterial species and even within the one species, for example, some *S. aureus* strains develop biofilms more promptly compared with other strains [103]. In addition, factors associated with external environment may change the capacity of certain strains to start the formation of a biofilm [103].

1.2.1.3. Stages of biofilm development

Biofilm development begins with an initial stage of adhesion to a biotic or abiotic surface, followed by further accumulation, formation of microcolony, established biofilm growth, and finally disassembly/dispersal of biofilms (Figure 1.1). While the microcolony formation does not have a precise definition, it is usually considered to be an intermediate phase of biofilm establishment which connects the initial stage of adhesion step with the complete biofilm growth. Further mature biofilm development ensured by continuous microcolony formation leads to the production of EPS, which is the surface structure of a well-established biofilm. This EPS matrix play significant role in developing extreme resistance mechanisms against a broad range of antimicrobial agents [104, 105]. The last step is the detachment/dispersal of the specific molecular factors from the biofilm cells which can function as spreading factors in distant areas. The biofilm matrix is usually targeted for degradation during this stage, this triggers cells to be released into the surrounding area. Biofilm dispersal restores the susceptibility of bacteria to effective chemotherapy and has gained attention as a potential field of research [106, 107]. Determining the degradation of biofilms may lead to deeper understanding of the components of the biofilm matrix with the possibility to explore more treatment options. In addition to these basic stages of biofilm development, *S. aureus* biofilm has two additional intermediate stages (multiplication and exodus) between initial attachment and maturation stages (Figure 1.1), which contribute to the EPS and cellular organisation differences in the mature biofilm [108]. The exodus phase is facilitated by the staphylococcal nuclease [108].

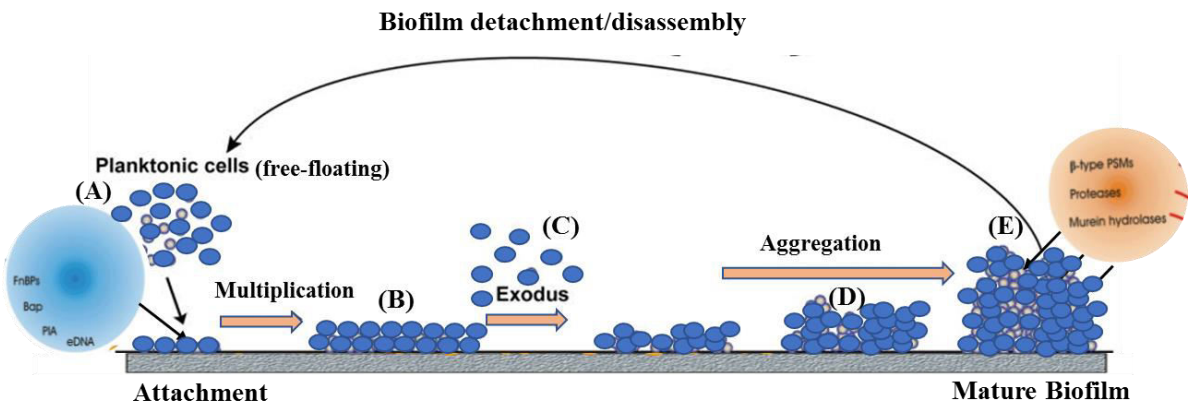

Figure 1.1: Scheme showing the phases of the formation of *S. aureus* biofilm; modified from [109]. (A) Individual planktonic bacterial cells adhere to a biotic or abiotic surface (B) Further continue to grow cells and multiply and ultimately develop microcolonies leading to the deposition of biofilm matrix (C) Exodus, premature detachment of a biofilm subpopulation. (D) Continue to produce excessive EPS matrix components results in the formation of a matured biofilm (E) Final step, biofilm cell detachment/disassembly occur and return to a planktonic mode of growth.

In biotic surfaces, the bacteria need to evade the host defence mechanisms and *S. aureus* MSCRAMMs plays significant role by forming covalent bond to the surface of bacterial cells which allows binding to the host matrix proteins [110, 111]. Surface proteins (e.g., autolysins, Atl) which are bound non-covalently, demonstrated to be the cell surface's most abundant protein and they can enhance bacterial adhesion to surfaces through their interaction with human extracellular proteins including vitronectin, fibronectin, matricellular protein thrombospondin 1 and plasma proteins [112]. In addition, the lipase GehD was described as having a functional role in adherence by acting as a cell surface-associated collagen adhesion [113].

1.2.1.5. Mechanism of biofilm resistance and tolerance

Biofilms are characterised by their notable resistance and tolerance to wide-ranging antibiotics, biocides, and host defenses that plays an important role in chronic infections due to their high level of persistence. Numerous mechanisms are thought to be involved in biofilm resistance and

tolerance. In particular, some of them are strictly regulated by the mechanisms specific to biofilm. However, others are associated with physiological adaptations to the biofilm microenvironment [114].

Biofilm matrix

Several reports have suggested that biofilm matrix or EPS can decrease or delay antibiotic and disinfectant penetration, resulting in an enhanced biofilm resistance or tolerance to these agents. For example, EPS accounted for a significant decrease in the antimicrobial efficacy of vancomycin, teicoplanin, and pefloxacin, mainly due to diffusion barriers [115-117]. Interestingly, bacterial cell-wall hydrophobicity has been shown to change the nanoparticles diffusion within the biofilm [118], suggests that interface elements of the cell wall (e.g., peptidoglycan, capsules, and fimbriae) may also impact the biofilm component diffusion. Although diffusion may partly explain biofilms resistance, very small level of inactivation has been accomplished as a consequence of efficient biocide penetration into a biofilm [119]. For instance, resistance mechanism in the complex *S. aureus* biofilm to a quaternary ammonium compounds (QACs) has been assigned to phenotypic changes in cells instead of the defensive existence of a biofilm matrix [120].

Extracellular enzymes

Various extracellular enzymes present in the biofilm matrix can accumulate within the biofilm EPS. These enzymes (e.g., aminoglycoside modifying enzymes, and secreted β-lactamases) can play significant role in the degradation and modification of antimicrobials, and as a result these agents can not reach their desired cellular targets. Resistance to β-lactams is due to the secreted β-lactamases hydrolysing the antibiotic's β-lactam ring and has been reported in multiples studies [121, 122]. Mechanisms of bacterial resistance to aminoglycosides (AGs) mainly based on ribosomal mutation and chemical modifications by enzymes. A very recent review highlighted the possible resistance mechanism to AGs, where AGs can target the A-site of the bacterial ribosome resulting in mutations of the ribosome including modification of the ribosomal structure by methyltransferases at the AG binding site [123]. In addition, Garneau-Tsodikova *et al.* (2016) have also mentioned a mechanism of resistance to AG is chemical modification by

aminoglycoside-modifying enzymes, in particular, bifunctional enzymes such as AAC(6′)-Ie/APH(2″)-Ia from *S. aureus*, which are capable of multiple types of AG modification [123].

Heterogeneity in metabolism and growth rate

Metabolic activity and growth rate of the bacteria are impacted by the changes in the gradient of oxygen as well as several other nutrients within the biofilm. Many studies have demonstrated that cells within oxygen deficient regions have decreased metabolic activity and are in a condition of stationary phase [124-126]. Cellular enzyme synthesis is arrested in stationary phase or slow-growing bacteria [127]. This slow pace of development gives tolerance because antimicrobials are most efficient against fast-growing cells [128-130].

A biofilm's development is also connected with physiological adaptations of cells resulting from the expression of particular genes in reaction to their immediate micro-environmental circumstances, which can lead to increased biocide resistance. For example, a study by Folsom *et al.* (2010), 3-day old *P. aeruginosa* biofilms was characterised in terms of the availability of oxygen, nutritional limitation and antibiotic tolerance, and observed low oxygen concentrations in biofilms (initial from 6mg/l to decreased down to 0.2mg/l). They also observed *P. aeruginosa* biofilm cells showed higher levels of persistence to antibiotics (e.g. tobramycin) in comparison to planktonic culture, which suggests that these physiological adaptations may lead to increased resistance to antibiotics [131].

Efflux pumps

Efflux pumps are resistant to distinct antimicrobials that correspond to the same or distinct families [132, 133]. Efflux pumps protect cells by removing antimicrobials from their intracellular targets and returning them to extracellular space [134]. Multiple studies have reported that the encoding genes of the efflux pump are located either on the chromosome or plasmids with resistance to numerous antibiotics, detergents, and biocides [135].

Bacterial efflux pumps can be divided into several superfamilies: “the major facilitator superfamily (MF), the resistance-nodulation-division family (RND), the small multidrug resistance family (SMR), the ATP-binding cassette family (ABC) and the multidrug and toxic compound extrusion family (MATE)” [136]. To drive antimicrobial agent efflux, the family of

MF, RND and MATE family function as secondary transporters, catalysing drug ion antiproton reactions, whereas the family of ABC involved in the hydrolysis of ATP [137].

Although the role of efflux pumps in planktonic bacteria in terms of the resistance of antibiotics is well recognised, their role in the resistance of biofilm antibiotics remains ambiguous. In some studies, downregulation of multidrug efflux systems has been observed in *P. aeruginosa* biofilm mode of growth [131, 138]. In another study of *P. aeruginosa* strain PA14, the gene encodes multidrug efflux system was upregulated in biofilms compared to planktonic bacteria [139]. However, due to their versatile roles and highly diverse expression in biofilm architecture, determining the response of particular efflux systems is difficult [140, 141].

Genetic diversity

Genetic diversity arises when breaks are repaired by a mechanism capable of inducing mutation which involved recombinatorial DNA repair genes. Studies from Boles *et al.* (2008) and Lebeaux *et al.* (2014), demonstrated an "insurance effect" mechanism by which biofilm mode of growth enhance the ability to adjust and withstand in diverse environments by employing mutagenic mechanism [142, 143]. They also reported that endogenous oxidative stress in *P. aeruginosa*, influences the breakage of double-stranded DNA in certain biofilm cells. Various genes (e.g. katA and sodB) are downregulated when cells are in the biofilm mode of growth and these may play an important role in the protection against oxidative stress associated DNA damage [143, 144]. Mutation studies in staphylococci revealed that, *S. aureus* biofilms with mutability 60-fold and 4-fold in *S. epidermidis* higher compared to planktonic growth mode [143, 145], thereby these mutations can result in resistance or tolerance mechanisms toward antimicrobial agents.

1.3. Biofilm infections associated with implantable medical devices

With the continuous advancement of modern medical sciences, the use of implanted medical devices has become an essential component of modern medicine. Implantable medical devices are used for life-saving purposes like artificial hearts as well as for cosmetic purposes like a breast implants. But, the problem of implant-associated infections (IAIs) is expected to grow as the number of implants used increases. Currently, IAIs rate ranges from 2% to 40%, depending on the type of surgical implant, such as 19 to 30% for breast implants [146] and "2% for joint

prostheses, 4% for mechanical heart valves, 10% for ventricular shunts, 4% for pacemakers and defibrillator, and about 40% for ventricular-assisted devices" [147, 148]. Many of these infections are due to bacterial biofilms involving both Gram-positive and Gram-negative bacteria with the most common ones including "*Enterococcus faecalis*, *S. aureus*, *S. epidermidis*, *Streptococcus viridans*, *E. coli*, *K. pneumoniae*, *Proteus mirabilis* and *P. aeruginosa*" [149]. The staphylococcal species accounts for about two thirds of the IAIs [147, 150]. It has been estimated that, *S. aureus* and *S. epidermidis* alone, are responsible for approximately 40 to 50% of infections associated with prosthetic heart valve, 87% of bloodstream and 50 to 70% of biofilm-associated infections caused by catheters [149]. Diagnostic difficulties and absence of appropriate biomarkers are major challenges in the treatment of biofilms, and biofilms can also be hard to eradicate in the clinic because of their elevated tolerance to antibiotics [109].

Breast implants

Breast augmentation with breast implants is a popular surgical procedure used for breast enlargement, asymmetry correction or post-mastectomy reconstruction [146]. In 2016, in the US alone, more than 290,000 procedures were performed, and this figure represents a 37% increase from 2000 [151]. Despite advances in implant invention and surgical procedures, complications may arise after implant arrangement [152]. One of the most frequent post-operative problems of breast augmentation and reconstruction is capsular contracture (CC) [153, 154], and in the past it has been reported as having incidence rates of between 5 to 74% [155-159]. Persons with breast implants also have a risk of developing a rare type of non-Hodgkin's lymphoma, known as breast implant-associated anaplastic large-cell lymphoma (BIA-ALCL). As a result, in 2016 the American FDA made it compulsory to inform them of adverse events/reoperation/removal associated with their breast implants allowing for better determination of the incidence of BIA-ALCL and CC. As of 2018, the FDA had received a total of 660 medical device reports, 457 of which were for BIA-ALCL [146]. In Australia, there have been 90 reported cases of BIA-ALCL, including four deaths [160]. While CC, one of the most common reasons for reoperation, occurred in 38.9% of the 5,290 breast implant revision cases that took place between 2012 and 2016 [161].

CC is a hardening and tightening of the tissue that forms around the breast implant leading to pain and discomfort [162]. CC is classified according to the Baker classification system, specifically: grade I, looks and feels natural breast; grade II, minimum contracture; grade III, breasts will be firm to touch and appear abnormal but causes little or no pain; and grade IV, breasts become hard and patients experience soreness that is painful to the touch [163]. The mechanisms that lead to CC are remained unclear, but the cause appears to be largely multifactorial [6]. Several potential risk factors have been identified for CC [164], the principal risk factors including: bacterial infections, gel exudations and contaminants, foreign-body reactions, tissue responses to implanted materials, propensity for hypertrophic scars, postoperative hematomas, the surgical position of the prosthesis, and site of the surgical cut.

Despite the large amount of risk factors that may lead to the formation of CC, multiple lines of evidence suggest the involvement of subclinical infections and bacterial biofilm formation [6, 165-171]. It has been evidenced by several studies that microbial biofilms on breast implants may promote a chronic inflammatory reaction and consequently lead to the development of intense capsular fibrosis with contracture following [6, 172, 173]. The inflammatory response itself, however, also contributes to tissue destruction by continually recruiting proinflammatory cells such as lymphocytes, and macrophages, releasing proteases, and inflammatory mediators [6]. Although proteases help dislodge biofilms, they also harm ordinary and curative tissues, whereas macrophages may develop a fibrous capsule around the implants [174]. Various kinds of fibroblasts which includes myofibroblasts, play a key role in healing. These molecular factors rise in number in CC [175, 176], and it has been shown that transforming growth factor beta-1 (TGF-β1) and mechanical stress play vital role in the regulation of CC as well as in wound healing [175]. A recent study by Mazhar *et al.* (2014) found a positive correlation between bacterial biofilms and TGF-β1 expression in patients with airway tracheal stenosis [177]. Myofibroblasts are able to produce collagen (such as types I and III) and a precise shape of fibronectin [178], which may contribute to the establishment of a contracted capsule around a breast implant [179]. The excessive deposition of collagen and fibronectin may also be exploited by bacteria since several bacterial species generate proteins that binds to collagen and fibronectin which facilitate bacterial adhesion to extracellular matrix molecules [180-183]. Bacteria multiply and form

biofilms once they are attached. Hence, we ponder that the enhanced count and activity of myofibroblasts may lead to the development of biofilm and likely CC.

The majority of isolates from breast implant infection cases are *S. aureus,* coagulase-negative staphylococci (CoNS) including *S. epidermidis, Cutibacterium acnes* (formally *Propionibacterium acnes*) and streptococci [170, 184, 185]. Potential sources of infection with breast implants may include: (a) implants with contaminated surface and/or inner solution; (b) surgical technique; (c) working conditions; (d) the patient's skin and the resident bacterial flora that may come into contact with the breast implant during its insertion; (e) mammary ducts that host bacterial colonies in more than 90% of cases [186, 187], thus representing the most important potential source of prosthetic surface colonisation; (f) late bacteremia originating in a different position from the mammary gland (e.g. dental operations) [188]; and (g) hematomas, which constitute an aggravating factor able to increase the risk of CC [189] in view of the higher availability of iron that is essential for bacterial growth.

Multiple studies using animal models have demonstrated a link between biofilms and CC such as the role of *S. epidermidis* biofilms in CC using a rabbit model [190], and *S. aureus* biofilms in CC using a guinea pig model [191]. In addition, an excellent study design using a porcine model successfully established a correlation between biofilms and the formation of CC [171]. Further, several clinical studies showed a significant correlation between biofilm and breast implant CC [170, 172, 192]. In addition to the significant correlation between biofilm and CC, recent studies also represent a trigger for chronic peri-implant inflammation [193, 194]. Given the vast amount of evidence of the significant correlation between biofilm and CC, more advanced research on the identification of the involvement of bacteria and/or host marker proteins in biofilm formation are needed to develop an early stage diagnosis and therapeutic regime.

Orthopaedic implants

Despite the advancement in the best medical practice and surgical management, none of the preventative and/or therapy for infections associated with orthopaedic implant is efficient in all instances and contribute to infections that have a negative effect on clinical outcomes and considerably boost healthcare spending [195]. The overall burden of infection in primary and revision hip and knee arthroplasties are projected to increase by 4% between 2005 and 2030 [196,

197]. Every year in US alone it has been reported that more than 12 million people impacted by biofilm-related infections with a projected yearly financial load of $6 billion [198]. Among them, biofilm-associated infections in orthopaedic practice attract greatest attention because the surfaces of frequently used orthopaedic materials (e.g., stainless steel, titanium, cobalt-chromium, numerous polymeric biomaterials, and polymethylmethacrylate cement) are all vulnerable to colonisation by biofilm producing bacteria [198-201].

The most prevalent bacteria responsible for infections associated with prosthesis are *S. aureus* and coagulase-negative staphylococci, which account for about half of the infections or more [202-204]. Highly virulent microorganisms such as *S. aureus* or *E. coli* were found to be responsible for early infections after implantation, while in contrast, less virulent bacteria such as coagulase-negative staphylococci were related to delayed infections (3-24 months after operation) [198]. It has been revealed that polysaccharide intercellular adhesin (PIA) produced by staphylococci is a key virulent factor that assists staphylococci to develop biofilm on implants or orthopaedic biomaterials [205, 206].

Evidence suggested that both early and delayed infections are generally caused by perioperative contamination and are regarded as the most prevalent cause of infections related to biomaterials [198, 207-209]. Usually, these infections are linked with symptoms locally and systemically (such as localised pain, swelling, and congestion. Further, increased responses to inflammation that came with raised inflammatory markers in the laboratory (e.g., C-reactive protein (CRP), leukocyte count, and white cell count levels). It is also possible to use positive blood and tissue cultures to detect infection in the early stages. However, molecular diagnostic methods indicate a substantial percentage of culture-negative infections (5% -34%) [210-212]. These infections have often been shown to be caused by bacterial biofilms showing little or no systemic signs and minor inflammatory reactions at the local level [202, 213-216].

Cardiovascular implants

Over 100,000 cardiovascular devices are implanted in the United States each year, and infections of the cardiac valve account for 30% of implant-associated fatalities. The most frequently reported bacteria causing cardiac implant infections (pacemakers, prosthetic valves, defibrillators and coronary artery bypass grafts) include Gram-positive and Gram-negative bacteria such as *S.*

aureus, *S. epidermidis*, *P. aeruginosa*, *Acinetobacter baumannii*, *K. pneumonia*, *E. coli*, and *C. acnes* [147, 217-219]. Other microorganisms also develop biofilms on cardiovascular devices, such as *Enterococcus* and yeasts [220]. The source of these microorganisms may initiate from the skin or various medical devices for instance central venous catheters or works associated with dental implants [221]. Tissue harm can happen at the time of surgical implantation of prosthetic heart valves as a consequence of the accumulation of platelets and fibrin at the suture place and on the devices, and bacterial cells have the capability to colonise these sites [78, 222]. Biofilms developed on heart valve may affect the blood flow by reducing its flow in the valve, which leads to hematogenous spread, infection and the growth of emboli in other body parts [219].

Indwelling urinary catheters

Urinary catheters are usually produced by silicon or latex and are regularly used in hospitalised patients to perform various activities such as collection of urine during surgical operation, measurement of urine production, and prevention of urine retention [219]. Colonisation of the periurethral skin causes bacterial contamination, this can lead to the migration of the bladder and the development of biofilms on catheters [223]. The microorganisms that frequently contaminate these devices and develop biofilms are include *S. aureus*, *S. epidermidis*, *E. faecalis*, *E. coli*, *P. mirabilis*, *K. pneumoniae*, *P. aeruginosa*, as well as various Gram-negative bacteria [224, 225]. Urine contamination in the drainage bag of the catheter can also be a source of bacteria that can lead to the cause of infection [223]. Further, some urease producing bacteria such as *P. mirabilis*, *Proteus vulgaris*, *Pseudomonas*, and *Klebsiella*, causes a rise in the urinary pH, that helps the establishment of crystalline biofilms within catheters [226]. These crystalline biofilms can form deposits on the outer surfaces, tips, and balloons of catheters, which can lead to severe complications, such as urinary bladder injury [223].

Moreover, biofilm debris may also be shed after a catheter balloon has been deflated, that can prevent the flow of urine through the catheter [227]. Studies have shown that patients with short-term catheterisation (≤7 days) undergo biofilm development 10 to 50% of the time; however, it is found that nearly all patients with long-term catheterisation (>28 days) have biofilm formation [51]. The key approaches used to avoid infections associated with urinary catheters are to utilise catheters when highly recommended to use, circumvent long-term catheterisation and regularly

change catheters. Recurrent replacement and interruption can, however, lead to serious complications, the spread of bacteria through biofilm shedding to uncontaminated locations [228-230].

1.4. Biofilm on hospital surfaces

Environmental surfaces in healthcare facilities play an important role in terms of disease transmission [231-235], and the development of biofilms on the surfaces in these settings [90, 104, 236-239]. Biofilms can function as pathogen's reservoirs in the hospital setting and provide favourable situations to allow pathogens to persist for prolonged durations [239-241]. The structure of biofilms also prevents integrated pathogens from many antimicrobials, (e.g., antibiotics and biocides) [104, 242, 243], which makes it so hard to eliminate these pathogens using normally used decontamination methods [244-246].

It has been speculated that the formation of biofilms may be enhanced by a thin film of water resulting from condensation on surfaces or that the relative humidity of intensive care units is sufficiently high to allow biofilm development [239]. However, recent findings of biofilms on dry hospital surfaces emphasises the failures in current cleaning practices and disinfection [239, 247]. Biofilms contain a high bacterial load capable of surviving for a long time on dry hospital surfaces, also showing an increased resistance towards inactivation by disinfectants. In fact, bacteria in the biofilm are up to 1,000 times more resistant to disinfectants than their respective planktonic state [244, 248-250].

Recent studies reported that 50% [239] or more [251] of dry surface biofilms recovered from hospital surfaces contain *S. aureus*, which is a serious concern in terms of increased transmission of disease from healthcare settings and the failing of current cleaning and disinfectant protocols. A novel dry surface biofilm (DSB) model by Almatroudi *et al.* (2015) was developed to test the multiple roles played by DSB in a hospital setting, in particular cleaning and disinfectant efficacy testing. For example, they studied the effectiveness of hypochlorite against DSB and found that DSB was more tolerant to hypochlorite than hydrated biofilm which in turn was more tolerant than planktonic organism [244]. Another recent study reported that disinfectants were unable to remove all *S. aureus* biofilm protein in the presence of biological soil [245]. These studies highlight the possible negative impact that biofilms have on infection control.

However, so far, no research has examined the development of the complicated dry surface biofilms on environmental surfaces in healthcare facilities [239, 251]. Almatroudi *et al.* (2015), reported that DSB contain more protein and less carbohydrate than wet biofilm, and thicker extracellular polymeric substances [252]. Within DSB, bacteria are highly protected against desiccation and have enhanced tolerance by disinfectants and cleaning agents for removal. Therefore, there is a dire need to understand the deeper biology of complex biofilm formation to prevent transmission of pathogens from healthcare surfaces, and develop more advanced targeted design of cleaning agents and disinfectants by destabilising biofilm architecture.

1.5. *Staphylococcus aureus* and biofilms

1.5.1. *Staphylococcus aureus*

S. aureus is a Gram-positive cocci commonly found in the environment [253] and it is also normal human microbiota which is linked with an symptomless commensal colonisation of the skin, nose, throat, hair, nails, perineum, and axillae as shown in Figure 1.2 [254]. *S. aureus* can grow over a widespread range of temperatures from 6 to 48ºC, but its optimal growth is between 35 to 41ºC. Similarly, it can grow over a wide pH range from pH 4 to pH 10, but optimal growth happens at pH 6 to 7. *S. aureus* is salt tolerant surviving in media containing up to 20% of salt but optimal growth also happens in the absence of NaCl. While it has high water activity (a_w) limits ($a_w = 0.83 \geq 0.99$, optimal at 0.99), *S. aureus* also tolerates desiccation [255, 256]. *S. aureus* is non-fastidious due to its production of a wide range of various enzymes (such as lipases, proteases, thermonucleases, hyaluronidases, collagenases, catalases) and exotoxins (e.g., haemolysins) [257, 258].

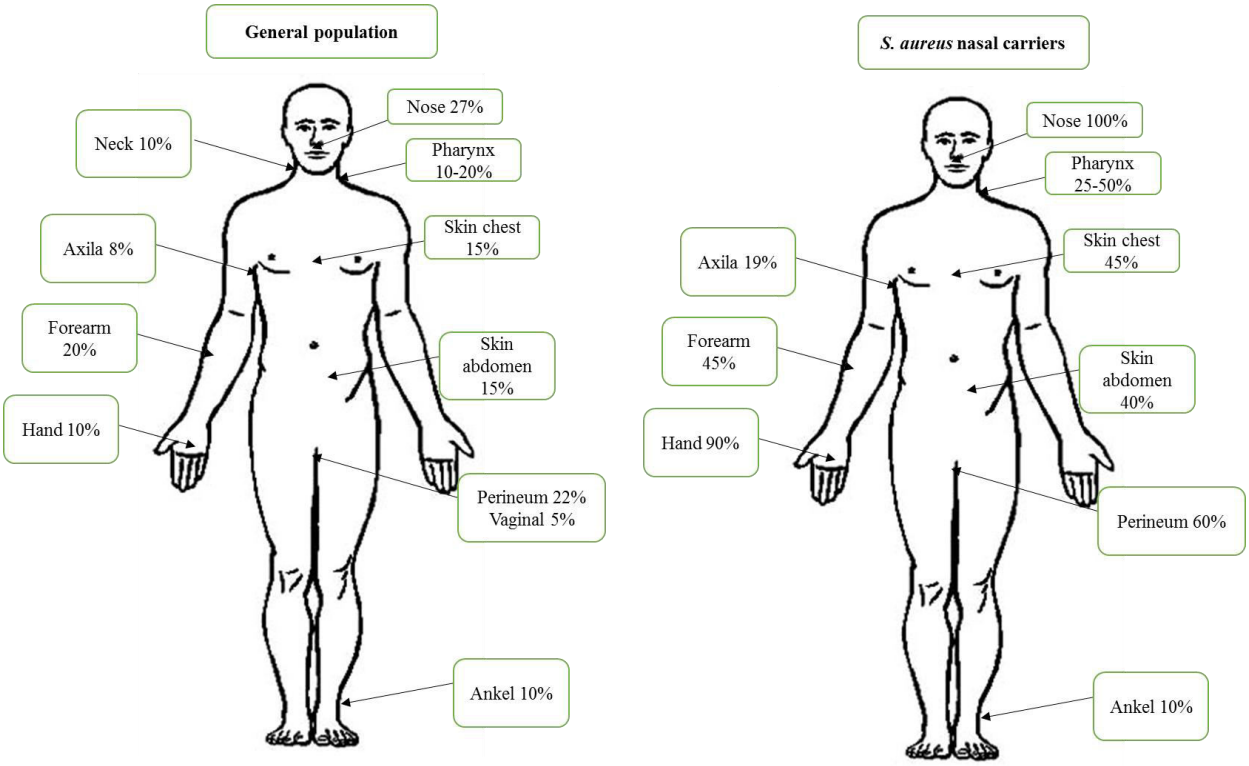

Figure 1.2: *S. aureus* colonisation sites in the human body. Modified from web site: https://www.coloringsky.com/human-body-coloring-pages-for-kids/.

1.5.2. *Staphylococcus aureus* pathogenicity and pathogenic determinants

In human carriers, *S. aureus* acts as an opportunistic bacterial pathogen [259]. *S. aureus* can infect people when the mucocutaneous barrier is broken such as those occurring through skin injuries (e.g., burns, wounds, acne, styes) or secondary to medical treatment (urinary or intravenous catheters) or following surgery (prosthetic devices, sutures). In immune-compromised patients or those with co-morbidity, for example, infection with other pathogens or chronic underlying diseases (e.g., heart disease, cancer), the chance of getting *S. aureus* infections can also be enhanced [260-262].

S. aureus has a multitude of extracellular and cell-surface-associated virulence factors encoded in phages, plasmids, staphylococcus cassette chromosome and pathogenicity islands. They are expressed in a coordinated manner during the various phases of infection, constituting

colonisation and host tissue invasion, the multiplication of bacteria and spread [263]. Universal regulators, for instance, the staphylococcal accessory regulator (sarA), the accessory gene regulator (agr), and the sigma factor B (σB), mediate the production of pathogenic determinants during infection, which are influenced by the activity of various environmental signals (e.g., temperature, pH, osmolarity, alterations in the availability of nutrient) [263, 264].

MSCRAMMs (e.g., Clf, CnA, Fnbp1) produced by *S. aureus* play important role in the host tissue colonisation and invasion [110, 263, 265]. *S. aureus* may internalise and continue forever in the host cells, or produce rapid cellular apoptosis or necrosis, or even multiply and further disseminate [265]. Multiple studies demonstrated that, *S. aureus* produces several virulence factors (e.g., extracellular adherence proteins, Eap, extracellular capsular polysaccharides, extracellular complement-binding proteins, Ecb, efb, PSM, haemolysins, leukocidins, and others), [266], and showed various evasive responses which play a vital role in the survivability of bacteria against the immune system [257, 258, 267-274].

1.5.3. *Staphylococcus aureus* biofilms

S. aureus is an opportunistic biofilm-producing pathogen and reported to be the most common causes of infections associated with biofilms. *S. aureus* have been isolated from approximately 65% of infections associated with implantable medical devices such as prosthetic joints, catheters, and pace makers [2-5]. Upon insertion of implantable medical devices, implanted biomaterials has the potential to come into contact with surface associated matrix-binding proteins produced by *S. aureus* which ease the adhesion to host proteins leading to a biofilm formation [275, 276]. *S. aureus* produces a comprehensive range of virulence factor proteins, and the secretion of these proteins and biofilm formation are regulated by an advanced network of virulence regulators (e.g., agr, sarA, saeR/S) [277]. The production of diverse range of *S. aureus* pathogenic molecular factors and its high potential to develop infections associated with biofilms poses a challenging task for the host immune defense to completely eliminate the bacteria given high tolerance to antimicrobials, which results in persistent chronic infections [109].

Chronic infections associated with biofilms caused by *S. aureus* most often results in significantly increased morbidity and mortality, and increased duration of hospitalisation. This has resulted in a significant increase in expenses associated with *S. aureus* infections and an

estimated annual cost of approximately $450 million in 2010 [9, 10]. Therefore, a better understanding of the complex *S. aureus* biofilm formation at the molecular level is an unmet need to develop new/potential diagnostic and therapeutic approaches for biofilm-related infections and to decrease the substantial health-associated loads triggered by this pathogen.

1.6. *Staphylococcus aureus* biofilm regulation

Biofilm cells show a changed profile of gene expression [278] and metabolism in comparison with their planktonically grown bacterial cells [279, 280] and global changes in gene expression occur throughout the lifespan of Staphylococcal biofilms. These changes are coordinated through several regulatory systems such as quorum sensing, and sigma factors (SigB) [280-283]. Regulatory systems also include a transcriptional regulatory protein rbf which play an important role in biofilm formation [284-286]. Cramton *et al.* (2001) highlight the additional PIA regulatory mechanism whereby anaerobic conditions induced PIA expression. As depicted in the (Figure 1.3), both PIA dependent/independent regulatory networks mediated by the changes in differential gene expression level.

Among all regulators, the accessory gene regulator (agr) quorum-sensing system, the staphylococcal accessory regulator (sarA), and the stress response sigma factor B (sigB) are key players in this process (Figure 1.4).

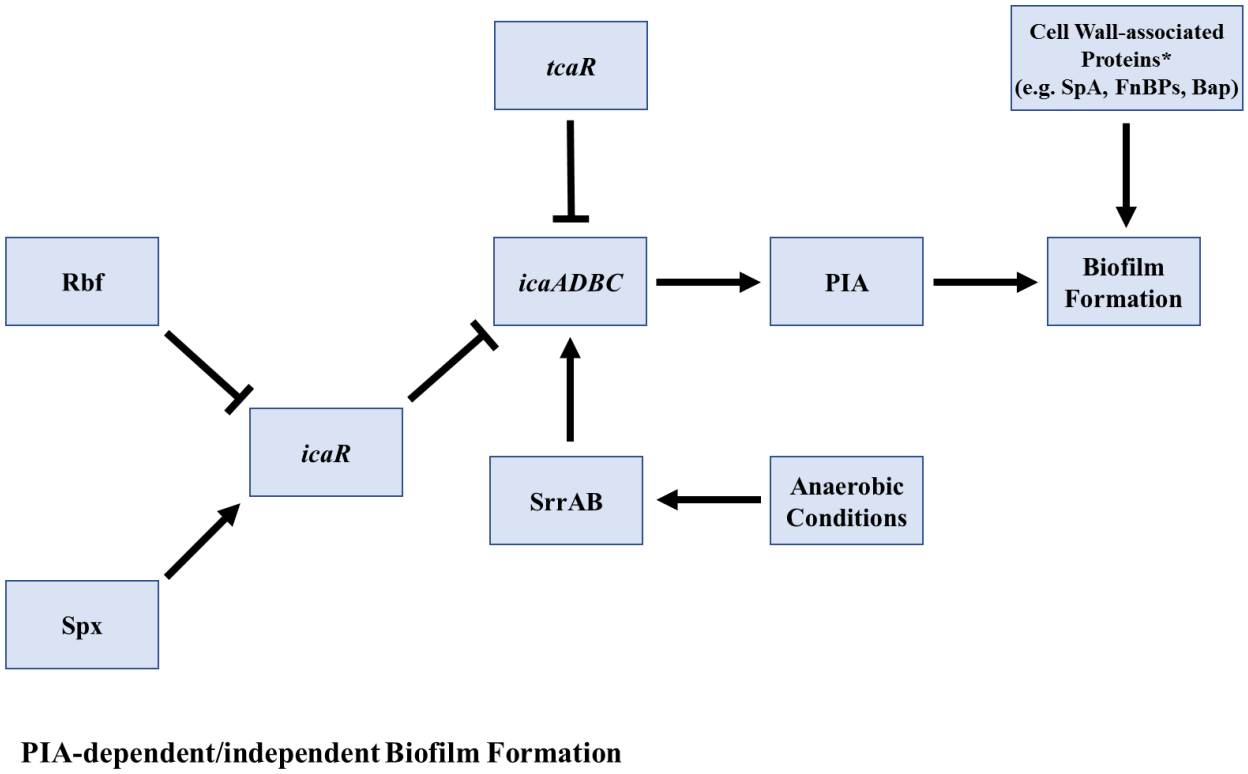

Figure 1.3: Schematic representation of the regulatory network of *S. aureus* biofilm development based on PIA dependent/independent. Biofilm development based on PIA, the icaADBC gene cluster play a central role to initiate the expression of PIA by downregulating the activity of icaR and tcaR. The regulation of icaR gene can be controlled by upregulating the activity of Spx and downregulating the activity of Rbf genes. SrrAB gene plays a vital role in triggering the expression of icaADBC during oxygen deficient conditions. In contrast, PIA independent biofilm development is controlled via the proteins associated with cell-wall and attachment. Modified from [83].

1.6.1. Agr quorum-sensing system

Quorum sensing is a phenomenon through which a cell-to-cell communication occurs that permits bacteria to synthesise and respond to signalling molecules and adjust gene expression accordingly. The agr system involves the quorum-sensing system that existing in *S. aureus* and leading regulators of virulence, biofilm formation and disassembly [282, 287]. The agr system

are responsible for the production of autoinducing peptides (AIPs) that function as a vital signalling molecules. AIPs contains a structure of eight residue peptides, in which the last five residues are linked with a cyclic thiolactone ring [287, 288]. The chemical nature of this AIP signal varies between different species and within species. Once AIP is released from the cell, it can accumulate and binds to the surface-exposed AgrC histidine kinase at a concentration in the low nM range, leading to a two-component response activation [289]. This results in the phosphorylation of the AgrA response regulator, inducing the RNAIII regulatory transcript expression [289]. RNAIII is one of the major regulatory system that is directly involved in the regulation of the production of pathogenic molecular factors and the toxin repressor (Rot) translation [290].

The agr system trigger multiple response which results in the upregulation of secreted enzymes and at the same time adhesives are downregulated, whereas agr-dependent differences in the gene expression have also been reported in *S. aureus* [291]. RNAIII interacts directly with the target protein mRNA to enable or prevent its translation. This applies to numerous transcripts of the virulence factor, including coa, hla, and spa [290]. Phenol-soluble modulins are other important agr-regulated factors associated with biofilm dispersion [292]. These peptides have surfactant properties which act in an anti-biofilm nature. Studies have shown that the process of dispersion is mediated by agr-regulated proteases, most notably Staphopain enzymes [293]. Protease agr regulation is via Rot, the transcriptional repression of which is relieved when agr is induced [294, 295]. A model for this regulatory pathway is shown in Figure 1.4.

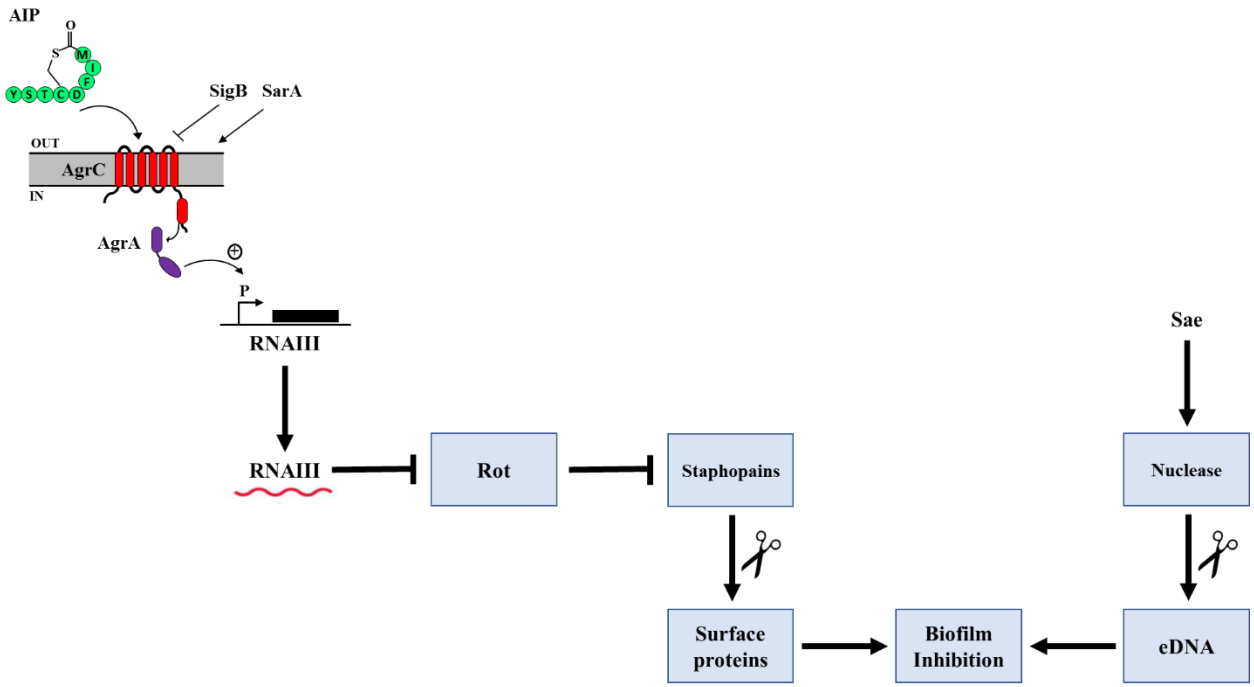

Figure 1.4: Schematic representation of the networks in the formation of biofilm regulation. The agr quorum-sensing system triggers the expression of surface proteins (e.g., proteases) of Staphopain by downregulating the activity of Rot (toxin repressor). On the Staphylococcal surface and in the biofilm matrix, these proteases then degrade proteins. SaeRS induces nuclease enzyme production that breaks eDNA in the biofilm matrix. SigB downregulates agr expression whereas it has been demonstrated that SarA directly enhances agr expression. Adapted from [109].

The function of agr system is also significantly controlled by environmental conditions, such as the suppression of agr activity by low pH, which is generated from short-chain fatty acid excretion [296]. In the host environment, control of agr function is also beginning to be appreciated. It is known that proteins found in human serum suppress *S. aureus* agr activity [297], including apolipoprotein B [298, 299]. Another abundant host protein with known agr inhibitor properties is haemoglobin [300]. Environmental contaminants, such as triclosan, which accumulate in the body, have also been connected to enhanced biofilm development [301].

The function of the agr system has also been examined in chronic infections involving host tissue. In chronic infections, low concentrations of agr expression are usually recognised [302-304], which suggest that agr's damage or reduced activity is an adaptation to enable it to persist within the host condition.

The complexity of the quorum sensing system and the molecular factors that change its expression can, however, lead to a variety of *in vivo* effects of the agr system. Moreover, investigations have begun looking into whether inhibition of agr or increase expression of agr to cause biofilm dispersal are possible treatment(s) for *S. aureus* infections [305-307]. Thus, further work is needed to gain a deeper understanding of the types of *in vivo* environments and infections.

1.6.2. SarA (Staphylococcal accessory regulator)

Multiple studies have reported that SarA is required for *in vitro* and *in vivo* biofilm development in *S. aureus* [308-311]. Omics studies has been conducted to observe the sarA regulation that demonstrate the upregulation of the gene in biofilms and sarA mutants showed reduced activity to develop biofilms [309, 310]. SarA also positively regulates bap, a cell wall adhesin found in bovine *S. aureus* isolates, through direct binding with its promoter [312]. Further studies on the regulation of biofilms demonstrated that the agr quorum sensing system involved in the downregulation of genes associated with cell-wall and attachment factors [313]. SarA, even in the absence of agr, suppresses the transcription of the collagen adhesion cna and directly binds it to the cna promoter region [314, 315].

1.6.3. Sigma B regulation

An alternative RNA polymerase sigma factor is sigma B (SigB), which is activated in response to stress [316]. SigB also regulates biofilm formation [317] by down regulating icaR and repressing icaADBC (Figure 1.4) [318, 319]. Multiple functions has been observed by SigB system such as the upregulation of biofilm formation and cell adherence associated molecular factors (e.g., clumping factor, FnbpA), whereas downregulation of the cell detachment associated factors (e.g., hla, enterotoxin B, leukotoxin D, SplA, SplB, Aur) [316, 320, 321]. A list of major proteins

involved in biofilm dispersal are mentioned in Table 1.2. Studies by Archer *et al.* (2011), demonstrated that the activity of sigB system may be specific to particular strains [83].

Table 1.2: List of major biofilm dispersal proteins adapted from [322].

Dispersal agent	Mechanism	Specific factor
Proteases	Degradation of proteinaceous matrix components	V8 protease (SspA)
		Staphopains (Cysteine Proteases)
		Aureolysin (Aur)
		Aur, SspA
		Proteinase K
		sarA regulation
		sigB, *agr* regulation
agr activation by AIP	Expression of agr regulated factors (proteases and PSMs)	AIP
Phenol-soluble modulins	Surfactant-mediated dispersal	PSMs
S. epidermidis Esp	Degradation of proteinaceous matrix components; inhibition of autolysis through Atl degradation	Esp
Nucleases	Degradation of eDNA	Nuc
		Nuc2
Dispersin B	Degradation of polysaccharide matrix components	DisB
D-amino acids	Protein synthesis inhibition in *B. subtilis*, unknown in *S. aureus*	D-amino acids
Stringent response inhibition	Unknown	Peptide 1018

1.7. Bacterial biofilm proteomics

With the emergence of proteomics technology and protein database advancement has helped comprehend the molecular processes behind the development of biofilms in bacteria. In general, biofilm proteomics denotes to the comparative recognition of the whole set of proteins in the complex biofilm/EPS matrix expressed by the bacteria under different environments [323, 324], followed by interpretation of complicated biological processes at the fundamental physiological level or more complicated regulations owing to enforced starvation and stress response. Improvement in the biofilm proteomics analysis started with gel-based (2D PAGE) mass spectrometry (MS). For example, a study conducted by Resch *et al.* (2006), to identify differentially expressed cytoplasmic and secreted cell-wall associated proteins grown under planktonic and biofilm state from *S. aureus*. They reported that among the upregulated proteins nine proteins were involved in the glycolysis pathway in biofilm growth mode. In addition, they also identified upregulated proteins involved in cell-wall synthesis, cell adhesion, pyruvate metabolism and SarA [278, 325]. In contrast, immunodominant antigen A, staphylococcal secretory antigen A, and proteases were downregulated in the biofilm growth mode (Resch *et al.*, 2005, 2006). Another study by Chew *et al.* (2012) have also performed 2-dimensional gel electrophoresis (2DE) based MS to explore the biofilm proteome under alkaline-induced environments from *Fusobacterium nucleatum* [326]. So far, numerous studies have demonstrated the comparative proteomic profiling of planktonic and biofilm growth mode using bacteria, for example, *S. aureus*, *Desulphovibrio vulgaris*, *Xylella fastidiosa*, *Streptococcus suis*, *Listeria monocytogenes*, *E. coli, S. enterica*, and *Neisseria meningitidis* [324, 327-333]. On the other hand, less studies have been performed on the comparative proteomic analysis of bacterial biofilms cultivated under ordinary circumstances and unfavourable environments. Changing protein expression under stress conditions exhibits either upregulation or downregulation of those proteins that are usually expressed moderately, whereas the expression of several proteins also remains unchanged. However, in recent times, high-resolution quantitative proteomic techniques using isobaric labeling such as iTRAQ (isobaric tag for relative and absolute quantitation)/TMTs is gaining popularity due to several advantages including the possibility of performing multiplexed quantification of up to ten samples simultaneously [334-336], saves instrument time,

make simpler to experimental design [337], with the ability to identify several thousand non-redundant proteins at once [335, 338, 339].

1.7.1. *Staphylococcus aureus* proteomics

Given the significant research on fundamental physiology, pathogenesis and potential new targets for antimicrobial treatment against *S. aureus*, along with the advent of modern proteomic technologies, there is now a greater ability to have a better and comprehensive understanding of basal cell physiology or more multifaceted regulations of diverse environmental conditions, and behavior of the pathogen in the host. As mentioned earlier, proteomic's achievement as a study area is strongly associated with the implementation of 2DE. For example, a review by Otto *et al.* (2014) demonstrated the multiple physiological investigations that have been conducted using 2D gel-based of starvation experiments such as reducing the availability of nutrient sources (e.g. limited use of glucose), the influence of a oxygen deficient environment on staphylococcal physiology, and the effect of stress response (oxidative) on *S. aureus* [340]. Besides planktonic development, as mentioned in chapter 1.2.1, bacteria can develop as biofilms. Furthermore, attempts to comprehend the biochemical foundation of biofilm formation and resilience have continuously demonstrated variations in protein expression in *S. aureus* [325, 327, 341-343] compared with planktonic counterparts.

A study by Islam *et al.* (2014), looking at the proteome changes under fluid shear stress in *S. aureus* biofilm, showed approximately 30% and 20% of the identified proteins were associated with carbohydrate and protein metabolism, respectively. Among the significantly downregulated proteins, nine proteins were downregulated under shear stress (1000 s^{-1}) and were associated with glycolysis/Krebs (TCA) cycle, while glyceraldehydes-3-phosphate dehydrogenase displayed downregulation with elevated shear stress [341].

A separate study by Foulston *et al.* (2014), reported interesting observations that the *S. aureus* biofilm matrix consist mostly of cytoplasmic proteins that reversibly interact pH dependently with the cell surface. They suggested that, instead of utilising a devoted matrix protein, *S. aureus* seems to recycle multifunctional cytoplasmic proteins that act as parts of the extracellular matrix [344].

Studies by Lei *et al.* (2017), applied the proteomic based analysis to gain more deeper insights into biofilm matrix proteins using a rat model of orthopedic implant-associated *S. aureus* acute and chronic infection. During chronic infection, they identified leukocidins (LukAB and HlgAB) in the biofilm matrix. This suggests that identified toxins could play a part in the host immune system at a later phase of orthopedic implant-associated infection. During acute infection, in contrast, surface associated proteins such as Ebh and SasF were identified in the infected bone tissue. In addition to these proteins, they also identified stress response associated proteins and emphasised the importance of these proteins for virulence regulation, and adaptation during chronic infection of orthopaedic implant-associated *S. aureus* biofilm infection [345].

Such studies emphasise the significance of biofilms in diverse environmental conditions as well as in bacterial infections. In addition, continuous improvement in the field of proteomics and associated database enrichment has been shown to be a strong instrument for giving molecular insight into biofilms and later diseases.

1.8. Transcriptomics of bacterial biofilms

A transcriptome refers to the whole genome gene expression by RNA transcripts [346]. Comparative transcriptomics and proteomics analysis using both approaches remain the most comprehensive study of the differential expression of genes and gene products between two cell populations such as during planktonic state and biofilm development [346]. Early studies by Resch *et al.* (2005), highlighted that genes associated with formate fermentation, urease activity, and stress response are upregulated in biofilm growth mode which could lead to growth, survival, and persistence in a biofilm state [278]. Furthermore, there have been several studies analysing the transcriptomic profile of *S. aureus* biofilms to test the effect of sublethal concentrations of disinfectants [347], the effect of low concentration drug [348], and the role of CymR gene in biofilm formation [349].

However, transcriptomics are now extensively used to validate proteomic results due to relatively easy analysis, rapid turn-around and its cost-effectiveness [350]. Although the association between transcriptomics and proteomics may be small owing to distinct variables such as multiple half-lives and post-transcription processes. A combined analysis can therefore supply

new understandings that can not be transcribed from individual mRNA or protein expressions analysis.

1.9. Human proteomics

With the advancement of modern proteomics technology that has allowed the detailed characterisation of multifaceted organelles and biological fluids, plasma samples hold the promise to discover clinically effective human disease biomarkers [351]. Plasma proteomics is an attractive concept in medicine as its inexpensive, the ease of sampling and excellent reproducibility [352]. Plasma contains actual plasma proteins that maintain physiological homeostasis. In addition, it also contains lower-abundance "leakage" proteins from damaged tissues, which may provide direct information about the pathology of disease and may serve as clinical biomarkers for diagnosis and therapeutic intervention [353]. However, due to the variable composition and wide dynamic range of protein concentrations (greater than 10 orders of magnitude) there pose tremendous challenges in the identification of clinically relevant biomarkers especially amongst the background of higher-abundant proteins such as albumin, IgG, and transferrin [354]. Therefore, the identification of novel or specific for a particular disease biomarker has been hampered by higher-abundant proteins, even with current high-resolution proteomic approaches, as higher-abundant proteins mask signals from lower-abundance proteins. The depletion of higher-abundant proteins from human plasma/serum has been revealed to enhance the identification of relatively lower-abundant proteins which is clinically important [354-356].

With the emergence of proteomic technologies used for biomarker screening such as TMT, it is now possible to achieve multiplexing and quantifying of up to ten samples at the same time [334-336], which saves instrument time and reduce in complexity to design experiments [337], with the ability to identify proteins between samples even in the lower mass region [357, 358]. Various studies have demonstrated the differential expression of many proteins and identified novel/potential candidate plasma biomarkers for infectious diseases [355, 359-363]. For example, studies by Rehman *et al.* (2012) identified the potentially useful serum biomarkers, eukaryotic translation elongation factor 1 alpha 1, which is linked with human prostate cancer's metastatic progression. Moreover, a review by Ray *et al.* (2014), reported differential expressions of

plasma/serum proteins in different infectious diseases such as Malaria, Dengue, AIDS, Hepatitis A and B, and Tuberculosis [355]. Furthermore, several studies have reported the increased expression of plasma/serum proteins in various diseases such as tropomyosin alpha 4 chain in liver cirrhosis [364], talin-1 in inflammatory diseases [365-367], and lipopolysaccharide-binding protein in sepsis, septic shock, and in acute and chronic infections [368-372].

1.10. MS-based proteomics and bioinformatics

1.10.1. MS-based proteomics workflow

The term "proteome" can be described as the overall protein composition of a cell which is characterised with respect to their (i) subcellular compartment, (ii) interactions, (iii) post-translational modifications (PTMs) and (iv) turnover, at a specific time. Meanwhile, "proteomics" deals with the proteome such as, (i) differential expression changes, (ii) structural variations, (iii) cell type(s) and subcellular localisation(s), (iv) interactions and (v) PTMs of proteins, at any time [373]. However, determining such variations/changes with precision for any comprehensive proteome, is a challenge. The advancement of mass spectrometry (MS) technologies has become a powerful tool to overcome these issues, providing a deeper understanding into the variations of the proteome of complex mixtures (such as identification, quantitation, subcellular localisation(s) and biological significance, etc.), all of which influence biology [374].

Recent strategies of MS-based proteome analysis can be broadly classified into discovery and targeted proteomics. Discovery proteomics is the identification of protein components present in any given sample. In this analysis, automatic selection of peptide ion fragmentation is mostly based on signal intensities. In contrast, targeted proteomics aims to identify the proteins of interest against a control sample (also called relative protein profiling), or on an absolute scale, using a pre-set peptide ion fragmentation model [374, 375].

Proteome analysis is further classified into two different approaches, namely "top-down" and "bottom-up" strategies. Top-down proteomics deals with the analysis of intact proteins by liquid chromatography (LC)MS without proteolytic digestion steps, which is advantageous in terms of higher precision and greater sequence coverage [374, 376]. However, due to technical issues such

as difficulty of proteome-wide study at the intact protein level, this approach is often challenging and hence less frequently used. In contrast, bottom-up approaches (also termed "shotgun proteomics"), which is the most widely used in proteomics research, involves proteolysis, labelling (for labelling-based approaches), chromatographic fractionation and/or LCMS analysis for the identification of proteins. In this thesis, we applied bottom-up strategies, with the processing of samples, MS instrumentation, peptide fragmentation, protein identification and relative quantification methods detailed in the subsequent sections.

1.10.2. Processing of samples

The first step in proteomics analysis begins with the preparation of samples, which is a very important step as it can impact the overall MS performance and detection accuracy [377]. Specimens such as microbial, human or other biological samples are usually highly complex and require further processing to reduce their complexity prior to starting MS analysis. Therefore, multi-level processing steps are required starting with lysis, extraction, fractionation (e.g., extracellular, cell wall, membrane, etc.) of proteins followed by proteolytic digestion after the reduction and alkylation steps [377]. Among the enzymatic digestion methods, trypsin-based digestion is the most frequently used approach for the digestion of proteins due to its ability to cleave the C-terminal next to arginine (R) and lysine (K) [378]. In more recent times, multi-enzyme digestion approaches using Lys-c and trypsin combined, have gained popularity due to its greater proteome coverage in comparison to single enzyme digestion [379, 380].

After the proteolysis step(s), protein/peptides can be labeled with chemical tags. Label-based MS analysis including, iTRAQ and TMT have seen an increase in popularity. The advantages of TMT label-based techniques is that they allow multiplex assays and the quantification of up to ten samples at the one time (**Figure 1.5**) [334-336]. This saves instrument time, reduces the complexity associated with designing experiments [337] and it is possible to identify proteins between samples in even the lower mass region [357, 358].

Chromatographic fractionation occurs following labelling. Various chromatographic separation techniques such as high pH fractionation, isoelectric focusing, strong anion and cation exchange, etc. can be utilised to facilitate in reducing sample complexity [381], and as a result increases the proteome coverage. However, the presence of unwanted impurities such as detergents, salts and

polymers can affect the overall efficiency of fragmentation and peak intensity during LCMS analysis [382]. Therefore, sample clean-up steps are performed to help in removing residual salts and detergents prior to loading the sample in the LCMS, hence greatly improving ionisation efficiency during LCMS.

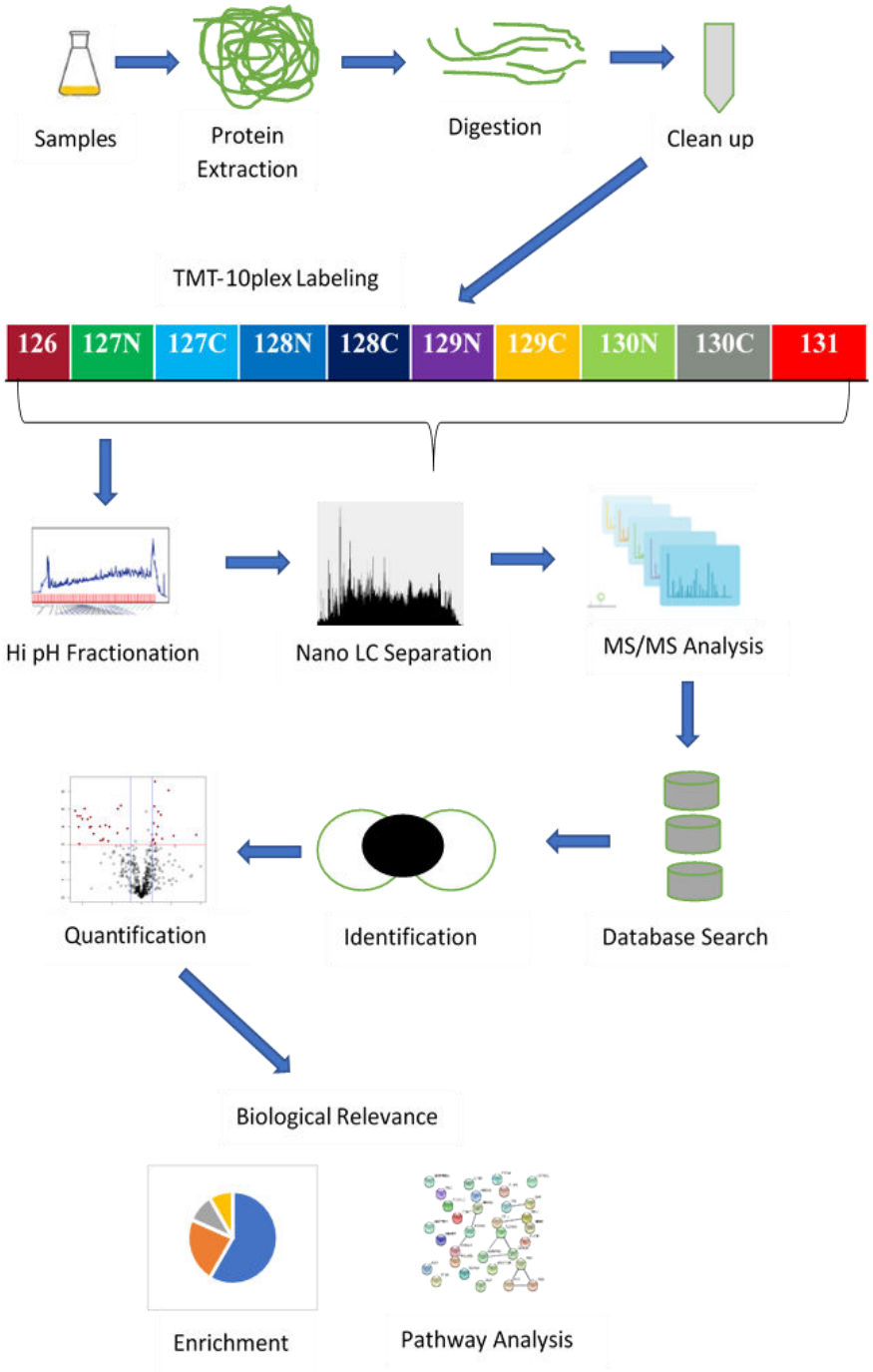

Figure (1.5): An overview of TMT-labeling based MS analysis.

1.10.3. MS instrumentation and peptide fragmentation

MS-based proteomics is one of the most popular methods for identifying and quantifying an organism's proteome. All MS instruments measure the mass-to-charge (m/z) of ionised molecules and are designed to distinctly perform ionisation and mass analysis [383]. The more widely utilised "bottom-up" approach begins with complex protein mixtures being exposed to enzymatic cleavage and results in peptide products that are fragmented based on their chemical or physical properties, which are then analysed by MS [383]. Peptide identity is determined from the mass and the fragmentation pattern, while the precursor ion intensity can be used to quantify peptide abundances.

Spectrum-specific information is acquired during a MS in two modes. In the MS mode, mass and intensity profiles are acquired from co-eluting peptides. In tandem MS (MS/MS) mode, fragmentation of the peptides along their peptide bonds results in a fragmentation spectral pattern [384]. The speed and sensitivity of MS instruments make it possible for the fragmentation and quantitation of intensity within only a portion of a second for up to thousands of ion species [384]. The most common fragmentation methods include (i) collision-induced dissociation (CID), (ii) electron capture dissociation (ECD), (iii) electron transfer dissociation (ETD) and (iv) high-energy collisional dissociation (HCD).

In MS/MS, precursor ions that have peaks showing the highest abundance are fragmented and scanned once again. In CID, collision with a neutral gas causes the precursor ions to be fragmented leading to the cleavage of the amide bond along the peptide backbone, forming b- and y- ions. This fragmentation technique results in obscure spectra during neutral loss, and in order to identify such patterns additional fragmentation modes on a MS workflow are required [385].

ECD and ETD fragmentation techniques cause an electron to be transferred from a radical anion to a protonated peptide [386], thereby increasing the internal energy and hence neutralising the positive charge [387, 388]. As a result, c- and z-ions are produced and leaves the side-chains along with a peptide bond intact. Thus, the fragmentation pattern that is observed should match with its theoretical pattern, as long as the search database contains its peptide sequence.

In contrast to CID, HCD fragmentation takes place in a collision cell and it is here ions are transported to a c-trap to allow for high-resolution analysis in an Orbitrap instrument [389]. Although HCD spectra analysis generates high-quality spectra in the Orbitrap, there is however an increase in spectral acquisition times resulting from the requirements of Fourier transform-based detection. This is in contrast to electron-multiplier-based detection in CID. Nevertheless, the development of efficient HCD collision cells with enhanced performance has enabled HCD fragmentation to be widely implemented [390].

In a typical MS instrument, the key components are the ion source, mass analyser and ion detector. The ion source is responsible for adding charge (proton) to the peptides. The most common ionisation methods include (i) electron impact, (ii) chemical ionisation, (iii) field desorption, (iv) laser desorption and (v) electrospray ionisation (ESI). The mass analyser is important for the sensitivity, resolution and the mass accuracy of a MS. It has the ability to identify low abundant peptides, differentiate between ions with similar m/z values and achieve mass measurements close to reality. Some basic mass analysers include (i) quadrupole (Q), (ii) ion-trap (IT), (iii) time-of-flight (TOF), (iv) Fourier transform ion cyclotron resonance (FTICR) and (v) Orbitrap.

Current MS instruments, including nano LC system [391] or ion mobility component [392], can be combined with an extra online separation component to allow for continuous separation, which enhances the efficiency of separating peptides. In shotgun proteomics, linear ion trap (LIT)-Orbitrap and Quadrupole-TOF configurations are mainly used for the selection, fragmentation and detection of ion species [384]. In Quadrupole-TOF configurations, entire ion species can be transmitted in MS mode via the Quadrupole mass filter and, alternatively, selected ion species can be transmitted around a precursor mass range in MS/MS mode. The fragmented ions generated in a collision cell are then analysed by TOF. Separation is achieved when peptides pass through the first Quadrupole or TOF, where only the selected mass-range ion species can maintain a stable trajectory to reach the detector. This process is commonly referred to as peptide separation “in space”. This is in contrast to the fragmentation of peptides in ion trap instruments, which occurs through an electrostatic field. Only selected peptide fragments that are within a

specific mass-range can remain stable within a trap and this is known as peptide separation "in time" [393]. In an Orbitrap mass analyser, the frequency of oscillation of ion species going round a centred spindle-shaped electrode using FTICR can produce a mass spectrum [394, 395]. The axial oscillation frequency of the ion species is directly proportionate to the square root of m/z. Thus, the more precise the oscillation frequency, the more accurate the m/z measurement in an Orbitrap [396].

MS instruments such as LTQ-Orbitrap can also have a combination of both low-resolution LIT and high-resolution Orbitrap, which have become widely implemented in proteomic studies. In MS mode, the peptide population is collected and transferred to an intermediate c-trap by the LIT, which injects ions into Orbitrap for high-resolution analysis. In the MS/MS mode, at low-resolution LIT carries out precursor ion isolation, fragmentation and mass scan. Thus, LTQ-Orbitrap enables a combination of both high-resolution MS and low-resolution MS/MS scan in tandem [397, 398], as demonstrated in instruments such as the Thermo Orbitrap Velos and Thermo Q Exactive.

1.10.4. MS data processing for protein identification

In bottom-up proteomics, the identification of proteins is often achieved by firstly comparing the MS features that are observed to those of the predicted or those features identified previously in a database. For example, by MS/MS or based on previous analysis of a well-characterised sample. Given MS analysis deals with thousands of MS/MS spectra, computational algorithms are needed to solve a "many-to-many" relationship between peptide and proteins. Especially in instances where the same peptide sequence from different proteins (i.e. degenerate peptides) are produced upon proteolytic digestion [399].

There are numerous database search algorithms available for peptide-spectrum match (PSM) assignment, which use either probabilistic or heuristic approaches including (i) Mascot, (ii) SEQUEST, (iii) X!Tandem and (iv) Andromeda [400-404]. However, the presence of degenerate peptides and what has been termed "one-hit-wonder" peptides, protein inference combined with PSM alone remains questionable [405]. Thus, it is essential for PSM assignment to be validated during protein inference procedures [406].

For FDR estimation, target-decoy approaches (TDA) are often used to infer that the probability of a random match occurring is similar between the target and corresponding decoy databases, whether it be reversed, shuffled or random. FDR estimation of the peptides is therefore a measure of the number of targets matching the decoy and target databases. The number of target and decoy matches above a certain threshold can then be used to control the levels of FDR at the peptide and protein level [400].

The heterogenic nature of proteomics data presents a challenge when assigning a FDR to the fragment ion spectra produced from MS analysis [407]. Moreover, as the number of peptide spectra or the database size increases the more complex the FDR assignment becomes, and thus when combining multiple datasets the multiplicative tendencies of FDR need to be taken into account [407]. A disadvantage in the use of TDA for FDR estimation is that it focuses only on the peptide level and quality control is not guaranteed at the protein level. Instead, MAYU allows for the quantification of FDR on protein levels based on the PSM assembly at a certain FDR threshold [407]. Therefore, unlike the TDA approach, which applies a single FDR threshold to a dataset, p-value based confidence level analysis in MAYU reports the p-value for individual PSM. MAYU aligns the score distribution with a parametric model to determine the p-value and also uses the properties of the spectra to increase confidence scoring efficiency [406].

1.10.5. Protein quantification

Protein quantitation is focused on quantifying and comparing the abundance of proteins that are present in diverse conditions. Two approaches are utilised: (i) label and label-free methods and (ii) relative and absolute quantification [378]. Labelling quantification involves incorporating a stable isotope into a peptide or protein via chemical or metabolic processes [408]. Multiple samples can be combined in a single MS run since MS instruments are able to differentiate the isotopic variant induced by labelling.

Metabolic labelling is also possible whereby a heavy isotope is added during the growth phase of a cell or organism to allow only selective labelling on newly synthesised proteins [409]. Because chemical labelling can incorporate isotopomeric tags onto peptides or proteins, multiplexed protein quantitation of different samples is possible in a single MS run [410]. The most

commonly utilised chemical labelling with multiple isotope variants includes iTRAQ, TMT, dimethyl labelling and SILAC [411-414].

In TMT-based protein quantitation, the relative abundance of peptides is calculated as the ratios of the reporter ion intensities, and subsequent incorporation of the relative quantification at the peptide level would give the relative expression of the proteins. In this thesis, we implemented TMT-based proteomics approach which has been described briefly in the next section.

1.10.6. Tandem mass tag (TMT) liquid chromatography MS/MS

In MS analysis, to quantify proteins with stable isotopes is based on the change in mass between labeled and unlabeled ions. Thompson *et al.* in 2003, were the first to apply isobaric labels enabling the simultaneous identification and quantification of peptide pairs [412]. In their study, peptide pairs containing TMTs were synthesised and they demonstrated that this technique can be used for relative quantification during the analysis of tandem mass spectrometry (MS/MS). The structure of TMT reagents, in general, involves a primary amine reactive group and a mass reporter region separated by a fragmentation-vulnerable linker from the mass normalisation moiety. Labeled peptides release the group of mass reporters during MS2 fragmentation and the ratio of these reporters is used for the relative quantification of peptides. The multiplexing capacity of TMT reagents was later improved by means of differential stable isotope incorporation (^{15}N, ^{13}C) across the reporter and mass balancing regions of the tag, resulting in 6-plex and 10-plex sets for relative quantitative profiling of multiple conditions, such as time courses, dose responses or parallel sample comparisons [415]. Quantification of TMT-labelled peptides needs fragmentation (to obtain structural or sequence information) utilising higher-energy collision dissociation (HCD) [408, 416-418], electron transfer dissociation (ETD) [419], and collision-induced dissociation (CID) [420]. HCD is more effective than collision-induced dissociation and advantageous for quantifying isobaric tag (TMT and iTRAQ) labeled peptides in the lower mass zone [357, 358]. Relative quantification of peptides using TMT reagents is supported by multiple software packages, including Proteome Discoverer 2.1, Mascot 2.5, Biowork 3.3, MaxQuant 1.6, and Scaffold Q+S.

The excellent benefit of TMT-labeling based LC-MS/MS is the chance of multiplexing and quantification of up to ten samples simultaneously [335, 336], saves instrument time and make

simpler in the design of experiments [337]. In the future, the multiplexing capability of the TMT reagents can theoretically be expanded to 18-plex by substituting ^{15}N with ^{13}C in the reporter region [421].

After LC-MS/MS run, mass spectra containing raw data file converted to required file format for further processing, quality control cheking, and data analysis. Specifically designed software program (e.g., Proteome Discoverer) is utilised to identify mass and developing comparisons between samples based on multiple criteria such as abundance, peak shape, and others [422, 423]. The false discovery rate (FDR) can then be minimized by performing further analysis including mass chromatogram extraction, noise filtering and normalization [424]. Furthermore, in order to enhance the robustness of the experimented data normalisation calculation also been included in the analysis. Multiple statistical analysis has been performed to test the significance of the data. After data processing, diverse and continuously improved databases (Table 1.3) such as: GenBank, UniProt, SwissProt, KEGG etc. assist in the annotation, identification of proteins, and various level of bioinformatics analysis.

Table 1.3: List of commonly used database searching tools, subcellular localisation, pathway analysis, and PPI analysis tools, and others.

Name	Type	Web links
GenBank	Database	http://www.ncbi.nih.gov/entrez/query.fcgi?db=protein
RefSeq	Database	https://www.ncbi.nlm.nih.gov/refseq/
nr	Database	http://www.ncbi.nlm.nih.gov/BLAST/
UniProt	Database	http://www.pir.uniprot.org/
UniRef	Database	http://www.pir.uniprot.org/database/nref.shtml
UniParc	Database	http://www.pir.uniprot.org/database/archive.shtml
TrEMBL	Database	http://kr.expasy.org/sprot/
SwissProt	Database	http://kr.expasy.org/sprot/
PIR	Database	http://pir.georgetown.edu/
OWL	Database	http://www.bioinf.man.ac.uk/dbbrowser/OWL/
BLASTP	BLAST	http://blast.ncbi.nlm.nih.gov
TBLASTN	BLAST	https://blast.ncbi.nlm.nih.gov
PSI-BLAST	Position Specific Iterated BLAST	https://blast.ncbi.nlm.nih.gov
PHI-BLAST	Pattern Hit Initiated BLAST	https://blast.ncbi.nlm.nih.gov
DELTA-BLAST	Domain Enhanced Lookup Time Accelerated BLAST	https://blast.ncbi.nlm.nih.gov
InterProScan	Protein domain servers	http://www.ebi.ac.uk/lnterProScan/
CD server	Protein domain servers	http://www.ncbi.nlm.nih.gov/Structure/cdd/cdd.shtml
ProWleScan	Protein domain servers	http://hits.isb-sib.ch/cgi-bin/PFSCAN

ScanProsite	Protein domain servers	http://us.expasy.org/tools/scanprosite/
PATTINPROT	Protein motif search tools	http://pbil.ibcp.fr/html/pbiljndex.html
SIRW	Protein motif search tools	http://sirw.embl.de/index.html
Match Box	Motif based alignment server	http://www.sciences.fundp.ac.be/biologie/bms/help.html
MEME	Motif based alignment server	http://meme.sdsc.edu/meme/website/meme.html
Gibbs	Motif based alignment server	http://bayesweb.wadsworth.org/gibbs/gibbs.html
Dialign	Motif based alignment server	http://bibiserv.techfak.uni-bielefeld.de/dialign/
BlockMakei	Motif based alignment server	http://blocks.fhcrc.org/make_blocks.html
PDB	Protein structure databases	http://www.rcsb.org/pdb/
SwissModel	Protein structure databases	http://swissmodel.expasy.org/repository/
SCOP	Protein structure databases	http://scop.mrc-lmb.cam.ac.uk/scop/
ModBase	Protein structure databases	http://alto.compbio.ucsf.edu/modbase-cgi/index.cgi
CATH	Protein structure databases	http://www.biochem.ucl.ac.uk/bsm/cath/
MMDD	Protein structure databases	http://www.ncbi.nlm.nih.gov/Structure/
ConSurf	Protein structure analysis server	http://consurf.tau.ac.il/
CASTp	Protein structure analysis server	http://sts.bioe.uic.edu/castp/index.php
ProtSkin	Protein structure analysis server	http://www.mcgnmr.ca/ProtSkin/intro/
LigandProtein	Protein structure analysis server	http://bip.weizmann.ac.il/oca-bin/lpccsu
PredictProtein	Protein structure prediction sever	http://www.embl-heidelberg.de/predictprotein
O-GlycoBase	Protein structure prediction sever	http://www.cbs.dtu.dk/services/NetOGIyc/
PhosphoBase	Protein structure prediction sever	http://www.cbs.dtu.dk/services/NetPhos
SwissModel	Protein structure modeling server	http://www.expasy.org/swissmod

Whatlf	Protein structure modeling server	http://www.cmbi.kun.nl/gv/servers/WIWWWI
ESyPred3D	Protein structure modeling server	http://www.fundp.ac.be/urbm/bioinfo/esypred
EBI	Protein structure modeling server	http://biotech.ebi.ac.uk:8400/

1.10.7. Gene Ontology (GO) and enrichment analysis

In shotgun proteomics or more targeted approaches, the output from a proteome analysis usually involves a long list of the identified factors, along with their associated probability score and quantitative value. This list needs to be classified and filtered to interpret their meaning and generate a hypothesis that can be tested based on the proteome's systemic response to a specific scientific question [425]. In the functional analysis of a long list of proteins, the first step is to link the name of the protein to a unique identifier. Despite the numerous databases available, a challenge for bioinformaticians is that the names of proteins can differ significantly between various databases, which can lead to important information being lost. Web-based algorithms that are available to link the name of proteins to their corresponding gene names include PICR or CRONOS [426, 427]. Alternatively, Uniport knowledge base, Ensembl or the International Protein Index (IPI) functional databases can use protein identifiers as input [425].

The first stage in interpreting the functionality of a list of proteins is to relate the identified protein the Gene Ontology (GO) term it is associated with (http://www.geneontology.org) [428]. This allows for the characterisation of a gene based on their (i) biological process, (ii) molecular function or (iii) cellular component. To perform a GO term functional annotation for single proteins, one would use the Amigo tool available on the GO website and look for the corresponding terms. For larger data, proteomic database search algorithms including (i) MaxQuant, (ii) Proteome Discoverer and (iii) X!tandem [403, 429] have included a GO term annotation step. However, because the list of GO terms is incomplete and often changes with new discoveries means not all protein entries are going to be completely annotated with the corresponding GO terms. In these instances, the BLAST2GO tool can be used to obtain the closest related protein (GO terms) through a BLAST similarity search [430].

The next step is the GO term enrichment analysis, which compares the specific GO terms' abundance in the dataset with the abundance of those in the reference dataset such as cell lines, growth rates, etc. [431]. To determine which specific GO term(s) are significantly overrepresented or are enriched in a sample over another sample, the p-value needs to be calculated. This calculation can be done using software tools such as (i) http://neurolex.org/wiki/Category:Resource:Gene_Ontology_Tools, (ii) DAVID and (iii)

Babelomics [425]. These software tools can be classed into different enrichment algorithms. The simplest algorithm being singular enrichment analysis (SEA), including GOStat, BinGO or EasyGO, where one annotation term is tested at a time from a list of the genes of interests [432]. More complex algorithms include gene set enrichment algorithms (GSEA), which takes every gene in the analysis into consideration and not just the ones with significant changes in abundance. Modular enrichment analysis (MEA) provides associations between annotation terms, which avoids the loss of biologically relevant correlations that often result when relationships are lacking and hence reduces redundancies [432]. An advantage of these aforementioned programs is that they are not just restricted to GO enrichment term but can also be used to (i) look up the network of proteins networks, (ii) change protein identifiers or (iii) even link any information and/or publications that corroborate the gene function observed.

1.10.8. Subcellular localisation

The identification of a bacterial proteins subcellular localisation can be of considerable aid to microbiological research. It can be used to infer potential protein function, determine its prospective interaction partners and identify elements that are exposed to the cell surface. The cell wall plays an important role for pathogenic bacteria during host invasion, colonisation and evasion of the immune system and thus serves as a potential diagnostic and therapeutic target. To identify subcellular localisation, a number of bioinformatics tools are available such as PSortB [433], SignalP [434], SecretomeP [435], TargetP [436], and CELLO [437]. PSortB is a widely used high precision multi-component subcellular localisation prediction method and can predict four Gram-positive localisations (cytoplasmic, cytoplasmic membrane, cell wall and extracellular) and five Gram-negative localisations (cytoplasmic, inner membrane, periplasmic, outer membrane and extracellular) (Peabody et al., 2015). Multiple studies have been reported to predict subcellular localisation of *S. aureus* biofilm proteins using PSortB [438-440].

1.10.9. Pathway analysis

In omics research, pathway analysis (PA) is a set of widely used tools which are also identified as functional diversity evaluation. PA tools are broadly intended to give significance to biological data of high-resolution and have a wide variety of applications in recent medical research. In terms of PA in proteomics, the incorporation of previous information on how protein groups

work together or with other proteins/genes has enabled the complexity intrinsic in cellular function assessment to be unraveled [441]. The protein pathways are a sequence of responses within the cell that have a specific biological impact. Biological pathways may be considered as signalling, metabolic, and gene regulatory pathways. PA can help to organise a large list of proteins on a small list of pathway information maps so that molecular mechanisms implicit in these changed proteins, or their differential expressions can be easily interpreted [442]. The proteins directly engaged in the response are coupled in pathway databases with those that regulates the processes. Thus, several databases and resources are existing for the protein pathways such as the KEGG [443], the Human Pathway Database (HPD) [444], BioCarta [445], Ingenuity Pathway Analysis (commercial), Reactome [446] etc., are some of the commonly used pathway databases with extensive information in relation to metabolism, signalling and interactions.

1.10.10. Protein-protein interaction network analysis

In most cases, proteins do not act independently and build temporary or steady complexes with closely related functional/other proteins. The protein may have complexes of varying constitution and it is crucial to explore the protein-protein network complexes together with the circumstances which lead to their development or dissociation in order to fully understand the biological system. It has been reported that more than 80% of proteins operate in complexes [447] and complex networks of proteins derived from complicated diseases, for example, numerous cancers including type II diabetes and Alzheimer's disease etc. A complicated disease is most often one disease but may have various symptoms, and as a result the multiple symptom phenotypes and thousands of proteins react to factors that drive disease and sensitivity/resistance to drugs. Therefore, in order to uncover secret molecular mechanisms for early diagnosis and therapeutic intervention, it is necessary to address wide-scale protein networks for particular disease with hierarchical functional interactions under distinct circumstances. Databases such as STRING [448], BioGRID [449], IntAct [450], MINT [451], and HPRD [452] include data on protein interactions in complexes. However, STRING is not just a broadly used database for information on protein-protein interaction, but also links to other mining tools from literature, as mentioned in Table 1.3 [425, 453].

1.11. Aims and scope of the PhD project

Project hypotheses

In vitro

- The protein composition of planktonic (free floating) bacteria, hydrated biofilm and biofilms grown under limited water availability will be different.
- The protein composition of hydrated biofilm will change as the biofilm ages
- The protein composition of hydrated biofilm will be different from that of biofilm subjected to periodic dehydration and nutrition (dry surface biofilm – DSB)
- The tolerance of *S. aureus* to disinfectants will be reflected by changes in the protein composition of the various growth phases.

In vivo

- Patients suffering capsular contracture around breast implants due to biofilm infection will secrete proteins associated with biofilm infection along a concentration gradient, eventually ending up in the plasma.
- Biofilm infection will produce changes in the plasma proteome.

Project objectives

In vitro

- Construct a comprehensive reference map of planktonic and biofilm-associated proteins.
- Identification of potential marker proteins associated with biofilm formation.
- Identification of biofilm-associated virulence factor proteins.
- Metabolic pathway analysis and design of novel regulatory pathways.
- Subcellular localisation and protein-protein interaction network mapping.
- Validation of potential genes by qRT-PCR.

In vivo

- Construct a comprehensive reference map of healthy patients and patients suffering capsular contracture around breast implants due to biofilm infection.
- Identification of potential bacterial and/or host marker proteins in the plasma of patients with biofilm-related capsular contracture.
- Metabolic pathway analysis of significant differentially expressed host proteins.
- Subcellular localisation and protein-protein interaction network mapping of host proteins.

Chapter 2: Materials and Methods

2.1. Microorganism and culture conditions

2.1.1. *S. aureus* planktonic growth conditions

S. aureus reference strain (ATCC 25923) was grown on solid horse blood agar (HBA; Micro Media Laboratories, Australia) overnight at 37°C. A single colony *S. aureus* was inoculated onto 250ml glass bottle containing 50ml of sterile 100% tryptone soya broth (TSB; Oxoid, Threbarton, Australia) and incubated for 24 hours with constant agitation at 130 rotations per minute (rpm) in an Innova 42™ shaker incubator (John Morris Scientific, Australia) at 37°C.

2.1.2. Bacterial colony forming units (CFU) counting

The number of bacteria in a solution was determined by serial ten-fold dilution and plate culture of 100µl of each dilution. The number of CFU on the plate with between 30 and 300 colonies was counted and the bacterial concentration/ml calculated.

For initiation of biofilm growth, 1ml of overnight bacterial culture diluted with sterile 100% TSB to an absorbance of 0.3 at 600nm wavelength (V-1200 Spectrophotometer, VWR™, Belgium) was added to the biofilm generator. This was equivalent to approximately 10^8 CFU/ml.

2.1.3. Biofilm growth conditions

Biofilm was generated in the Centres for Disease Control (CDC) biofilm reactor (BioSurface Technologies Corp, Bozeman, USA) on 24 polycarbonate coupons (BioSurface Technologies Corporation, Bozeman, USA) which were 1.27cm diameter and 0.3cm thick (Figure 2.1). To ensure the sterility, the CDC bioreactor with coupons was autoclaved prior to each use. During all liquid phases (batch phases) of biofilm development, mixing and shear were provided by baffle rotation at 130rpm, generated by a magnetic stir plate. Temperature was monitored by the same magnetic stir plate coupled with temperature sensor. In addition, filter-sterilised air-conditioned air was pumped at 3L/minute into the biofilm generator.

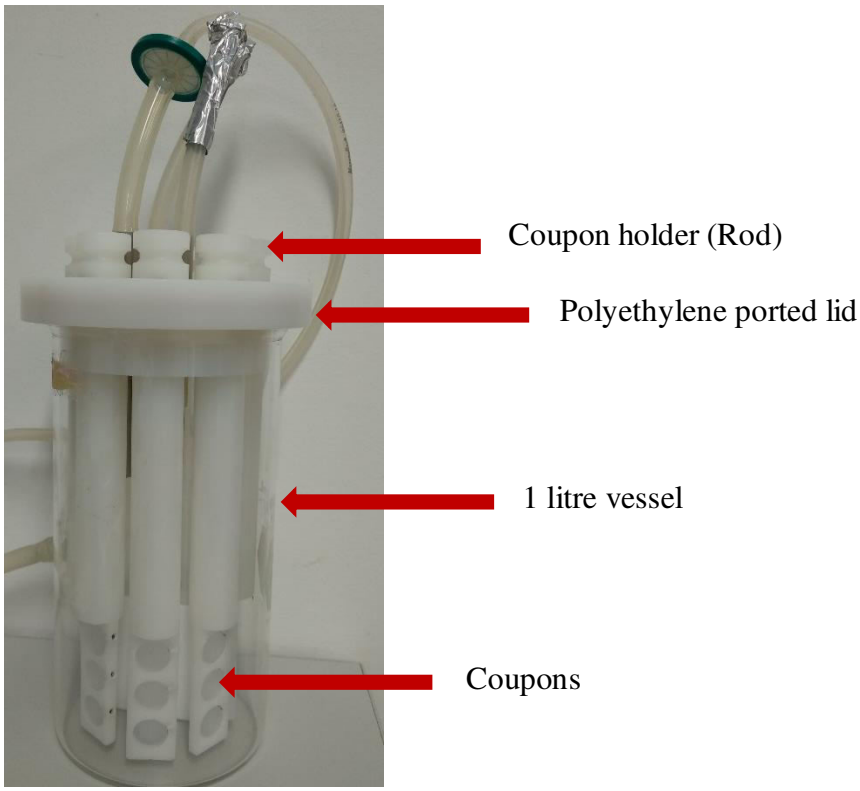

Figure 2.1: Centre for disease control (CDC) bioreactor. The CDC biofilm reactor comprises of eight (8) polypropylene coupon holders (rods) and each rod can hold three removable polycarbonate coupons (1.27cm diameter and 0.3cm thick) suspended from a polyethylene ported lid. The lid with rods and removable coupons is equipped in a 1 litre glass vessel with sidearm discharge port. During all liquid phases (batch phases) of biofilm development, mixing and shear were provided by baffle rotation generated by a magnetic stir plate.

2.1.4. 3-day wet biofilm (3dwb)

A 1ml aliquot of *S. aureus* liquid culture containing approximately10^8 organisms was added to 500ml sterile 50% TSB within the CDC biofilm reactor and biofilm grown in batch phase, at 37°C, for 48 hours. At 48 hours the media was drained and replaced with 20% TSB and incubated batch phase for the next 24 hours. Biofilm was grown and harvested from three separate experiments.

2.1.5. 12-day wet biofilm (12dwb)

A 1ml aliquot of liquid culture of *S. aureus* (10^8/ml) was added to the CDC biofilm reactor containing 500ml sterile 50% TSB and biofilm grown in batch phase, at 37°C, for 48 hours. At 48 hours the media was exchanged with sterile 20% TSB which was repeated every 48 hours over 12-days as shown in Table 2.1.

Table 2.1: Culture conditions for the formation of 12dwb from *S. aureus*.

Phases	Growth conditions	Cumulative operating time
1	48 hours batch phase in 50% TSB	48 hours
2	48 hours batch phase in 20% TSB	96 hours
3	48 hours batch phase in 20% TSB	144 hours
4	48 hours batch phase in 20% TSB	192 hours
5	48 hours batch phase in 20% TSB	240 hours
6	48 hours batch phase in 20% TSB	288 hours

2.1.6. 12-day dry surface biofilm (DSB)

S. aureus DSB was grown on removable polycarbonate coupons in the CDC biofilm reactor using Almatroudi's method [252] of alternating nutrition and dehydration phases over 12-days as shown in Table 2.2. To develop DSB, 1ml of liquid culture of *S. aureus* (10^8/ml) was added to the biofilm reactor vessel containing 500ml sterile 5% TSB and biofilm grown in batch phase, at 37°C for 48 hours followed by 48 hours of dehydration at room temperature (RT) (22-25°C). Additionally, three more cycles of batch culture for 6 hours at 37°C, were interspersed with prolonged dehydration phases of 66, 42 and 66 hours at room temperature [252]. Biofilm was grown and harvested from three separate experiments.

Table 2.2: Culture conditions for the formation of DSB from *S. aureus*.

Phases	Growth conditions	Cumulative operating time
1	48 hr batch phase in 5% TSB followed by 48 hours dehydration	96 hours
2	6 hr batch phase in 5% TSB followed by 66 hours dehydration	168 hours
3	6 hr batch phase in 5% TSB followed by 42 hours dehydration	216 hours
6	6 hr batch phase in 5% TSB followed by 66 hours dehydration	288 hours

2.2. Protein extraction, fractionation and processing for MS/MS analysis

Extraction and fractionation were performed using a modified method described by Sadovskaya [454].

2.2.1. Protein extraction from 24 hour planktonic culture

Planktonic culture samples (n=3) were divided into 2x1.5ml aliquots each (total of 6) for extraction. Each 1.5ml aliquot was mixed with lysis buffer containing 100mM Triethylammonium bicarbonate (TEAB; Sigma-Aldrich, Australia) pH 8.5 and 1% (weight per volume, w/v) sodium deoxycholate (Sigma-Aldrich) at 10:1 ratio (supernatant:lysis buffer) and probe sonicated in ice-cold environment (Sonic Ruptor; Omni international, USA) for 2 minutes at 50% power and 70% pulse followed by centrifugation at 12,000xg for 10 minutes. The supernatants from one sample (n=2) were loaded onto an Amicon ultra membrane filter tube (MWCO; Sigma-Aldrich, Merck Millipore) with a 10kDa molecular weight cut off and concentrated to 2ml. TSB and lysis buffer was removed by washing the concentrated sample with phosphate buffered saline (PBS; Gibco, Life Technologies Corp., USA) three times, followed by protein concentration using a 3kDa MWCO (Sigma Aldrich) filtration.

2.2.2. Extraction of biofilm proteins

Biofilm coated coupons (n=24) were washed with 1x PBS, pH 7.2 to remove loosely attached bacteria. Each coupon was individually placed into 2ml of 1x PBS and 200µl of lysis buffer and incubated overnight with a gentle shaking at 4°C followed by probe sonication in ice-cold environment for 2 minutes at 70% pulses. The sonicates were pooled (52.8ml) and centrifuged at

12,000xg for 30 minutes at 4ºC. The supernatant was concentrated to 2mls by centrifuging through a 10kDa MWCO. TSB and lysis buffer was removed by washing the concentrated sample with PBS three times, followed by protein concentration using 3kDa MWCO filtration.

2.2.3. Determination of protein concentration

At this stage, the three replicate planktonic samples were pooled whilst the biofilm triplicate samples were kept separate. The concentration of protein in each sample was measured by bicinchoninic acid (BCA) assay (Pierce™ BCA protein kit assay, Thermofisher, USA) at 562nm wavelength (PHERAstar FS, BMG Labtech, Germany) as per manufacturer's instructions.

Microplate assay procedure

The BCA assay working reagent was mixed at 1:50 (reagent B: reagent A) ratio. 10µl of sample and 10µl of standard solution were added to each well followed by 200µl working reagent. Samples were mixed well and incubated at 37°C for 30 minutes. After incubation samples were then kept at room temperature for 10 minutes to cool down. The concentration of protein in each triplicate sample was measured at 562nm wavelength using bovine serum albumin (BSA) as a standard (shown in Figure 2.2).

Preparation of diluted albumin (BSA) standards

Serial dilution of BSA for standard curve			
Vial	**Volume of diluent (µl)**	**Volume and source of BSA (µl)**	**Final BSA concentration (µg/ml)**
A	0	200µl of stock (1mg/ml)	1000
B	100	100µl of stock (1mg/ml)	500
C	120	80µl of stock (1mg/ml)	400
D	140	60µl of stock (1mg/ml)	300
E	160	40µl of stock (1mg/ml)	200
F	180	20µl of stock (1mg/ml)	100
G	100	100µl of vial F dilution	50
H	100	100µl of vial G dilution	25
I	200	0	0 = Blank

Measurement of protein concentration

Protein concentration (ug/ml)	1000	500	400	300	200	100	50	25
Absorbance at 562	0.888	0.467	0.377	0.28	0.2	0.123	0.044	0.022

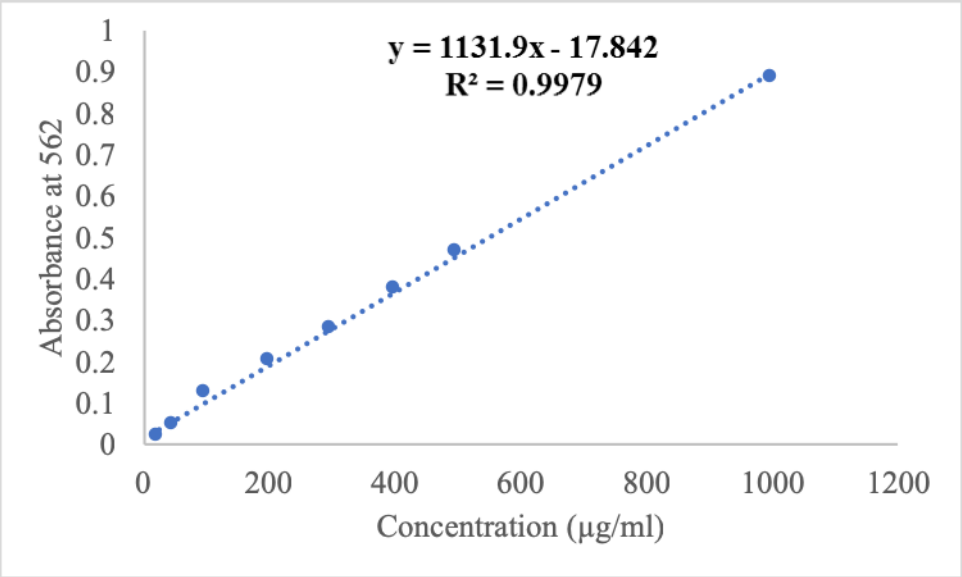

Figure 2.2: An example of BCA protein assay standard curve generated.

2.2.4. Protein reduction, alkylation, and digestion

The protein concentration in the ten samples (one planktonic, three 3dwb, three 12dwb and three DSB) was adjusted to 1µg protein/µl using PBS and 40µg protein used for reduction, alkylation and digestion (Figure 2.3). Each sample was reduced with 5mM dithiothreitol (DTT; Sigma-Aldrich) for 15 minutes at RT and alkylated with 10mM iodoacetamide (IAA; Sigma-Aldrich) in the dark for 30 minutes at RT. Alkylated samples were then diluted with 20µl of 100mM TEAB pH 8.5. For digestion, Lys-C (Promega, USA) was added at a ratio of 1:30 for overnight at RT followed by the addition of trypsin (Sigma-Aldrich) at a ratio of 1:30 for 5.5 hours at 37°C. Samples were adjusted to 1% (v/v) trifluoroacetic acid (TFA; Sigma-Aldrich), and the precipitated deoxycholate was removed by centrifugation. Samples were centrifuged at 14,100xg and desalted using Styrene Divinylbenzene-Reversed Phase Sulfonate (SDB-RPS; 3M-Empore,

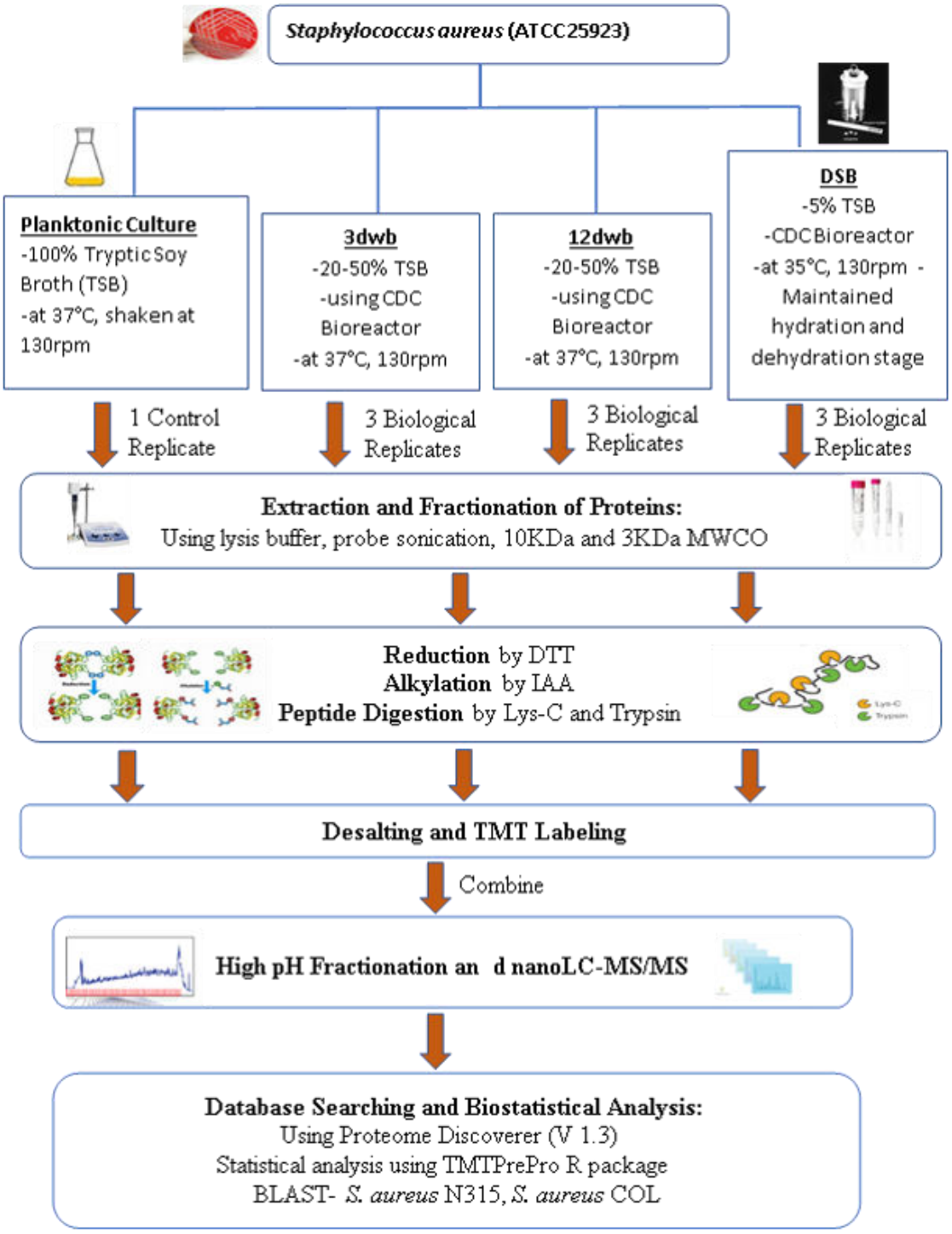

Figure 2.3: Experimental workflow for TMT labeling and analysis. *S. aureus* strain cultivated in TSB to grow a planktonic culture pooled from biological triplicates, and biofilms (3-day, 12-day, and DSB) in biological triplicates. The Centres for Disease Control biofilm reactor was used

to grow biofilms. Proteins were extracted from the 9 replicates of 3 biofilm conditions, and a pooled control from planktonic culture was generated from equal aliquots of protein from the control triplicates. Proteolytically digested peptides were labeled with TMT 10-plex reagents and subjected to high pH RP-HPLC fractionation followed by LC−MS/MS analysis. TMT-10-plex experimental design adapted from Samantha et al., (2016) [336].

USA) stage tips. To make the stage tip, 3 layers of SDB-RPS disks were cut and stacked using a 16-G Hamilton syringe needle into bottom of a 200µl pipette tip. Each stage tip was placed onto a 1.5ml Eppendorf tube. Each sample was added to the stage tip and centrifuged 1000xg for 5 minutes. Stage tip containing samples were washed twice with 0.2% TFA and centrifuged at 1000xg for 5 minutes. Samples were eluted with 100µl of elution buffer containing 5% ammonium hydroxide (Sigma-Aldrich) in 80% acetonitrile (ACN; Acros Organics, USA) and centrifuged at 1000xg for 5 minutes. Samples were vacuum dried (miVac, Genevac Ltd, England) and stored at -20°C until further processing.

2.2.5. TMT labeling and high pH fractionation

The vacuum dried samples were reconstituted in 100µl of 100mM TEAB pH 8.5. Tandem Mass Tag (TMT; Thermo Fisher Scientific, Germany) reagents (0.8mg) were dissolved in ACN (85µl) of which 41µl was added to the reconstituted samples and incubated for 1hr at RT. A volume of 8µl of 5% Hydroxylamine (Sigma-Aldrich) was added to each TMT labeled sample and incubated for 15 minutes at RT. A volume of 2µl of each labeled sample was pooled and vacuum dried and reconstituted in 30µl 0.1% formic acid (FA; Merck Pty Ltd, Finland) solution, centrifuged for 5 minutes at 14000xg and analysed with mass spectrometer (for detailed information see section 2.1.6.1).

Data searching was conducted using Proteome Discoverer 1.3 (for detailed information see section 2.2.7). Based on the applied normalisation values from this search result an equal amount of peptides were taken from each sample, pooled and vacuum dried. The pooled labeled sample was fractionated by high pH reverse phase-high pressure liquid chromatography (RP-HPLC; Agilent Technologies, USA). The buffer A was 5mM ammonia solution (pH 10.5) and buffer B

was 5mM ammonia solution with 90% acetonitrile (pH 10.5). The dried labeled sample was resuspended in loading buffer which was the same as the buffer A. After sample loading and washing with 97% buffer A for 10 minutes, buffer B concentration was increased from 3% to 30% buffer B for 55 minutes; 70% for 10 minutes; 90% for 5 minutes at a flow rate of 300µl/minute. The eluent was collected every 2 minutes until the 16 minutes time point and thence every 1 minute for the remainder of the gradient. The fractionated sample by high pH RP-HPLC was pooled to 20 fractions according to the following chart (Table 2.3) and vacuum dried. Finally, each fraction was resuspended in 55µl of 0.1% FA for mass spectrometry analysis.

Table 2.3: Pooled 20 fractions after high pH RP-HPLC.

Pooled fraction name	**F1**	**F2**	**F3**	**F4**	**F5**	**F6**	**F7**	**F8**	**F9**	**F10**
High pH fraction	E1	F1	G1	H1	H2	G2	F2	E2	D2	C2
	G3	H3	H4	G4	F4	E4	D4	C4	B4	A4
	H6	G6	F6	E6	D6	C6	B6	A6	A7	B7
	F8	E8	D8	C8	B8	A8	A9	B9	C9	D9
	D10	C10								
Pooled fraction name	**F11**	**F12**	**F13**	**F14**	**F15**	**F16**	**F17**	**F18**	**F19**	**F20**
High pH fraction	B2	A2	A3	B3	C3	D3	E3	F3	A1	C1
	A5	B5	C5	D5	E5	F5	G5	H5	B1	D1
	C7	D7	E7	F7	G7	H7	H8	G8		
	E9	F9	G9	H9	H10	G10	F10	E10		

2.2.6. Nanoflow liquid chromatography electrospray ionisation tandem mass spectrometry (Nanoflow LC-ESI-MS/MS)

The samples were run on two mass spectrometer systems.

2.2.6.1. Nanoflow LC-ESI-MS/MS using Orbitrap Elite

An Orbitrap Elite (Thermo Fisher Scientific, Germany and USA) mass spectrometer equipped with PicoView 550 Nanospray Source (New Objective, Inc.), an Eksigent ultra-pressure liquid chromatography (UPLC) system (AB SCIEX) consisting of an ekspert™ nanoLC 425 UPLC pump and ekspert™ nanoLC 400 (Thermo Fisher Scientific) autosampler was used for acquiring

data. A 20µl aliquot of each fraction was loaded onto a self-packed 100µm x 3.5cm trap column with Halo® 2.7µm 160 Å ES-C18 (Advanced Materials Technology) and desalted with loading buffer [0.1% FA] at a flow rate of 4µl/minute for 10 minutes. Peptides were eluted onto a self-packed analytical column 100µm x 30cm with Halo® 2.7µm 160 Å ES-C18 (Advanced Materials Technology) with the linear gradients of mobile phase A [0.1% FA/5% dimethyl sulfoxide (DMSO)] and mobile phase B [0.1% FA/5% dimethyl sulfoxide (DMSO)/94.9% ACN] starting with B (1–10%) for 0.1 minutes, B (10–20%) for 52 minutes, B (20–32%) for 48 minutes followed by (32%-43%) for 20 minutes with a flow rate of 450nl/minute across the gradient. The eluent from the trap was diluted with 100nl/minute of buffer A before reaching the analytical column. The peptides refocused and separated over the analytical column at 60°C. Peptides were ionised by electrospray ionisation and data-dependent MS/MS acquisition carried out using an Orbitrap Elite consisting of 1 full MS1 (R=120 K) scan acquisition from 380 to 1600 m/z, and 15 higher energy collisional dissociation (HCD) type MS2 scans (R=30 K), (spray voltage=3.0KV; automatic gain control (AGC) target=1e6; HCD collision energy=40; dynamic exclusion window=90s; maximum injection time=200ms).

2.2.6.2. Nanoflow LC-ESI-MS/MS using Q Exactive

A Q Exactive (Thermo Fisher Scientific) Mass Spectrometer equipped with Nano spray Source and Easy nLC 1000 (Thermo Fisher Scientific) was used for acquiring data. Each fraction (10µl) was loaded onto a self-packed 100µm x 3.5cm reversed phase peptide trap with Halo® 2.7µm 160 Å ES-C18 (Advanced Materials Technology) desalted with 20µl of loading buffer [0.1% FA] and the peptide trap was then switched on line with the analytical column a self-packed 75µm x 3.5cm Halo® 2.7µm 160 Å ES-C18 column. Peptides were eluted with the linear gradients of mobile phase A [0.1% FA] and buffer B [100%(v/v) ACN, 0.1%(v/v) formic acid] starting with (1–30%) for 110 minutes, B (30–85%) for 2 minutes followed by 85% B for 8 minutes with a flow rate of 300nl/minute. Peptides were ionised by electrospray ionisation and data-dependent MS/MS acquisition performed utilising a Q-Exactive consisting of 1 full MS1 (R=70 K) scan acquisition from 350 to 1850 m/z, and 10 HCD type MS2 scans (R=70 K), (spray voltage=3.0KV; automatic gain control (AGC) target=1e6; HCD collision energy=35; dynamic exclusion window=30s; maximum injection time=250ms).

2.2.7. Database search, statistical analysis, and bioinformatics

The raw data files were submitted to Proteome Discoverer (version 1.3, Thermo Fisher Scientific). The data were processed using Sequest and Mascot (Matrix Science, London, UK) against *S. aureus* reference strain (ATCC 25923) from the gene bank. To identify proteins, the following selections were applied: (i) peptide mass tolerance = 10 ppm; (ii) MS/MS tolerance = 0.1 Da; (iii) enzyme = trypsin, (iv) missed cleavage = 1; (v) fixed modification, carbamidomethyl (C), TMT10-plex (K) and TMT10-plex (N-term); (vi) variable modification, oxidation (M), Deamidated (N, Q) and Acetyl (N-Terminus). Relative quantification was carried out dependent on the peak intensities of reporter ions in the MS/MS spectra. Below 1% false discovery rate was selected as the cut-off for peptide identification. The quantification of proteins was based on the total intensity of the peptides allocated. After the extraction of protein ratios with Proteome Discoverer, further processing and statistical analysis was conducted using the TMTPrePro R package [455]. In this study, our proteomics database processed through very powerful and specifically designed TMTPrePro R package to analyse TMT-based proteomics work. This software performed various multivariate analysis to assess the overall data quality and FDR based on replicates (Boxplots and density plots, heatmap correction), unsupervised analyses (Pearson correlation coefficients (PCC), clustering and PCA), ANOVA, etc. Pearson correlation coefficients (PCC) were calculated to measure the reproducibility between samples by the TMTPrePro R package and degree of variation of proteins to be counted less than 5%. In addition, Principal Component Analysis (PCA) also showed that the individual biofilm sample replicates cluster closely against the pooled control. Therefore, statistical assessment of the dataset by comparing individual biofilm sample replicates against the pooled planktonic control indicated that levels of variability across all 10 samples were very low. BLAST search was performed using highly annotated strains *S. aureus* N315 and *S. aureus* COL. Proteins were considered upregulated when the TMT ratio was above 1.5 and downregulated when the TMT ratio was lower than 0.665 (1/0.665=1.5-fold) in biofilm growth compared to planktonic growth with significant p-value < 0.05. When we processed our database through the TMTPrePro R package, we considered the cutoff range >1.5 fold, $p < 0.05$. But, in our thesis we specifically focused on only proteins dysregulated >2 fold, $p < 0.05$. Significant differentially expressed proteins (>2fold) were determined by using VENNY (v.2.1)

http://bioinfogp.cnb.csic.es/tools/venny/ and processed further to gain more functional insights. Significant differentially expressed proteins (>2fold) were examined using the PANTHER program (http://www.pantherdb.org/) for gene ontology (GO) annotation based on protein function into four domains: protein classes, biological processes, cellular components, and molecular functions. Metabolic pathways of identified proteins were analysed by using Kyoto Encyclopedia of Genes and Genomes (KEGG) mapper (https://www.genome.jp/kegg/tool/map_pathway2.html). Subcellular localisation of identified proteins was analysed by using PSORTb (version3.0.2) (http://www.psort.org/psortb/index.html) [456]. The protein–protein interaction (PPI) network of significantly differentially expressed proteins was analysed by STRING software v.10.0 (http://string-db.org/) [457]. Identification of virulence factors was performed using the Virulence Factors of Pathogenic Bacteria Database (VFDB) (http://www.mgc.ac.cn/VFs/).

2.3. Validation of biofilm proteomics results by quantitative reverse-transcription PCR

An experimental overview is illustrated in Figure 2.4.

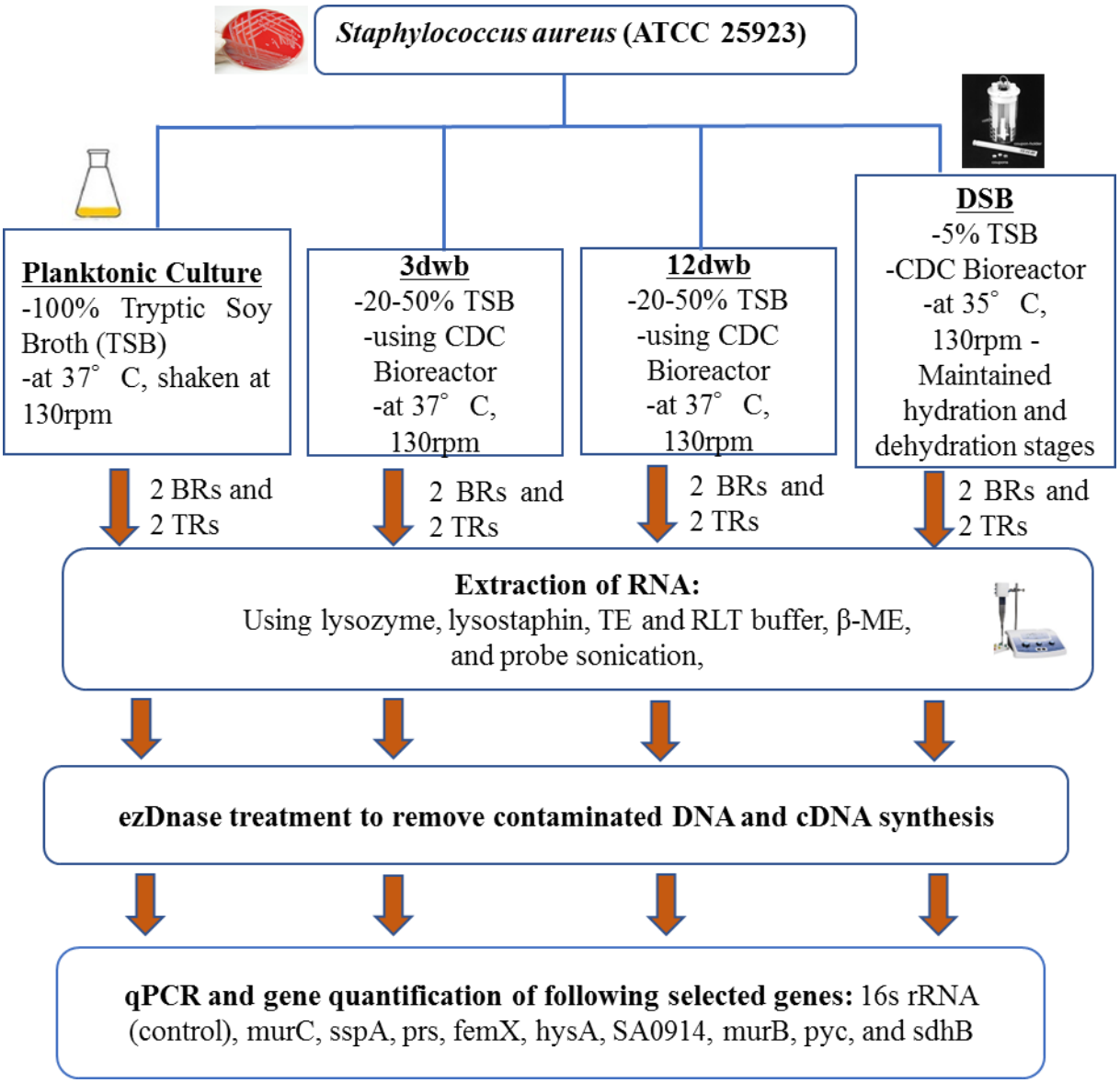

Figure 2.4: Experimental workflow for RNA extraction and qPCR analysis. *S. aureus* strain cultivated in TSB to grow a planktonic culture, and biofilms (3-day, 12-day, and DSB). The Centres for Disease Control biofilm reactor was used to grow biofilms. Each growth condition was conducted in two biological replicates (BR) and two technical replicates (TR). RNA was extracted and subjected to ezDNase treatment to remove genomic DNA and cDNA synthesis followed by qPCR analysis of selected genes.

2.3.1. Planktonic and biofilms culture conditions

***S. aureus* planktonic culture:** *S. aureus* 24 hours planktonic culture was prepared according to the procedure described in 2.1.3.

Biofilm culture conditions: *S. aureus* 3dwb, 12dwb, and DSB were developed according to the procedure described in 2.1.4.

2.3.2. RNA extraction from planktonic cultures

To extract RNA from 24 hours culture of planktonic bacteria, 200µl liquid culture immediately mixed with 80µl lysozyme (20mg/ml; Sigma-Aldrich), and 3µl TE buffer [10mM Tris-HCl, 1mM EDTA (Sigma-Aldrich)]. A volume of 100µl RLT buffer (obtained from a commercially available RNA extraction Qiagen RNeasy Mini Kit; Qiagen, Australia) plus 3µl β-mercaptoethanol was added and incubated for 10 minutes at 37°C with shaking. A volume of 10µl proteinase k (25mg/ml; Sigma-Aldrich) was added and incubated for 10 minutes at RT followed by 30 seconds probe sonication at 50% power and 70% pulses. The solution was then used in RNA extraction using Qiagen RNeasy Mini Kit, according to the manufacturer's recommendations for prokaryotic RNA isolation. The RNA was eluted with 30µl of RNase free water and concentrations were measured using the Nanodrop 2000 (Thermo Fisher Scientific).

2.3.3. RNA extraction from biofilms

Total RNA in biofilm coated coupons was preserved by adding 1ml/coupon of RNA later (Qiagen) to cover the coupon and placing at 4°C overnight. To extract the RNA, the coupons were washed in RNase-free water and placed in a tube containing 200µl lysozyme (20mg/ml), 50µl lysostaphin (2.5mg/ml; Sigma-Aldrich), and 7µl TE buffer [10mM Tris-HCl, 1mM EDTA]. A volume of 350µl RLT buffer plus 7µl β-mercaptoethanol was added and incubated for 10 minutes at 37°C with shaking. A volume of 15µl proteinase k (25mg/ml, Sigma-Aldrich) was added and incubated for 10 minutes at RT followed by 2 minutes probe sonication at 50% power and 70% pulses. The solution was then used in RNA extraction using Qiagen RNeasy Mini Kit, according to the manufacturer's recommendations for prokaryotic RNA isolation. The RNA was eluted with 30µl of RNase free water and concentrations were measured using the Nanodrop 2000.

2.3.4. Reverse transcription

Genomic DNA was removed using ezDNase (Thermo Fisher Scientific) following the manufacturer's instructions with slight modification of incubation at 37°C for 5 minutes instead of 2 minutes to ensure DNA removal. ezDNase removes residual contaminated genomic DNA from RNA preparations without affecting the quality or quantity of target RNA. The amount of RNA was quantified again using the Nanodrop 2000 after ezDNase treatment.

cDNA was produced using with a cDNA synthesis kit using SuperScript™ IV VILO™ Master Mix (Thermo Fisher Scientific) as per the manufacturer's instructions. Briefly, 200ng of RNA was added to 20µl reverse transcription reaction and, incubation at 25°C for 10 minutes, followed by incubation at 50°C for 10 minutes and the reaction was terminated by incubation inactivated at 85°C for 5 minutes in an Eppendorf mastercycler gradient PCR machine (Eppendorf, Germany). A no reverse transcription control (no -RT control) reaction was also included, which included all reaction components except the reverse transcriptase enzyme, which was replaced with nuclease free water. The cDNA was used immediately in quantitative real-time PCR or stored at -80°C.

2.3.5. Primers

The primers used in this study (Table 2.4) were designed based on the published *S. aureus* (ATCC 25923) genome sequences (GenBank CP009361 and CP009362) [458]. The primers were produced commercially by Sigma Aldrich, Australia. Upon receipt, the lyophilised primers were resuspended with nuclease free water to obtain a 100µM stock solution. From this, 10µM working solutions were prepared and frozen in aliquots to prevent freeze-thawing cycles. The primers were stored at -20°C.

Table 2.4: Primer sequences used in this study.

Gene name	Primer name	Primer sequence (5'-3')	Position in gene	PCR size (bp)	Ta (°C)
16s rRNA	Staphy_16sF	GGCGAAGGCGRCTTTCTGG	704-720	95bp	55
	Staphy_16sR	CGTTTACGGCGTGGACT	782-798		
hysA	hysA F	TCTTCTTAGGAACTGGCATT			
	hysA R	GGTTGTTTGCGTATCATCTT	1727-1839	113	55
mucC	murC F	TAATTGGTGATGGCACAGG			
	murC R	GTCATAATTGCGTAATCAGG	395-506	112	50
murB	murB F	AGGTGGTAATGCCGACTTT			
	murB R	TAATTACAATGCCGCGAATA	99-253	155	55
SA0914	SA0914 F	ATTGCGATGATGCTATTTA			
	SA0914 R	GGCGCTCATACACAGGTTC	1124-1207	84	55
sspA	sspA F	CAGCGACACTTGTGAGTTC			
	sspA R	TCTGCGTTTGTTGTGGAT	53-130	109	55
prs	prs F	TCAGGACCGGCTAAAGAAC			
	prs R	AGCTTGTGCGATTAAACCAG	784-918	55	55
femX	femX F	ATTAACGAAATGGGCAGAAA			
	femX R	GTCACGACCTACAGCGATT	75-144	70	55
pyc	pyc F	TCGTACAACGGCTATCAAGG			
	pyc R	AATCATTAGCGGGAAACCAG	366-480	60	60
sdhB	sdhB F	GCCACGTATGCCAGAGAAA			
	sdhB R	CGAACTTGCGAGATTGCTT	462-599	60	60

2.3.6. Quantitative real-time PCR

Quantitative real-time PCR (qPCR) was conducted in an Applied Biosystems quantitative real-time PCR machine (ViiA™ 7 qPCR, Life Technologies, USA).

A volume of 25µl of qPCR reaction mix containing 12.5µl 2X PowerUp™ SYBR™ Green Master Mix (Applied Biosystems, Thermo Fisher Scientific), 1µl each of 10µM reverse and forward primer for a final primer concentration of 400nM, 8.5µl of water and 2µl of 1:5 diluted cDNA. Controls in each run included a no template control (NTC) for each primer set, which consisted of all PCR components except cDNA template which was replaced by nuclease free

water. A no reverse transcription control (no RT control) was also included in initial experiments for each targeted gene. No RT controls consisted of the cDNA sample with no reverse transcriptase enzyme to determine if there was contaminating genomic DNA in the RNA. Cycling conditions for real-time PCR were set as an initial activation step of 95°C for 10 minutes to activate the polymerase, followed by 40 cycles of denaturation at 95°C for 15 seconds, annealing at 50°C or 55°C for 40 seconds and extension at 72°C for 30 seconds, or annealing and extension at 60°C for 1 minute (see annealing temperature Ta in Table 2.4).

Standard samples of known concentrations 10^6,10^5,10^4, 10^3 copies/µl of *S. aureus* genome were included in each qPCR run to generate a standard curve for each target gene. Copy number of each expressed target gene was generated according to the corresponding standard curve.

2.3.7. Relative quantification of gene expression

Relative quantitation of gene expression was conducted using the Pfaffl method [459] where changes in gene expression were normalised to a reference gene. In this study, a single reference gene, 16s rRNA was used as its stable expression [460]. The expressed copy number of each target gene was normalised to 16s rRNA copy number within same growth condition first. Then expression fold changes of each gene were compared between different growth conditions, such as 24 hours planktonic, 3dwb, 12dwb, and DSB.

2.4. Depletion of human plasma protein and processing for MS/MS analysis

2.4.1. Patients and ethics

Human ethics approval was obtained from the Macquarie University Human Research Ethics Committee (Reference number 5201600427). Informed consent was sought from study participants. Human ethics approval mentioned in Appendix 1 and participant information and consent forms mentioned in Appendix 2A and 2B.

Blood was collected from ten healthy patients receiving breast implants for the first time (control patients: C) and from ten patients with symptomatic contracted capsules surrounding breast implants (D) (Table 2.5).

Table 2.5: Details of selected patients used in this study.

SN	MQ Patient ID	Diagnosis	Age (years)	Short ID	State
1	1623	Control	33	C1	Kingsway Day Surgery, NSW
2	1624	Control	34	C2	Kingsway Day Surgery, NSW
3	1625	Control	25	C3	Kingsway Day Surgery, NSW
4	1628	Control	31	C4	Kingsway Day Surgery, NSW
5	1629	Control	29	C5	Kingsway Day Surgery, NSW
6	1630	Control	39	C6	Kingsway Day Surgery, NSW
7	1704	Control	Not available	C7	Kingsway Day Surgery, NSW
8	1705	Control	35	C8	Kingsway Day Surgery, NSW
9	1706	Control	29	C9	Kingsway Day Surgery, NSW
10	1843	Control	32	C10	MUH, NSW

SN	MQ Patient ID	Diagnosis	Age at diagnosis (years)	Short ID	Bacteria from Culture	State
1	1621	Capsule contracture	42	D1	Enterococcus, Staph	MUH, NSW
2	1711	Capsule contracture	58	D2	Staphylococcus	Cabrini Hospital, VIC
3	1712	Capsule contracture	62	D3	N/A	VIC
4	1722	Capsule contracture	39	D4	N/A	St Luke's Hospital, NSW
5	1732	Capsule contracture	49	D5	N/A	Mater Health, QLD
6	1733	Capsule contracture	64	D6	N/A	Mater Health, QLD
7	1804	Capsule contracture	49	D7	N/A	Kareena Private Hospital, NSW
8	1814	Capsule contracture	37	D8	N/A	MUH, NSW
9	1825	Capsule contracture	44	D9	*S. epidermidis*	Princess Alexandra Hospital, QLD
10	1826	Capsule contracture	52	D10	N/A	Pacific Private Day Hospital, QLD

2.4.2. Collection and processing of human plasma samples

Up to 5ml of blood was collected in ethylenediamintetraacetic acid (EDTA) tubes (BD Biosciences, Australia) and the plasma separated by centrifugation at 800xg for 15 minutes at RT. Between 2 to 3ml of plasma was removed and transferred in aliquots to 1.5ml microcentrifuge tubes (Axygen; Fisher Biotech, Australia) and centrifuged again at 1600xg for 10 minutes at RT to remove cellular debris. The plasma was then stored in 500µl aliquots at -80°C.

2.4.3. Depletion of human plasma proteins

Plasma (40µl) from each patient (10 healthy control, 10 capsular contracture) was processed for the depletion of high abundant proteins using the multiple affinity removal systems (MARS-14) (Agilent Technologies, USA). As mentioned in the Agilent Technologies brochure, "MARS-14 high capacity affinity column was specifically designed to employ anti-human plasma protein monoclonal antibodies to remove the 14 most abundant proteins (human serum albumin, IgG, antitrypsin, IgA, transferrin, haptoglobin, fibrinogen, α2-macroglobulin, α1-acid glycoprotein, IgM, apolipoprotein AI, apolipoprotein AII, complement C3 and transthyretin) from human biological fluids such as plasma, serum, and cerebral spinal fluid (CSF)". To deplete high-abundant plasma proteins, each sample was diluted 1:4 with buffer A and transferred to a 0.22µm spin filter (Merck Millipore Ltd, Ireland) and centrifuged for 2 minutes at 10,000×g and 4°C to remove particulates. Depletion of each sample was performed on an Agilent 1260 HPLC system using MARS-14 column (4.6×100 mm) and proteins eluted following the manufacturer's instructions (Agilent Technologies). During each sample run, approximately 2ml of flow-through fractions (at first low-abundant proteins were eluted, appeared between 11-15 minutes) were collected from each sample run followed by bound plasma proteins (high-abundant proteins) were eluted. Each flow-through fraction containing low-abundant plasma proteins sample was concentrated to approximately 200µl using 5kDa MWCO membrane filter (Vivaspin, Sartorius) at 3200xg and 4°C. Then equal volume (2ml) of 1x PBS buffer exchanged at the same conditions and concentrated to approximately 200µl. BCA protein assay was performed to measure the final low-abundant protein concentration (described in section 2.1.6).

2.4.4. Protein reduction, alkylation, and digestion

A total of 40µg protein from each sample was processed further for reduction, alkylation, and digestion. Each sample was reduced with 10mM DTT for 30 minutes at 60°C followed by alkylated with 20mM iodoacetamide IAA in the dark for 30 minutes at RT. Reduction step was repeated once to quench further alkylation for 15 minutes at RT. Alkylated samples were then diluted with 10µl 1M TEAB pH 8.5. For digestion, Lys-C (FUJIFILM Wako Pure Chemical Corporation, Japan) was added at a ratio of 1:100 overnight at RT followed by the addition of trypsin at a ratio of 1:100 for 5 hours at 37°C and 400rpm. After which, samples were acidified

using 1% (volume per volume, v/v) TFA and centrifuged at 14,100xg prior to desalting using SDB-RPS stage-tips. To make the stage tip, 2 layers of SDB-RPS disks were cut and stacked using a 16-G Hamilton syringe needle into the bottom of a 200µl pipette tip. Each stage tip was placed onto a 1.5ml Eppendorf tube. Stage-tip containing samples were washed with 0.2% TFA and centrifuged at 1000xg for 5 minutes twice. Samples were eluted with 100µl elution buffer containing 5% ammonium hydroxide in 80% ACN and centrifuged at 1000xg for 5 minutes. Samples were then vacuum dried) and stored at -20°C until further processing.

2.4.5. TMT labeling and high pH fractionation

Samples were reconstituted in 100µl of 200mM HEPES (4-(2-Hydroxyethyl) piperazine-1-ethanesulfonic acid; Sigma, Australia) pH 8.8 and labeled with 20µl of TMT for 1 hour at RT, which had been prepared by dissolving 0.8mg of TMT reagents in 85µl of anhydrous ACN. To each TMT labeled sample (Figure 2.5), 8µl of 5% Hydroxylamine was added and incubated for 15 minutes at RT. A volume of 3.2µl of each labeled sample was then pooled, dried and reconstituted in 10µl 0.1% formic acid and 2% ACN solution. This was centrifuged for 5 minutes at 14000xg and analysed by MS (for detailed information see section 2.9).

The data was searched using Proteome Discoverer 2.1 (for detailed information see section 2.10). Based on the applied normalisation values from this search result an equal amount of peptides were taken from each sample, pooled and vacuum dried. The pooled labeled sample was fractionated by high pH RP-HPLC (Agilent Technologies). The dried labeled sample was resuspended in buffer A (5mM ammonia solution, pH 10.5). After sample loading and washing with 97% buffer A for 10 minutes, buffer B (5mM ammonia solution with 90% acetonitrile, pH 10.5). Concentration was increased from 3% to 30% over 55 minutes; 70% for 10 minutes; 90% for 5 minutes at a flow rate of 300µl/minute. The eluent was collected every 2 minutes at the beginning until 16 minutes and every 1 minute's intervals for the remainder of the gradient. The fractionated sample by high pH RP-HPLC was pooled to 17 fractions according to the following chart (Table 2.6), dried in vacuum. Finally, each fraction was resuspended in an appropriate volume of 0.1% FA and 2% ACN for mass spectrometry analysis.

Table 2.6: Pooled 17 fractions after high pH RP-HPLC.

Pooled fraction name	F1	F2	F3	F4	F5	F6	F7	F8	F9	F10
High pH fraction	B2	A2	A3	B3	C3	D3	E3	F3	G3	H3
	D4	C4	B4	A4	A5	B5	C5	D5	E5	F5
	F6	E6	D6	C6	B6	A6	A7	B7	C7	D7
	H8	G8	F8	E8	D8	C8	B8	A8	A9	B9
	G9	H9	H10	G10	F10	E10				
Pooled fraction name	**F11**	**F12**	**F13**	**F14**	**F15**	**F16**	**F17**			
High pH fraction	H4	G4	F4	E4	C2	E1	A1			
	G5	H5	H6	G6	D2	F1	B1			
	E7	F7	G7	H7	E2	G1	C1			
	C9	D9	E9	F9	F2	H1	D1			
					G2					
					H2					

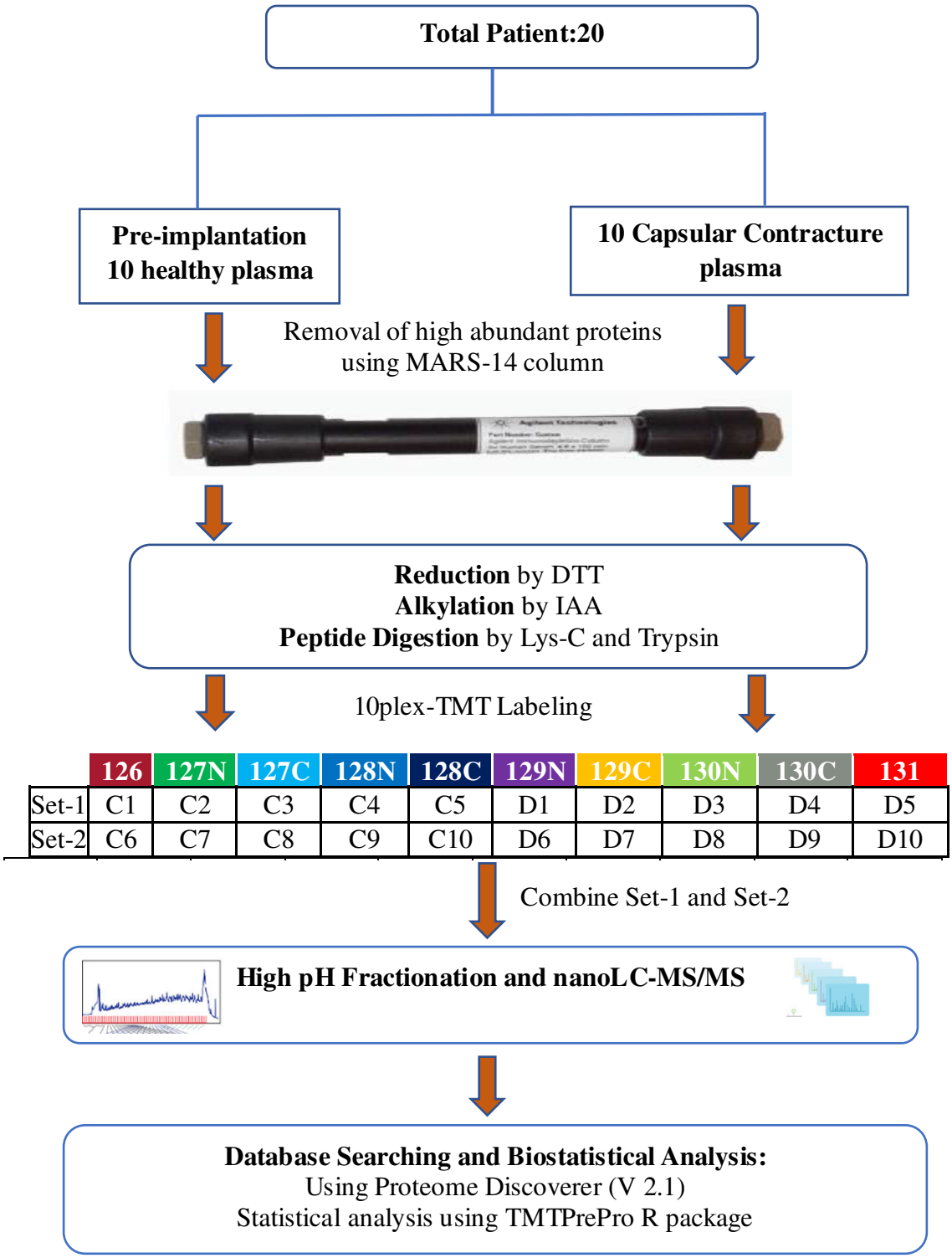

Figure 2.5: Experimental workflow for plasma depletion, TMT labeling and analysis. Plasma from each patient (10 healthy control, 10 CC) was processed for the depletion of high-abundant proteins using MARS-14 to improve depth of detection in plasma samples.

Proteolytically digested peptides were labeled with TMT 10-plex reagents and subjected to high pH RP-HPLC fractionation followed by LC−MS/MS analysis.

2.4.6. Nanoflow LC-ESI-MS/MS using Q Exactive

A Q Exactive Mass Spectrometer equipped with Nano spray source and Easy nLC 1000 was used for acquiring data. A volume of 10µl of each fraction was loaded onto a self-packed 100µm x 3.5 cm reversed phase peptide trap with Halo® 2.7µm 160 Å ES-C18 desalted with 20µl of loading buffer [0.1% FA] and the peptide trap was then switched on-line with the analytical column a self-packed 75µm x 3.5cm Halo® 2.7µm 160 Å ES-C18 column. Peptides were eluted with the linear gradients of mobile phase A [0.1% FA] and buffer B [100%(v/v) ACN, 0.1%(v/v) formic acid] starting with (1–30%) for 110 minutes, B (30–85%) for 2 minutes followed by 85% B for 8 minutes with a flow rate of 300 nl/minute. Peptides were ionised by electrospray ionisation and data-dependent MS/MS acquisition performed utilising a Q-Exactive consisting of 1 full MS1 (R=70 K) scan acquisition from 350 to 1600 m/z, and 10 HCD type MS2 scans (R=70 K).

2.4.7. Database search, statistical analysis, and bioinformatics

The raw data files were submitted to Proteome Discoverer (version 2.1, Thermo Scientific). The data were processed using Sequest and Mascot against all bacteria (taxonomy, 333711 reviewed sequences, release date 04/12/2018) and human (taxonomy, release date 04/12/2018) from Uniprot database. To avoid false-positive result, despite the large number of bacterial search database, we set high confidence criterion which includes: master proteins, FDR <1%, PSMs (high confidence), > 10 amino acid, and at least 1 unique peptide. Therefore, we can speculate that the bacterial proteins reported in this study meet acceptable criteria. To identify proteins, the following selections were applied: (i) peptide mass tolerance = 10 ppm; (ii) MS/MS tolerance = 0.1 Da; (iii) enzyme = trypsin, (iv) missed cleavage = 1; (v) fixed modification, carbamidomethyl (C), TMT10-plex (K) and TMT10-plex (N-term); (vi) variable modification, oxidation (M), Deamidated (N, Q) and Acetyl (N-Terminus). Relative quantification was carried out dependent on the peak intensities of reporter ions in the MS/MS spectra. At least 7 amino acids for peptide, greater than 2 peptides were essential per protein. Below 1% FDR was selected as the cut-off for

peptide identification. The quantification of proteins was based on the total intensity of the peptides allocated. Following the extraction of protein ratios with Proteome Discoverer, further processing and statistical analysis was conducted using the TMTPrePro R package [455]. Metabolic pathways of identified proteins were analysed by using Kyoto Encyclopedia of Genes and Genomes (KEGG) mapper (https://www.genome.jp/kegg/tool/map_pathway2.html). The protein–protein interaction (PPI) network of significantly differentially expressed proteins was analysed by STRING software v.10.0 (http://string-db.org/) [457].

Chapter 3: Comparison of the proteome of *Staphylococcus aureus* planktonic culture and 3-day biofilm reveals potential role of key proteins in biofilm

In this chapter, we aimed to establish a comprehensive proteomic reference map between *S. aureus* planktonic and an early stage biofilm. *S. aureus* is a well-known biofilm producing pathogen, and biofilm-related infections caused by *S. aureus* frequently lead to significantly increased morbidity and mortality. *S. aureus* expresses a comprehensive array of virulence factor proteins, and the secretion of these proteins and complex biofilm formation are still poorly understood. The multiplicity of *S. aureus* virulence factors coupled with the ability to form biofilms, which allows them to have an increased tolerance to antibiotics and the immune defence system in comparison to their planktonic states, suggests that the biofilm mode of growth have an altered protein expression profile and metabolic activity. Therefore, a better understanding of the complex *S. aureus* biofilm formation at the molecular level is an unmet need to develop new/potential diagnostic and therapeutic approaches for biofilm-related infections and to decrease the substantial health-associated loads triggered by this pathogen.

Abstract

Background

Staphylococcus aureus and coagulase-negative staphylococci account for about 80% of infections associated with medical devices and are associated with an increased virulence due to their ability to form biofilm. Currently, there is no effective technique for early identification of biofilms. Thus, we aimed to generate a wide-ranging reference map followed by the identification of potential biomarker proteins in biofilm development, and then performed further analysis associated with significant pathways, subcellular localisation and PPI network mapping.

Methods

S. aureus reference strain (ATCC 25923) was grown in tryptic soy broth to produce a 24-hour planktonic, 3-day wet biofilm (3dwb). The Centres for Disease Control biofilm reactor was used to grow biofilms. Tandem Mass Tag (TMT)-based mass spectrometry was performed, and protein identification and relative quantitation of protein levels were performed using Proteome Discoverer (version 1.3). Statistical analysis was done using the TMTPrePro R package.

Results

We identified 1636 total biofilm extractomes. 82 biofilm proteins were significantly (>2-fold) upregulated and 35 of these were involved in recognised protein pathways. Proteins associated with secondary metabolites, ABC transporters, biosynthesis of amino acids, response to stress, and amino sugar and nucleotide sugar metabolism were significantly upregulated in biofilms. In particular, hyaluronidase (hysA) an exo-enzyme involved in disseminating recognised biofilms by degradation of hyaluronic acid was upregulated. In contrast, 191 biofilm proteins were significantly (>2-fold) downregulated and of these, 74 were involved in recognised protein pathways. Proteins associated with virulence factors, microbial metabolism in diverse environments secondary metabolites, translation, and energy metabolism were significantly downregulated in biofilms. Among them, chitinase (SA0914) an exo-enzyme involved in quorum sensing that prevents the initial stage development of biofilms. Interestingly, hyaluronic acid is the structural constituent of N-acetyl-D-glucosamine which can be hydrolysed by chitinase.

Therefore, hysA in conjunction with chitinase may play significant role in the elimination and/or prevention of biofilm development.

Conclusions

This TMT-based quantitative strategy advances the current *S. aureus* subproteomes and establishes a basis for the identification and study of potential pathways significant to biofilm biology in *S. aureus*. These pioneering findings might be useful in developing novel and/or potential candidates for diagnostic biomarkers, anti-biofilm agents, vaccines, etc. for biofilm-infections related with implantable medical devices.

Keywords: *Staphylococcus aureus*, Bacterial Biofilms, CDC Bioreactor, TMT, Mass Spectrometry

Introduction

The Gram-positive opportunistic pathogen *S. aureus* represents a serious public health burden worldwide, particularly within healthcare settings where they are often associated with an increased virulence due to their ability to form biofilm. To establish infection bacteria initially have to attach to the tissue. *S. aureus* does this using Microbial Surface Components Recognising Adhesive Matrix Molecules abbreviated as MSCRAMMs, and Secreted Expanded-Repertoire Adhesive Molecules termed SERAMs. In addition, various types of enzymes also produced by *S. aureus* including exotoxins such as exfoliative toxins A and B (which increase host tissue invasion), lipases, proteases, thermonucleases, and hyaluronidases [274, 461]. Planktonic cells (free-floating) generally cause acute infections by producing extracellular enzymes and secreted toxins [462]. In chronic infections, *S. aureus* play significant role because of its capacity to withstand therapeutic intervention by developing biofilms on host tissues or on implantable medical devices (e.g. prosthetic joints, catheters, breast implants, and pace makers) [2-6, 170].

Biofilms are microbial communities embedded in a self-produced EPS matrix which can be found on any surface [89, 104]. Although the exact composition of EPS differs between various bacterial species and environmental conditions, EPS consists mainly of polysaccharides, proteins, and extracellular DNA (eDNA) [89]. In general, biofilm development is characterised by three

stages: initial attachment, biofilm maturation, and dispersal. Several studies highlighted primarily on the elucidation of individual molecular variables that are essential in the growth of *S. aureus* biofilms. A very recent study by Graf *et. al.* (2019) mentioned some of the proteinaceous and non-proteinaceous factors responsible for various phases of biofilm formation and the synthesis and expression of these molecular factors are closely regulated by several biofilm regulators such as AgrA and RNAIII, Rot, SigB, SarA, IcaR, CodY, and othres [463].

Attempts to comprehend the biochemical framework of biofilm formation and resilience have constantly demonstrated alterations in protein expression profile in *S. aureus* [325, 327, 341-343] compared with planktonic counterparts. However, numerous facets of complex structure and role of biofilms have yet to be elucidated.

Recent advances in isobaric multiplexed labeling techniques have considerably enhanced the depth, effectiveness, and performance of MS-based proteomics. TMTs are isobaric compounds with a key amine reactive group and a mass reporter region separated by a fragmentation-vulnerable linker from the mass normalisation moiety. In TMTs labeling, each isotopic variant contains unique reporter masses but has the same overall mass, allowing precise general quantification along with accurate measurement of the relative abundance of proteins between samples even in the lower mass region [357, 358]. The excellent benefit of TMT is the chance of multiplexing up to ten samples simultaneously [334-336], saves instrument time, make simpler of the experimental design [337], with the ability to identify several thousand non-redundant proteins at once [335, 338, 339].

In the present study, we aimed to construct a comprehensive proteomic reference map between *S. aureus* planktonic and 3-day biofilm by employing TMT-based high-resolution MS. In addition, identified potential marker proteins further analysed for pathway analysis, subcellular localisation and protein-protein interaction (PPI) network mapping. This work provides new insight into the impact of planktonic and biofilm on the protein expression profile as well as the potential role of key proteins in *S. aureus* biofilms.

Materials and Methods

The objective of this study was to construct a comprehensive proteomic framework of *S. aureus* cells progressing through planktonic and biofilm lifestyles. To do this, we performed in-solution digestion followed by TMT-based high-throughput mass spectrometry (Figure 3.1).

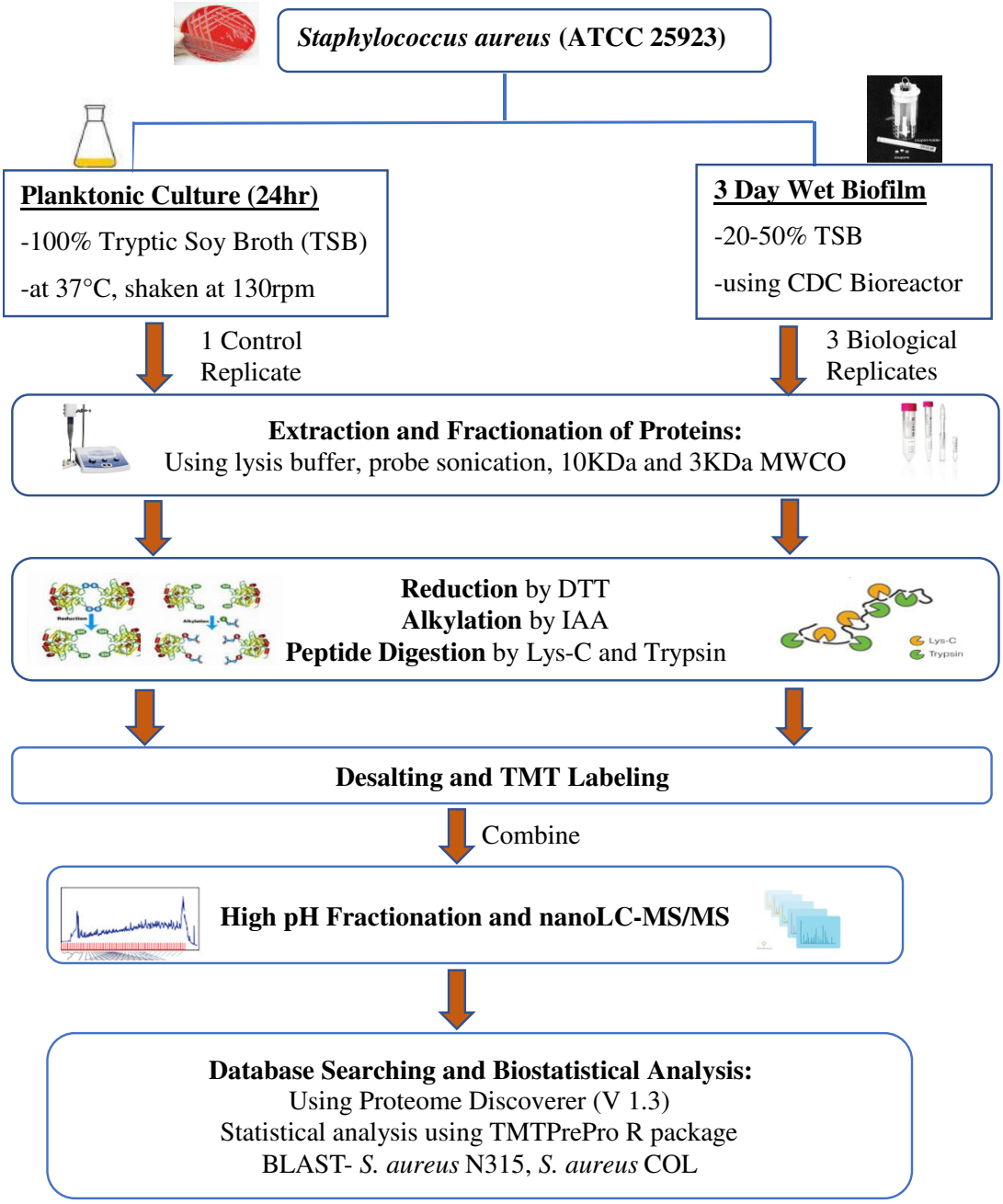

Figure 3.1: Experimental workflow for the analysis of *S. aureus* planktonic and biofilm proteome using TMT labeling based MS. *S. aureus* strain cultivated in TSB to grow a

planktonic culture pooled from biological triplicates, and 3-day biofilm in biological triplicates. The Centres for Disease Control biofilm reactor was used to grow biofilms. Proteolytically digested peptides were labeled with TMT 10-plex reagents and subjected to high pH RP-HPLC fractionation followed by LC−MS/MS analysis.

Microorganism and culture conditions

S. aureus (ATCC 25923) 24 hour planktonic culture were grown as described in Chapter 2, section 2.1.3 whilst 3-day hydrated biofilm cultures were grown as described in section 2.1.4.1.

Sample Processing

Extraction and fractionation were performed using a modified method described by Sadovskaya [454] as described in Chapter 2, section 2.2.1 for planktonic culture and section 2.2.2 for 3-day biofilm culture.

The amount of protein in extracted samples was measured using the BCA protein assay (Thermo Fisher Scientific, Australia) as described in Chapter 2, section 2.2.3.

A total of 40µg protein of each sample was processed further for protein reduction, alkylation, and digestion (Chapter 2, 2.2.4).

Samples were reconstituted in 100µl of 100mM TEAB pH 8.5 and labeled with TMT (Thermo Fisher Scientific, Germany) reagents as described in Chapter 2, section 2.2.5. A volume of 2µl of each labeled sample was pooled and vacuum dried and reconstituted in 30µl 0.1% FA solution, centrifuged for 5 minutes at 14000xg and analysed with mass spectrometer (nanoLC-ESI-MS/MS using Orbitrap Elite) as described in Chapter 2, section 2.2.6.1.

Based on the applied normalisation values from this search result an equal amount of peptides were taken from each sample, pooled and vacuum dried (miVac). The pooled labeled sample was fractionated by high pH RP-HPLC (Agilent Technologies). The fractionated sample by high pH RP-HPLC was pooled to 20 fractions, dried in miVac. Finally, each fraction was resuspended in 55µl of 0.1% FA for mass spectrometry analysis.

Nanoflow LC-ESI-MS/MS

All samples were run on two sequential mass spectrometer systems.

Nanoflow LC-ESI-MS/MS using Orbitrap Elite

An Orbitrap Elite (Thermo Fisher Scientific) mass spectrometer was used for acquiring data (Chapter 2, 2.2.6.1). Briefly, 20µl of each fraction was loaded onto a self-packed 100µm x 3.5cm trap column with Halo® 2.7µm 160 Å ES-C18 and desalted with loading buffer [0.1% FA] at a flow rate of 4µl/minute for 10 minutes. Peptides were eluted onto a self-packed analytical column with the linear gradients with a flow rate of 450nl/minute across the gradient. The eluent from the trap was diluted with 100nl/minute of buffer A before reaching the analytical column. The peptides refocused and separated over the analytical column at 60°C. Peptides were ionised by electrospray ionisation, and data-dependent MS/MS acquisition carried out using an Orbitrap Elite consisting of 1 full MS1 (R=120 K) scan acquisition from 380 to 1600 m/z, and 15 higher energy collisional dissociation (HCD) type MS2 scans (R=30 K).

Nanoflow LC-ESI-MS/MS using Q Exactive

A Q Exactive (Thermo Fisher Scientific) mass spectrometer was used for acquiring data (Chapter 2, 2.2.6.2). Briefly, each fraction (10µl) was loaded onto a self-packed 100µm x 3.5cm reversed phase peptide trap with Halo® 2.7µm 160 Å ES-C18 desalted with 20µl of loading buffer [0.1% FA] and the peptide trap was then switched on-line with the analytical column. Peptides were eluted with the linear gradients with a flow rate of 300nl/minute. Peptides were ionised by electrospray ionisation and data-dependent MS/MS acquisition carried out using a Q Exactive consisting of 1 full MS1 (R=70 K) scan acquisition from 350 to 1850 m/z, and 10 HCD type MS2 scans (R=70 K).

Database search, statistical analysis, and bioinformatics

The raw data files were submitted to Proteome Discoverer (version 1.3, Thermo Scientific) and processed using Sequest and Mascot (Matrix Science, London, UK) against *S. aureus* reference strain (ATCC 25923) as described in Chapter 2, 2.2.7). After the extraction of protein ratios with Proteome Discoverer, additional processing and statistical analysis was conducted using the TMTPrePro R package [455]. BLAST search was performed using highly annotated strains *S. aureus* N315 and *S. aureus* COL. Proteins were considered upregulated when the TMT ratio was above 1.5 and downregulated when the TMT ratio was lower than 0.66 in biofilm growth compared to planktonic growth with significant p-value < 0.05. Significant differentially

expressed proteins (>2-fold) were determined by using VENNY, metabolic pathway analysis using KEGG mapper, subcellular localisation using PSORTb [456], and protein–protein interaction (PPI) network of significantly differentially expressed proteins were analysed by STRING software [457].

Correlation of TMT data with real-time qPCR results

Five genes encoding (1) Hyaluronate lyase HysA, (2) Chitinase SA0914, (3) Glutamyl endopeptidase sspA, (4) pyruvate carboxylase pyc, and (5) Succinate dehydrogenase sdhB were chosen as targets to analyse the RNA expression difference to validate the protein expression differences in planktonic and biofilms revealed by TMT method. The 16S rRNA was used as an endogenous control to normalise the data, and the level of differential expression of the four genes between planktonic and biofilm were compared.

RNA was extracted using a RNeasy Mini Kit (Qiagen, Germany) and cDNA synthetised from 200ng of RNA using the SuperScript™ IV VILO™ Master Mix (Thermo Fisher Scientific) as described in Chapter 2, sections 2.3.2, 2.3.3 and 2.3.4. Real-time (RT)-PCR was performed in duplicate on two biological replicates as described in Chapter 2 section 2.3.6.

Primer sequences used in this study as described in Chapter 2 section 2.3.5.

Results

TMT identification

A total of 1636 non-redundant proteins with at least one unique peptide and <1% FDR were identified and quantitated across at 10 replicates. In this study, we specifically focused on only extractomes (extracted supernatant proteins) to explore the proteome changes that exist between different stages of biofilms. We have not considered a large part of precipitated cell pellet fractions in this study. In addition, present study, we considered master proteins, FDR <1%, PSMs (high confidence), peptide length >5 amino acids per protein with at least 1 unique peptide. Therefore, it is considered as a comprehensive coverage of proteome in this model organism. For example, iTRAQ-based cell surface shaving proteomics using *S. epidermidis* reported a total of 1610 proteins [460]. Of these, 273 proteins were significantly ($p < 0.05$) differentially regulated

significant proteins (DRSPs) greater than 2-fold change during biofilm growth in comparison to planktonic bacteria. These 273 DRSPs could be regarded as potential variables responsible for difference in the proteome of biofilm compared with planktonic growth. Of these, 82 proteins were upregulated (Table 3.2) and 191 were downregulated in the biofilm (Table 3.3). Of the upregulated biofilm proteins 35 proteins (42.7%) were associated with recognised protein pathways. Similarly, 74 (38.7%) of the downregulated biofilm proteins were associated with recognised protein pathways. Among the DRSPs, we identified a total of 34 hypothetical proteins and hypothetical protein KQ76_04110 had the highest differential expression being upregulated 5.09-fold. We identified a molybdenum ABC transporter permease (4.68-fold upregulated) and transport of molybdenum via ABC transporter into the cells is essential for bacterial growth [464]. Further, we identified DNA-directed RNA polymerase subunit omega (4.50-fold) which is involved in RNA polymerase, pyrimidine and purine metabolism, glycosyltransferase (4.32-fold), and branched-chain amino acid transporter II carrier protein (4.04-fold).

The most downregulated protein was delta-hemolysin (-34.02-fold) which is involved in quorum sensing. Delta-hemolysin is a small amphipathic membrane-damaging virulence factor protein and showed potential antimicrobial activity. Delta-hemolysin may act either by binding to the surface of the cell and aggregating to form transmembrane pores, thus destabilising the cytoplasmic membrane by affecting the membrane curvature, or function as a detergent by solubilising the membrane at higher concentration [465]. Significant downregulation of this protein may prevent the dispersal of cells thereby enhance the biofilm formation. Spermidine/putrescine ABC transporter substrate-binding protein (potD) was also downregulated 22.02-fold and functions in the ABC transporter pathway. PotD is a periplasmic substrate-binding protein that binds extracellular polyamines (e.g. spermidine, putrescine) and binding of spermidine to PotD is essential for building more compact protein structure and cell growth. PotD negatively regulates the spermidine-preferential uptake system transcription of the operon, thereby decrease in spermidine uptake activity leads to increased polyamines accumulation in cells [466, 467]. In addition, extracellular proteins including alpha-hemolysin (-13.82-fold), phosphodiesterase (-12.33-fold), cysteine protease (-11.44-fold), and transglycosylase (-10.14-fold) were also downregulated. Several ribosomal proteins were also downregulated (Table 3.3).

In addition, we identified 20 virulence factor proteins using VFDB among the DRSPs (Table 3.4).

Table 3.2: List of the significantly upregulated proteins in *S. aureus* biofilm in comparison to planktonic culture (fold change >2, p <0.05). * CM denotes Cytoplasmic Membrane.

Accession ID	Protein Name	Gene Names	Fold Change	Protein Pathways	Subcellular Localisation	p Value
AIO20486.1	hypothetical protein KQ76_04110	SA0772	5.09		Unknown	0.000397681
AIO21910.1	molybdenum ABC transporter permease	modB	4.68	ABC transporters	CM*	0.001089457
AIO20812.1	DNA-directed RNA polymerase subunit omega	rpoZ SA1053	4.52	Metabolic pathways, Pyrimidine metabolism, RNA polymerase, Purine metabolism	Unknown	0.000904083
AIO20306.1	glycosyltransferase	tagX SA0596	4.32		Unknown	0.013477413
AIO19852.1	branched-chain amino acid transporter II carrier protein	SA0180	4.04		CM	0.011555503
AIO21307.1	hypothetical protein KQ76_08425	SA1443	3.57		Cytoplasmic	0.008662183
AIO20635.1	hypothetical protein KQ76_04890	SACOL1046	3.43		Unknown	0.000370515

AIO21316.1	hypothetical protein KQ76_08470	SAS049	3.38		Unknown	0.001552903
AIO21773.1	membrane protein	SA1937	3.32		CM	8.57136E-05
AIO21982.1	hypothetical protein KQ76_12230	SACOL2344	3.30		Cytoplasmic	0.003244436
AIO21211.1	2-oxoisovalerate dehydrogenase	bfmBAA	3.19	Metabolic pathways, Biosynthesis of secondary metabolites, Biosynthesis of antibiotics, Propanoate metabolism, Valine, leucine and isoleucine degradation	Cytoplasmic	0.003348128
AIO20267.1	NAD(P)H-dependent oxidoreductase	SA0558	3.17		Unknown	2.972E-05
AIO21660.1	DNA-binding protein		3.12		Cytoplasmic	0.001652037
AIO22226.1	fructosamine kinase	SA2374	2.97		Cytoplasmic	0.000268392
AIO19750.1	transposase	SA0379	2.91		Cytoplasmic	0.001955142
AIO19867.1	peptide ABC transporter substrate-binding protein	SACOL0187	2.91	Quorum sensing	Unknown	0.005248609
AIO21786.1	lytic regulatory protein	truncated-SA	2.89		CM	0.014079978

AIO22040.1	formate/nitrite transporter	SACOL2401	2.84		CM	0.005637221
AIO22234.1	pantoate--beta-alanine ligase	panC SACOL2614	2.82	Metabolic pathways, Biosynthesis of secondary metabolites, beta-Alanine metabolism, Pantothenate and CoA biosynthesis	Cytoplasmic	0.000736711
AIO20180.1	2-amino-4-hydroxy-6-hydroxymethyldihydropteridine pyrophosphokinase	folK SACOL0560	2.78	Metabolic pathways, Folate biosynthesis	Cytoplasmic	0.008211938 0.002109738
AIO20754.1	fibrinogen-binding protein	SA1000	2.78		Extracellular	0.000777275
AIO21317.1	hypothetical protein KQ76_08475	SA1452	2.76		Extracellular	0.011894905
AIO20178.1	dihydropteroate synthase	folP SA0472	2.76	Metabolic pathways, Folate biosynthesis	Cytoplasmic	0.006085794
AIO20957.1	30S ribosomal protein S14	rpsN rpsN2 SA1171	2.76	Ribosome	Cytoplasmic	0.001910489
AIO20787.1	cell division protein FtsA	ftsA	2.74		Cytoplasmic	0.002524267

		SA1028				
AIO20718.1	glycerophosphodiester phosphodiesterase	SA0969	2.72	Glycerophospholipid metabolism	Cytoplasmic	0.003643299
AIO21337.1	50S ribosomal protein L27	rpmA SA1471	2.64	Ribosome	Cytoplasmic	0.007344563
AIO21082.1	zinc metallopeptidase	SACOL1500	2.59		CM	0.006616234
AIO21503.1	restriction endonuclease subunit S	hsdS	2.57		Unknown	0.002887605
AIO21727.1	membrane protein	yidC SA1893	2.53	Quorum sensing, Protein export, Bacterial secretion system	CM	0.002808562
AIO21819.1	hypothetical protein KQ76_11385	SA1986	2.52		CM	0.001362946
AIO21839.1	hyaluronate lyase	hysA	2.50		Extracellular	0.011121186
AIO22003.1	L-lactate permease	SACOL2363	2.47		CM	0.002058241
AIO21769.1	hypothetical protein KQ76_11075	SA1933	2.47		Cytoplasmic	0.000623182
AIO20806.1	orotidine 5'-phosphate	pyrF	2.42	Metabolic pathways,	Cytoplasmic	0.006355221

	decarboxylase	SA1047		Pyrimidine metabolism		
AIO20697.1	spermidine/putrescine ABC transporter ATP-binding protein	potA SA0950	2.39	ABC transporters	CM	0.001682293
AIO21790.1	glucosamine--fructose-6-phosphate aminotransferase	glmS SACOL2145	2.37	Metabolic pathways, Amino sugar and nucleotide sugar metabolism, Alanine, aspartate and glutamate metabolism, Biosynthesis of antibiotics	Cytoplasmic	0.000709148
AIO20817.1	peptide deformylase	SA1058	2.35		Cytoplasmic	0.005310652
AIO21826.1	PTS system lactose-specific transporter subunit IIA	lacF SA1993	2.34	Metabolic pathways, Galactose metabolism, Phosphotransferase system (PTS)	Cytoplasmic	0.001945845
AIO20444.1	glyceraldehyde-3-phosphate	gapA1 gap	2.34	Metabolic pathways,	Cytoplasmic	0.000923701 0.002367404 0.000366962

	dehydrogenase	gapA SA0727		Biosynthesis of antibiotics, Biosynthesis of amino acids, Microbial metabolism in diverse environments, Carbon metabolism, Biosynthesis of secondary metabolites, Glycolysis / Gluconeogenesis		
AIO21863.1	30S ribosomal protein S5	rpsE SA2031	2.33	Ribosome	Cytoplasmic	4.37428E-05
AIO21333.1	ATP-dependent DNA helicase RuvB	ruvB SACOL1696	2.33	Homologous recombination	Cytoplasmic	0.001784239
AIO20122.1	cystathionine gamma-synthase	metB	2.33	Metabolic pathways, Biosynthesis of antibiotics, Biosynthesis of amino acids, Cysteine and methionine metabolism, Glycine, serine and threonine metabolism, Sulfur metabolism	Cytoplasmic	0.000472788
OOC89123.1	heme ABC transporter ATP-	SACOL07	2.3293		Cytoplasmic	0.024741395

	binding protein	79				
AIO22129.1	helicase	SACOL2499	2.28		Unknown	0.001134695
AIO20958.1	guanosine 5'-monophosphate oxidoreductase	guaC SACOL1371	2.28	Purine metabolism	Cytoplasmic	0.004134617
AIO21372.1	helicase DnaB	SACOL1732	2.27		Cytoplasmic	0.000430905
AIO20949.1	threonine synthase	thrC SACOL1363	2.27	Metabolic pathways, Biosynthesis of secondary metabolites, Microbial metabolism in diverse environments, Vitamin B6 metabolism, Glycine, serine and threonine metabolism, Biosynthesis of amino acids	Cytoplasmic	0.019360539
AIO21528.1	hypothetical protein KQ76_09615	SA1657	2.26		Unknown	0.00265363
AIO19973.1	5'-nucleotidase	SA0295	2.23		Unknown	0.002111067
AIO20535.1	argininosuccinate lyase	argH	2.21		Cytoplasmic	0.002967449

		SA0821		Metabolic pathways, Biosynthesis of secondary metabolites, Biosynthesis of antibiotics, Biosynthesis of amino acids, Alanine, aspartate and glutamate metabolism, Arginine biosynthesis		0.018119505
AIO21844.1	acetolactate synthase	alsS	2.21	Metabolic pathways, Biosynthesis of secondary metabolites, Biosynthesis of antibiotics, Biosynthesis of amino acids, Pantothenate and CoA biosynthesis, 2-Oxocarboxylic acid metabolism, C5-Branched dibasic acid metabolism, Butanoate metabolism, Valine, leucine and isoleucine biosynthesis	CM	0.00129439

AIO21768.1	pantothenate kinase	coaW SA1932	2.17	Metabolic pathways, Pantothenate and CoA biosynthesis	Unknown	0.00725931
AIO21133.1	capsid protein		2.17		Extracellular	0.004077618
AIO20460.1	coagulase	SACOL0857	2.17		Extracellular	0.003958347
AIO21800.1	chromosome partitioning protein ParA	SA1969	2.16		Cytoplasmic	0.004630227
AIO21846.1	ATP-dependent DNA helicase RecG		2.15		Cytoplasmic	0.012274163
AIO21327.1	adenine phosphoribosyltransferase	apt SA1461	2.15	Metabolic pathways, Purine metabolism	Cytoplasmic	0.019154857
AIO20536.1	argininosuccinate synthase	argG SA0822	2.15	Metabolic pathways, Biosynthesis of secondary metabolites, Biosynthesis of antibiotics, Biosynthesis of amino acids, Alanine, aspartate and glutamate metabolism,	Cytoplasmic	0.011986456

				Arginine biosynthesis		
AIO20205.1	50S ribosomal protein L10	rplJ SA0497	2.15	Ribosome	Cytoplasmic	0.001090509
AIO21502.1	NTPase		2.13		Unknown	0.003400651
AIO19985.1	N-acetylmannosamine-6-phosphate 2-epimerase	nanE SACOL0315	2.13	Amino sugar and nucleotide sugar metabolism	Cytoplasmic	0.039199547
AIO21111.1	lipoprotein	SACOL1528	2.12		Unknown	0.002267015
AIO20869.1	prolyl-tRNA synthetase	proS SA1106	2.12	Aminoacyl-tRNA biosynthesis	Cytoplasmic	0.001404809
AIO21190.1	aldo/keto reductase	SACOL1543	2.11		Cytoplasmic	0.000866702
AIO22278.1	amino acid APC transporter	arcD	2.10		CM	0.008765176
AIO19888.1	coagulase	coa	2.10		Extracellular	0.02084422
AIO20778.1	hypothetical protein KQ76_05635	SA1019	2.09		Unknown	0.01903872
AIO21086.1	3-phosphoshikimate 1-carboxyvinyltransferase	aroA SACOL15	2.09	Metabolic pathways, Biosynthesis of secondary	Cytoplasmic	0.001855961

		04		metabolites, Biosynthesis of antibiotics, Biosynthesis of amino acids, Phenylalanine, tyrosine and tryptophan biosynthesis		
AIO21153.1	hypothetical protein KQ76_07625	SACOL0347	2.08		Cytoplasmic	0.009574964
AIO20531.1	NADH-dependent flavin oxidoreductase	SACOL0959	2.08		Cytoplasmic	0.018402847
AIO20985.1	LytR family transcriptional regulator	msrR SA1195	2.08		CM	0.005089303
AIO20616.1	glycosyl transferase family 1	SACOL1043	2.08		Cytoplasmic	0.023847212
AIO20898.1	(dimethylallyl)adenosine tRNA methylthiotransferase	miaB SA1134	2.06		Cytoplasmic	0.008502906
AIO22086.1	epimerase	SA2231	2.06		Cytoplasmic	0.032173983
OOC90965.1	glutamine ABC transporter ATP-binding protein	SA1674	2.05		CM	0.007892711
AIO20143.1	thymidylate kinase	tmk SA0440	2.03	Metabolic pathways,	Cytoplasmic	0.002141712

AIO20221.1	HAD family hydrolase	SACOL0602	2.02	Pyrimidine metabolism Metabolic pathways, Biosynthesis of secondary metabolites, Biosynthesis of antibiotics, Glyoxylate and dicarboxylate metabolism	Cytoplasmic	0.000172417
AIO19823.1	UDP-N-acetylglucosamine 2-epimerase	capG	2.02	Metabolic pathways, Amino sugar and nucleotide sugar metabolism	Cytoplasmic	0.000397681
AIO21443.1	hypothetical protein KQ76_09120	SA1573	2.01		Unknown	0.001089457
AIO22323.1	histidinol-phosphate aminotransferase	SACOL2701	2.01	Metabolic pathways, Biosynthesis of secondary metabolites, Biosynthesis of antibiotics, Biosynthesis of amino acids, Phenylalanine, tyrosine and tryptophan biosynthesis, Novobiocin biosynthesis, Tyrosine metabolism, Histidine	Cytoplasmic	0.000904083

				metabolism, Phenylalanine metabolism		
AIO21737.1	UDP-N-acetylglucosamine 1-carboxyvinyltransferase	murA1 murA SA1902	2.01	Metabolic pathways, Peptidoglycan biosynthesis, Amino sugar and nucleotide sugar metabolism	Cytoplasmic	0.013477413

Table 3.3: List of the significantly downregulated proteins in *S. aureus* biofilm in comparison to planktonic culture (fold change >-2, p <0.05). * CM denotes Cytoplasmic Membrane.

Accession ID	Protein Name	Gene Names	Fold Change	Protein Pathways	Subcellular Localisation	p Value
AIO21667.1	delta-hemolysin	hld SA1841.1 SAS065	-34.02	Quorum sensing	Cytoplasmic	0.004019645
AIO20700.1	spermidine/putrescine ABC transporter substrate-binding protein	potD	-22.04	ABC transporters	Unknown	0.001406803
AIO20763.1	alpha-hemolysin	SA1007	-13.83		Extracellular	0.00070713
AIO22369.1	phosphodiesterase	hlb SACOL2003	-12.33		Extracellular	0.000441333
OOC90902.1	calcium-binding protein	SACOL1846	-11.77		Unknown	0.001335183
AIO20644.1	cysteine protease	sspB SACOL1056	-11.44		Extracellular	0.00107553
AIO22207.1	transglycosylase	isaA SACOL2584	-10.14		Extracellular	0.00664751
AIO20556.1	hypothetical protein KQ76_04470	SA0841	-9.46		CM*	0.001704132
AIO19942.1	peptidase M23	lytM	-9.30		Extracellular	0.000232208

		SACOL0263				
AIO20056.1	hypothetical protein KQ76_01725		-8.47		CM	0.000575663
AIO20660.1	chitinase	SA0914	-8.44		Unknown	0.001488005
AIO19870.1	peptidase M23	SA0205	-8.28		Extracellular	0.003345954
AIO21024.1	cold-shock protein	cspA SA1234	-8.08		Cytoplasmic	0.000433667
AIO19947.1	staphyloxanthin biosynthesis protein	SACOL0270	-7.54		Extracellular	0.008160513
AIO21349.1	DNA-3-methyladenine glycosylase	tag	-7.16	Base excision repair	Unknown	0.005926526
AIO21509.1	serine protease	splC SACOL1867	-6.98		Extracellular	0.001464329
AIO20463.1	thermonuclease	nuc SACOL0860	-6.97		Extracellular	0.000965933
AIO20332.1	peptidase M23B	SA0620	-6.86		Cell wall	0.000571171
AIO20645.1	glutamyl endopeptidase	sspA SACOL1057	-6.52	Quorum sensing	Extracellular	0.000496544
AIO20716.1	SCP-like extracellular protein	SA0967	-6.49		Unknown	0.00154168
AIO19770.1	1-phosphatidylinositol phosphodiesterase	plc	-5.85	Inositol phosphate metabolism	Extracellular	0.001894738

AIO20387.1	glycerol phosphate lipoteichoic acid synthase	ltaS SA0674	-5.84	Metabolic pathways, Glycerolipid metabolism	CM	0.001375108
AIO22290.1	N-acetylmuramoyl-L-alanine amidase	SACOL2666	-5.80		Extracellular	0.000585867
AIO21492.1	hypothetical protein KQ76_09365	SACOL1852	-5.35		Unknown	9.36522E-05 0.002501282
AIO20326.1	response regulator GraR	graR SACOL0716	-5.34	Two-component system, Cationic antimicrobial peptide (CAMP) resistance	Cytoplasmic	0.020751891
AIO21221.1	acetyl-CoA carboxylase	accB	-5.16	Metabolic pathways, Microbial metabolism in diverse environments, Biosynthesis of secondary metabolites, Biosynthesis of antibiotics, Pyruvate	Cytoplasmic	0.007095826

				metabolism, Carbon metabolism, Fatty acid metabolism, Propanoate metabolism, Fatty acid biosynthesis		
AIO19779.1	peptigoglycan-binding protein LysM	spa SACOL0095	-4.71	*Staphylococcus aureus* infection	Cell wall	0.0024712
AIO20739.1	ribonuclease HIII	rnhC SACOL1150	-4.61	DNA replication	Unknown	0.001713369
AIO20228.1	hydrolase	sdrD SA0520	-4.49	*Staphylococcus aureus* infection	Cell wall	0.001796636
AIO20762.1	hypothetical protein KQ76_05550	SA1005	-4.44		Unknown	0.000463513
AIO20126.1	N-acetylmuramoyl-L-alanine amidase	sle1 aaa SA0423	-4.42		Cell wall	0.000244056
AIO20637.1	acetyltransferase	SA0893	-4.41		Cytoplasmic	0.001147454
AIO21273.1	molecular chaperone DnaJ	dnaJ SA1408	-4.24		Cytoplasmic	0.002410513
AIO20577.1	competence negative regulator MecA	mecA SA0857	-4.19		Cytoplasmic	0.000921482

AIO20418.1	ABC transporter	SACOL0811	-4.18		Cytoplasmic	0.000873147
AIO21353.1	delta-aminolevulinic acid dehydratase	hemB SA1492	-4.18	Metabolic pathways, Microbial metabolism in diverse environments, Biosynthesis of secondary metabolites, Porphyrin and chlorophyll metabolism	Cytoplasmic	0.001447915
AIO21508.1	serine protease	splE SACOL1865	-4.18	Quorum sensing	Extracellular	0.000743712
AIO19905.1	nucleoside hydrolase	SACOL0225	-4.17		Cytoplasmic	0.00138688
AIO20630.1	hypothetical protein KQ76_04865	SACOL1575	-4.12		Unknown	0.001714034
AIO19987.1	lipase	lip2 geh SA0309	-4.12	Metabolic pathways, Glycerolipid metabolism	Extracellular	0.004220453
AIO20479.1	arsenate reductase	SA0759	-4.06		Cytoplasmic	0.000110371
AIO20651.1	mannosyl-glycoprotein endo-beta-N-	atl nag SACOL1062	-4.01		Extracellular	0.00201878 0.002648041

	acetylglucosamidase					
AIO21549.1	Fur family transcriptional regulator	perR SACOL1919	-4.00		Cytoplasmic	0.006150869
AIO22042.1	glutathione S-transferase	SACOL2402	-3.94		Unknown	0.005307007
AIO21406.1	Free methionine-(R)-sulfoxide reductase	SACOL1768	-3.85	Cysteine and methionine metabolism	Cytoplasmic	0.000152835
AIO20229.1	bis(5'-nucleosyl)-tetraphosphatase	sdrE SACOL0610	-3.82	*Staphylococcus aureus* infection	Cell wall	0.003530896
AIO22060.1	gamma-hemolysin subunit A	hlgC SA2208	-3.79	*Staphylococcus aureus* infection	Extracellular	0.001213016
AIO20738.1	phenylalanyl-tRNA synthase subunit beta	pheT SA0986	-3.75	Aminoacyl-tRNA biosynthesis	Cytoplasmic	0.003960157
AIO21601.1	cysteine protease	sspP scpA SA1725	-3.73		Extracellular	0.003999966
AIO20874.1	50S ribosomal protein L7	SA1111	-3.73		Unknown	0.004018714
AIO21505.1	serine protease	splF SA1627	-3.71	Quorum sensing	Extracellular	0.004462777
AIO22081.1	sodium:proton antiporter	SA2228	-3.68		CM	0.00388415
AIO20884.1	zinc protease	SA1121	-3.66		Cytoplasmic	0.002193235
AIO20093.1	superantigen-like protein	set11	-3.63	*Staphylococcus aureus* infection	Extracellular	0.00334413

AIO21182.1	transcriptional regulator	srrA SA1323	-3.63	Two-component system	Cytoplasmic	0.016280333
AIO20960.1	secretion protein	SACOL1373	-3.63		Unknown	6.47033E-05
AIO22350.1	peptidase		-3.61		Extracellular	0.005235913
AIO21805.1	uridylyltransferase	SA1974	-3.60		Cytoplasmic	0.002126712
AIO21491.1	hypothetical protein KQ76_09360	SACOL1851	-3.58		Cytoplasmic	0.005303318
AIO20144.1	hypothetical protein KQ76_02220	SA0441	-3.57		Unknown	0.002311961
AIO21160.1	single-stranded DNA-binding protein	ssb	-3.53	Homologous recombination, Mismatch repair, DNA replication	Unknown	0.002752116
AIO22099.1	peptidase M28	SA2244	-3.47		Cytoplasmic	0.002128977
AIO22349.1	hypothetical protein KQ76_14165		-3.46		Unknown	0.006679391
AIO20756.1	formyl peptide receptor-like 1 inhibitory protein	flr SA1001	-3.39	*Staphylococcus aureus* infection	Unknown	0.00128061
AIO20951.1	HAD family hydrolase	SA1167	-3.34		Cytoplasmic	0.001232071
AIO22292.1	adhesin	sasF SACOL2668	-3.28		Cell wall	0.001048986

AIO19988.1	alpha/beta hydrolase	SACOL0391	-3.27		Cytoplasmic	0.001019697
AIO20737.1	phenylalanine--tRNA ligase	pheS SA0985	-3.27	Aminoacyl-tRNA biosynthesis	Cytoplasmic	0.001302771
AIO21246.1	penicillin-binding protein	pbp3	-3.24	Metabolic pathways, beta-Lactam resistance, Peptidoglycan biosynthesis	CM	0.002031879
OOC94232.1	aureolysin	aur SACOL2659	-3.22	*Staphylococcus aureus* infection, Cationic antimicrobial peptide (CAMP) resistance	Extracellular	0.002259606
AIO21853.1	50S ribosomal protein L17	rplQ SA2022	-3.19	Ribosome	Cytoplasmic	0.000160943
AIO21391.1	oligoribonuclease	SA1526	-3.17	Metabolic pathways, Microbial metabolism in diverse environments, Sulfur metabolism	Cytoplasmic	0.003855623
AIO21842.1	toxin	SACOL2197	-3.14		CM	0.004486491
AIO22206.1	acetyltransferase	oatA SA2354	-3.12		CM	0.02919433
AIO21365.1	50S ribosomal protein L20	rplT SA1502	-3.09	Ribosome	Cytoplasmic	0.00887712

AIO21565.1	hypothetical protein KQ76_09970	SAS054	-3.08		Cytoplasmic	0.002630488
AIO22160.1	lactate dehydrogenase	ldhD ddh SACOL2535	-3.04	Pyruvate metabolism, Microbial metabolism in diverse environments	Cytoplasmic	0.000224831
AIO20515.1	hypothetical protein KQ76_04260	SACOL0943	-3.00		Cytoplasmic	0.001038762
OOC94758.1	alpha/beta hydrolase	SA1990	-2.98		Unknown	0.011935531
AIO22074.1	glycerate kinase	SA2220	-2.97	Metabolic pathways, Microbial metabolism in diverse environments, Biosynthesis of antibiotics, Glycerolipid metabolism, Glyoxylate and dicarboxylate metabolism, Glycine,	Cytoplasmic	0.000826686

				serine and threonine metabolism		
AIO21275.1	heat shock protein GrpE	grpE SA1410	-2.97		Cytoplasmic	0.015942198
AIO22275.1	clumping factor B	clfB SA2423	-2.96	*Staphylococcus aureus* infection	Cell wall	0.002326341
AIO20071.1	NADPH-dependent oxidoreductase	nfrA SACOL0453	-2.92	Metabolic pathways, Riboflavin metabolism	Cytoplasmic	0.003816543
AIO22317.1	lipase	lip1 SA2463	-2.89	Metabolic pathways, Glycerolipid metabolism	Extracellular	0.00077633
AIO19780.1	MarR family transcriptional regulator	sarS sarH1 SA0108	-2.87		Cytoplasmic	0.005480508
AIO21530.1	peptidylprolyl isomerase	prsA SA1659	-2.86		CM	0.002588729
AIO21602.1	staphostatin A	SA1726	-2.86		Unknown	0.000622091
AIO20100.1	hypothetical protein KQ76_01960	SA0395	-2.85		Unknown	0.002487361
AIO20776.1	phenol soluble modulin	SACOL1186	-2.85	Quorum sensing	Unknown	0.006037462
AIO20863.1	elongation factor Ts	tsf SACOL1276	-2.82		Cytoplasmic	0.003329166
OOC93971.1	phosphoglucomutase	pgcA SA2279	-2.81	Metabolic pathways, Microbial metabolism	Cytoplasmic	0.0095828

				in diverse environments, Biosynthesis of secondary metabolites, Biosynthesis of antibiotics, Purine metabolism, Amino sugar and nucleotide sugar metabolism, Starch and sucrose metabolism, Streptomycin biosynthesis, Glycolysis / Gluconeogenesis, Pentose phosphate pathway, Galactose metabolism		
AIO21506.1	serine protease	splE SACOL1865	-2.81		Extracellular	0.003993169
AIO20279.1	hypothetical protein	SA0570	-2.80		Unknown	0.009827721

AIO21343.1	KQ76_03005 membrane protein	SA1476	-2.76		Unknown	0.003236219 0.010605903
AIO20368.1	PTS fructose transporter subunit IIC	fruA	-2.73	Metabolic pathways, Microbial metabolism in diverse environments, Fructose and mannose metabolism, Phosphotransferase system (PTS)	CM	0.000934546
AIO20534.1	glycerophosphodiester phosphodiesterase	glpQ	-2.73	Glycerophospholipid metabolism	Unknown	0.00302594
AIO20049.1	pathogenicity island protein	SA1824	-2.72		Unknown	0.000674744
AIO21274.1	molecular chaperone DnaK	dnaK SA1409	-2.68	RNA degradation	Cytoplasmic	0.000354591
AIO21449.1	leucyl-tRNA synthetase	leuS SA1579	-2.67	Aminoacyl-tRNA biosynthesis	Cytoplasmic	8.97721E-05

AIO21282.1	competence protein ComE	comEB	-2.67	Metabolic pathways, Pyrimidine metabolism	Cytoplasmic	0.001919851
AIO21436.1	peptidase M28	SA1566	-2.66		Cytoplasmic	0.001579626
AIO20170.1	hypothetical protein KQ76_02355	SA0464	-2.65		Cytoplasmic	0.004619411
AIO21073.1	hypothetical protein KQ76_07205	SACOL1491	-2.65		Unknown	0.019763356
AIO21788.1	HAD family hydrolase	SA1957	-2.64		Cytoplasmic	0.000298696
AIO22136.1	fibronectin-binding protein	fnbA SA2291	-2.60	Bacterial invasion of epithelial cells	Cell wall	1.7344E-05
AIO21371.1	primosomal protein DnaI	dnaI	-2.59		Cytoplasmic	0.001092641
AIO20579.1	oligopeptidase PepB	SA0859	-2.58		Cytoplasmic	8.04135E-05
AIO20152.1	methionine--tRNA ligase	metG metS SA0448	-2.58	Selenocompound metabolism, Aminoacyl-tRNA biosynthesis	Cytoplasmic	0.006707407
AIO20286.1	recombinase	SA0577	-2.58		Cytoplasmic	0.002044168
OOC92415.1	sphingomyelin phosphodiesterase	hlb SACOL2003	-2.56	Quorum sensing, Metabolic pathways, Inositol phosphate	Extracellular	0.001875872

				metabolism, Glycerophospholipid metabolism, Biosynthesis of secondary metabolites		
AIO20439.1	Clp protease	clpP SA0723	-2.55		Cytoplasmic	0.004844428
AIO21970.1	ribose 5-phosphate isomerase	rpiA SA2127	-2.54	Metabolic pathways, Microbial metabolism in diverse environments, Carbon metabolism, Biosynthesis of secondary metabolites, Biosynthesis of antibiotics, Biosynthesis of amino acids, Pentose phosphate pathway	Cytoplasmic	3.53798E-05
AIO20435.1	thioredoxin reductase	trxB SA0719	-2.54	Selenocompound	Cytoplasmic	0.000526989 0.000441124

				metabolism		
				Metabolic pathways, Microbial metabolism in diverse environments, Biosynthesis of secondary metabolites, Biosynthesis of antibiotics, Pyruvate metabolism, Carbon metabolism, Fatty acid metabolism, Propanoate metabolism, Fatty acid biosynthesis		0.008090389
AIO21298.1	acetyl-CoA carboxylase biotin carboxylase subunit	SA1434	-2.52		Cytoplasmic	
AIO21363.1	DNA mismatch repair protein MutT	SA1501	-2.50		Cytoplasmic	0.010264455
AIO20575.1	tryptophanyl-tRNA synthetase	trpS SA0855	-2.50	Aminoacyl-tRNA biosynthesis	Cytoplasmic	0.00033905
AIO21606.1	nicotinate	SA1729	-2.49	Metabolic pathways,	Cytoplasmic	0.010264455

	phosphoribosyltransferase			Nicotinate and nicotinamide metabolism		
AIO22387.1	replication-associated protein (plasmid)	SAP031	-2.49		Unknown	0.002059029
AIO20282.1	transcriptional regulator	sarA SA0573	-2.48		Cytoplasmic	0.000422988
AIO20202.1	antitermination protein NusG	nusG SA0494	-2.48		Cytoplasmic	0.000206252 0.000682766
AIO21595.1	lipoprotein	SA1719	-2.46		Unknown	0.007153735
AIO22291.1	isochorismatase	SA2438	-2.45		Unknown	0.0042208
AIO21531.1	3'-5' exonuclease	cbf1	-2.44		Cytoplasmic	0.019574424
AIO20398.1	7-cyano-7-deazaguanine reductase	queF SA0683	-2.44	Metabolic pathways, Folate biosynthesis	Cytoplasmic	0.006065134
AIO21033.1	hypothetical protein KQ76_06965	SA1242	-2.44		Unknown	0.001266785
AIO19802.1	cell wall surface anchor family protein	sasD SACOL0119	-2.43		Cell wall	0.000152791
AIO21623.1	thioredoxin	SA1743	-2.41		Unknown	0.000401156
AIO20231.1	glycosyl transferase family	SACOL0612	-2.41		Cytoplasmic	0.001570981

	1					
AIO20885.1	zinc protease	SACOL1298	-2.40		Unknown	0.001377871
AIO21583.1	ferritin	ftnA SA1709	-2.39		Cytoplasmic	0.002264344
AIO22235.1	3-methyl-2-oxobutanoate hydroxymethyltransferase	panB SA2392	-2.37	Metabolic pathways, Biosynthesis of secondary metabolites, Pantothenate and CoA biosynthesis	Unknown	0.006828514
AIO20406.1	iron ABC transporter substrate-binding protein	SA0691	-2.37	ABC transporters	CM	0.016825507 0.005828318
AIO20712.1	pyruvate carboxylase	pyc SACOL1123	-2.35	Metabolic pathways, Pyruvate metabolism, Microbial metabolism in diverse environments, Biosynthesis of amino acids, Carbon metabolism, Citrate cycle (TCA cycle)	Cytoplasmic	0.00039883

				Metabolic pathways, Microbial metabolism in diverse environments, Benzoate degradation, Xylene degradation, Degradation of aromatic compounds		0.00129283
AIO22158.1	glyoxalase	SA2310	-2.35		Unknown	
AIO20704.1	hypothetical protein KQ76_05255	SA0957	-2.34		Cytoplasmic	0.010138105
				Metabolic pathways, Biosynthesis of secondary metabolites, Arginine biosynthesis, Arginine and proline metabolism		0.001364193
AIO21607.1	nitric oxide synthase	nos SA1730	-2.34		Cytoplasmic	
AIO22191.1	TetR family transcriptional regulator	SA2340	-2.33		Cytoplasmic	0.003622702
AIO22006.1	acetyltransferase	SA2159	-2.33		Cytoplasmic	0.003897145
AIO20913.1	glutamine synthetase	glnA	-2.32	Metabolic pathways,	Cytoplasmic	0.004517754

		SACOL1329		Two-component system, Biosynthesis of amino acids, Glyoxylate and dicarboxylate metabolism, Arginine biosynthesis, Microbial metabolism in diverse environments, Alanine, aspartate and glutamate metabolism, Nitrogen metabolism		
AIO20225.1	HAD family hydrolase	SA0517	-2.32		Cytoplasmic	0.002140455
AIO22285.1	hypothetical protein KQ76_13835	SACOL2661	-2.31		Extracellular	0.001359211
AIO19949.1	type VII secretion protein EsaA	esaA SA0272	-2.29		CM	3.70988E-05
AIO21929.1	transcriptional regulator	SA2091	-2.28		Unknown	0.004084917
AIO21020.1	hydrolase	SACOL1433	-2.28		Cytoplasmic	0.000580316
AIO21157.1	replication protein		-2.28		Cytoplasmic	0.006259143

						0.011553995
AIO22336.1	pyrrolidone-carboxylate peptidase	pcp SACOL2714	-2.27		Cytoplasmic	0.00040605
				Metabolic pathways, Microbial metabolism in diverse environments, Carbon metabolism, Biosynthesis of secondary metabolites, Biosynthesis of antibiotics, Biosynthesis of amino acids, Methane metabolism, Glycolysis / Gluconeogenesis, Glycine, serine and threonine metabolism		0.004996645
AIO22054.1	phosphoglyceromutase	gpmA SA2204	-2.24		Unknown	
OOC89529.1	dUTP pyrophosphatase	dut SACOL0357	-2.23	Metabolic pathways, Pyrimidine metabolism	Cytoplasmic	0.001411317

AIO21679.1	ABC transporter ATP-binding protein	vga	-2.23		Cytoplasmic	0.004454181
AIO21204.1	hypothetical protein KQ76_07895	SACOL1555	-2.22		Cytoplasmic	0.001343001
						0.000940318
AIO21459.1	riboflavin synthase subunit alpha	ribE SACOL1819	-2.22	Metabolic pathways, Riboflavin metabolism, Biosynthesis of secondary metabolites	Cytoplasmic	0.008971334
AIO20749.1	succinate dehydrogenase	sdhB	-2.21	Metabolic pathways, Microbial metabolism in diverse environments, Biosynthesis of secondary metabolites, Biosynthesis of antibiotics, Carbon metabolism, Citrate cycle (TCA cycle),	Cytoplasmic	0.007493272

AIO20507.1	alanine-phosphoribitol ligase	dltA SACOL0935	-2.20	Oxidative phosphorylation, Butanoate metabolism Two-component system, Cationic antimicrobial peptide (CAMP) resistance, D-Alanine metabolism, *Staphylococcus aureus* infection	Cytoplasmic	0.004426841
AIO21007.1	oligoendopeptidase F	SA1216	-2.19		Cytoplasmic	0.002416275
AIO21222.1	elongation factor P	efp SA1359	-2.19		Cytoplasmic	0.003124498
AIO22338.1	adhesin		-2.18		Cell wall	0.000859809
AIO20422.1	sigma-54 modulation protein	hpf SA0707	-2.16		Cytoplasmic	0.005765903
AIO20857.1	ATP-dependent protease subunit HslV	hslV clpQ SA1096	-2.16		Cytoplasmic	6.19699E-06
AIO21536.1	Cro/Cl family transcriptional regulator	SA1665	-2.15		Cytoplasmic	0.004711143
AIO20783.1	penicillin-binding protein	pbpA	-2.15	Metabolic pathways,	CM	0.000352212

				beta-Lactam resistance, Peptidoglycan biosynthesis		
AIO20880.1	polynucleotide phosphorylase	pnp pnpA SA1117	-2.14	Purine metabolism, Pyrimidine metabolism, RNA degradation	Cytoplasmic	0.000231614
AIO19900.1	nitric oxide dioxygenase	SA0231	-2.14		Cytoplasmic	0.004114259
AIO21401.1	peroxidase	tpx SACOL1762	-2.14		Unknown	0.012659894
				Metabolic pathways, Microbial metabolism in diverse environments, Carbon metabolism, Biosynthesis of amino acids, Pentose phosphate pathway, Methane metabolism		0.002601172
AIO20237.1	6-phospho 3-hexuloisomerase	SA0529	-2.13		Unknown	
AIO21562.1	RecX family transcriptional regulator	recX SA1690	-2.13		Cytoplasmic	0.033059551

AIO21223.1	peptidase M24	SACOL1588	-2.12		Cytoplasmic	0.004797302
AIO21854.1	DNA-directed RNA polymerase subunit alpha	rpoA SA2023	-2.12	Metabolic pathways, Purine metabolism, Pyrimidine metabolism, RNA polymerase	Cytoplasmic	0.0186629
AIO20194.1	glutamyl-tRNA synthetase	gltX SA0486	-2.11	Metabolic pathways, Aminoacyl-tRNA biosynthesis	Cytoplasmic	0.012541864
AIO20273.1	arginine--tRNA ligase	argS SACOL0663	-2.11	Aminoacyl-tRNA biosynthesis	Cytoplasmic	0.00539229
AIO21926.1	MarR family transcriptional regulator	sarR SA2089	-2.10		Cytoplasmic	0.001173203
AIO20259.1	dihydrolipoamide dehydrogenase	SA0551	-2.09		Cytoplasmic	0.002933012
AIO20623.1	conjugal transfer protein	SACOL1582	-2.08		Unknown	0.002265429
AIO22143.1	hypothetical protein KQ76_13105	SACOL2519	-2.08		Cytoplasmic	0.004411129
AIO21116.1	gamma-hemolysin subunit A	hlgC SA2208	-2.06		Extracellular	0.001641133

AIO21055.1	membrane protein	SA1265	-2.06		CM	0.004565373
AIO21194.1	ribonuclease Z	rnz SACOL1548	-2.06		Cytoplasmic	0.002351995
AIO20555.1	phosphatidylethanolamine-binding protein	SACOL0984	-2.06		Unknown	0.001380911
AIO20895.1	2-oxoglutarate ferredoxin oxidoreductase subunit alpha	SA1131	-2.06	Metabolic pathways, Microbial metabolism in diverse environments, Carbon metabolism, Biosynthesis of antibiotics, Glycolysis / Gluconeogenesis, Butanoate metabolism, Pyruvate metabolism, Citrate cycle (TCA cycle)	Cytoplasmic	0.014034899 0.008074246
AIO20402.1	ribonucleotide-diphosphate reductase subunit beta	nrdF	-2.06	Metabolic pathways, Purine metabolism, Pyrimidine metabolism	Cytoplasmic	0.028267467

AIO19739.1	50S ribosomal protein L9	rplI SA0014	-2.05	Ribosome	Cytoplasmic	0.018585116
AIO20584.1	GTP pyrophosphokinase	SA0864	-2.04	Purine metabolism	Cytoplasmic	0.004580621
AIO21458.1	GTP cyclohydrolase	ribBA SACOL1818	-2.04	Metabolic pathways, Riboflavin metabolism, Biosynthesis of secondary metabolites, Folate biosynthesis	Cytoplasmic	0.003861302
AIO20455.1	hypothetical protein KQ76_03935	SACOL0851	-2.04		Unknown	0.004019645
AIO20695.1	hypothetical protein KQ76_05210	SA0947	-2.04		Unknown	0.001406803 0.00070713
AIO20687.1	hypothetical protein KQ76_05170	SA0941	-2.04		Cytoplasmic	0.000441333
AIO20819.1	16S rRNA methyltransferase	SA1060	-2.03		Cytoplasmic	0.001335183
AIO20413.1	peptidase T	pepT SA0698	-2.03		Cytoplasmic	0.00107553
AIO20838.1	cell division protein FtsY	ftsY SACOL1251	-2.03	Quorum sensing, Protein export, Bacterial secretion	CM	0.00664751

				system		
AIO21057.1	ribonuclease H	SACOL1471	-2.03	DNA replication	Cell wall	0.001704132
OOC91307.1	hypothetical protein BWO94_08325	SA1008	-2.02		Unknown	0.000232208
AIO20835.1	acyl carrier protein	acpP hmrB SA1075	-2.01		Cytoplasmic	0.000575663

Table 3.4: List of the significantly differentially expressed virulence factor proteins identified by VFDB in *S. aureus* biofilm in comparison to planktonic culture (fold change >2, p <0.05). * CM denotes Cytoplasmic Membrane.

Function	Accession ID	Virulence factors	Related genes	Fold change	Protein Pathway	Subcellular Localisation	
Adherence	AIO22275.1	Clumping factor B	clfB	-2.96	*S aureus* infection	Cell wall	0.000826686
	AIO22136.1	Fibronectin-binding protein A	fnbA SA2291	-2.60	Bacterial invasion of epithelial cells	Cell wall	0.004619411
	AIO19779.1	Immunoglobulin G binding protein A	spa SACOL 0095	-4.71	*S aureus* infection	Cell wall	0.007095826
	AIO20229.1	Serine-aspartate repeat-containing protein E	sdrE SACOL 0610	-3.82	*S aureus* infection	Cell wall	0.005307007
	AIO20228.1	Serine-aspartate repeat-containing protein D	sdrD SA0520	-4.49	*S aureus* infection	Cell wall	0.001713369
Toxins	AIO20763.1	Alpha-Hemolysin	SA1007	-13.83		Extracellular	0.00070713

				Quorum sensing, Inositol phosphate metabolism, Glycerophospholipid metabolism, Biosynthesis of secondary metabolites		0.000441333
AIO22369.1	Phospholipase C (EC 3.1.4.3) (Beta-hemolysin) (Beta-toxin) (Sphingomyelinase) (SMase)	hlb SACOL 2003	-12.33		Extracellular	
AIO21667.1	Delta-hemolysin (Delta-lysin) (Delta-toxin)	hld SA1841.1	-34.02	Quorum sensing	Extracellular	0.004019645
AIO22060.1	Gamma-hemolysin component C	SAS065 hlgC SA2208	-3.79	*Staphylococcus aureus* infection	Extracellular	0.000152835
AIO20093.1	Exotoxin 11 (superantigen-like protein)	set11	-3.63	*Staphylococcus aureus* infection	Extracellular	0.00388415

Antiphagocytosis (Capsule)	AIO19823.1	Capsular polysaccharide synthesis enzyme Cap5G	capG	2.018	Amino sugar and nucleotide sugar metabolism	Cytoplasmic	0.032173983
Exoenzyme	AIO21508.1	Serine protease SplE	splE	-4.18	Quorum sensing	Extracellular	0.001447915
	AIO21601.1	Cysteine proteinase A	scpA	-3.73		Extracellular	0.001213016
	AIO20644.1	Cysteine proteinase B	sspB	-11.44		Extracellular	0.00107553
	AIO19987.1	lipase	geh	-4.12		Extracellular	0.001714034
	AIO21839.1	Hyaluronate lyase	hysA	2.50		Extracellular	0.001362946
	AIO20645.1	glutamyl endopeptidase	sspA	-6.52	Quorum sensing	Extracellular	0.000496544
	OOC94232.1	aureolysin	aur	-3.22	*Staphylococcus aureus* infection, Cationic antimicrobial peptide (CAMP) resistance	Extracellular	0.001302771
	AIO19888.1	Staphylocoagulase	coa	2.10		Extracellular	0.002267015

Secretion system (Type VII secretion system)	AIO19949.1	type VII secretion protein EsaA	esaA SA0272	-2.29	CM*	0.001364193

GO analysis and annotation of DRSPs

We performed GO functional annotation for all DRSPs. PANTHER assessment showed that the involvement of 12 distinct classes of proteins in the entire global repository of proteins (Figure 3.2A). Nucleic acid-binding proteins (20.7%), hydrolases and transferases (17.2%), ligases (13.8%), transcription factors (8.6%) and oxidoreductases (6.9%) were the most prominent classes. According to the molecular function categories by PANTHER revealed the seven most represented molecular functions (Figure 3.2B). Among them, proteins involved in catalytic activity (50.7%) was the highest followed by binding (31.9%), and structural molecule activity (5.8%). According to the biological process evaluation, we identified seven most represented biological processes (Figure 3.2C). Of these, metabolic processes are the most prevalent biological processes, representing 60.5% of the protein repository followed by cellular component organisation or biogenesis (19.7%), biological regulations (9.2%), and cellular processes (3.9%).

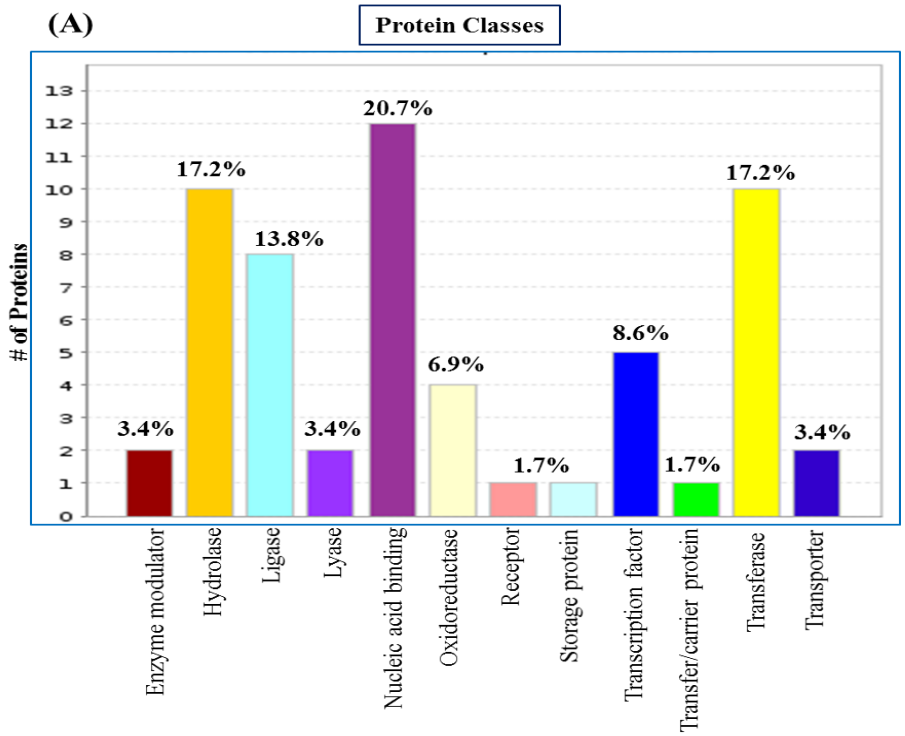

Figure 3.2: Classification of the DRSPs of *S. aureus* biofilm using Gene Ontology based on their functional annotations. (A) GO Protein Classes. We performed GO functional annotation

for significant differentially regulated proteins of 3dwb in comparison to planktonic. In this analysis we considered only proteins dysregulated >2 fold and p<0.05.

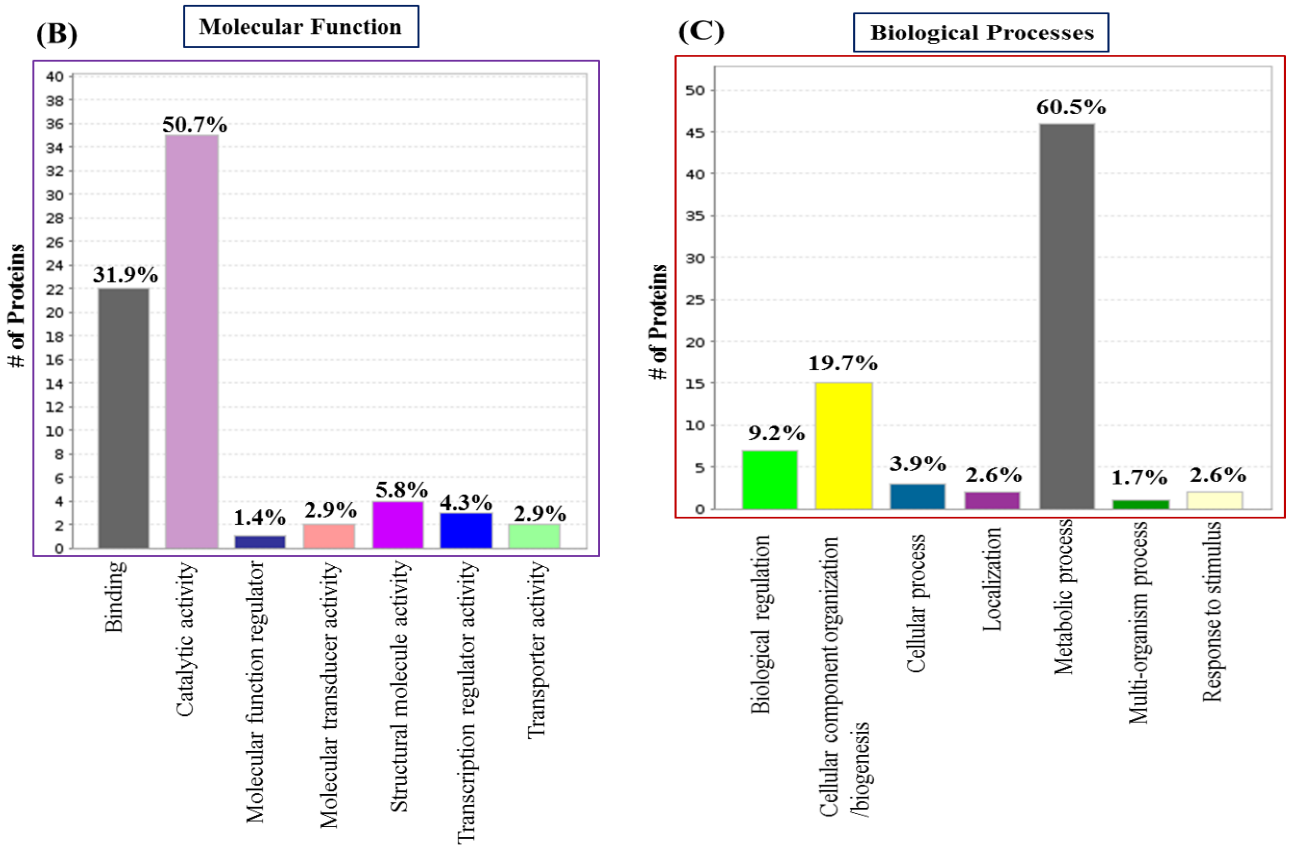

Figure 3.2: Classification of the DRSPs of *S. aureus* biofilm using Gene Ontology based on their functional annotations. (B) GO Molecular Function; (C) GO Biological Processes. We performed GO functional annotation for significant differentially regulated proteins of 3dwb in comparison to planktonic. In this analysis we considered only proteins dysregulated >2 fold and p<0.05.

KEGG pathway analysis of DRSPs

We analysed the TMT results using KEGG pathways to establish pathways impacted by bacterial biofilm formation in *S. aureus*. We annotated 289 DRSPs using the KEGG database, with all mapping onto 113 recognised pathways. Among these, 35 out of 82 significantly upregulated proteins were involved in recognised pathways. The 35 significantly upregulated proteins were

mainly involved in biosynthesis of secondary metabolites, biosynthesis of amino acids, microbial biosynthesis of antibiotics, metabolism in diverse environments, ABC transporters, alanine, aspartate and glutamate metabolism, amino sugar and nucleotide sugar metabolism, purine metabolism, ribosome, pyrimidine metabolism, arginine biosynthesis, tyrosine and tryptophan biosynthesis etc. (Figure 3.3A). In addition, upregulated proteins were also found to be involved in energy metabolisms such as glycolysis and galactose, and synthesis of cell-wall components such as peptidoglycan biosynthesis. On the other hand, 74 out of 191 significantly downregulated proteins were involved in recognised pathways. KEGG pathway analysis revealed that among the 74 significantly downregulated proteins these were mainly involved in quorum sensing, citrate cycle (TCA cycle), carbon metabolism, pyruvate metabolism, aminoacyl-tRNA biosynthesis, cationic antimicrobial peptide (CAMP) resistance, methane metabolism, glycerophospholipid metabolism, and two-component system, etc. (Figure 3.3B).

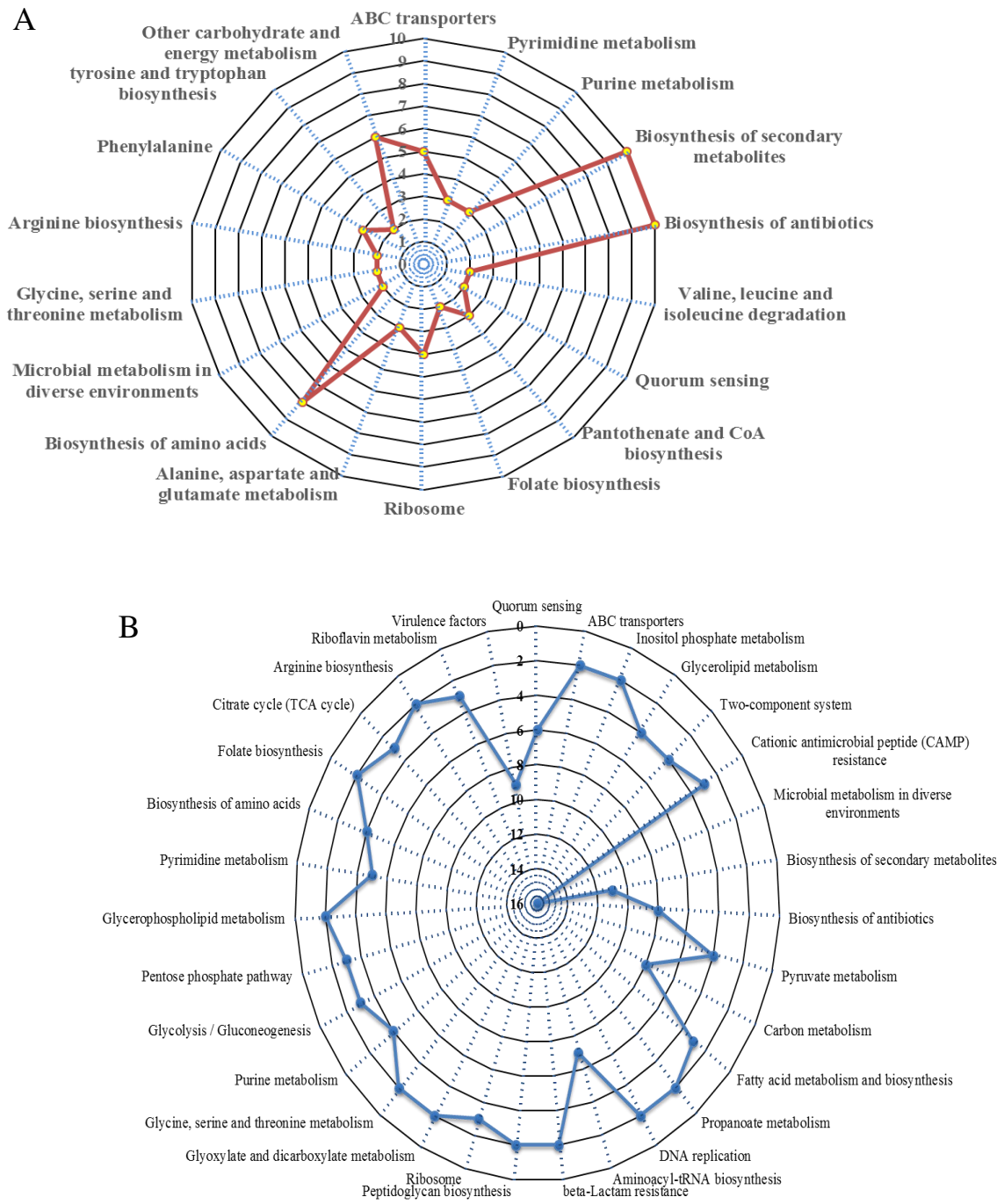

Figure 3.3: The DRSPs of *S. aureus* biofilm showed functional diversity using KEGG pathway analysis. (A) major pathways involved in significantly upregulated proteins; (B) major pathways involved in significantly downregulated proteins. Number scale represents; number of proteins identified in specific pathways.

Protein–protein interaction analysis of DRSPs

We established protein-protein interaction (PPI) networks using STRING software to assess the network of those proteins identified significantly to be expressed differentially in the biofilm mode of growth. In this PPI analysis, all predicted interactions tagged as "high-confidence" (≥0.7) and omitted nodes that are not connected in the network in STRING software. Among the 289 DRSPs, 129 nodes (proteins) and 145 edges (interactions) formed the final network. (Figure 3.4).

PPI network revealed that one protein symbolises a majority of connections: 30S ribosomal protein S5 (rpsE). This protein was found to be upregulated in the biofilm growth mode and could connect with 39 other proteins (Figure 3.4), and plays an important role in translational accuracy. Among these 39 possible connections, most of them are involved in metabolic, catalytic activity, and binding (such as ion, nucleic acid, metal, and drug). The findings of this subnetwork are in line with the top protein classes and biological processes acquired with PANTHER analysis (Figure 3.2). Further relevant subnetworks consist of nodes associated with gene expression, translation, ATP biosynthesis, virulence factors, glucose metabolism, and stress-response (Figure3.4).

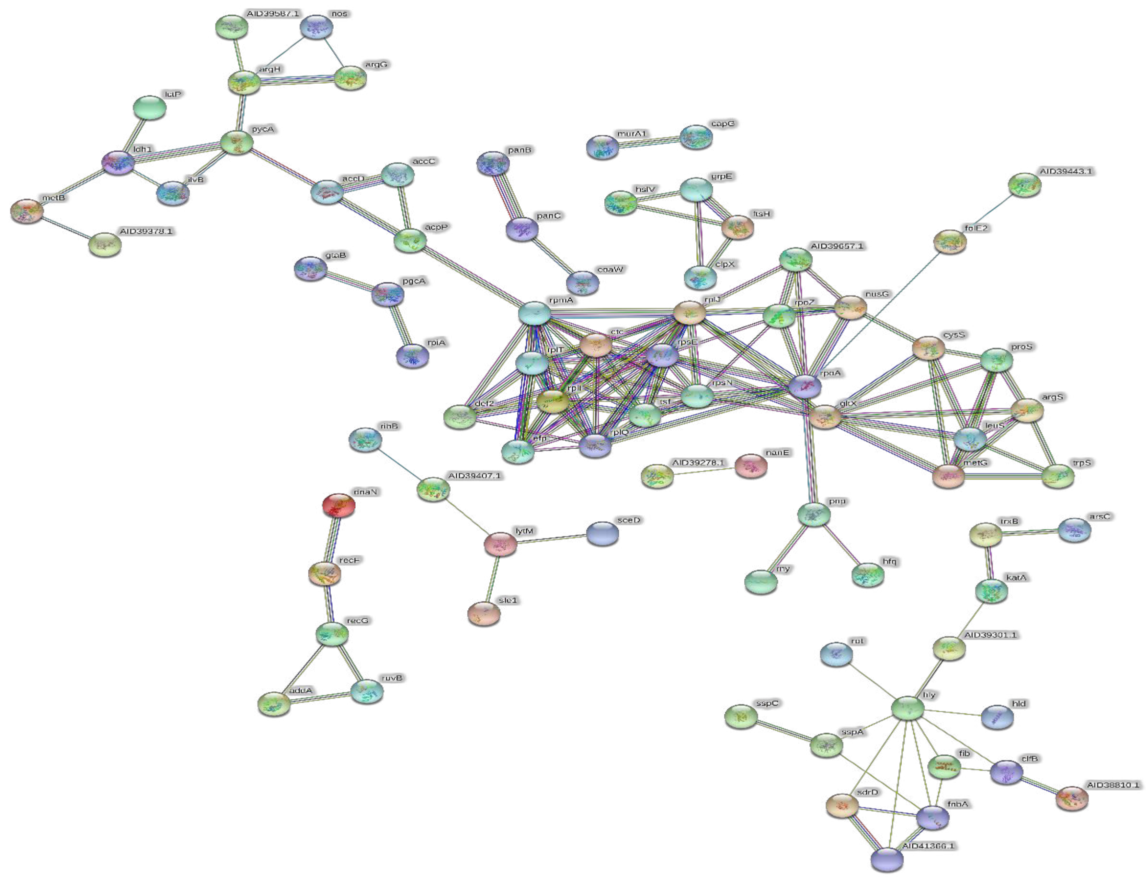

Figure 3.4: The network of DRSPs of *S. aureus* biofilm was analysed by STRING software (v.10.0). High-confidence interactions (≥0.7) and omitted nodes that are not connected in the network in STRING software were selected for this study.

Correlation of TMT data with real-time qPCR results

The ratios from the qPCR results were obtained by comparing with planktonic in 3dwb. Individual normalised qPCR results are shown in Appendix 3. Upregulated and downregulated protein expression and gene expression results were expressed in fold change (FC) (Table 3.5). qPCR results showed that, two gene (sspA and pyc) were downregulated in the 3dwb, indicated a relative consistency with the TMT data. Further, we also observed that, genes (hysA, SA0914, and sdhB) showed relatively lack of positive correlation between qPCR and TMT data (Table 3.5).

Table 3.5: Relative correlation of selected qPCR gene expression data to TMT protein expression data in 3dwb in comparison to planktonic culture. * FC denotes fold change

			TMT	qPCR
Accession ID	**Protein Name**	**Gene Name**	**3dwb (FC)***	**3dwb (FC)***
AIO21839.1	Hyaluronate lyase	hysA	2.503	0.047
AIO20660.1	chitinase	SA0914	0.118	1.528
AIO20645.1	glutamyl endopeptidase	sspA	0.152	0.010
AIO20712.1	pyruvate carboxylase	pyc	0.425	0.391
AIO20749.1	Succinate dehydrogenase	sdhB	0.452	1.10

Discussion

Whilst the proteomics of *S. aureus* biofilm have previously been investigated [325, 341, 342, 468], this is the first study to use TMT. TMT-labeling approach in combination with tandem MS has the potential to analyse high-resolution, proteins in the low mass region with the posibility to label up to 10 samples simultaneously [334, 336]. This powerful proteomic strategy can be helpful for deeper understanding of biological mechanisms as well as screening of biomarkers by examining the variations in protein expression levels.

Further, we also performed qPCR experiments of some selected significantly dysregulated genes to explore the correlation between qPCR and TMT data. qPCR results indicated that the ratios of the levels of gene expression were relatively partial consistent with the data acquired from the TMT-based MS analysis. In general, the correlation between transcriptomics and proteomics can be low owing to distinct variables such as unlike half-lives and post-transcription machinery. In addition, the lack of positive correlation between TMT and qPCR data might be affected by the differences in the cell lysis and extraction process of the samples.

In our proteomics data, we identified several proteins associated with transporters, mostly ABC transporters (Table 3.2, Figure 3.3A) as significantly upregulated in the *S. aureus* biofilm state: molybdenum ABC transporter permease (4.68 fold), peptide ABC transporter substrate-binding protein (2.91 fold), spermidine/putrescine ABC transporter ATP-binding protein potA (2.39 fold), heme ABC transporter ATP-binding protein (2.32 fold), and glutamine ABC transporter ATP-binding protein (2.05 fold). Proteins were also significantly downregulated in biofilm growth and included ABC transporter ATP-binding protein encoded by vga and iron ABC transporter substrate-binding protein encoded by SA0691. ATP-binding cassette transporters (ABC transporters) are members of a superfamily of proteins, that are transmembrane proteins which are linked with adenosine triphosphate (ATP) binding energy utilisation. They play substantial functions in molecular (macro and micro) uptake of nutrients, such as capsular polysaccharides, small molecule inhibitors, amino acids, lipids, and vitamins. To better understand of virulence and drug resistance, microbial ABC transporters are gaining attention as a potential target [469]. In previous studies, ABC transporters (such as ABC transporter lipoprotein, ABC transporter permease protein, ABC transporter periplasmic amino acid-binding protein, and ABC transporter ATP-binding protein) have been reported to be upregulated in biofilm formation in *S. aureus* [278, 341, 438, 440] and in numerous other bacteria, including *Cronobacter* sp., *Streptococcus uberis*, *Rhizobium leguminosarum*, *Pseudomonas fluorescens* and *Bacillus subtilis* [470-474], but have also been reported to be downregulated (putative ABC transporter permease) in *Listeria monocytogenes* [475], and ABC transporter ATP-binding protein in *S. aureus* [476]. In these instances, the specific role they have (i.e. up- or down-regulation) will depend on the substrates being supplied by the ABC transporters. Although the exact reason for the downregulation of ABC transporters yet to be explored, however, it could be

due to the lower metabolic rate of the biofilm and hence it didn't need to transport ATP as much. A study by Brady *et al.* (2006) revealed that the upregulation of a membrane-bound ABC transporter protein in *S. aureus* biofilm growth and suggested that it may be an excellent vaccine candidate, as previous work reported it as immunogenic in *S. aureus* infections in humans [440, 477]. Taken together, the unique or significant ABC transporter proteins (especially those that are membrane-bound) we identified in our study may play an important role in biofilm formation which may lead to potential marker proteins, vaccine and antimicrobial targets for biofilm-related infections.

Among the significant differentially regulated proteins in the biofilm extractomes, we identified most of the extracellular or cell-wall associated proteins to be primarily represented by virulence factors (Table 3.4). Proteins significantly upregulated include fibrinogen-binding protein (SA1000), hypothetical protein KQ76_08475 (SA1452), hyaluronate lyase (hysA), and coagulase, while downregulated proteins (Table 3.4, Figure 3.3B) include hemolysins (hld, SA1007, hlgCAB), proteases (sspABP, splCEF, SA1121, clpP), nucleases (nuc, rnhC, SA1526, cbf1, rnz), peptidases (lytM, SA0205, SA0620, sspA), lipases (lip1, lip 2), a chitinase (SA0914), a phenol soluble modulin (SACOL1186), fibronectin-binding protein (fnbA), and adhesin (sasF). Among the upregulated proteins, fibrinogen-binding protein is an MSCRAMM, vital for the attachment of *S. aureus* to human cells and thus for the spread of infections [478, 479]. A recent *in vitro* study by Kot *et al.* (2018), demonstrated that the expression levels of fibrinogen-binding protein in weakly attaching strain of *S. aureus* was considerably smaller than in strongly attaching strain of *S. aureus* [480]. Studies by Resch *et al.* (2006), reported the upregulation of fibrinogen-binding protein in biofilm growth mode compared with planktonic which shows a similar trend with our study. In an *in vivo* rat model of central venous catheter infection using *S. epidermidis*, rat lacking fibrinogen-binding motif observed more robust biofilm on the catheter, indicating its significance in the *in vivo* biofilm development [109]. In addition, binding of *S. aureus* to fibrinogen-binding protein and coagulase demonstrates various evasive responses that protect bacteria against the immune system, and its binding is influenced by Rot and Agr mediated regulatory systems [109, 342].

In our study, we also identified significantly downregulated other fibrinogen-binding proteins (such as clfB, sdrDE) may exhibit potential moonlighting/multiple functions in *S. aureus* biofilm

development. Proteomic studies by Hofbauer et al., (2018), reported that significant downregulation of several virulence proteins including fibrinogen-binding protein in *S. aureus* biofilm, suggested interesting perspective of putative antibiofilm effects [479]. Significant downregulation of these proteins may be function as a spreading factor/antibiofilm agents by disseminating bacterial cells from one place to another to form denser biofilm. However, further investigation is required to better understand the intriguing perspective of downregulated fibrinogen-binding proteins.

Hyaluronidase (hysA) an extracellular enzyme significantly upregulated in biofilm state and play an important role in disseminating recognised biofilms by the degradation of hyaluronic acid (HA) (Figure 3.5). HA is an extracellular matrix component and revealed to enhance biofilm development in Gram-positive pathogens, including *Streptococcus intermedius*, and *Streptococcus pneumoniae*. A very recent in-depth study by Ibberson *et al.* (2016) demonstrated that *S. aureus* integrates HA into the biofilm matrix both *in vivo* (murine implant-associated infection model) and *in vitro*, and HysA acts as a spreading factor by dispersing the biofilm and disseminating to new locations of infection [481]. On the other hand, among the significantly downregulated proteins, chitinase (SA0914) an exo-enzyme involved in quorum sensing that prevents the initial stage development of biofilms. Interestingly, HA is the structural constituent of N-acetyl-D-glucosamine (Figure 3.5) which can be hydrolysed by chitinase [482]. Therefore, we can speculate that hysA in conjunction with chitinase may play significant role in the elimination and/or prevention of biofilm development.

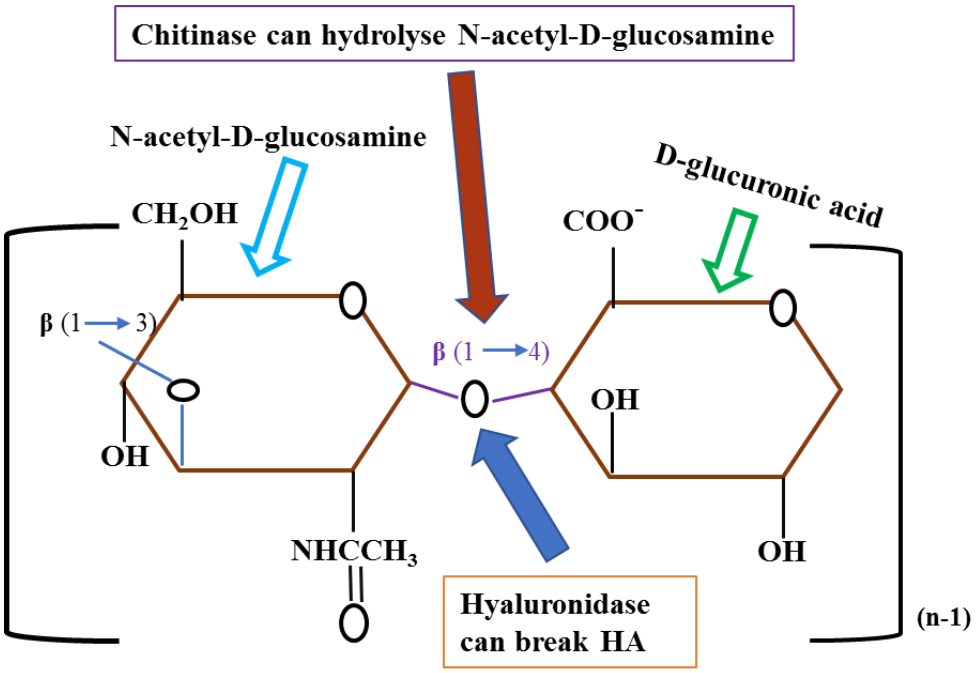

Figure 3.5: This figure showing structural component of hyaluronic acid (HA) and breaking point. HA comprises of repeating disaccharides units of N-acetyl-D-glucosamine and D-glucuronic acid, and the units are linked by repeating glycosidic bonds beta-1,4 and beta-1,3.

Further, the significant downregulation of virulence-related and cell wall proteins showed that the bacteria adapted to the diverse biofilm condition by reducing some less essential roles such as adhesion, invasion, and virulence. For example, agr quorum-sensing system regulates the expression of virulence genes and contributes to the dispersal and structuring of biofilms by regulating extracellular proteases (e.g. sspAB) and phenol-soluble modulin (PSMs) surfactant peptides [106, 292]. Further, Staphylococcal accessory regulator (SarA) is a positive biofilm regulator through the downregulation of extracellular nuclease (nuc) and proteases [483]. Downregulation of these genes from our findings shows similarity with the findings of Resch et al [278]. Studies have shown that *S. aureus* produces proteases which in most cases act as a virulence factor that may influence the chronicity of *S. aureus* infections [484]. *In vivo* the inflammatory response itself also contributes to tissue destruction by continually recruiting proinflammatory cells such as lymphocytes and macrophages, releasing proteases and inflammatory mediators [6]. Although proteases help dislodge biofilms, they also harm ordinary

and curative tissues, whereas macrophages may form a fibrous capsule around the implants. [174].

Further pathway analysis revealed that, the upregulation of glyceraldehyde-3-phosphate dehydrogenase encoded by gapA1 (2.34 fold), cystathionine gamma-synthase encoded by metB (2.33 fold), threonine synthase encoded by thrC (2.27 fold), argininosuccinate lyase encoded by argH (2.21 fold), acetolactate synthase encoded by alsS (2.21 fold), argininosuccinate synthase encoded by argG (2.15 fold), 3-phosphoshikimate 1-carboxyvinyltransferase encoded by aroA (2.09 fold), and histidinol-phosphate aminotransferase encoded by SACOL2701 (2.01 fold) involved in biosynthesis of amino acid (Table 3.2 and Figure 3.3A). Besides protein parts, amino acids function as signals for gene expression molecules and regulators. In the meantime, changes in the metabolism of amino acids contribute to the development of biofilms *in vitro* and *in vivo* catheter infection [283, 485]. Studies by Ammons *et al.* (2014) reported that, in addition to the diverse role of amino acids in biofilm development, they also involved in substantial energy expenditure for adequate redox equilibrium maintenance, cell-wall synthesis components, and deposition of EPS matrix [279]. Notably, in our biofilm extractomes, we found significantly upregulated proteins involved in amino sugar and nucleotide sugar metabolism (such as glmS, nanE, capG) which is linked with peptidoglycan biosynthesis (Figure 3.6). As we know, peptidoglycan is the major component of the bacterial cell-wall, and our study also observed significant accumulation of peptidoglycan biosynthesis associated protein (e.g. murA). Therefore, we can speculate that the proper utilisation of amino acids will stimulate cell-wall formation leading to EPS matrix deposition and enhance biofilm formation.

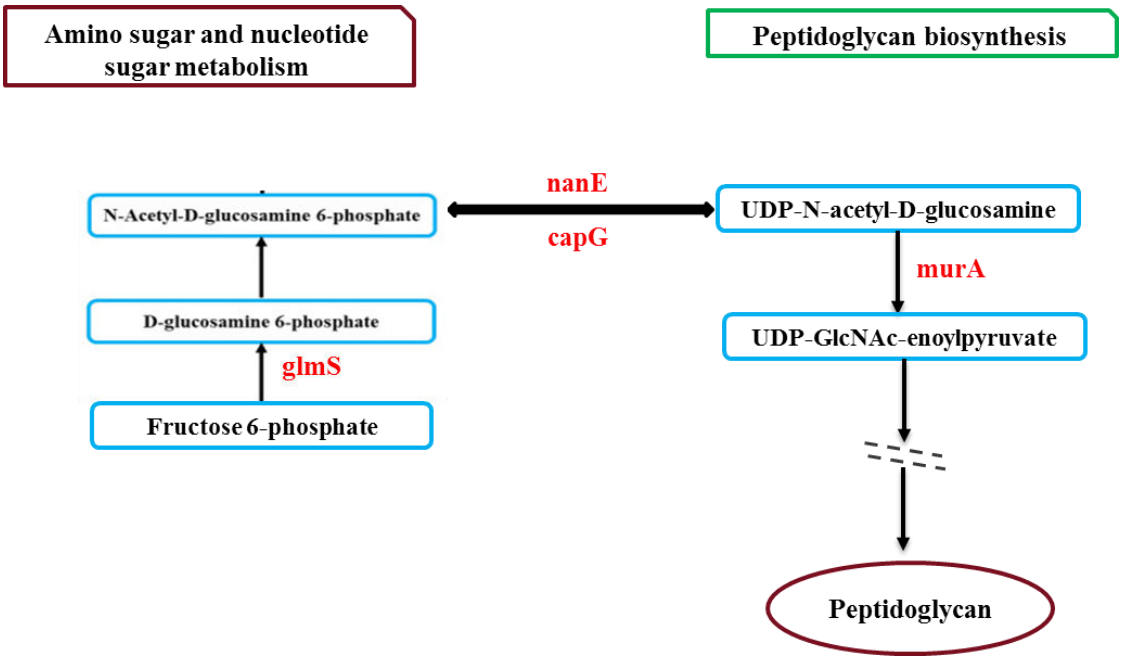

Figure 3.6: Pathway demonstration showing significantly upregulated proteins (red colour encoded genes) involved in amino sugar and nucleotide sugar metabolism and linked with peptidoglycan biosynthesis in 3dwb.

Many ribosomal subunit proteins such as 30S ribosomal protein S14 (rpsN), 50S ribosomal protein L27 (rpmA), 30S ribosomal protein S5 (rpsE), 50S ribosomal protein L10 (rplJ) were significantly upregulated (Table 3.2 and Figure 3.3A) under biofilm growth state, while 50S ribosomal protein L17 (rplQ) and 50S ribosomal protein L20 (rplT) were downregulated (Table 3.3 and Figure 3.3B). Usually, ribosomal subunit proteins play a significant role in regulating the expression of whole proteins. 50S involves the activity that catalyses the formation of peptide bonds, protects premature polypeptide hydrolysis, and helps to fold proteins after synthesis, etc. It stated that by synthesising some of the peptides or proteins helps to promote the resistance. For example, 50S ribosomal protein L27 (rpmA) plays a critical role in tRNA substrate stabilisation during the peptidyl transfer reaction as well as ribosome assembly and catalysis even with certain level of stress environment (e.g. deletion of some part) [486].

Among the significantly differentially regulated proteins, we identified several proteins related to different stress responses in the *S. aureus* biofilm extractomes: DNA-directed RNA polymerase subunit omega (RpoZ), dehydrogenases (e.g., bfmBAA, gap, ldhD), oxidoreductases (e.g., guaC,

SACOL0959, SA0558, nfrA), reductases (e.g., SACOL1543, SA0759, SACOL1768, trxB), glutathione S-transferase, and heat shock protein GrpE (Table 3.3 and 3.4). The formation of a stress response is a significant characteristic of biofilm life cycle as it leads to changes in many gene expressions which increase antimicrobial resistance and is generally regulated by alternative RNA polymerase sigma factor B (SigB). Multiples studies have reported increased or decreased expression of stress response associated proteins in *S. aureus* biofilm [341, 342, 487] and other bacterial [488-490]. However, notably, we identified a unique DNA-directed RNA polymerase subunit omega (RpoZ) which is 4.52-fold upregulated in the biofilm. Even though very little is known about RpoZ, a very recent study reported its significant roles in stability, complex assembly, maintenance of transcriptional integrity, and cellular physiology in response to stress in *S. aureus* biofilm [487]. Another protein glyceraldehyde-3-phosphate dehydrogenase (Gap) was significantly upregulated in biofilm growth mode and under oxidative stress environments, showed a significant positive correlation between development, ATP level and Gap activity in planktonic *S. aureus* [491]. Pathway analysis revealed that the Gap, an enzyme involved in multiple pathways (such as biosynthesis of amino acids, carbon metabolism, microbial metabolism in diverse environments, glycolysis/gluconeogenesis etc), play important role in the phosphorylation of glyceraldehyde-3 phosphate and contributes in phosphotransferase activity and repair apoptosis [492]. Gap is upregulated in biofilms developed by numerous bacterial species [330, 344, 493-495].

Metabolic activity and growth rate of the bacteria are affected by the changes in the gradient of oxygen and other nutrients within the biofilm. Many studies have demonstrated that cells within hypoxic conditions have decreased metabolic activity [124-126], this slow pace of development suggests tolerance as antimicrobials are most efficient against rapidly developing cells [128-130]. In addition, the deeper layers of cells are also located in biofilms with undergrowth-limiting conditions, with anaerobic or micro-aerobic conditions. Pyruvate fermentation could support these cells, allowing them to survive with little or no oxygen [496]. In our *S. aureus* biofilm extractomes, we observed significant upregulation of acetolactate synthase (alsS) which is responsible for the activation of butanediol pathway from pyruvate. Activation of this pathway will promote NADH oxidation and indicate that there is a tenuous redox balance during the

development of biofilms [283]. Another study reported that alsS utilise pyruvate to produce acetoin which is essential for acid tolerance within biofilms [497].

Among the 273 DRSPs, unique or significant proteins identified in *S. aureus* biofilm contain 34 of functionally unknown or very little-known hypothetical proteins (Table 3.2 and 3.3) including a hypothetical protein namely hypothetical protein KQ76_08425 encoded by SA0772 with the highest upregulation (5.09 fold), suggests that the complex metabolic and regulatory reaction to biofilm is not yet fully elucidated. Despite searching the UniProt database, identification of proteins with known function to hypothetical proteins KQ76_08425, KQ76_08425, KQ76_04890, KQ76_08470, etc. could not be found. Even though the role of the hypothetical protein remains unknown, it is probable to play a part in the distinct physiological state of the biofilm. In particular, we can speculate for those significantly upregulated in biofilm growth state. Although there have been previous reports of hypothetical proteins implicated in alterations in biofilm [326, 498, 499], more research is required to assess their role as these proteins are homologous to conserved hypothetical proteins from other organisms which include certain pathogenic strains.

Conclusions

In this study, we compared the proteome of *S. aureus* planktonic culture and 3-day biofilm using high-resolution TMT-based MS. We observed a significant range of abundance variation between planktonic and 3-day biofilm. Proteins associated with ABC transporters (modB, SACOL0187, potA, SACOL0779, etc.), extracellular/cell-wall (hysA, coa, SA1000, etc.) were significantly upregulated in 3-day biofilm. Pathway enrichment analysis revealed that, significantly differentially regulated proteins involved in pathways associated with biosynthesis of amino acid (gapA1, metB, thrC, argGH, alsS, aroA,etc.), amino sugar and nucleotide sugar metabolism (e.g. glmS, nanE, capG), stress responses (bfmBAA, gap, guaC, trxB, etc.), others in 3-day biofilm. Further downstream analysis such as GO, KEGG pathway, and PPI of significantly identified potential marker proteins may provide new insight into planktonic and early stage biofilm biology.

Chapter 4: Proteome of *Staphylococcus aureus* biofilm changes significantly with age

In Chapter 3, we showed significant changes in the protein expression profile between the planktonic and biofilm forms of *S. aureus*. Moreover, we found significant changes in metabolic processes, strong protein-protein interaction network, and identified a potential role for key proteins in *S. aureus* biofilm. In this chapter, we explored the proteomic profiles of the different stages of *S. aureus* biofilm and compared it to its planktonic state.

The biology of *S. aureus* biofilm may vary with the time since biofilm formation or its state of maturity. This may have implications when trying to either remove biofilm from surfaces or treat biofilm *in vivo*. More mature biofilm has been shown to be more tolerant to biocides *in vitro* [500, 501]. In addition, targeted antibiotic treatment of biofilm infecting medical implants usually results in treatment failure unless the infected device is removed [502]. Clinically, it is difficult to diagnose infected implantable medical devices, thus antibiotic treatment is often delayed so treatment is initiated on a more antibiotic resistant mature biofilm with its inherent slower growth rate and lower metabolic rate. There is presently no effective technique for early identification of biofilms.

With the advent of modern proteomic technologies and the development of protein databases, the changes in protein expression profile of the different stages (maturity) of biofilm can be analysed enabling the identification of potential marker proteins in biofilm development.

In this study, we aim to determine how the biofilm proteome differs at two time points i.e. modelling early biofilm and late biofilm development, which may shed novel insight and bridge the knowledge gap in the *S. aureus* subproteomes.

Abstract

Staphylococcus aureus is a notorious biofilm-producing pathogen that is frequently isolated from implantable medical device infections. As biofilm ages, it becomes more tolerant to antimicrobial treatment leading to treatment failure and necessitating the costly removal of infected devices. In this study, we investigated what changes occur in the proteome of *S. aureus* biofilm grown for 3-days and 12-days, using high-throughput TMT-based mass spectrometry. Comparison of *S. aureus* biofilm grown over 3-day wet biofilm (3dwb) and 12-day wet biofilm (12dwb) with 24hr planktonic showed that proteins associated with biosynthetic processes, energy metabolism, ABC transporter pathway, virulence proteins, and shikimate kinase pathway were significantly upregulated in 3-day biofilm, while proteins associated with sugar transporter, degradation, and stress response were downregulated. In 12-day biofilms, proteins associated with peptidoglycan biosynthesis, sugar transporters, and stress responses were upregulated, whereas proteins associated with ABC transporter pathway, DNA replication, and adhesion proteins were downregulated. Further analyses of pathways and gene ontology demonstrated that the significant variations in the formation of biofilms result from changes in the level of metabolic activity in the different growth mode of biofilms, with a higher level of metabolic activity being observed in the 3dwb. Therefore, changes in metabolic activity could be a significant factor of *S. aureus* biofilm maturation and persistence. In the current study, potential marker proteins were identified and further characterised to understand their exact role in *S. aureus* biofilm development which may shed light on possible new therapeutic regimes in the treatment of biofilm-related implant-associated infections.

Keywords: *Staphylococcus aureus*, Bacterial Biofilms, CDC Bioreactor, TMT, Mass Spectrometry

Introduction

It is projected that about 65 to 85% of all bacterial infections are associated with biofilms [503, 504]. *Staphylococcus aureus* is a notorious biofilm-producing pathogen and reported to be the most common causes of infections associated with biofilms in humans. Together with coagulase-negative staphylococci, *S. aureus* have been isolated from approximately 65% of

infections associated with implantable medical devices such as catheters, prosthetic joints, breast implants, and pace makers [2-8]. Once developed, biofilm is enormously hard to eliminate due to its high tolerance to both antimicrobials and host immune defenses [109]. Eradication often requires painful and expensive removal or replacement of contaminated medical devices.

Biofilm is a multilayered structure comprising of bacterial communities embedded in a self-produced matrix containing extracellular polymeric substances (EPS). In *Staphylococcus* biofilms, proteins such as fibronectin-binding proteins (FnBPs) and biofilm-associated proteins (Bap), polysaccharide intercellular adhesin (PIA), extracellular DNA (eDNA), and teichoic acids have been shown to be components of EPS matrix [92-95]. PIA is thought to be a principal extracellular component (80–85%) and is mainly composed of β-1,6-linked N-acetylglucosamine residues. *In vitro*, PIA is generated from UDP-N-acetylglucosamine through intercellular adhesin (ica) locus products [96]. In some strains of *S. aureus* biofilm development is dependent upon the ica locus [icaR (regulatory) and icaADBC (biosynthetic) genes] [97], however, ica-independent mechanisms have been shown to be sufficient for biofilm formation in some strains, *S. aureus* and in coagulase-negative staphylococci [98]. Studies by Houston et al. (2011) demonstrated that fibronectin-binding proteins (FnBPs) can mediate *S. aureus* biofilm development via a vital role by the major autolysin (Atl), agr, and sigB regulation [99]. However, accumulation-associated protein (Aap) play significant role in PIA-independent biofilm formation in *Staphylococcus epidermidis* [100, 101].

Biofilm-associated protein (Bap) plays a significant function among the adhesive proteins involved in the formation of biofilms, which has been shown to be crucial for both initial attachment and intercellular accumulation during the growth of *S. aureus* biofilm. The Bap gene is also found in *Staphylococcus chromogenes, S. epidermidis*, *Staphylococcus xylosus*, *Staphylococcus hyicus*, *Staphylococcus simulans* and several other staphylococcal species [102]. In addition, the differential expression and synthesis of these molecular variables during the distinct phases of biofilm development are tightly controlled by various biofilm regulators as listed by Graf *et al.* (2019) such as SarA, AgrA, RNAIII, Rot, IcaR, CodY, Spx, and others [463].

Global advances can be especially advantageous in unraveling the complex interaction among these regulatory networks and in identifying proteins with vital functions in biofilm

development. However, most of the omics studies focus on the profiling of early stage biofilm development and/or up to 3-days [278, 325, 327, 341-343]. Patients can be exposed to biofilm-infected medical devices long term. This could have an effect on the patient's immune response to the biofilm infection as well as affecting the physiology of the infecting biofilm.

In the current study, we aimed to construct a comprehensive quantitative proteomic framework to bridge the knowledge gap in *S. aureus* cells as they progress through planktonic and different stages of biofilm lifestyle. To do this, we performed TMT-based high-throughput MS of planktonic and two different stages (3-day and 12-day) of biofilm growth mode from *S. aureus*. In addition, the identified potential marker proteins were subjected to pathway analysis, subcellular localisation and protein-protein interaction (PPI) network mapping.

Materials and Methods

The objective of this research was to create quantitative proteomic profiling to define the distinctions between *S. aureus* cells that progress through the lifestyles of planktonic and biofilm. To accomplish this, we conducted in-solution digestion that enabled us to produce extremely complicated samples that could be analysed with TMT-based mass spectrometry (Figure 4.1).

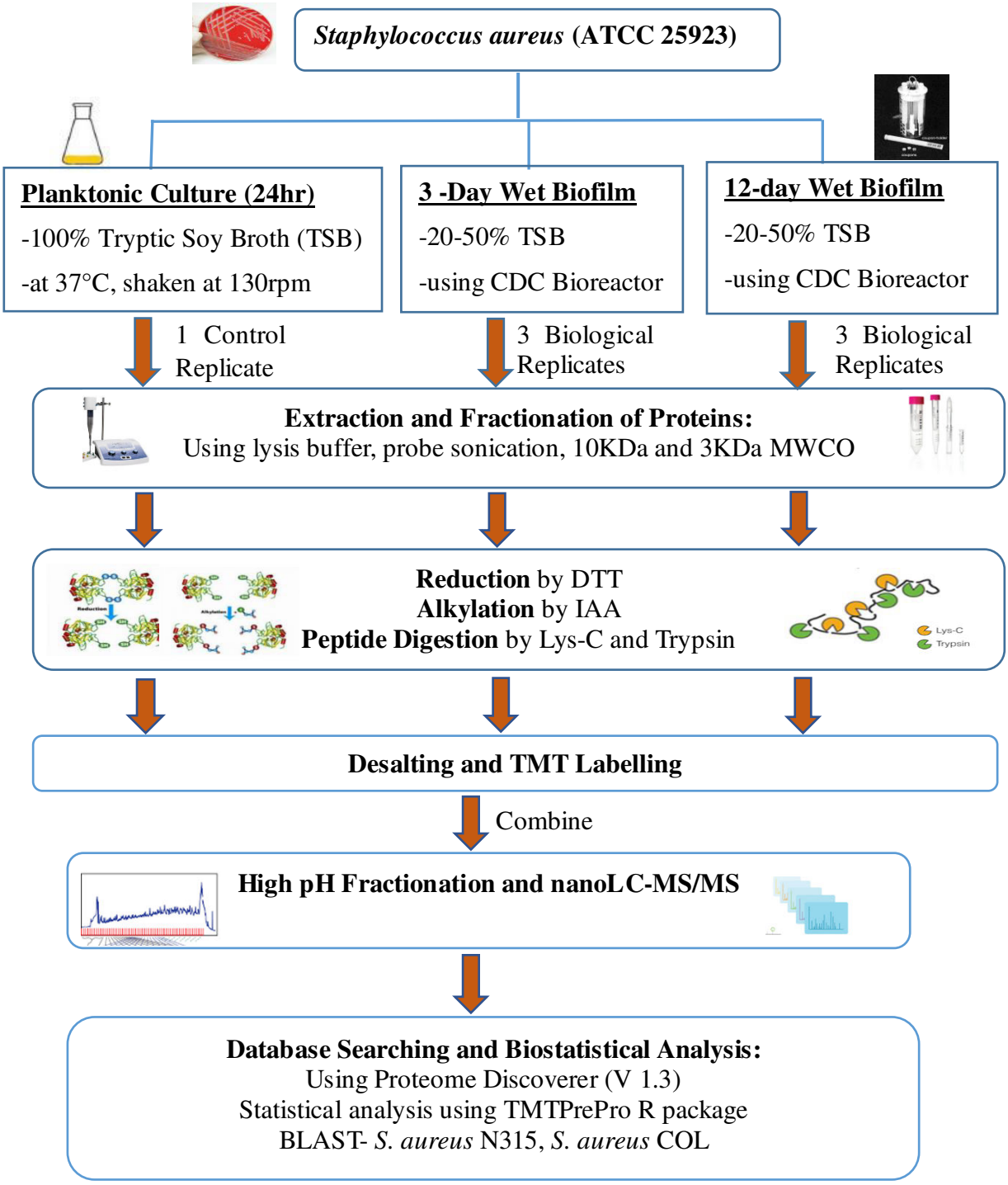

Figure 4.1: Experimental workflow for the analysis of *S. aureus* planktonic and two different growth stage of biofilm proteome using TMT labeling based MS. *S. aureus* strain cultivated in TSB to grow a planktonic culture pooled from biological triplicates, and biofilms (3-day and 12-day) in biological triplicates. The Centres for Disease Control biofilm reactor was used to grow biofilms. Proteolytically digested peptides were labeled with TMT

10-plex reagents and subjected to high pH RP-HPLC fractionation followed by LC−MS/MS analysis.

Microorganism and culture conditions

S. aureus (ATCC 25923) 24hr planktonic culture was grown as described in Chapter 2, section 2.1.3 whilst 3-day and 12-day hydrated biofilm cultures were grown as described in sections 2.1.4.1 and 2.1.4.2, respectively.

Sample Processing

Extraction and fractionation were performed using a modified method described by [454], as described in Chapter 2, section 2.2.1 for planktonic culture and section 2.2.2 for 3-day and 12-day biofilm culture.

The amount of protein in extracted samples was measured using the BCA protein assay (Thermo Fisher Scientific, Australia) as described in Chapter 2, section 2.2.3.

A total of 40µg protein of each sample was processed further for protein reduction, alkylation, and digestion (described in Chapter 2, 2.2.4).

Samples were reconstituted in 100µl of 100mM TEAB pH 8.5 and labeled with TMT (Thermo Fisher Scientific, Germany) reagents as described in Chapter 2, section 2.2.5. A volume of 2µl of each labeled sample was pooled and vacuum dried (miVac) and reconstituted in 30µl 0.1% FA solution, centrifuged for 5min at 14000xg and analysed with mass spectrometer (nanoLC-ESI-MS/MS using Orbitrap Elite) as described in Chapter 2, section 2.2.6.1.

Based on the applied normalisation values from this search result an equal amount of peptides were taken from each sample, pooled and vacuum dried. The pooled labeled sample was fractionated by high pH RP-HPLC (Agilent Technologies). The fractionated sample by high pH RP-HPLC was pooled to 20 fractions, dried in miVac. Finally, each fraction was resuspended in 55µl of 0.1% FA for mass spectrometry analysis.

Nanoflow LC-ESI-MS/MS

All samples were run on two sequential mass spectrometer systems.

Nanoflow LC-ESI-MS/MS using Orbitrap Elite

An Orbitrap Elite (Thermo Fisher Scientific) mass spectrometer was used for acquiring data (described in Chapter 2, 2.2.6.1). Briefly, 20µl of each fraction was loaded onto a self-packed 100µm x 3.5cm trap column with Halo® 2.7µm 160 Å ES-C18 and desalted with loading buffer [0.1% FA] at a flow rate of 4µl/min for 10min. Peptides were eluted onto a self-packed analytical column with the linear gradients with a flow rate of 450nl/min across the gradient. The eluent from the trap was diluted with 100nl/min of buffer A before reaching the analytical column. The peptides refocused and separated over the analytical column at 60°C. Peptides were ionised by electrospray ionisation, and data-dependent MS/MS acquisition carried out using an Orbitrap Elite consisting of 1 full MS1 (R=120 K) scan acquisition from 380 to 1600 m/z, and 15 higher energy collisional dissociation (HCD) type MS2 scans (R=30 K).

Nanoflow LC-ESI-MS/MS using Q Exactive

A Q Exactive (Thermo Fisher Scientific) mass spectrometer was used for acquiring data (described in Chapter 2, 2.2.6.2). Briefly, each fraction (10µl) was loaded onto a self-packed 100µm x 3.5cm reversed phase peptide trap with Halo® 2.7µm 160 Å ES-C18 desalted with 20µl of loading buffer [0.1% FA] and the peptide trap was then switched on-line with the analytical column. Peptides were eluted with the linear gradients with a flow rate of 300nl/minute. Peptides were ionised by electrospray ionisation and data-dependent MS/MS acquisition carried out using a Q Exactive consisting of 1 full MS1 (R=70 K) scan acquisition from 350 to 1850 m/z, and 10 HCD type MS2 scans (R=70 K).

Database search, statistical analysis, and bioinformatics

The raw data files were submitted to Proteome Discoverer (PD, version 1.3, Thermo Scientific) and processed using Sequest and Mascot (Matrix Science, London, UK) against *S. aureus* reference strain (ATCC 25923) as described in Chapter 2, 2.2.7. Following the extraction of protein ratios with PD, further processing and statistical analysis was carried out using the TMTPrePro R package [455]. BLAST search was performed using highly annotated strains *S. aureus* N315 and *S. aureus* COL. Proteins were considered upregulated when the TMT ratio was above 1.5 and downregulated when the TMT ratio was lower than 0.66 in biofilm growth compared to planktonic growth with significant p-value < 0.05. Significant differentially expressed proteins (>2-fold) were determined by using VENNY, metabolic

pathway analysis using KEGG mapper, subcellular localisation using PSORTb [456], and protein–protein interaction (PPI) network of significantly differentially expressed proteins were analysed by STRING software [457].

Validation of TMT data with qPCR results

Five genes encoding (1) Chitinase SA0914, (2) Glutamyl endopeptidase sspA, (3) Ribose-phosphate pyrophosphokinase prs, (4) Aminoacyltransferase femX, and (5) Succinate dehydrogenase sdhB were chosen as targets to analyse the levels of RNA expression to validate the expression differences in planktonic and biofilms. The 16S rRNA was used as an endogenous control to normalise the data, and the level of differential expression of the five genes between planktonic and biofilm were compared.

RNA was extracted using a RNeasy Mini Kit (Qiagen, Germany) and cDNA synthesised from 200ng of RNA using the SuperScript™ IV VILO™ Master Mix (Thermo Fisher scientific) as described in Chapter 2, sections 2.3.2, 2.3.3 and 2.3.4. Real-time (RT)-PCR was performed in duplicate on two biological replicates as described in Chapter 2 section 2.3.6.

Primer sequences used in this study as described in Chapter 2 section 2.3.5.

Results

TMT identification of differentially regulated proteins

A total of 1636 non-redundant proteins with at least one unique peptide and <1% FDR were identified and quantitated across all 10 replicates. The profile of differentially regulated proteins in 3dwb and 12dwb relative to planktonic cultures are depicted using volcano plots by implementing the fold change (>1.5-fold) and p-value (<0.05) cut off values (Figure 4.2 A&B). Initial analysis was conducted on a cut-off of >1.5-fold, and p <0.05. However, in Chapter 3, we analysed and discussed proteins with a >2-fold difference with a significance level of p <0.05, to make the changes more biologically relevant. That's why we observed significant variation in the number of proteins. Each comparison regarded the proteins with fold changes beyond the cut-off values collected from Figure 4.2 A & B and with p values < 0.05 as the most significantly impacted proteins. Among them, 350 and 137 significant differentially regulated significant proteins and 382 common proteins were identified

compared to planktonic bacteria in 3dwb and 12dwb, respectively (Figure 4.3). When we processed our database through the TMTPrePro R package, we considered the cutoff range >1.5 fold, p <0.05. But, in our thesis we specifically focused on only proteins dysregulated >2 fold, p <0.05. Of these, 39 and 33 proteins were significantly (>2-fold) upregulated compared to planktonic bacteria in 3dwb and 12dwb, respectively (Figure 4.3). Of which, 15 and 19 proteins were detected in recognised protein pathways in 3dwb and 12dwb, respectively (Figure 4.3). In contrast, 77 and 18 proteins were significantly (>2-fold) downregulated in 3dwb and 12dwb, respectively. Of which, 29 and 6 proteins were detected in recognised protein pathways in 3dwb and 12dwb, respectively (Figure. 4.3). Among the common proteins between 3dwb and 12wb, 42 proteins were significantly upregulated (>2-fold) in which 21 proteins were involved in recognised pathways, and 128 proteins were significantly downregulated (>2-fold) of which 49 proteins were involved in recognised pathways (Figure. 4.3).

In this Chapter, we were able to present significant differences observed between 3bwb and 12dwb. Further, based on abundance variation (>2-fold), it appears that relatively a smaller number of proteins (51) are significantly different (p<0.05) between 12dwb and planktonic bacteria and more proteins (116) were significantly different in 3bwb and planktonic. This may suggest that 12 day biofilm proteome is closer to planktonic proteome, however, interestingly, we observed a large number of 12dwb proteins were more abundant but the difference didn't reach statistical significance.

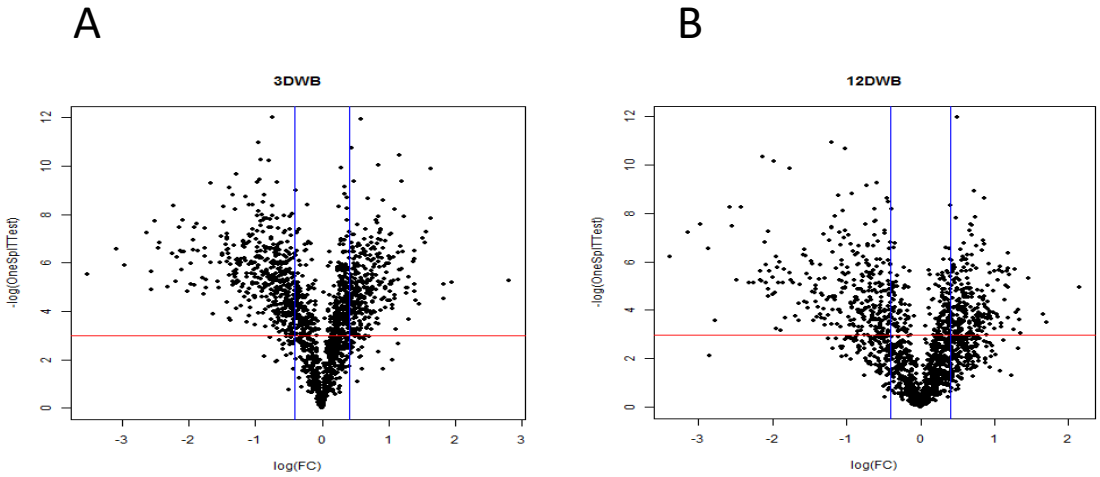

Figure 4.2: The volcano plot shows the distribution of the differential protein expression profile of (A) 3dwb compared to planktonic and; (B) 12dwb compared to planktonic. Y-axis in the form of −log 10 represents p-value; greater numerical value is associated with lower p-value and greater legitimacy. X-axis represents fold change (log_2) of the differentially regulated proteins are represented by blue lines. The two vertical blue lines represent fold changes of -1.5 and +1.5. Therefore, the dots above red line in the positive side are significantly (<0.05) upregulated proteins, and the dots in the negative side represent the significantly (<0.05) downregulated proteins.

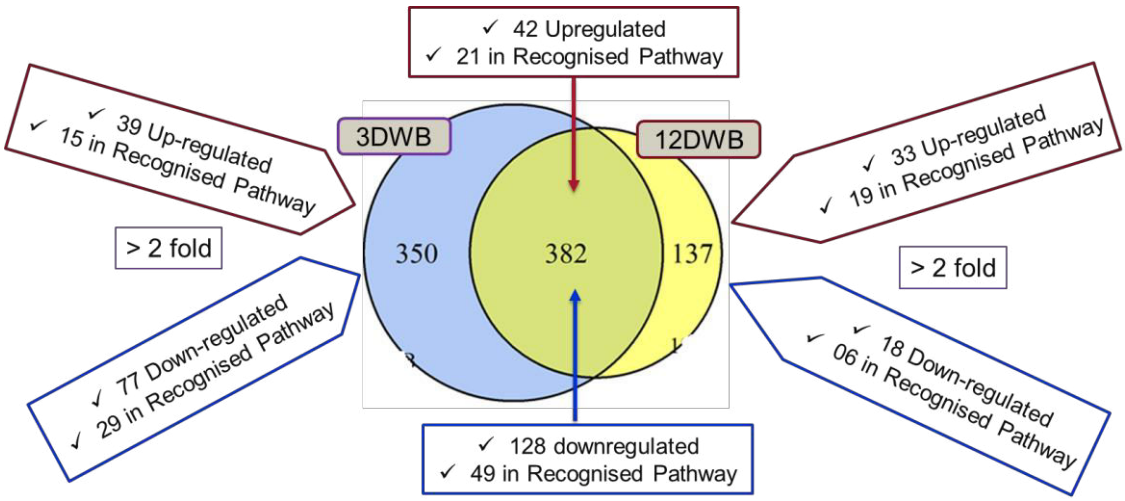

Figure 4.3: Venn diagram shows the dispersion of common and significant differential proteins in the 3dwb and 12dwb. Pathway analysis performed using KEGG.

GO analysis and annotation of differentially regulated proteins

We performed GO functional annotation for significant differentially regulated proteins of 3dwb and 12dwb in comparison to planktonic. In this analysis we considered only proteins dysregulated >2 fold and p<0.05. PANTHER analysis revealed the 5 most represented molecular functions in the complete global protein repository for both 3dwb and 12dwb (Figure 4.4 A&B). Among them, proteins involved in catalytic activity (44.8%) was the highest followed by binding (37.9%), and structural molecule activity (10.3%) in the 3dwb.

On the other hand, proteins involved in catalytic activity (40%) was the highest followed by binding (26.4%), structural molecule activity and transporter activity (13.3%) in the 12dwb.

Biological process evaluation identified the four most represented biological processes (Figure 4.5 A&B) for both 3dwb and 12dwb. Of the proteins significantly upregulated/downregulated >2 fold, 20 proteins (57.1%) involved in metabolic processes was found to be the highest followed by 10 proteins identified (28.6%) in cellular processes and 4 proteins (11.4%) involved in biological regulations in 3dwb. In contrast, 11 proteins (57.9%) involved in metabolic processes were identified in 12dwb followed by five proteins (26.3%) in cellular processes, and two proteins (10.5%) in localisations. These results suggest that more proteins are involved in metabolic processes in 3dwb compared with 12dwb.

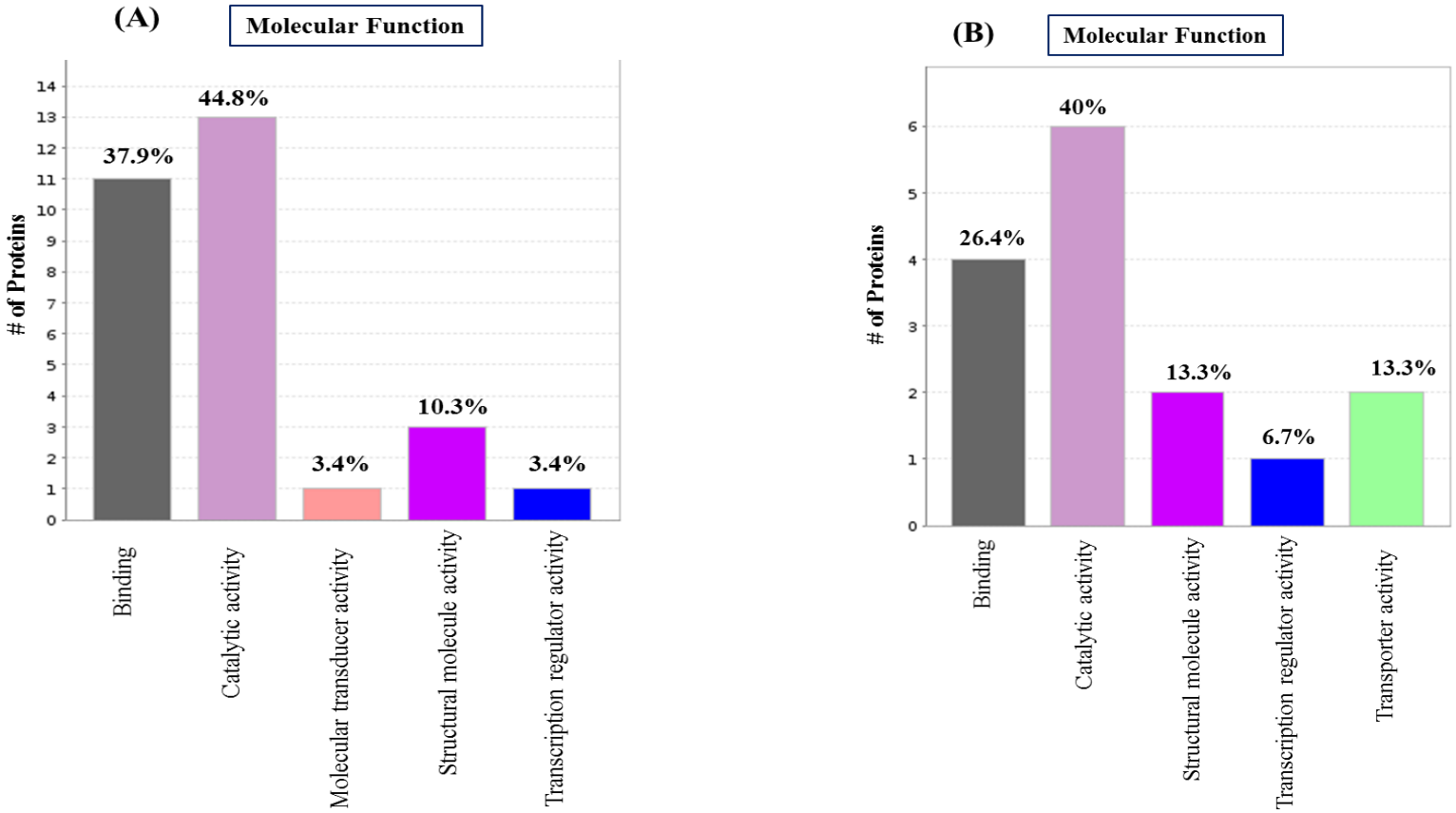

Figure 4.4: Classification of the significant differentially regulated proteins of 3dwb and 12dwb based on their functional annotations using Gene Ontology. In this analysis we considered only proteins dysregulated >2 fold and p<0.05. (A) GO Molecular Function for 3dwb; (B) GO Molecular Function for 12dwb.

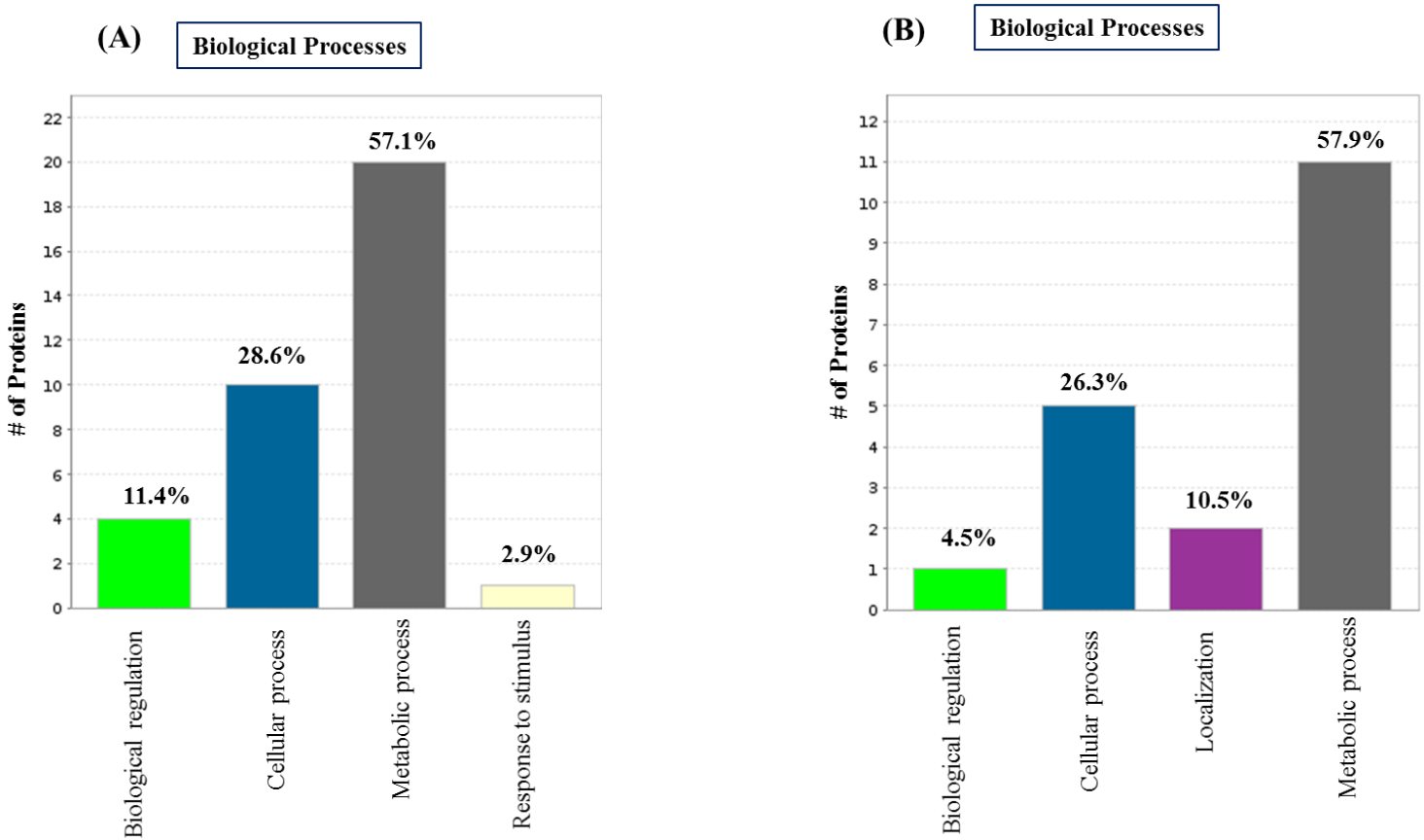

Figure 4.5: Classification of the significant differentially regulated proteins of 3dwb and 12dwb based on their functional annotations using Gene Ontology. (A) GO Biological Processes for 3dwb; (B) GO Biological Processes for 12dwb.

Significant differentially regulated proteins and pathway analysis in the 3dwb

The proteins that are significantly upregulated in 3-day biofilm in comparison with planktonic and 12-day biofilm are listed in Table 4.2. Of these proteins, acetyl-CoA acetyltransferase (>3.5-fold upregulated), a cytoplasmic enzyme, was significantly identified in 3-day biofilm and is involved in multiple metabolic pathways including fatty acid and pyruvate metabolism, indicating this enzyme plays a central role in energy metabolism (Figure 4.6), regulation of protein function under nutrient and oxygen-limiting conditions, and thus, ensures the survivability of biofilm [505-508]. Further, glyceraldehyde-3-phosphate dehydrogenase (gap) is significantly/significantly upregulated in 3-day biofilm and is involved in glycolysis pathway and is responsible for energy metabolism, which is also part of central metabolism (Figure 4.6). In addition, we observed 2-oxoglutarate ferredoxin oxidoreductase subunit alpha (SA1131) is significantly downregulated in 3dwb, involved in multiple pathways including pyruvate metabolism and tricarboxylic acid (TCA) cycle. This enzyme is a vital enzyme of the reductive TCA, and this cycle takes the opposite shape of the TCA cycle and is primarily disseminated in anaerobic autotrophs. 2-oxoglutarate ferredoxin oxidoreductase catalyses the carbon dioxide fixation reaction to succinyl-CoA resulting in 2-oxoglutarate production. (Figure 4.6). This reaction needs strong reducing power, and ferredoxin plays an important role in maintaining this redox balance. Studies have reported that 2-oxoglutarate ferredoxin oxidoreductase is important for maintaining bacterial growth under anaerobic conditions [509], and it also plays a role as a source for low-potential electron equivalents for nitrogen fixation [510]. A study by Dorner *et al.* (2002) reported that, 2-oxoglutarate ferredoxin oxidoreductase plays a pivotal role in the metabolism of aromatic compounds in the absence of molecular oxygen by catalysing the transfer of two electrons from decreased ferredoxin to benzoyl-CoA driven by ATP. They described that, reducing the benzene ring is a cycle that is energetically and mechanistically hard and needs exceptionally low redox potential and ferredoxin functions as an electron shuttle between the TCA cycle and benzoyl-CoA reductase by combining the oxidation of the benzoyl-CoA pathway end product, acetyl-CoA, with the decrease of the aromatic ring [510]. Therefore, it can be concluded that, the identified proteins involved in the central metabolism pathways maintained biofilm growth under diverse environments by providing an alternative metabolic route to utilise energy.

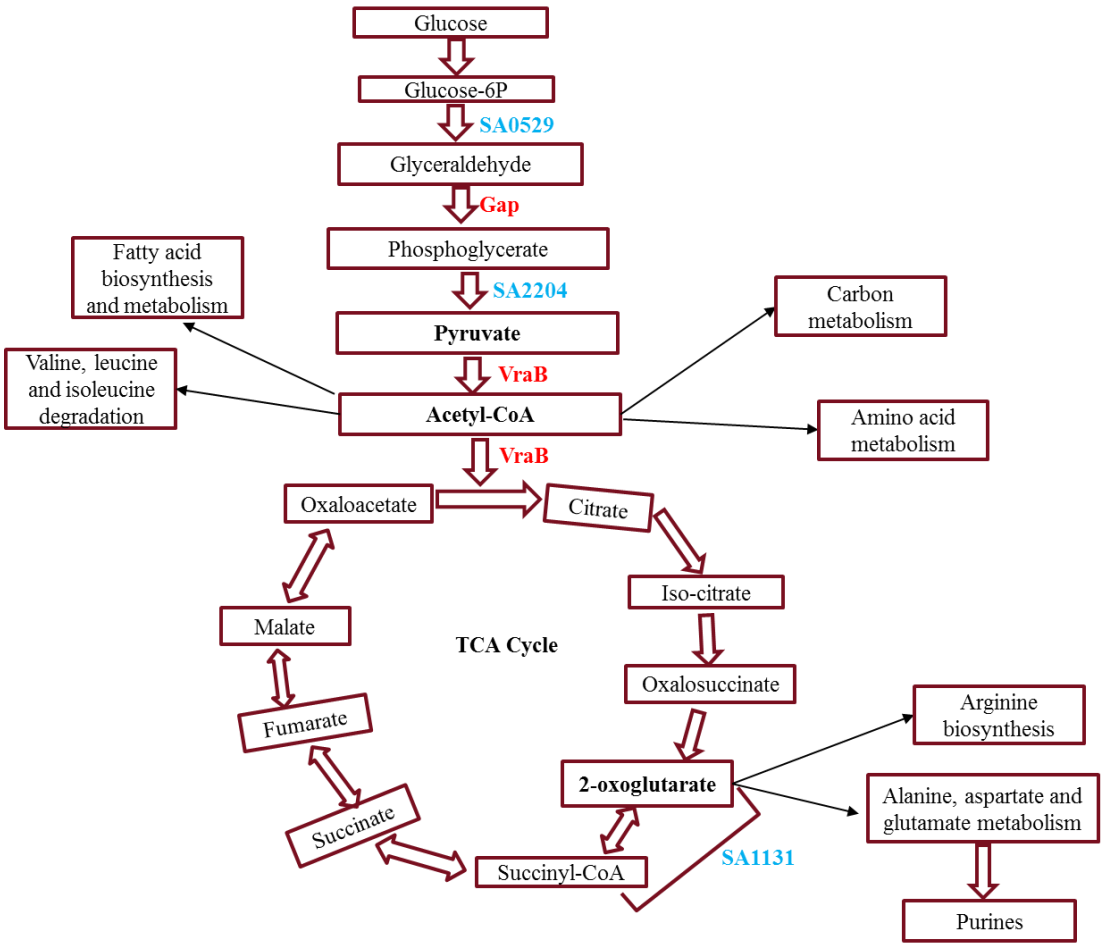

Figure 4.6: Significant differentially regulated proteins involved in central metabolism in 3dwb. Red names denote encoded genes with increased abundance while blue names denote encoded genes with decreased expression.

Cystathionine gamma-synthase (metB), 3-phosphoshikimate 1-carboxyvinyltransferase (aroA), and histidinol-phosphate aminotransferase were significantly upregulated in 3dwb and involved in multiple biosynthetic processes including amino acids, indicating increase the synthesis of amino acids. Selective amino acid uptake by the biofilm is significant for energy utilisation for maintenance of a proper redox balance, adaptation to diverse environmental conditions and nutrient availability thereby ensuring survivability [279].

We identified N-acetylmannosamine-6-phosphate 2-epimerase (nanE) and UDP-N-acetylglucosamine 1-carboxyvinyltransferase (murA) were significantly upregulated. These proteins are involved in amino sugar and nucleotide sugar metabolism and peptidoglycan biosynthesis. They are linked with the synthesis of cell-wall components which may lead to

EPS matrix deposition in the 3-day biofilm. Other upregulated cytoplasmic enzyme 2-amino-4-hydroxy-6-hydroxymethyldihydropteridine pyrophosphokinase (folk) is a part of folate biosynthesis which may favour intracellular accumulation of folate. 30S ribosomal protein S14 (rpsN) and 30S ribosomal protein S5 (rpsE) are significantly upregulated and such proteins may help cells adapt to the diverse conditions and guarantee cellular metabolism. However, zinc metallopeptidase is a cytoplasmic membrane protein, and hypothetical protein KQ76_08475, coagulase (coa) are extracellular enzymes involved in unrecognised pathways. Furthermore, glycosyltransferase (tagX), hypothetical protein KQ76_04890, restriction endonuclease subunit S (hsdS), etc are also involved in unrecognised pathways.

Table 4.2: Functional classification of the significantly upregulated proteins in 3dwb in comparison to 12dwb and planktonic (fold change >2, p<0.05).

Accession ID	Protein Name	Gene Name	Fold Change	Protein Pathways	Subcellular Localisation	p Value
						0.007028245
AIO20241.1	acetyl-CoA acetyltransferase	vraB SA0534	3.57	Metabolic pathways, Biosynthesis of antibiotics, Microbial metabolism in diverse environments, Carbon metabolism, Biosynthesis of secondary metabolites, Valine, leucine and isoleucine degradation, Two-component system, Terpenoid backbone biosynthesis, Fatty acid metabolism, Lysine degradation, Synthesis and degradation of ketone bodies, Propanoate metabolism, Glyoxylate and dicarboxylate metabolism, Benzoate degradation, Pyruvate metabolism, Tryptophan metabolism, Fatty acid degradation,	Cytoplasmic	

				Butanoate metabolism		
AIO19867.1	peptide ABC transporter substrate-binding protein	SACOL0187	2.91	Quorum sensing	Unknown	0.005248609
AIO20180.1	2-amino-4-hydroxy-6-hydroxymethyldihydropteridine pyrophosphokinase	folK SACOL0560	2.78	Metabolic pathways, Folate biosynthesis	Cytoplasmic	0.008211938
AIO20957.1	30S ribosomal protein S14	rpsN rpsN2 SA1171	2.76	Ribosome	Cytoplasmic	0.006085794
AIO20444.1	glyceraldehyde-3-phosphate dehydrogenase	gapA1 gap gapA SA0727	2.34	Metabolic pathways, Biosynthesis of antibiotics, Biosynthesis of amino acids, Microbial metabolism in diverse environments, Carbon metabolism, Biosynthesis of secondary metabolites, Glycolysis / Gluconeogenesis	Cytoplasmic	0.001945845
AIO21863.1	30S ribosomal protein S5	rpsE SA2031	2.33	Ribosome	Cytoplasmic	0.000923701

AIO20122.1	cystathionine gamma-synthase	metB	2.33	Metabolic pathways, Biosynthesis of antibiotics, Biosynthesis of amino acids, Cysteine and methionine metabolism, Glycine, serine and threonine metabolism, Sulfur metabolism	Cytoplasmic	0.000366962
AIO21327.1	adenine phosphoribosyltransferase	apt SA1461	2.15	Metabolic pathways, Purine metabolism	Cytoplasmic	0.004077618
AIO19985.1	N-acetylmannosamine-6-phosphate 2-epimerase	nanE SACOL0315	2.13	Amino sugar and nucleotide sugar metabolism	Cytoplasmic	0.019154857
AIO20869.1	prolyl-tRNA synthetase	proS SA1106	2.12	Aminoacyl-tRNA biosynthesis	Cytoplasmic	0.001090509
AIO21086.1	3-phosphoshikimate 1-carboxyvinyltransferase	aroA SACOL1504	2.09	Metabolic pathways, Biosynthesis of secondary metabolites, Biosynthesis of antibiotics, Biosynthesis of amino acids, Phenylalanine, tyrosine and tryptophan biosynthesis	Cytoplasmic	0.000866702
AIO20143.1	thymidylate kinase	tmk SA0440	2.03	Metabolic pathways, Pyrimidine	Cytoplasmic	0.023847212

				metabolism		
AIO20221.1	HAD family hydrolase	SACOL0602	2.02	Metabolic pathways, Biosynthesis of secondary metabolites, Biosynthesis of antibiotics, Glyoxylate and dicarboxylate metabolism	Cytoplasmic	0.008502906
AIO22323.1	histidinol-phosphate aminotransferase	SACOL2701	2.01	Metabolic pathways, Biosynthesis of secondary metabolites, Biosynthesis of antibiotics, Biosynthesis of amino acids, Phenylalanine, tyrosine and tryptophan biosynthesis, Novobiocin biosynthesis, Tyrosine metabolism, Histidine metabolism, Phenylalanine metabolism	Cytoplasmic	0.002141712
AIO21737.1	UDP-N-acetylglucosamine 1-carboxyvinyltransferase	murA1 murA SA1902	2.01	Metabolic pathways, Peptidoglycan biosynthesis, Amino sugar and nucleotide sugar metabolism	Cytoplasmic	0.000172417

Significantly upregulated proteins and pathway analysis in the 12dwb

The proteins that are significantly upregulated in the 12dwb in comparison with planktonic and 3dwb are listed in Table 4.3. Proteins such as octanoyltransferase (lipM), acetoin reductase (butA), nitrite reductase are involved in nitrite reduction, arginase (arg), 5-(carboxyamino)imidazole ribonucleotide mutase, are involved in multiple metabolic processes including galactose (lacAE) and pyrimidine metabolism (pyrEGHR). A cytoplasmic enzyme 2-oxoisovalerate dehydrogenase is part of biosynthesis of antibiotics, biosynthesis of secondary metabolites, valine, leucine and isoleucine degradation, and propanoate metabolism. Ribose-phosphate pyrophosphokinase (prs) is a cytoplasmic enzyme involved in multiple metabolism associated pathways including pentose phosphate and the glycolytic pathway. The high abundance of ribose may lead to metabolic change associated with TCA cycle stress and biofilm formation [511, 512]. A cytoplasmic enzyme 4'-phosphopantetheinyl transferase belongs to pantothenate and CoA biosynthesis was also upregulated. Proteins associated with cytoplasmic membrane include cytochrome C oxidase subunit III (qoxC) involved in oxidative phosphorylation, and preprotein translocase subunit SecY that is involved in quorum sensing, bacterial secretion systems, and protein export. Phosphotransferase system (PTS) lactose-specific transporter subunits IICB is a cytoplasmic membrane protein and is involved in metabolic pathways such as nitrogen metabolism, galactose metabolism, and phosphotransferase system.

A cytoplasmic enzyme aminoacyltransferase (femX) significantly upregulated in 12dwb and involved in peptidoglycan biosynthesis, plays an important role in cell-wall synthesis and may be very important for biofilm maintenance.

However, sodium:alanine symporter (alsT), and the transporter associated domain protein are cytoplasmic membrane proteins involved in unrecognised pathways. Furthermore, type II secretion protein (SA2371), GntR family transcriptional regulator (SACOL0120), hypothetical protein KQ76_05130 (SA0933), etc are also involved in unrecognised pathways and subcellular localisation are still unknown.

Table 4.3: Functional classification of the significantly upregulated proteins in 12dwb in comparison to 3dwb and planktonic (fold change >2, p <0.05). * CM denotes Cytoplasmic Membrane.

Accession ID	Protein Name	Gene Name	Fold Change	Protein Pathways	Subcellular Localisation	p Value
AIO21210.1	2-oxoisovalerate dehydrogenase	SACOL1561	3.11	Metabolic pathways, Biosynthesis of antibiotics, Biosynthesis of secondary metabolites, Valine, leucine and isoleucine degradation, Propanoate metabolism	Cytoplasmic	0.011919129
AIO20163.1	ribose-phosphate pyrophosphokinase	prs SA0458	2.81	Metabolic pathways, Biosynthesis of secondary metabolites, Biosynthesis of antibiotics, Microbial metabolism in diverse environments, Biosynthesis of amino acids, Carbon metabolism, Purine metabolism, Pentose phosphate pathway	Cytoplasmic	0.02178712

AIO21226.1	octanoyltransferase	lipM SA1363	2.68	Metabolic pathways, Lipoic acid metabolism	Cytoplasmic	0.008146779
AIO20800.1	phosphoribosyl transferase	pyrR SA1041	2.53	Metabolic pathways, Pyrimidine metabolism	Cytoplasmic	0.002716491
AIO19795.1	acetoin reductase	butA SA0122	2.49	Butanoate metabolism	Cytoplasmic	0.024617746
AIO21707.1	4'-phosphopantetheinyl transferase	acpS dpj SA1875	2.37	Pantothenate and CoA biosynthesis	Cytoplasmic	0.01457743
AIO21864.1	50S ribosomal protein L18	rplR SA2032	2.33	Ribosome	Cytoplasmic	0.001023369
AIO21765.1	CTP synthetase	pyrG ctrA SA1929	2.32	Metabolic pathways, Pyrimidine metabolism	Cytoplasmic	0.011333279
AIO20657.1	cytochrome C oxidase subunit III	qoxC SA0911	2.31	Metabolic pathways, Oxidative phosphorylation	CM*	0.008189133
AIO21825.1	PTS system lactose-specific transporter	lacE SACOL2181	2.27	Metabolic pathways, Phosphotransferase system,	CM	0.022621059

	subunits IICB			Galactose metabolism		
AIO21860.1	preprotein translocase subunit SecY	secY SA2028	2.15	Quorum sensing, Bacterial secretion system, Protein export	CM	0.016868331
AIO20807.1	orotate phosphoribosyltransferase	pyrE SA1048	2.13	Metabolic pathways, Pyrimidine metabolism	Cytoplasmic	0.029800669
AIO21830.1	galactose-6-phosphate isomerase	lacA SA1997	2.13	Metabolic pathways, Galactose metabolism	Unknown	0.022870023 0.000136083
AIO22037.1	nitrite reductase	nasD	2.08	Microbial metabolism in diverse environments, Nitrogen metabolism	Cytoplasmic	0.028564174
AIO20864.1	uridylate kinase	pyrH smbA SA1101	2.07	Metabolic pathways, Pyrimidine metabolism	Cytoplasmic	0.009286469
AIO21798.1	arginase	arg SA1968	2.04	Metabolic pathways, Biosynthesis of secondary metabolites, Biosynthesis of antibiotics,	Cytoplasmic	0.048277177

				Biosynthesis of amino acids, Arginine and proline metabolism, Arginine biosynthesis		
AIO21879.1	50S ribosomal protein L4	rplD SA2046	2.03	Ribosome	Unknown	0.049455485
AIO21892.1	aminoacyltransferase	femX fmhB SA2057	2.03	Metabolic pathways, Peptidoglycan biosynthesis	Cytoplasmic	0.001849203
OOC91313.1	5-(carboxyamino)imidazole ribonucleotide mutase	purE SA0916	2.01	Metabolic pathways, Biosynthesis of antibiotics, Purine metabolism	CM	0.011919129

Significantly downregulated proteins and pathway analysis in the 3dwb

The proteins that are significantly downregulated in the 3dwb in comparison with planktonic and 12dwb are listed in Table 4.4. Of these, response regulator GraR and alanine-phosphoribitol ligase (dltA) are cytoplasmic enzymes involved in two-component system, and cationic antimicrobial peptide (CAMP) resistance. A cytoplasmic membrane protein PTS fructose transporter subunit IICO is a part of fructose and mannose metabolism, oligoribonuclease and 7-cyano-7-deazaguanine reductase are cytoplasmic enzymes involved in sulfur metabolism and folate biosynthesis, indicating they reduce the utilisation of these molecules in the 3dwb. Tryptophanyl-tRNA synthetase (trpS), and methionine--tRNA ligase (metG) are cytoplasmic enzymes involved in aminoacyl-tRNA biosynthesis, and selenocompound metabolism. We identified several stress responses associated proteins that were significantly/significantly downregulated in 3-day biofilm such as cold-shock protein, Clp protease, thioredoxin reductase, glyoxalase, catalase, and general stress protein as well as other proteins (Table 4.4). Other downregulated proteins include, phenol soluble modulin is cytoplasmic enzyme belonging to the quorum-sensing pathway, ribonuclease H is a cell-wall enzyme belongs to DNA replication pathway. Proteins are significantly/significantly downregulated in 3-day biofilm such as oligoribonuclease, ribose 5-phosphate isomerase (rpiA), 6-phospho 3-hexuloisomerase, glutamine synthetase (glnA), phosphoglyceromutase, polynucleotide phosphorylase (pnp), ribonucleotide-diphosphate reductase subunit beta (nrdF), involved in multiple metabolism associated pathways including pentose phosphate and RNA degradation. However, acetyltransferase (oatA), peptidylprolyl isomerase (prsA), involved in unrecognised pathways.

Table 4.4: Functional classification of the significantly downregulated proteins in 3dwb in comparison to 12dwb and planktonic (fold change >2, p <0.05). * CM denotes Cytoplasmic Membrane.

Accession ID	Protein Name	Gene Name	Fold Change	Protein Pathways	Subcellular Localisation	p Value
AIO20326.1	response regulator GraR	graR SACOL0716	0.19	Two-component system, Cationic antimicrobial peptide (CAMP) resistance	Cytoplasmic	0.002501282
AIO21391.1	oligoribonuclease	SA1526	0.32	Metabolic pathways, Microbial metabolism in diverse environments, Sulfur metabolism	Cytoplasmic	0.002259606
AIO21365.1	50S ribosomal protein L20	rplT SA1502	0.32	Ribosome	Cytoplasmic	0.004486491
AIO20776.1	phenol soluble modulin	SACOL1186	0.35	Quorum sensing	Unknown	0.000622091
AIO20368.1	PTS fructose transporter subunit IIC	fruA	0.37	Metabolic pathways, Microbial metabolism in diverse environments, Fructose and mannose metabolism, Phosphotransferase system (PTS)	CM*	0.009827721

AIO20152.1	methionine--tRNA ligase	metG metS SA0448	0.39	Selenocompound metabolism, Aminoacyl-tRNA biosynthesis	Cytoplasmic	1.7344E-05
AIO21970.1	ribose 5-phosphate isomerase	rpiA SA2127	0.39	Metabolic pathways, Microbial metabolism in diverse environments, Carbon metabolism, Biosynthesis of secondary metabolites, Biosynthesis of antibiotics, Biosynthesis of amino acids, Pentose phosphate pathway	Cytoplasmic	0.002044168
AIO20435.1	thioredoxin reductase	trxB SA0719	0.39	Selenocompound metabolism	Cytoplasmic	0.001875872
AIO20575.1	tryptophanyl-tRNA synthetase	trpS SA0855	0.40	Aminoacyl-tRNA biosynthesis	Cytoplasmic	0.000526989
AIO21606.1	nicotinate phosphoribosyltransferase	SA1729	0.40	Metabolic pathways, Nicotinate and nicotinamide metabolism	Cytoplasmic	0.000441124
AIO20398.1	7-cyano-7-deazaguanine reductase	queF SA0683	0.41	Metabolic pathways, Folate biosynthesis	Cytoplasmic	0.000206252

AIO22235.1	3-methyl-2-oxobutanoate hydroxymethyltransferase	panB SA2392	0.42	Metabolic pathways, Biosynthesis of secondary metabolites, Pantothenate and CoA biosynthesis	Unknown	0.000152791
AIO22158.1	glyoxalase	SA2310	0.43	Metabolic pathways, Microbial metabolism in diverse environments, Benzoate degradation, Xylene degradation, Degradation of aromatic compounds	Unknown	0.001377871
AIO20913.1	glutamine synthetase	glnA SACOL1329	0.43	Metabolic pathways, Two-component system, Biosynthesis of amino acids, Glyoxylate and dicarboxylate metabolism, Arginine biosynthesis, Microbial metabolism in diverse environments, Alanine, aspartate and glutamate metabolism, Nitrogen metabolism	Cytoplasmic	0.00039883

AIO22054.1	phosphoglyceromutase	gpmA SA2204	0.45	Metabolic pathways, Microbial metabolism in diverse environments, Carbon metabolism, Biosynthesis of secondary metabolites, Biosynthesis of antibiotics, Biosynthesis of amino acids, Methane metabolism, Glycolysis / Gluconeogenesis, Glycine, serine and threonine metabolism	Unknown	0.003622702
OOC89529.1	dUTP pyrophosphatase	dut SACOL0357	0.45	Metabolic pathways, Pyrimidine metabolism	Cytoplasmic	0.003897145
AIO21459.1	riboflavin synthase subunit alpha	ribE SACOL1819	0.45	Metabolic pathways, Riboflavin metabolism, Biosynthesis of secondary metabolites	Cytoplasmic	0.001359211
AIO20507.1	alanine-phosphoribitol ligase	dltA SACOL0935	0.45	Two-component system, Cationic antimicrobial peptide (CAMP) resistance, D-Alanine metabolism, *Staphylococcus aureus* infection	Cytoplasmic	3.70988E-05

AIO20880.1	polynucleotide phosphorylase	pnp pnpA SA1117	0.47	Purine metabolism, Pyrimidine metabolism, RNA degradation	Cytoplasmic	0.006259143
AIO20237.1	6-phospho 3-hexuloisomerase	SA0529	0.47	Metabolic pathways, Microbial metabolism in diverse environments, Carbon metabolism, Biosynthesis of amino acids, Pentose phosphate pathway, Methane metabolism	Unknown	0.00040605
AIO21854.1	DNA-directed RNA polymerase subunit alpha	rpoA SA2023	0.47	Metabolic pathways, Purine metabolism, Pyrimidine metabolism, RNA polymerase	Cytoplasmic	0.004426841
AIO20895.1	2-oxoglutarate ferredoxin oxidoreductase subunit alpha	SA1131	0.49	Metabolic pathways, Microbial metabolism in diverse environments, Carbon metabolism, Biosynthesis of antibiotics, Glycolysis / Gluconeogenesis, Butanoate metabolism, Pyruvate metabolism, Citrate cycle (TCA cycle)	Cytoplasmic	0.000859809

AIO20402.1	ribonucleotide-diphosphate reductase subunit beta	nrdF	0.49	Metabolic pathways, Purine metabolism, Pyrimidine metabolism	Cytoplasmic	0.004711143
AIO19739.1	50S ribosomal protein L9	rplI SA0014	0.49	Ribosome	Cytoplasmic	0.001173203
AIO21458.1	GTP cyclohydrolase	ribBA SACOL1818	0.49	Metabolic pathways, Riboflavin metabolism, Biosynthesis of secondary metabolites, Folate biosynthesis	Cytoplasmic	0.002933012
AIO21057.1	ribonuclease H	SACOL1471	0.49	DNA replication	Cell wall	0.002265429
AIO20517.1	cytosol aminopeptidase	SACOL0945	0.50	Metabolic pathways, Glutathione metabolism	Cytoplasmic	0.001641133
AIO20955.1	catalase	katA SA1170	0.51	Carbon metabolism, Biosynthesis of secondary metabolites, Biosynthesis of antibiotics, Glyoxylate and dicarboxylate metabolism, Tryptophan metabolism	Cytoplasmic	0.018585116
AIO20165.1	50S ribosomal protein L25	rplY ctc SA0459	0.51	Ribosome	Cytoplasmic	0.001515076

Significantly downregulated proteins and pathway analysis in the 12dwb

The proteins that are significantly downregulated in the 12dwb in comparison with planktonic and 3dwb are listed in Table 4.5. Of these, DNA polymerase III subunit delta, and urease subunit gamma (urea), involved in several metabolic pathways including mismatch repair, and DNA replication. 30S ribosomal protein S14, cytoplasmic enzyme, is a part of ribosome metabolism. Proteins associated with transcription elongation factor (GreA), ribosome recycling factor, and cell division protein (FtsK) were significantly downregulated, indicating decreased metabolism of translation and post-transcriptional modification in the 12dwb. Hemin ABC transporter ATP-binding protein (hrtA), and amino acid ABC transporter substrate-binding protein are cytoplasmic membrane enzymes belong to ABC transporters pathway. Fibrinogen-binding protein encoded by SA1004 significantly identified in 12-day biofilm, is a virulence factor protein, and responsible for *S. aureus* infection in human, also downregulated in other *S. aureus* proteomic study [479].

Table 4.5: Functional classification of the significantly downregulated proteins in 12dwb in comparison to 3dwb and planktonic (fold change >2, p <0.05). * CM denotes Cytoplasmic Membrane.

Accession ID	Protein Name	Gene Name	Fold Change	Protein Pathways	Subcellular Localisation
AIO21867.1	30S ribosomal protein S14	rpsZ rpsN1 SA2034.1 SAS079	0.26	Ribosome	Cytoplasmic
AIO20145.1	DNA polymerase III subunit delta '	SACOL0526	0.31	Metabolic pathways, Mismatch repair, Pyrimidine metabolism, DNA replication, Purine metabolism, Homologous recombination	Cytoplasmic
AIO21919.1	urease subunit gamma	ureA SA2082	0.35	Metabolic pathways, Microbial metabolism in diverse environments, Purine metabolism, Arginine biosynthesis	Cytoplasmic
AIO21993.1	hemin ABC transporter ATP-binding protein	hrtA SA2149	0.45	ABC transporters	CM*

AIO20759.1	fibrinogen-binding protein	SA1004	0.47	*Staphylococcus aureus* infection	Unknown
AIO22050.1	amino acid ABC transporter substrate-binding protein	SACOL2412	0.51	ABC transporters	Unknown

Differentially regulated proteins common to both 3dwb and 12dwb

A total of 170 proteins (>2-fold, $p<0.005$) were detected in both 3dwb and 12dwb. Of these, 42 proteins were upregulated, 21 proteins detected in recognised pathways whereas 128 proteins were downregulated, and 49 proteins detected in recognised pathways. Among the upregulated proteins, amino acid biosynthesis and metabolism, purine and pyrimidine metabolism associated proteins showed an increased abundance trend in the 3dwb (Appendix 4). However, the majority of the upregulated proteins showed an even distribution. On the other hand, downregulated proteins were higher in the categories of amino acid biosynthesis, energy metabolism, translation, and post-translational modification indicating a lower metabolic activity profile in the 12dwb (Appendix 5) and supports the overall perspective of biofilms as slow-growing, metabolically lethargic communities which is more predominant for 12-day biofilm.

Protein-protein interaction (PPI) analysis

Because PPI plays important roles in most cellular biological processes, a network was constituted by PPI of the 116 and 51 significantly >2 fold differentially expressed proteins in 3dwb and 12dwb respectively, using the STRING online PPI prediction software (Figure 4.7). As depicted in Figure 4.7, a set of significant differentially regulated proteins were found to be actively interacting in 3dwb including: 30S ribosomal protein S14 (rpsN), 30S ribosomal protein S5 (rpsE), proline--tRNA ligase (proS), thymidylate kinase (tmk), adenine phosphoribosyltransferase (apt), 5'-nucleotidase (sasH), ribonucleotide-diphosphate reductase subunit beta (nrdF), thioredoxin reductase (trxB), DNA-directed RNA polymerase subunit alpha (rpoA), 50S ribosomal protein L25 (ctc). Further targeted experimental and PPI analysis of this group will be helpful to understand how they are biologically connected and what function they share.

For 12dwb, there was an active interaction between a group of significant differentially expressed proteins, including preprotein translocase subunit (secY), 50S ribosomal protein L18 (rplR), 50S ribosomal protein L4 (rplD), orotate phosphoribosyltransferase (pyrE), ribose-phosphate pyrophosphokinase (prs), uridylate kinase (pyrH), urease subunit gamma (ureA), hemin ABC transporter ATP-binding protein (hrtA). Therefore, proteins are differentially expressed in early biofilm when compared to more mature biofilm.

A

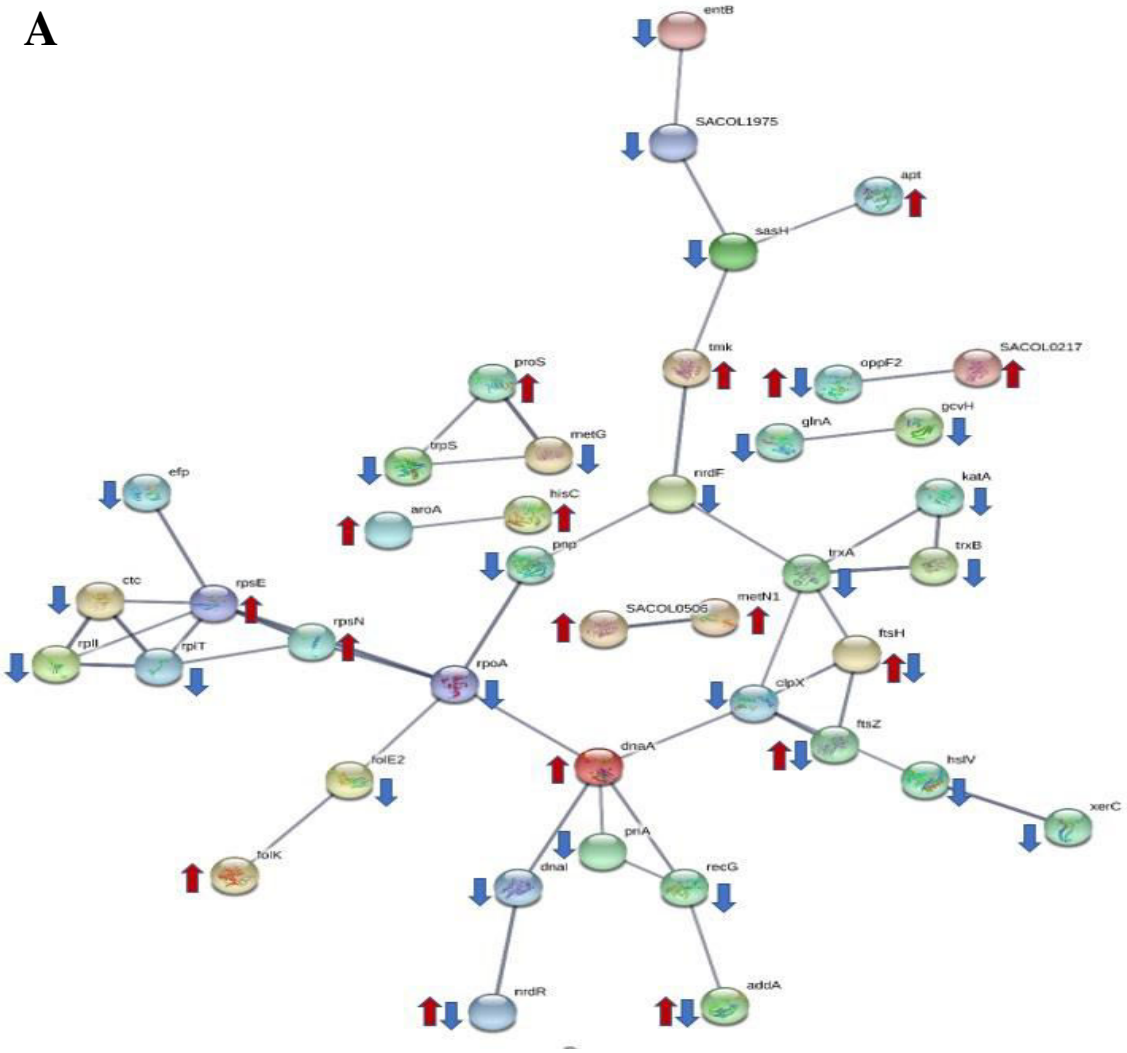
entB
SACOL1975
apt
sasH
tmk
SACOL0217
oppF2
proS
gcvH
glnA
metG
trpS
efp
nrdF
katA
hisC
aroA
pnp
trxA
trxB
ctc
rpsE
metN1
SACOL0506
rpsN
ftsH
rplI
rplT
rpoA
clpX
ftsZ
dnaA
hslV
folE2
xerC
priA
folK
dnaI
recG
nrdR
addA

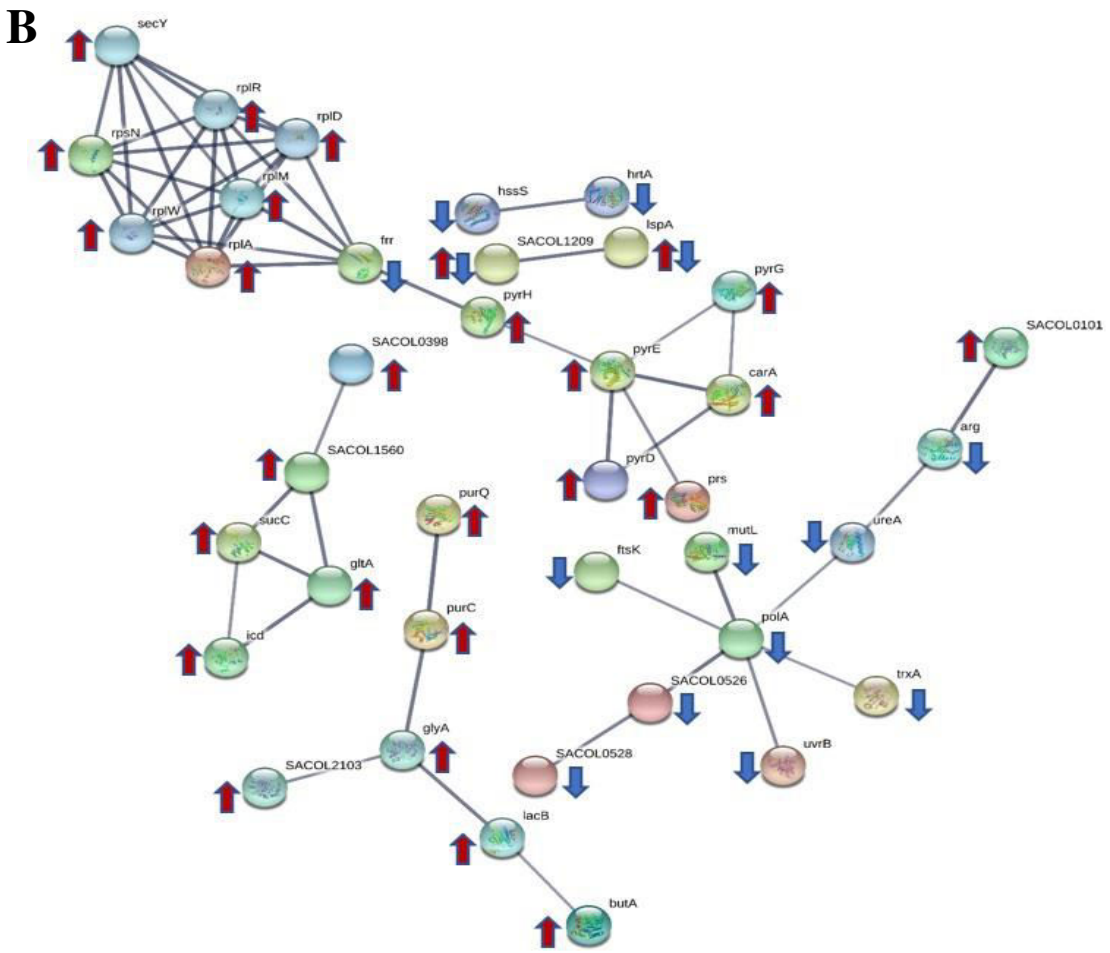

Figure 4.7. The protein-protein interaction network as analysed by STRING software with high confidence (0.700) and omitted nodes those are not connected to the network. Red arrows represent upregulation and blue arrows represent downregulation. The map of the significantly upregulated and downregulated proteins from (A) 3dwb and (B) 12dwb show high interactions, which indicates that the proteins are biologically linked, at least partly, as a group.

Validation of TMT data with real-time qPCR

The ratios from the qPCR results were obtained by comparing with planktonic in 3dwb and 12dwb. Individual normalised qPCR results are shown in Appendix 3. Upregulated and downregulated protein expression and gene expression results were expressed in fold change (FC). qPCR results showed that, in 12dwb, prs was significantly upregulated in both qPCR and TMT analysis. Between 3dwb and 12dwb, sspA was significantly downregulated in both qPCR

and TMT analysis, indicating a relative consistency with the TMT data for these proteins. However, for genes (SA0914, femX and sdhB) there was a dysregulation between qPCR and TMT data (Table 4.6).

Table 4.6: Relative correlation of the selected qPCR gene expression data to TMT protein expression data (significant and common) in 3dwb and 12dwb compared with planktonic. *FC denotes fold change

			TMT		qPCR	
Accession ID	**Protein Name**	**Gene Name**	**3dwb (FC)***	**12dwb (FC)***	**3dwb (FC)***	**12dwb (FC)***
AIO20660.1	chitinase	SA0914	0.118	0.088	1.528	0.902
AIO20645.1	glutamyl endopeptidase	sspA	0.152	0.149	0.010	0.083
AIO20163.1	ribose-phosphate pyrophosphokinase	prs		2.814		3.94
AIO21892.1	aminoacyltransferase	femX		2.026		0.646
AIO20749.1	Succinate dehydrogenase	sdhB	0.452	0.283	1.10	3.30

Discussion

A wide spectrum of Gram-positive organisms such as *S. aureus, Staphylococcus epidermidis, Streptococcus,* and *Enterococcus faecalis* as well as Gram-negative organisms such as *Pseudomonas aeruginosa*, and *Escherichia coli* have been associated with biofilm infection of medical devices [174, 513] and healthcare equipment [514] and surfaces [239, 249, 251, 514]. Nevertheless, the potential molecular markers and mechanism associated with the formation of *S. aureus* biofilm are still poorly understood. In our previous study (Chapter 3), we observed significant variations in the expression of proteomic profile of *S. aureus* relating to numerous

metabolic and cellular processes, virulence factors, and transporters of the *S. aureus* biofilm compared to planktonic growth mode. Take a step forward, in this TMT-based high-resolution proteomics study, we mainly focused on the profiles of the protein expression in the 3-day biofilm and 12-day biofilm of *S. aureus* as compared to the planktonic growth mode.

Further, we also performed qPCR experiments of some selected significantly dysregulated genes to explore the correlation between qPCR and TMT data. Gene expression levels utilising qPCR were found to be comparably consistent with the data obtained from TMT-based MS analysis. The lack of an association between transcriptomics and proteomics is likely attributable to differences in half-lives and post-transcription machinery. Moreover, the absence of any correlation between data obtained from TMT and qPCR analysis could be due to differences in cell lysis and extraction methods performed on the samples.

Proteomic profiling analysis at various phases of biofilms highlighted interesting findings on metabolic processes, biosynthetic processes, transport systems such as sugar and ABC transporters, and stress response (e.g. gap, nanE, nasD, SA1692) involved in *S. aureus* biofilm formation (Figure 4.10).

For instance, the upregulation of 3-phosphoshikimate 1-carboxyvinyltransferase (aroA) involved in the shikimate pathway shows an enhanced synthesis of aromatic amino acids in the 3dwb. Some studies demonstrated that aroA production can result in glyphosphate resistance in pathogenic bacteria such as *S. aureus* and the plant pathogen *Burkholderia glumae*'s growth, virulence, and UV tolerance [515-517]. This suggests that a higher accumulation of glyphosphate in biofilm may show increased resistance levels to glyphosphate and virulence mechanisms, probably resulting in enhanced biofilm formation. PIA is a major component of the biofilm matrix and its formation also depends on the phosphotransferase system (PTS), a distinct method used by bacteria to uptake sugar. The phosphoenolpyruvate-protein (PEP) PTS is a carbohydrate-specific active transport mechanism, and is responsible for transporting sugar substrates (such as glucose, lactose, fructose, and cellobiose) during translocation across the cell membrane. We observed interesting findings with sugar transporter systems such as PTS, upregulation of lactose-specific transporter subunits IICB (lacE), galactose-6-phosphate isomerase (lacA) involved in galactose metabolism, and aminoacyltransferase (femX) involved in peptidoglycan

biosynthesis in the 12-day old biofilm. These three proteins are linked with energy metabolism and cell-wall synthesis (Figure 4.8) which might lead to higher EPS matrix deposition. This could be one possible mechanism by which more mature biofilm utilise energy consumption and increase cell-wall protein formation which increases tolerance to antimicrobials.

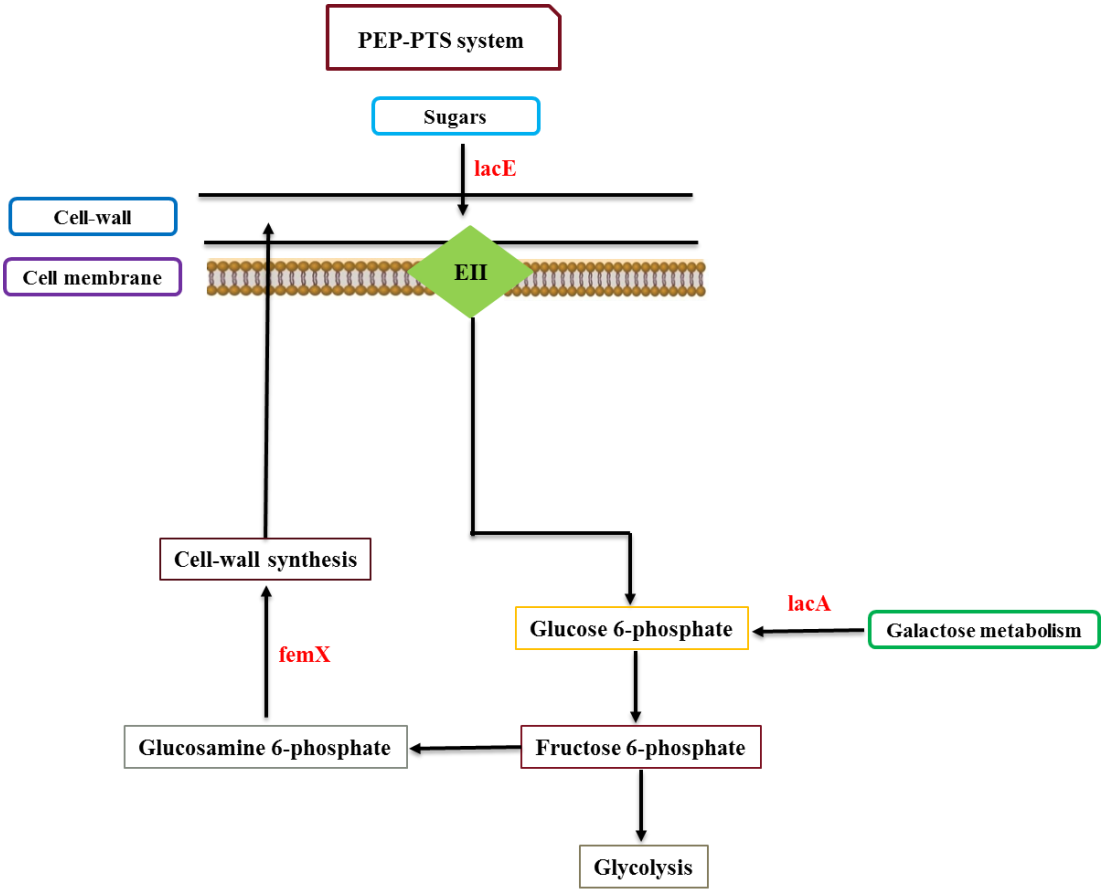

Figure 4.8: Linking pathway demonstration of phosphotransferase (PTS), galactose metabolism, and peptidoglycan biosynthesis in 12dwb. Bacterial biofilm can uptake sugars by specific sugar transport systems (e.g. PTS) and non-PTS system (e.g. galactose metabolism). LacAE involved in the metabolism of sugar molecules via fructose 6-phosphate which is also linked with glycolysis and synthesis of cell-wall components. In addition, peptidoglycan biosynthesis proteins (e.g. femX) is also directly linked with cell-wall formation. EII: Enzyme II; Red names denote encoded genes with increased abundance in 12dwb.

Aminoacyltransferase is a fem family enzyme that incorporates L-amino acids into the interchain cross bridge of Gram-positive cell-wall peptidoglycan. This enzyme plays important roles in stabilising peptidoglycan chains and cell viability in *S. aureus* [518]. FemX is a novel non-ribosomal peptidyl transferases which utilise aminoacyl-tRNA as a donor of amino acids [519, 520]. The interchain peptide is highly specific to a selective species, for example in *S. aureus*, femX was demonstrated to be involved in the incorporation of glycine$_1$ of the pentaglycine interchain peptide (Figure 4.9), while the femA and femB genes were accountable for glycine$_{2\text{-}3}$ and glycine$_{4\text{-}5}$ integration, respectively [521].

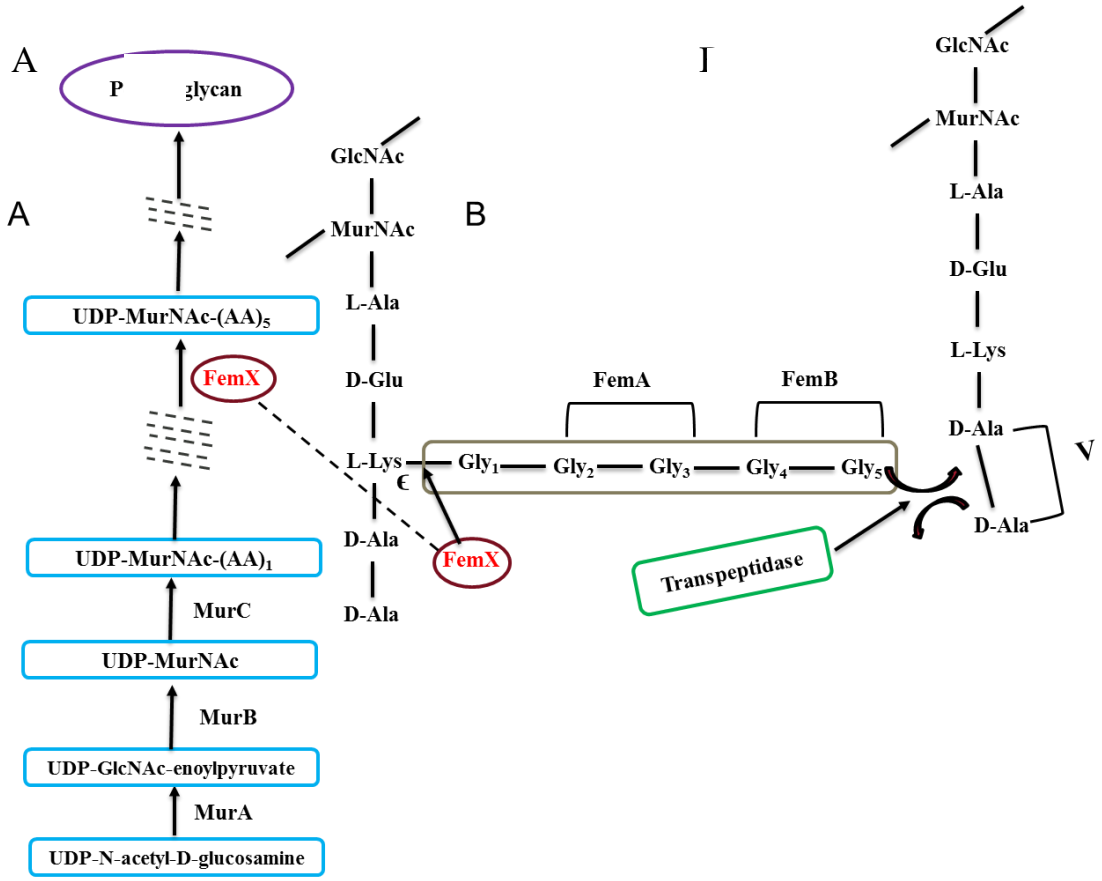

Figure 4.9: (A) General view of the selected part of the peptidoglycan biosynthesis pathway; (B) Selected part of the structure of *S. aureus* peptidoglycan which is linked with the potential role of femX significantly identified in 12dwb; modified from [521]. FemX from *S. aureus* play vital role in the transfer of Gly$_1$ to the ϵ-NH$_2$ group of Lys from glycyl-tRNA. Further chain elongation process initiated by the help of femA and femB which is ultimately

ended up of the terminal Gly_5. Gly_5 is cross-linked to the second last D-Ala residue and this step regulated by transpeptidase reaction, and inactivated by both β-lactams and vancomycin. V denotes vancomycin which is binds to the terminal D-Ala-D-Ala.

Fem family enzymes have a unique catalytic mechanism [521, 522], and essential for expression of β-lactam resistance mediated by low-affinity penicillin-binding protein family (PBPs) [520], suggesting that this enzyme might be potential targets molecules for the design of novel antimicrobial agents against multi-resistant bacteria.

Further, studies reported that PTS systems inhibition showed reduced virulence in *S. aureus* using a murine model [523]. Multiple proteomics and transcriptomics analysis demonstrated both increased and decreased abundance of PTS system associated proteins under various conditions (such as varying growth stages of biofilms, drug treatments, stress response) in several organisms including *S. aureus* [348, 524-527]. Therefore, it can be concluded that PTS systems (especially sugar transport) are expressed differentially in terms of the stress response, virulence, and the isolate nature and may be potentially associated with the formation of *S. aureus* biofilm.

Similarly, ABC transporter system proteins such as peptide ABC transporter substrate-binding protein encoded by SACOL0187 and heme ABC transporter ATP-binding protein (SACOL0779) are significantly upregulated in the 3dwb, whereas hemin ABC transporter ATP-binding protein (hrtA) and amino acid ABC transporter substrate-binding protein (SACOL2412) are significantly downregulated in the 12dwb. In 3dwb, we observed significant upregulation of ABC transporter proteins (such as SACOL0187, SACOL0779), and these proteins play important roles in the delivery of molecules (e.g., metabolic products, proteins) with diverse structures and functions to maintain cellular integrity, survivability and to support sufficient nutrient supply inside the cell. It is likely, that during early biofilm development , the bacteria are more metabolically active and biofilm formation requires a better nutrient supply, thus the ABC transporter proteins are upregulated. On the other hand, as biofilm ages, the cells are less metabolically active and the biofilm is mature so less nutrients are required. This is reflected by loss of upregulation of ABC transporter proteins SACOL0187, SACOL0779 and significant downregulation of other ABC transporter proteins (such as hrtA, SACOL2412).

As expected, over time biofilm produces thicker EPS matrix and significant upregulation of energy metabolism (e.g., lacAE) and cell-wall synthesis (femX) proteins might play significant role in producing thicker EPS matrix in the maturing biofilms. Several ABC transporter proteins have been shown to play a role in *S. aureus* pathogenesis and antimicrobial resistance [528-531]. For example, heme upregulates an ABC transport system when *S. aureus* is exposed to sub-lethal concentrations of iron, and a mechanistic explanation for this adaptation could be the redirection of central metabolism to increase iron availability [532]. Further, *S. aureus* relies on various amino acids under limited resources and multiple amino acid transporters play an important role to fulfil their metabolic requirements for virulence, growth, and persistence [530]. In addition, it has been reported that ABC transporter acts as a positive regulator during biofilm development in acute and chronic *S. aureus*-associated osteomyelitis in the pig [533], whilst it is a negative regulator of biofilm formation for *Listeria monocytogenes* [475]. In another study, the ABC transporter of *S. aureus* was shown to attenuate virulence by changing the composition and role of the cell-wall [534]. In addition, proteomics and transcriptomics studies have reported the differential expression of ABC transporter proteins during biofilm development in various bacteria including *S. aureus* [341, 470, 475, 476, 525]. Taken together, identified significant differentially regulated ABC transporter proteins may exhibit potential moonlighting/multiple functions in different stages of *S. aureus* biofilm development.

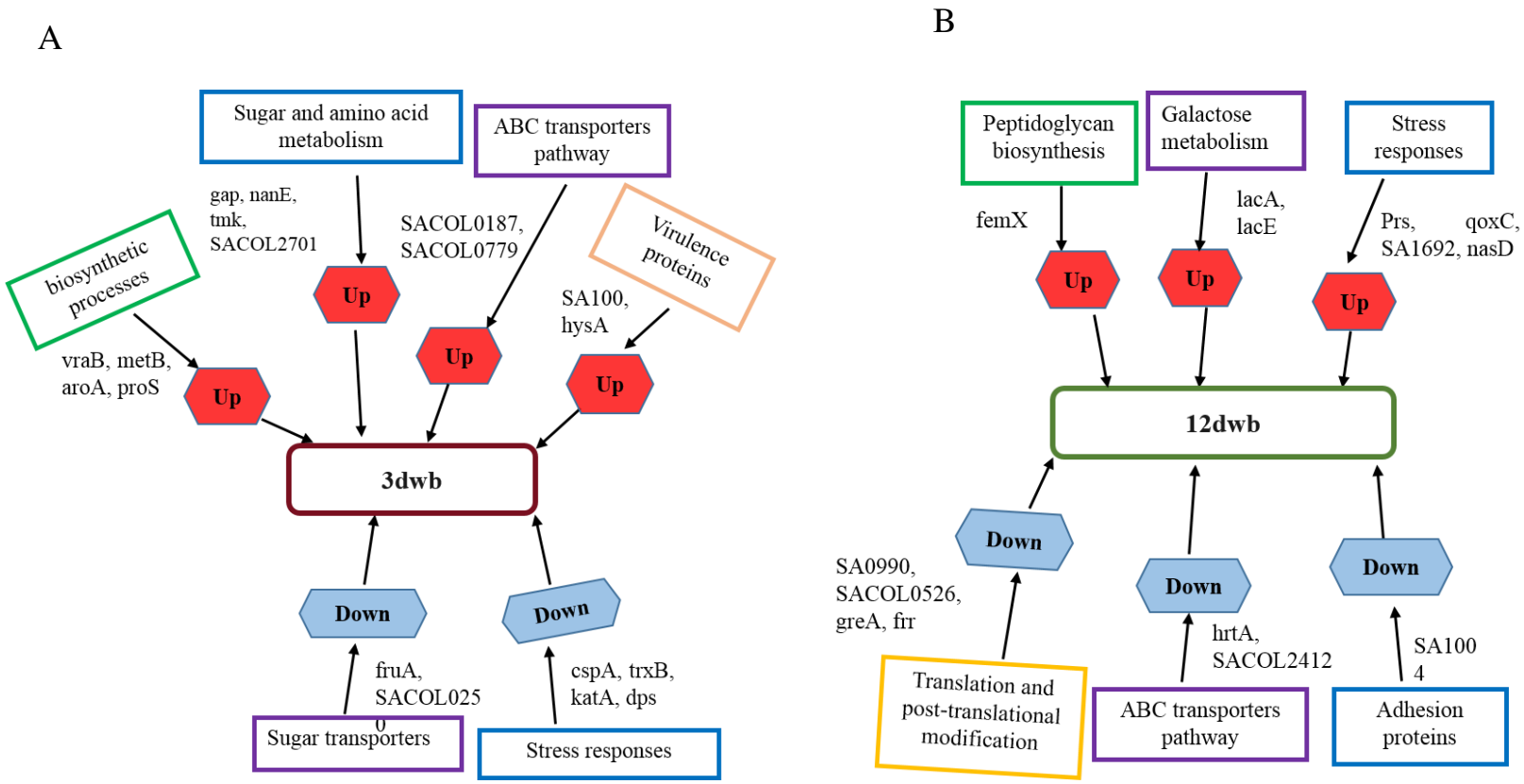

Figure 4.10. Novel regulators of *S. aureus* biofilm formation in (A) 3-day biofilm, and (B) 12-day biofilm identified from TMT-based analysis.

Further KEGG pathway analysis of the significant differentially expressed proteins showed interesting understandings into the metabolic profiles during different growth stages of biofilm development. In the 3dwb, small molecules, amino sugar and nucleotide metabolism, amino acid biosynthesis and metabolism, and energy metabolism associated proteins were significantly upregulated, indicating a higher metabolic activity profile in the 3dwb compared to 12dwb. In the 12dwb, translation, post-translational modification, ribosomal, cell division, attachment, and cofactor metabolic process associated proteins are significantly downregulated, indicating a lower metabolic activity profile in the 12dwb. This also suggested that the more mature biofilm adapted to adherent growth and utilised alternative metabolic pathways during biofilm development. On the other hand, it is likely that the metabolically active biofilm growth mode that we observed in 3dwb promote dispersal rather than adhesion, leading to biofilms with less mass. This notion also supported by Suriyanarayanan *et al.* (2018) where they compared the proteome of weak biofilm producer versus strong biofilm producer from *Enterococcus faecalis* [517]. They reported that strong biofilm producer showed lower metabolic activity compared to weak biofilm producer and suggested that it may be likely that the metabolically active biofilm cells (weak biofilm producer) promote dispersal rather than adhesion, leading in less mass of biofilms.

Biofilms are organised as tightly packed communities with bacteria exhibiting different metabolic states partly due to the availability of nutrients and oxygen declines gradually due to consumption and impairment of diffusion and is thus, limited in the biofilm's deeper layers. We expected to observe oxygen limitation due to the higher cell densities reached during different stages of biofilm development especially in 12-day biofilm compared to planktonic growth. Therefore, we observed nitrite reductase encoded by nasD significantly upregulated in 12-day biofilm which is responsible for the production of energy under oxygen-limited environments. Oxygen limitation also has been demonstrated for biofilms of several species including *S. aureus* [126, 342, 463, 476, 535, 536].

The expression of PIA synthesising proteins IcaADBC is influenced by oxygen availability and nutrient, cell density, and numerous stress responses, and we observed several stress responses associated proteins were differentially regulated in 3-day biofilm (such as SA0558, helicase DnaB, aldo/keto reductase, SACOL0959, response regulator GraR, trxB, glyoxalase, katA, dps,

etc), and in 12-day biofilm (such as SACOL1561, qoxC, SA1692, SA0758, glyoxal reductase, etc). We observed that oxidative stress associated proteins were more downregulated in 3-day biofilm which has also been shown by Graf *et al.*, 2019 [463]. In addition, due to oxygen limitation and oxidative stress within the biofilm, cytochrome C oxidase subunit III (qoxC), was significantly upregulated in 12-day biofilm, and is involved in electron transport chain maintenance. A recent proteomic study by Lei *et al.*, (2017), emphasises the importance of stress response associated proteins for virulence regulation, and adaptation during chronic infection in a rat model of orthopedic implant-associated biofilm infection from *S. aureus* [345]. The changes in protein synthesis and metabolic activity we identified in different stages of biofilm may shed new insight in the *S. aureus* biofilm biology.

Conclusions

In this study, the comparison of stationary phase planktonic bacteria with 3-day biofilm and 12-day biofilm demonstrated a significant range of quantitative proteomic shifts. Our analyses provide new understanding about the impact on the protein expression profile of growth mode for both planktonic and different stages of biofilm, potential biofilm regulators and the probable mechanisms for the development of *S. aureus* biofilms. Among the significantly upregulated proteins in 12-day biofilm, we observed proteins linked with energy metabolism (PTS, lacAE), and cell-wall synthesis (femX) which might lead to higher EPS matrix deposition. This interesting finding suggests one possible mechanism by which more mature biofilm increases resistance to antimicrobials. Further, proteins were significantly upregulated in the 3-day biofilm suggested a higher metabolic activity profiles whereas significantly downregulated proteins revealed a lower metabolic activity profiles in the 12-day biofilm. Moreover, PPI network showed significantly more interactions for 3-day and 12-day biofilms. Identified proteins may probably offer a new set of tools to design novel therapeutic approaches for *S. aureus* biofilm-associated infections related with implantable medical devices.

Chapter 5: One step forward with dry surface biofilm: TMT-based quantitative proteomic analysis reveals proteomic shifts between traditional hydrated biofilm and DSB from *Staphylococcus aureus*

In Chapters 3 and 4, we showed that significant abundance variation exists between planktonic and different stages of biofilm from *S. aureus*. Comparing the proteome of planktonic and biofilm revealed a potential role of key proteins in biofilm, which may advance our knowledge in the existing biofilm community. Further, comparing the proteome of different stages of biofilm showed altered metabolic profiles and over time the biofilm adapted to the adherent mode of growth.

The pioneering discovery of dry surface biofilm present on hospital surfaces, by our group, has raised serious concern in terms of infection control and the failing of current cleaning and disinfectant protocols. Almatroudi's study demonstrated that DSB contains more protein and less carbohydrate than wet biofilm and contains thicker extracellular polymeric substances (EPS). The authors surmised that these factors may be responsible for the increased tolerance to detergents and/or disinfectants [252]. However, so far, no study addressed the formation of complex DSB which urges more research to understand deeper biology of complex biofilm formation.

Therefore, in this study, we took a novel approach to better understand DSB biology by comparing the proteome of wet and DSB from *S. aureus*. This pioneering study may be helpful in designing advanced targeted cleaning agents and disinfectants to destabilising biofilm architecture.

Abstract

The Gram-positive bacterium *S. aureus* is responsible for serious acute and chronic infections worldwide and is well known for its biofilm formatting ability. Recent findings of biofilms on dry hospital surfaces emphasise the failures in current cleaning practices and disinfection and the difficulty in removing these dry surface biofilms (DSB). Many aspects of the formation of complex DSB biology on environmental surfaces in healthcare settings remains limited. Unlike traditional hydrated biofilms (wet), DSB are mainly composed of protein with little carbohydrate. In the present study, we aimed to determine how the protein component varied between wet and DSB. We did this by first constructing a comprehensive reference map of wet biofilm and DSB associated proteins of *S. aureus* using high-throughput TMT-based mass spectrometry. Further pathway analysis of significantly differentially expressed marker proteins revealed that proteins associated with energy metabolism such as phosphoribosyl transferase (pyrR), glucosamine--fructose-6-phosphate aminotransferase (glmS), galactose-6-phosphate isomerase (lacA), argininosuccinate synthase (argG) were significantly upregulated whereas ribosomal and ABC transporters were significantly downregulated in the wet. Proteins significantly upregulated in DSB include PTS glucose transporter subunit IIBC (ptaA), UDP-N-acetylmuramate-L-alanine ligase (murC) and UDP-N-acetylenolpyruvoylglucosamine (murB). These three proteins are all linked with peptidoglycan biosynthesis pathway and are responsible for cell-wall formation. Increased cell-wall formation may lead to increased EPS matrix deposition and contribute to the persistence of DSB on dry surfaces. For the first time, TMT-based proteomics study with DSB has shed novel insights and provides a basis for the identification and study significant pathways vital for biofilm biology in this reference microorganism. Identifying new/potential protein markers could lead to the development of much required advanced, targeted disinfectants and detergents, especially for decontaminating dry hospital environments.

Keywords: *Staphylococcus aureus*, Bacterial Biofilms, DSB, CDC Bioreactor, TMT, Mass Spectrometry

Introduction

Staphylococcus aureus frequently causes healthcare-associated infections (HAI) worldwide, and its virulence is increased due to its ability to form biofilm. Biofilms are problematic in healthcare settings, accounting for 65% of HAI including indwelling medical devices such as prostheses, peripheral venous catheters and urinary catheters. In addition, biofilms have been found to contaminate surgical equipment such as endoscopes [537]. Environmental surfaces in healthcare facilities play a vital role in terms of disease transmission [231-235], and development of biofilms on the surfaces in these settings complicate environmental decontamination [90, 104, 236-239]. Biofilms can function as reservoirs of pathogens in the hospital setting and provide favourable environments for long-term persistence of pathogens [239-241]. The structure of biofilms also protects engrafted pathogens against several antimicrobials, including antibiotics and biocides [104, 242, 243], which makes it very difficult to eliminate these pathogens using frequently used decontamination methods [244-246].

It has been speculated that the formation of biofilms may be enhanced by a thin film of water resulting from condensation on surfaces or that the relative humidity of intensive care units is sufficiently high to allow biofilm development [239]. However, recent findings of biofilms on dry hospital surfaces emphasise the failures in current cleaning practices and disinfection [239, 247]. Biofilms contain a high bacterial load capable of surviving for a long time on dry hospital surfaces, and also showing an increased resistance towards inactivation by disinfectants. In fact, bacteria in the biofilm are up to 1000 times more resistant to disinfectants than their respective planktonic state [244, 248-250].

Recent studies reported that more than 50% [239, 251] dry surface biofilms recovered from hospital surfaces contain *S. aureus*. A novel dry surface biofilm (DSB) model was developed by [252] to test the efficacy of disinfectants. They found that hypochlorite was less effective against DSB than its efficacy against hydrated biofilm which in turn was more effective against planktonic organisms [244]. Another recent study reported that disinfectants were unable to remove all *S. aureus* biofilm protein in the presence of biological soil [245]. These studies highlight the possible negative impact that biofilms have on infection control. Therefore, it is a dire need to understand deeper biology of complex biofilm formation to prevent transmission of

pathogens from healthcare surfaces, and advanced targeted design of cleaning agents and disinfectants by destabilising biofilm architecture. However, so far, none of the studies described the development of complex dry surface biofilm on environmental surfaces in healthcare settings.

Studies by Almatroudi et al (2015), reported that DSB contains more protein and less carbohydrate than wet biofilm, and thicker extracellular polymeric substances (EPS), with clinical dry biofilm containing between 42-95% protein [252]. In *Staphylococcus* biofilms, proteins such as fibronectin-binding proteins (FnBPs) and biofilm-associated proteins (Bap), polysaccharide intercellular adhesin (PIA), extracellular DNA (eDNA), and teichoic acids have been shown to be components of EPS matrix [92-95].

In this pioneering study, we have discussed this knowledge gap by using a TMT-based high-resolution proteomic analysis of *S. aureus* wet and DSB. The present study used a novel strategy to examine the changes in protein expression profiles by comparing the proteomic profiles of *S. aureus* wet and DSB with planktonic culture. This new strategy and a thorough analysis of proteomics profiles facilitated in gaining new knowledge on the protein composition of both wet and DSB followed by direct proof on biofilm regulators and the probable mechanisms for the formation of *S. aureus* biofilms in these modes of growth.

Materials and Methods

The aim of this work was to construct a comprehensive quantitative proteomic reference map to elucidate the differences of *S. aureus* cells progressing through planktonic, 12-day wet biofilm (wet), and DSB lifestyles. To do this, we performed in-solution digestion which enabled us to generate extremely complex samples that could be analysed with high-resolution TMT-based mass spectrometry (Figure 5.1).

Microorganism and culture conditions

S. aureus (ATCC 25923) 24 hour planktonic culture were grown as described in Chapter 2, section 2.1.3. whilst wet and DSB cultures were grown as described in Chapter 2, section 2.1.4.2 and section 2.1.4.3), respectively.

Sample processing

Extraction and fractionation were performed using a modified method described by Sadovskaya [454] as described in Chapter 2, section 2.2.1 for planktonic culture and section 2.2.2 for 3-day and 12-day biofilm culture.

The amount of protein in extracted samples was measured using the BCA protein assay (Thermo Fisher Scientific, Australia) as described in Chapter 2, section 2.2.3.

A total of 40µg protein of each sample was processed further for protein reduction, alkylation, and digestion (described in Chapter 2, 2.2.4).

Samples were reconstituted in 100µl of 100mM TEAB pH 8.5 and labeled with TMT (Thermo Fisher Scientific, Germany) reagents as described in Chapter 2, section 2.2.5. A volume of 2µl of each labeled sample was pooled and vacuum dried and reconstituted in 30µl 0.1% FA solution,

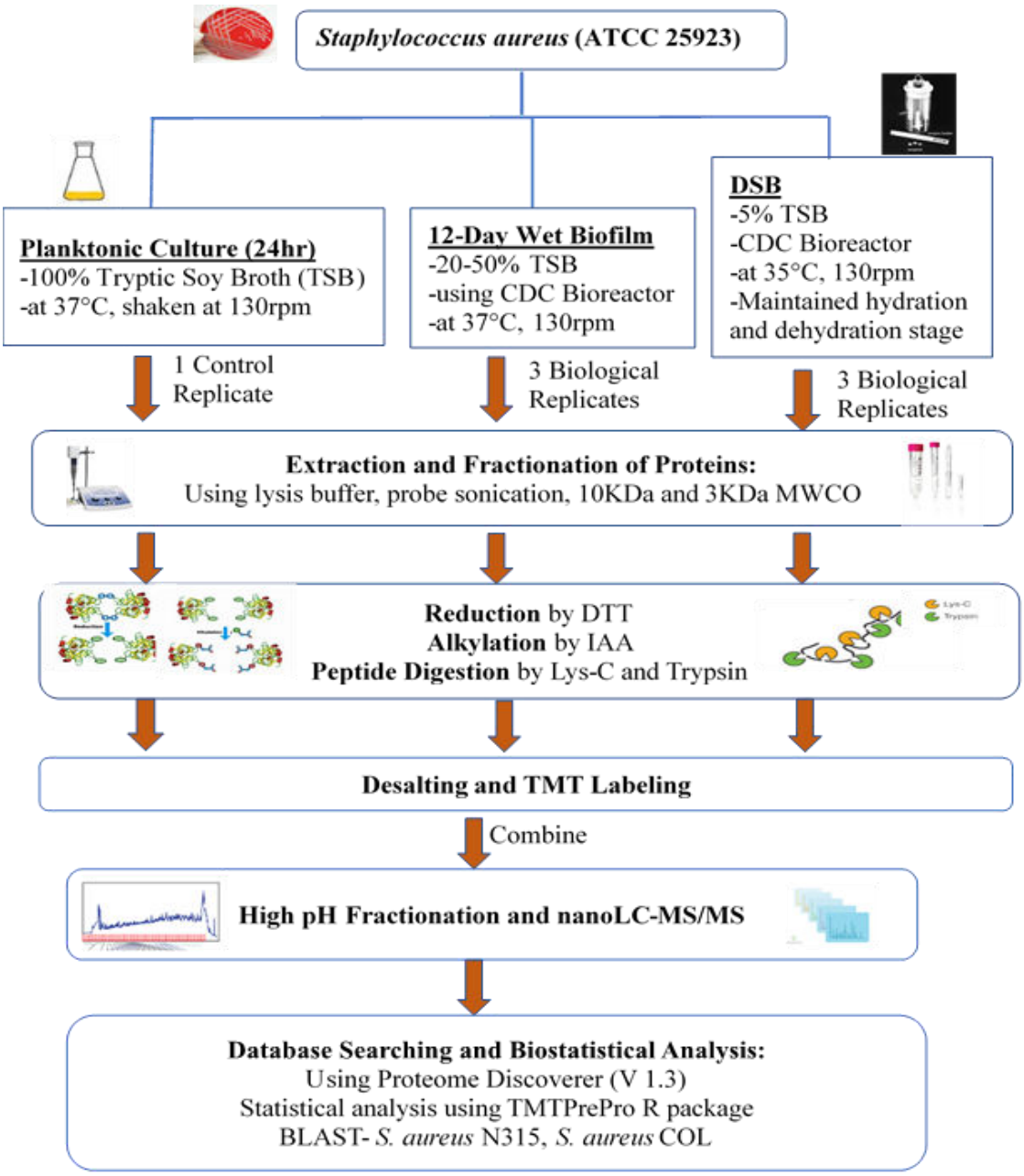

Figure 5.1: Experimental workflow for the analysis of *S. aureus* planktonic, wet, and DSB proteome using TMT labeling based MS. *S. aureus* strain cultivated in TSB to grow a planktonic culture pooled from biological triplicates, and biofilms (12-day and DSB) in biological triplicates. The Centres for Disease Control biofilm reactor was used to grow biofilms. Proteolytically digested peptides were labeled with TMT 10-plex reagents and subjected to high pH RP-HPLC fractionation followed by LC−MS/MS analysis.

centrifuged for 5 minutes at 14000xg and analysed with mass spectrometer (nanoLC-ESI-MS/MS using Orbitrap Elite) as described in Chapter 2, section 2.2.6.1.

Based on the applied normalisation values from this search result an equal amount of peptides were taken from each sample, pooled and vacuum dried (miVac). The pooled labeled sample was fractionated by high pH RP-HPLC (Agilent Technologies). The fractionated sample by high pH RP-HPLC was pooled to 20 fractions, dried in miVac. Finally, each fraction was resuspended in 55µl of 0.1% FA for mass spectrometry analysis.

Nanoflow LC-ESI-MS/MS

All samples were run on two sequential mass spectrometer systems.

Nanoflow LC-ESI-MS/MS using Orbitrap Elite

An Orbitrap Elite (Thermo Fisher Scientific) mass spectrometer was used for acquiring data (described in Chapter 2, 2.2.6.1). Briefly, 20µl of each fraction was loaded onto a self-packed 100µm x 3.5cm trap column with Halo® 2.7µm 160 Å ES-C18 and desalted with loading buffer [0.1% FA] at a flow rate of 4µl/minute for 10 minutes. Peptides were eluted onto a self-packed analytical column with the linear gradients with a flow rate of 450nl/minute across the gradient. The eluent from the trap was diluted with 100nl/minute of buffer A before reaching the analytical column. The peptides refocused and separated over the analytical column at 60°C. Peptides were ionised by electrospray ionisation, and data-dependent MS/MS acquisition carried out using an Orbitrap Elite consisting of 1 full MS1 (R=120 K) scan acquisition from 380 to 1600 m/z, and 15 higher energy collisional dissociation (HCD) type MS2 scans (R=30 K).

Nanoflow LC-ESI-MS/MS using Q Exactive

A Q Exactive (Thermo Fisher Scientific) mass spectrometer was used for acquiring data (described in Chapter 2, 2.2.6.2). Briefly, each fraction (10µl) was loaded onto a self-packed 100µm x 3.5cm reversed phase peptide trap with Halo® 2.7µm 160 Å ES-C18 desalted with 20µl of loading buffer [0.1% FA] and the peptide trap was then switched on-line with the analytical column. Peptides were eluted with the linear gradients with a flow rate of 300nl/minute. Peptides were ionised by electrospray ionisation and data-dependent MS/MS acquisition carried out using

a Q Exactive consisting of 1 full MS1 (R=70 K) scan acquisition from 350 to 1850 m/z, and 10 HCD type MS2 scans (R=70 K).

Database search, statistical analysis, and bioinformatics

The raw data files were submitted to Proteome Discoverer (PD, version 1.3, Thermo Scientific) and processed using Sequest and Mascot (Matrix Science, London, UK) against *S. aureus* reference strain (ATCC 25923) as described in Chapter 2, 2.2.7). Following the extraction of protein ratios with PD, further processing and statistical analysis was conducted using the TMTPrePro R package [455]. BLAST search was performed using highly annotated strains *S. aureus* N315 and *S. aureus* COL. Proteins were considered upregulated when the TMT ratio was above 1.5 and downregulated when the TMT ratio was lower than 0.66 in biofilm growth compared to planktonic growth with significant p-value < 0.05. Significant differentially expressed proteins (>2-fold) were determined by using VENNY, metabolic pathway analysis using KEGG mapper, subcellular localisation using PSORTb [456], and protein–protein interaction (PPI) network of significantly differentially expressed proteins were analysed by STRING software [457].

Validation of TMT data with qPCR results

In order to validate the reliability of the TMT analysis, six genes encoding (1) UDP-N-acetylmuramate-alanine ligase murC, (2) UDP-N-acetylenolpyruvoylglucosamine reductase murB, (3) Glutamyl endopeptidase sspA, (4) Ribose-phosphate pyrophosphokinase prs, (5) Pyruvate carboxylase pyc, and (6) Succinate dehydrogenase sdhB were chosen as targets to analyse the levels of RNA expression to validate the expression changes in planktonic and biofilms (wet and DSB). The 16S rRNA was used as an endogenous control to normalise the gene expression data, and the level of differential expression of the six genes between planktonic and biofilms were compared.

RNA was extracted using a RNeasy Mini Kit (Qiagen, Germany) and cDNA synthesised from 200ng of RNA using the SuperScript™ IV VILO™ Master Mix (Thermo Fisher scientific, Australia) as described in Chapter 2, sections 2.3.2, 2.3.3 and 2.3.4. Quantitative PCR (qPCR) was performed in duplicate on two biological replicates as described in Chapter 2 section 2.3.6.

Primer sequences used in this study as described in Chapter 2 section 2.3.5.

Results and Discussion

TMT identification of differentially regulated proteins in the wet and DSB

A total of 1636 non-redundant proteins with at least one unique peptide and <1% FDR were identified and quantitated. The profile of differentially regulated proteins in wet and DSB were depicted using volcano plots by implementing the fold change (>1.5-fold) and p-value (<0.005) cut off values (Figure 5.2 A&B). In the *S. aureus* biofilm proteomics study planktonic bacteria were used as a control and arbitrarily assigned a control value normalized to 1. So, the ratios obtained for wet and DSB was relative to the planktonic value. Each comparison regarded the proteins with fold changes beyond the cut-off values collected from Figure 5.2 A & B and with p values < 0.05 as the most significantly impacted proteins. Among them, 113 and 134 significant differentially regulated significant proteins and 406 common proteins were identified compared to planktonic bacteria in wet and DSB, respectively (Figure 5.3). Of these, 20 and 10 proteins were significantly (>2-fold) upregulated compared to planktonic bacteria in wet and DSB, respectively (Figure 5.3). Of which, 10 proteins were detected in recognised protein pathways in wet and DSB, respectively (Figure 5.3). In contrast, 24 and 11 proteins were significantly (>2-fold) downregulated in wet and DSB, respectively. Of which, 06 and 03 proteins were detected in recognised protein pathways in wet and DSB, respectively (Figure 5.3).

In the current study, we specifically focused on only extractomes (extracted supernatant proteins) to explore the proteome changes exist between different stages of biofilms. We have not considered large part of precipitated cell pellet fractions in this study.

Therefore, this is a proof of concept that, we can observe potential changes between wet and DSB even with comparatively small number of significant proteins. Identified potential marker proteins reported in this study might add valuable information in the global proteome repository, especially novel dry surface biofilm proteome. However, further deep fractionation study might be helpful to explore the large-scale differences between wet and DSB.

Among the common proteins between wet and DSB compared to planktonic, 61 proteins were significantly upregulated (>2-fold) with respect to planktonic cultures. Of these proteins 34 were

involved in recognised pathways. There were 127 proteins were significantly downregulated (>2-fold) in biofilm of which 51 proteins were involved in recognised pathways (Figure. 5.3). Among the upregulated proteins, energy metabolism, amino acid biosynthesis and metabolism, purine and pyrimidine metabolism associated proteins showed comparatively increased abundance in the wet (Appendix 6). For example, isocitrate dehydrogenase was upregulated 3.05-fold in wet while in DSB it was a 2.17-fold upregulation. Isocitrate dehydrogenase is involved in multiple biosynthesis and metabolism pathways including amino acid and central metabolism (e.g. TCA cycle), indicating wet biofilm has a higher energy metabolism rate when compared to DSB. On the other hand, downregulated proteins were higher in the categories of pyruvate metabolism, energy metabolism, amino acid biosynthesis, and translation indicating a lower metabolic activity profile in the DSB (Appendix 7). For instance, acetyl-CoA carboxylase (accB) was downregulated 4.35-fold in DSB whereas there was a 2.50-fold downregulation in wet. AccB is involved in multiple biosynthesis and metabolism pathways including pyruvate metabolism, which suggests that DSB has significantly lower energy metabolism rate in comparison to wet biofilm.

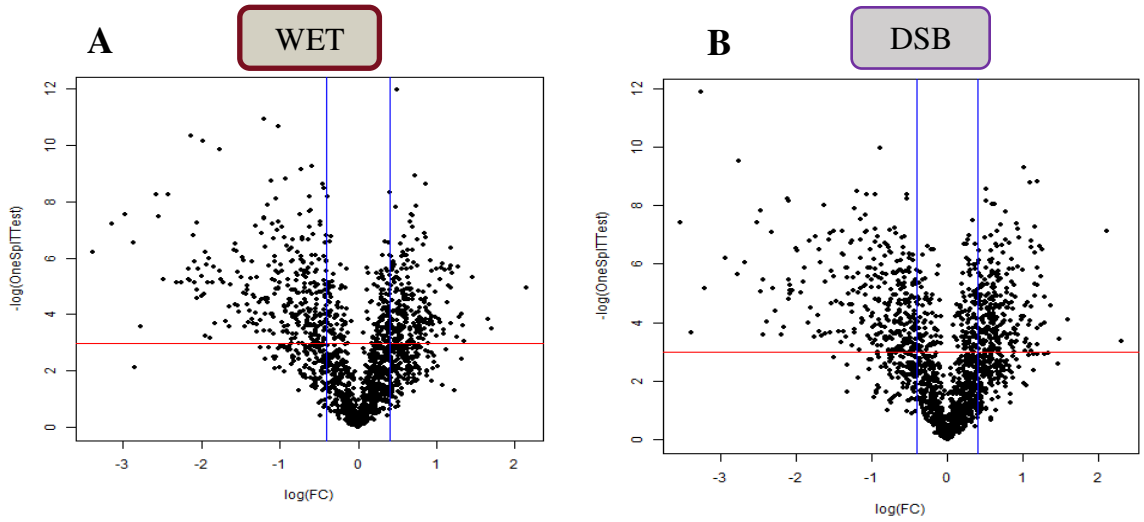

Figure 5.2: The volcano plot shows the distribution of the differential protein expression profile of (A) wet compared to planktonic; (B) DSB compared to planktonic. Y-axis in the form

of −log 10 represents p-value; greater numerical value is associated with lower p-value and greater legitimacy. X-axis represents fold change (log_2) of the differentially regulated proteins are represented by blue lines. The two vertical blue lines represent fold changes of -1.5 and +1.5. Therefore, the dots above red line in the positive side are significantly (<0.05) upregulated proteins, and the dots in the negative side represent the significantly (<0.05) downregulated proteins.

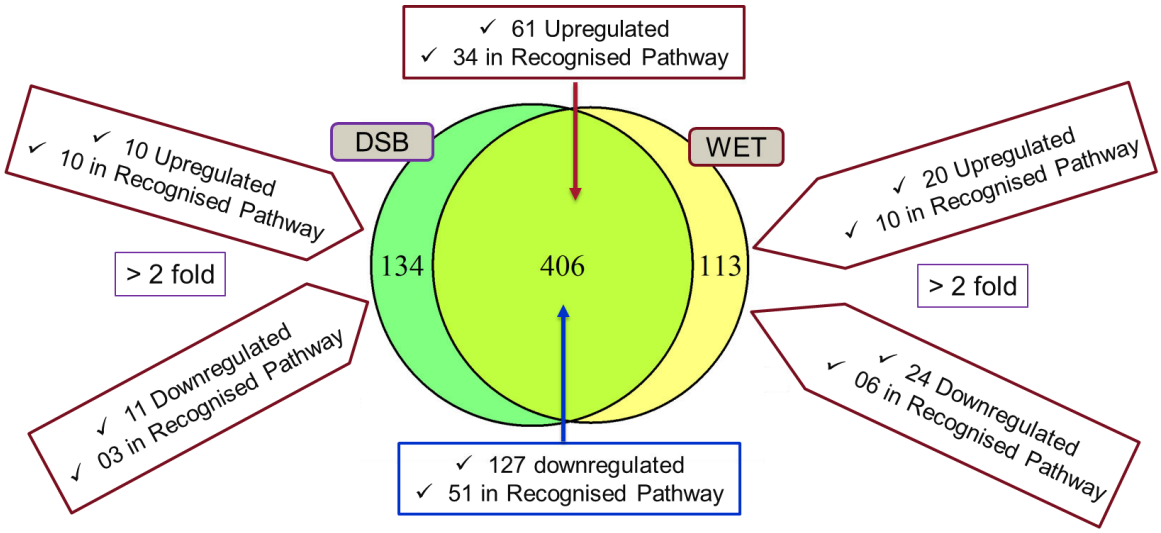

Figure 5.3: Venn diagram shows the dispersion of common and significant differential proteins in the wet and DSB. Pathway analysis was performed using KEGG.

Energy metabolism associated proteins are significantly upregulated in the wet

The proteins that are significantly upregulated in the wet in comparison with planktonic and DSB are listed in Table 5.2. Of these proteins, glucosamine-fructose-6-phosphate aminotransferase (glmS), and argininosuccinate synthase (argG) are cytoplasmic enzymes involved in alanine, aspartate and glutamate pathway. Galactose-6-phosphate isomerase (lacA) is a part of galactose metabolism pathway. These proteins are responsible for energy metabolism and are the vital points to support regular cell development and replication processes for biofilms.

Multiple studies reported that the selective amino acid uptake for *S. aureus* biofilm mode of growth versus planktonic cultures [279, 342, 538, 539], and suggested they may be an important feature distinguishing between planktonic and biofilm growth conditions. In our study, arginase encoded by arg significantly upregulated in wet and is involved in arginine metabolism, and is suggested to play a significant role in biofilm survival [538, 539]. A recent study by Ammons *et al.* (2014) and other studies suggested that, amino acid metabolism not only serves as a significant source of energy for the biofilm growth but also initiates an adaptive approach to nutrient availability, redox balance, and environmental conditions [279, 538].

A cytoplasmic enzyme aminoacyltransferase (femX) involved in peptidoglycan biosynthesis pathway which is important for cell-wall synthesis. Other upregulated proteins include phosphoribosyl transferase (pyrR) involved in pyrimidine metabolism, and 5-(carboxyamino)imidazole ribonucleotide mutase (purE) involved in both biosynthesis of secondary metabolites and purine metabolism pathway. This demonstrates the use of secondary carbon sources for energy production, supporting a role for purine and pyrimidine metabolism in biofilm formation. Furthermore, hypothetical protein KQ76_04110 (SA0772), tributyrin esterase (SA2422) are also involved in unrecognised pathways and subcellular localisation are still unknown.

Sugar transporter and cell-wall synthesis proteins are highly abundant in the DSB

The proteins that are significantly upregulated in the DSB in comparison with planktonic and wet are listed in Table 5.3. Of these, phosphotransferase system (PTS) glucose transporter subunit IIBC (ptaA) is significantly upregulated in DSB, suggesting that sugar uptake and PIA mediated biofilm matrix deposition became active in DSB through PTS. Multiple proteomics analysis has demonstrated increased abundance of PTS system associated proteins under various biofilm growth stages and stress associated conditions in several Gram-positive organisms including *S. aureus* [524, 525, 527]. Additionally, ptaA is also involved in amino sugar and nucleotide sugar metabolism and is responsible for energy metabolism and linked with peptidoglycan biosynthesis pathway. In particular, UDP-N-acetylmuramate-L-alanine ligase (murC) and UDP-N-acetylenolpyruvoylglucosamine reductase (murB) are cytoplasmic enzymes involved in the peptidoglycan biosynthesis pathway, which is essential for cell-wall formation and may play a

role in biofilm formation. Cell-wall synthesis involves the construction of peptidoglycan monomers (polymeric mesh) from precursors UDP-N-acetylglucosamine and UDP-N-acetylmuramate.

Table 5.2: Functional classification of the significantly upregulated proteins in 12-day wet biofilm in comparison to DSB and planktonic (fold change >2, p<0.05). *CM denotes Cytoplasmic Membrane.

Accession ID	Protein Name	Gene Name	Fold Change	Protein Pathways	Subcellular Localisation	p Value
AIO21660.1	DNA-binding protein		2.968		Cytoplasmic	0.036545851
AIO20800.1	phosphoribosyl transferase	pyrR SA1041	2.527	Metabolic pathways, Pyrimidine metabolism	Cytoplasmic	0.002716491
AIO22003.1	L-lactate permease	SACOL2363	2.495		CM*	0.01739001
AIO20486.1	hypothetical protein KQ76_04110	SA0772	2.359		Unknown	0.010439563
AIO21982.1	hypothetical protein KQ76_12230	SACOL2344	2.319		Cytoplasmic	0.029769068
AIO20657.1	cytochrome C oxidase subunit III	qoxC SA0911	2.312	Metabolic pathways, Oxidative phosphorylation	CM	0.008189133
AIO22274.1	tributyrin esterase	SA2422	2.304		Unknown	0.001531411

AIO21564.1	general stress protein	SA1692	2.294		Cytoplasmic	0.043782436
AIO20599.1	peptide chain release factor 3	prfC SACOL1025	2.272		Cytoplasmic	0.031511123
AIO20680.1	hypothetical protein KQ76_05130	SA0933	2.177		Unknown	0.041597244
AIO21790.1	glucosamine--fructose-6-phosphate aminotransferase	glmS SACOL2145	2.130	Metabolic pathways, Biosynthesis of antibiotics, Alanine, aspartate and glutamate metabolism, Amino sugar and nucleotide sugar metabolism	Cytoplasmic	0.001307313
AIO21830.1	galactose-6-phosphate isomerase	lacA SA1997	2.127	Metabolic pathways, Galactose metabolism	Unknown	0.022870023
AIO22037.1	nitrite reductase	nasD	2.078	Microbial metabolism in diverse environments, Nitrogen metabolism	Cytoplasmic	0.000136083

						0.009286469
AIO21798.1	arginase	arg SA1968	2.039	Metabolic pathways, Biosynthesis of secondary metabolites, Biosynthesis of antibiotics, Biosynthesis of amino acids, Arginine biosynthesis, Arginine and proline metabolism	Cytoplasmic	0.002965917
AIO20370.1	transporter associated domain protein	SA0657	2.038		CM	0.049455485
AIO21892.1	aminoacyltransferase	femX fmhB SA2057	2.026	Metabolic pathways, Peptidoglycan biosynthesis	Cytoplasmic	0.018377427
AIO21786.1	lytic regulatory protein	truncated-SA	2.024		CM	0.001849203

OOC91313.1	5-(carboxyamino)imidazole ribonucleotide mutase	purE SA0916	2.007	Metabolic pathways, Biosynthesis of secondary metabolites, Biosynthesis of antibiotics, Purine metabolism	CM	0.000823542
AIO20536.1	argininosuccinate synthase	argG SA0822	2.006	Metabolic pathways, Biosynthesis of secondary metabolites, Biosynthesis of antibiotics, Biosynthesis of amino acids, Arginine biosynthesis, Alanine, aspartate and glutamate metabolism	Cytoplasmic	0.008786571
AIO20949.1	threonine synthase	thrC SACOL1363	2.004	Metabolic pathways, Biosynthesis of secondary metabolites, Microbial metabolism in diverse environments, Glycine, serine and threonine metabolism, Vitamin B6 metabolism,	Cytoplasmic	0.036545851

Biosynthesis of amino acids

They are synthesised in the cytoplasm of *S. aureus*, and simultaneously play a major role in maintaining structural and cellular integrity against osmotic forces within the environmental niche as well as permitting essential fluidity of the cell-wall to adapt during different stages of growth, division, and infection to changes in bacterial cell shape [540, 541]. The metabolism associated with cell wall synthesis is well recognised in *S. aureus*, and we observed significantly higher abundance of precursor proteins in DSB which may contribute to the distinguishing features of the DSB in comparison with wet and planktonic mode of growth. In addition, increased abundance of amino and nucleotide sugar metabolism, and fermentation pathway associated proteins, (such as ptaA, lacG, purD), which are also involved in the production of cell wall components and EPS matrix deposition. Taken together, significantly identified proteins associated with cell-wall synthesis and the link to energy metabolism associated proteins in DSB, keep cells alive and produce thicker EPS matrix leading to increased persistence to biocides [244, 245, 252]. In Figure 5.5, we have demonstrated novel regulators of *S. aureus* biofilm formation in the DSB identified from TMT-based analysis.

In comparison between 12dwb and DSB, we observed relative higher abundance of energy metabolism associated proteins in the 12dwb. 12dwb was constantly supplied with better nutrition (ie 20 versus 5% TSB) throughout its growth. In contrast, very strict, limited nutrient (5%) and water supply was provided to DSB during its growth. In this state, DSB are in an extreme nutrient deficient condition in the deeper layer of cells. In addition, lower level of water content limits the penetration and consumption of nutrients into the adjacent cell clusters. In this harsh condition, DSB utilize major fermentation pathway associated products because these products are situated just below the surface. In addition, we observed higher abundance of cell-wall synthesis proteins in the DSB. The presence of a thicker cell wall would aid the biofilm to survive prolonged desiccation. Thicker cell walls are present in spores which are highly tolerant to desiccation. Therefore, in DSB environment, cells are mainly active on the biofilm surface level whereas cellular organelles might be in a state of shrinkage condition inside the DSB cell. To support this notion, we performed TEM analysis and observed thicker cell wall in the DSB compared to wet biofilm. In addition, we also observed more shrinkage cellular organelles inside the DSB compared to wet biofilm (data not shown).

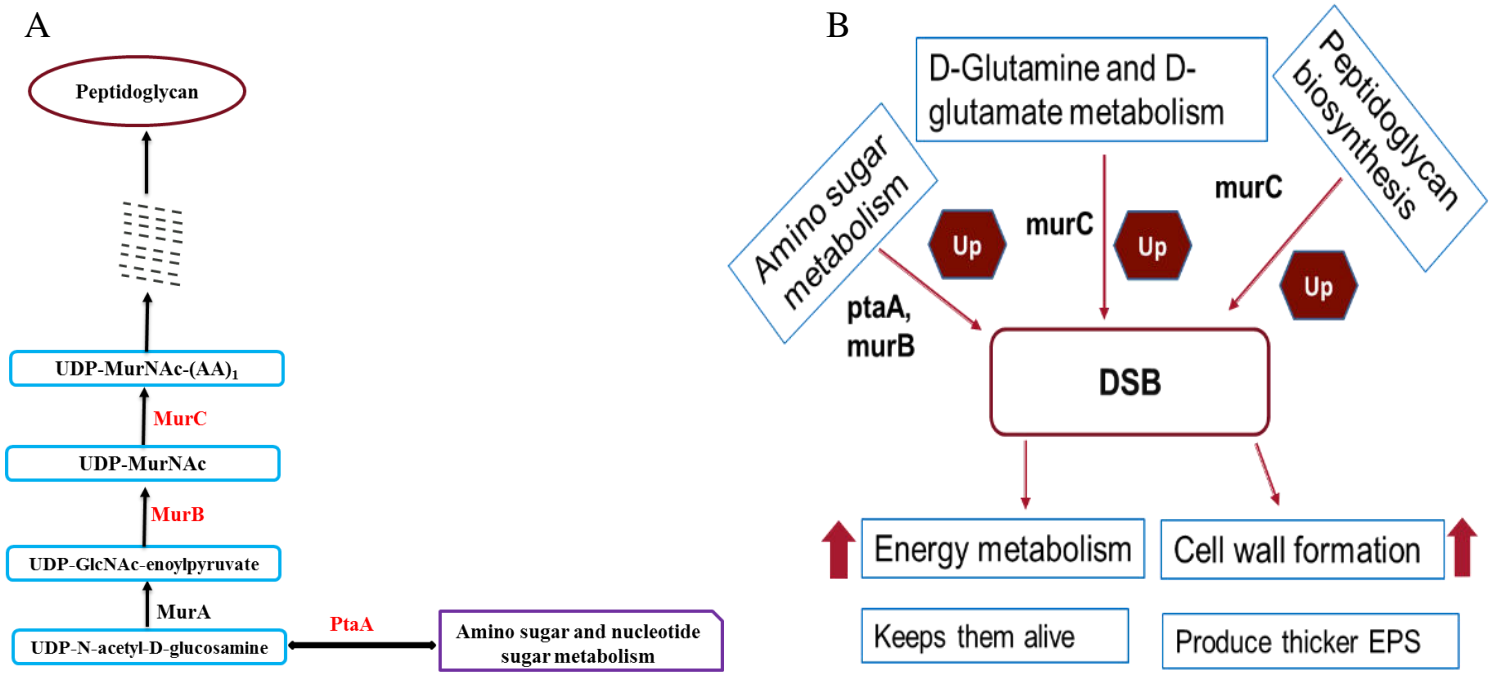

Figure 5.5. (A) Selected part of the peptidoglycan biosynthesis pathway and link with amino sugar metabolism; (B) Novel regulators of *S. aureus* biofilm formation in the DSB identified from TMT-based analysis.

Fatty acid pathway could be a novel target for DSB

A cytoplasmic membrane enzyme enoyl-ACP reductase (fabI) is a vital enzyme, significantly involved in fatty acid biosynthesis and metabolism and was significantly upregulated in DSB. Enoyl-ACP reductase plays an essential role in finishing cycles of the chain elongation process in the essential fatty acid biosynthesis pathway and is vital for cell survival (Figure 5.6) [542]. FabI is a remote member of an expanded protein family called short-chain alcohol reductases/dehydrogenases consisting of the motif Tyr-Xaa_6-Lys. Although, *S. aureus* FabI is extremely *E. coli* enzyme homologous, but *S. aureus* FabI is NADPH specific. In addition to the FabI enzymes regulatory importance, Fab1 is the target of the broad spectrum biocides such as triclosan [543, 544], and hexachlorophene [545, 546]. The possible mechanism of these two biocides, triclosan is a slow-binding inhibitor that deactivates the enzyme through the formation of a non-covalent, stable, ternary complex of FabI-NAD^+-triclosan with the oxidised cofactor in the active site, whereas hexachlorophene act by disrupting bacterial membranes [546]. Further, multiple studies suggested that this enzyme might be a potential target for biocides to treat bacterial infections including biofilm-associated infections [542, 546-549]. Therefore, significant upregulation of fabI enzyme we identified in this study may play a pivotal role in biofilm formation through fatty acid synthesis pathway and this enzyme might be a potential target for designing advanced cleaning agents and disinfectants to eradicate complex DSB from dry environmental surfaces.

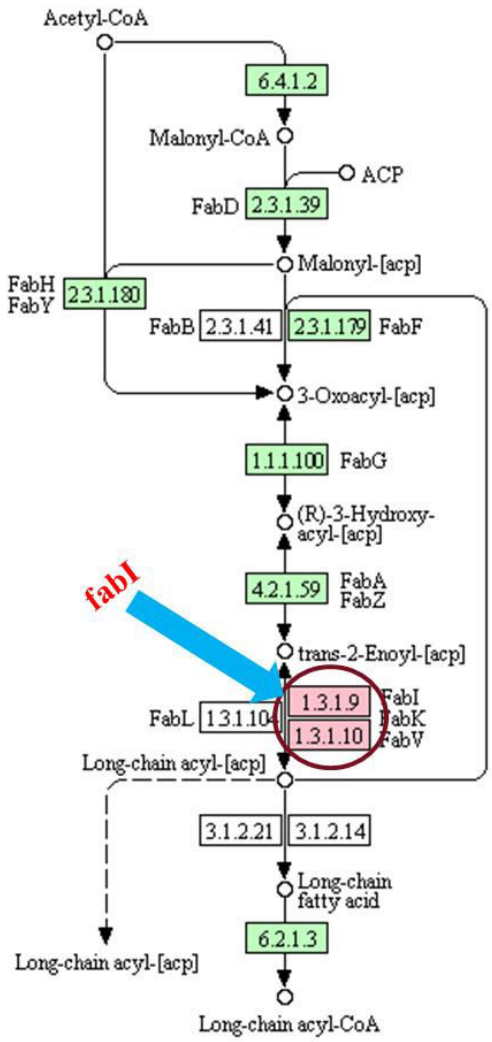

Figure 5.6: Selected part of type II fatty acid synthesis pathway for bacteria and the significant role of FabI in the last step of the elongation cycle in the synthesis of fatty acids. Modified from KEGG mapping online tool (https://www.genome.jp/kegg/).

Table 5.3: Functional classification of the significantly upregulated proteins in DSB in comparison to 12-day wet biofilm and planktonic (fold change >2, p<0.05). *CM denotes Cytoplasmic Membrane.

Accession ID	Protein Name	Gene Name	Fold Change	Protein Pathways	Subcellular Localisation	
OOC91425.1	serine acetyltransferase	cysE SA0487	2.322	Metabolic pathways, Microbial metabolism in diverse environments, Biosynthesis of secondary metabolites, Cysteine and methionine metabolism, Sulfur metabolism, Biosynthesis of amino acids, Carbon metabolism	Cytoplasmic	0.036545851
AIO21414.1	PTS glucose transporter subunit IIBC	ptaA	2.318	Amino sugar and nucleotide sugar metabolism, Phosphotransferase system (PTS)	CM*	0.002716491

AIO21824.1	6-phospho-beta-galactosidase	lacG SA1991	2.196	Metabolic pathways, Galactose metabolism	Cytoplasmic	0.01739001
AIO20705.1	inositol monophosphatase	SACOL1116	2.128	Metabolic pathways, Streptomycin biosynthesis, Inositol phosphate metabolism	Cytoplasmic	0.010439563 0.029769068
AIO20408.1	UDP-N-acetylenolpyruvoylglucosamine reductase	murB SA0693	2.122	Metabolic pathways, Amino sugar and nucleotide sugar metabolism, Peptidoglycan biosynthesis	Cytoplasmic	0.008189133
AIO22036.1	nitrite reductase	nasE	2.091	Microbial metabolism in diverse environments, Nitrogen metabolism	Cytoplasmic	0.001531411
AIO20589.1	enoyl-ACP reductase	fabI	2.086	Metabolic pathways, Biotin metabolism, Fatty acid biosynthesis and metabolism,	CM	0.043782436

				Biosynthesis of antibiotics		
AIO20891.1	recombinase RecA	recA SA1128	2.036	Homologous recombination	Cytoplasmic	0.031511123
AIO20673.1	phosphoribosylamine-glycine ligase	purD SA0926	2.011	Metabolic pathways, Biosynthesis of secondary metabolites, Biosynthesis of antibiotics, Purine metabolism	Cytoplasmic	0.041597244

Ribosomal and ABC transporter proteins revealed decreased abundance in the wet

The proteins that are significantly downregulated in the wet biofilm are listed in Table 5.4. Of these, a cytoplasmic protein 50S ribosomal protein L17 (rplQ) is a part of ribosomal pathway and changes in ribosomal protein expression can help cells adapt to the diverse conditions and guarantee cellular metabolism. It is expected that, cells have to make relative transcription and translation changes in order to create differential regulatory proteins to meet the necessities of various conditions. Hemin ABC transporter ATP-binding protein (hrtA), and amino acid ABC transporter substrate-binding protein (SACOL2412), are significantly downregulated in wet biofilm and are involved in ABC transporter systems. This suggests that the active transport of hemin and amino acid are downregulated in the wet biofilm, and several ABC transporter proteins have been demonstrated to play a role in *S. aureus* pathogenesis and antimicrobial resistance [528-531]. For example, *S. aureus* relies on various amino acids under conditions of limited resources and multiple amino acid transporters play an important role to fulfil their metabolic necessities for virulence, growth, and persistence [530]. Furthermore, studies have shown that ABC transporter of *S. aureus* reduces virulence by changing the structure and function of the cell wall [534] and, multiple omics studies have reported differential expression of ABC transporter proteins during biofilm growth [341, 470, 475, 476, 525]. Sulfite reductase [NADPH] flavoprotein alpha-component (SA2413), and cell division protein (ftsY) are cytoplasmic membrane proteins involved in different metabolic pathways such as microbial metabolism, sulfur metabolism, protein export and bacterial secretion system, respectively. Other downregulated proteins include GTP pyrophosphokinase (SA0864) associated with purine metabolism. Additional proteins such as hypothetical protein KQ76_13105 (SACOL2519), transcription elongation factor (greA), acyl carrier protein (acpP), etc. are cytoplasmic proteins involved in unrecognised pathways.

Table 5.4: Functional classification of the significantly downregulated proteins in 12-day wet biofilm in comparison to DSB and planktonic (fold change >2, p<0.05). *CM denotes Cytoplasmic Membrane.

Accession ID	Protein Name	Gene Name	Fold Change	Protein Pathways	Subcellular Localisation	p Value
AIO22143.1	hypothetical protein KQ76_13105	SACOL2519	0.303		Cytoplasmic	0.032278
AIO20170.1	hypothetical protein KQ76_02355	SA0464	0.427		Cytoplasmic	0.043671
OOC90925.1	serine protease splA	splB SA1630	0.431		Cytoplasmic	0.002837106
AIO19949.1	type VII secretion protein EsaA	esaA SA0272	0.432		CM*	0.018233713
AIO21302.1	transcription elongation factor GreA	greA SA1438	0.435		Cytoplasmic	0.002684595
AIO20865.1	ribosome recycling factor	frr SA1102	0.435		Cytoplasmic	0.019835972
AIO21853.1	50S ribosomal protein L17	rplQ	0.436	Ribosome	Cytoplasmic	0.037078395

		SA2022				
AIO21993.1	hemin ABC transporter ATP-binding protein	hrtA SA2149	0.448	ABC transporters	CM	0.018658212
AIO20742.1	DNA polymerase	SA0990	0.451		Cytoplasmic	0.007574497
AIO19898.1	uroporphyrin-III methyltransferase	SA0230	0.453		Unknown	0.014124961
AIO20835.1	acyl carrier protein	acpP hmrB SA1075	0.473		Cytoplasmic	0.008688479
AIO20893.1	hypothetical protein KQ76_06215	SACOL1306	0.480		Cytoplasmic	0.002573086
AIO20478.1	thioredoxin	SA0758	0.484		Cytoplasmic	0.003713384
AIO22260.1	sulfite reductase [NADPH] flavoprotein alpha-component	SA2413	0.486	Metabolic pathways, Microbial metabolism in diverse environments, Sulfur metabolism	CM	0.012461387
AIO20838.1	cell division protein FtsY	ftsY	0.486	Protein export, Bacterial secretion system, Quorum	CM	0.002345214

		SACOL1251		sensing		
AIO19963.1	QueA protein	SACOL0282	0.489		Cytoplasmic	0.001177358
AIO20555.1	phosphatidylethanolamine-binding protein	SACOL0984	0.491		Unknown	0.001282914
AIO20584.1	GTP pyrophosphokinase	SA0864	0.496	Purine metabolism	Cytoplasmic	0.016231399
AIO20515.1	hypothetical protein KQ76_04260	SACOL0943	0.497		Cytoplasmic	0.002810301
AIO21475.1	glyoxal reductase	SA1606	0.499		Cytoplasmic	0.030687304
AIO20687.1	hypothetical protein KQ76_05170	SA0941	0.501		Cytoplasmic	0.008284848
AIO21223.1	peptidase M24	SACOL1588	0.505		Cytoplasmic	0.004173793
AIO22050.1	amino acid ABC transporter substrate-binding protein	SACOL2412	0.508	ABC transporters	Unknown	0.006216264
AIO21432.1	cell division protein FtsK	SA1562	0.510		CM	0.010529055

Significantly downregulated Proteins in the DSB

The proteins that are significantly downregulated in the DSB are listed in Table 5.5. Of these, glycerophosphodiester phosphodiesterase (SACOL1770) is a part of glycerophospholipid metabolism. RNA polymerase encoded by sigB is a cytoplasmic enzyme belongs to sigma factor protein. Proteins involved in unrecognised pathways include membrane protein (cytoplasmic membrane) encoded by SACOL1113, ribonuclease III (mrnC), cell division protein ZapA, etc.

Table 5.5: Functional classification of the significantly downregulated proteins in DSB in comparison to 12-day wet biofilm and planktonic (fold change >2, p<0.05). *CM denotes Cytoplasmic Membrane.

Accession ID	Protein Name	Gene Name	Fold Change	Protein Pathways	Subcellular Localisation	p Value
AIO20286.1	recombinase	SA0577	0.388		Cytoplasmic	0.01982937
AIO20702.1	membrane protein	SACOL1113	0.409		CM*	0.019012267
AIO21531.1	3'-5' exonuclease	cbf1	0.441		Cytoplasmic	0.009724983
AIO20231.1	glycosyl transferase family 1	SACOL0612	0.463		Cytoplasmic	0.017494184
AIO21551.1	thiol peroxidase	SA1680	0.467		Cell-wall	0.029610209
AIO20579.1	oligopeptidase PepB	SA0859	0.477		Cytoplasmic	0.008196644
AIO21461.1	pyridine nucleotide-disulfide oxidoreductase	SACOL1821	0.493		Cytoplasmic	0.003239646
AIO20197.1	ribonuclease III	mrnC SA0489	0.496		Cytoplasmic	0.017354946
AIO21408.1	glycerophosphodiester phosphodiesterase	SACOL1770	0.497	Glycerophospholipid metabolism	Cytoplasmic	0.01856191

AIO21699.1	RNA polymerase sigma factor SigB	sigB	0.509	Cytoplasmic	0.00706
AIO20740.1	cell division protein ZapA	SA0988	0.509	Cytoplasmic	0.000867291

Significant differentially expressed stress response proteins in the wet and DSB

In this novel study, we identified several significant differentially expressed proteins associated with stress responses in wet biofilm such as L-lactate permease (SACOL2363), cytochrome C oxidase subunit III (qoxC), general stress protein (SA1692), thioredoxin (SA0758), glyoxal reductase (SA1606), and in DSB such as nitrite reductase (nasE), thiol peroxidase (SA1680), and pyridine nucleotide-disulfide oxidoreductase (SACOL1821). Among them, L-lactate permease regulates uptake and utilisation of L-lactate, and studies have reported that L-lactate uptake and utilisation is influenced by various stress response conditions such as oxygen limitation and acid stress [550-552], and play a significant role in biofilm formation under such diverse environments [333, 553, 554]. Acquisition of L-lactate has been shown to promote bacterial colonisation and enhance pathogenesis [553]. Under hypoxic conditions, a sudden drop in NAD^+ regeneration and ATP synthesis, increase glycolytic activity and activate fermentation pathways. In the wet biofilm, we observed significant upregulation of L-lactate permease suggesting it may have a pivotal role in biofilm formation or maintenance. The upregulation of L-lactate permease was also reported in a transcriptomics study by Morrison *et al.* (2018), where they grow *S. aureus* culture in the human spaceflight environment and their corresponding ground control cultures. In the same study, they observed L-lactate permease was downregulated in the *Bacillus subtilis* [555]. Another study by Clark *et al.* (2012), reported that L-lactate permease was downregulated in *Desulfovibrio vulgaris* biofilm growth mode compared to planktonic culture [333]. In addition, cytochrome C oxidase subunit III (qoxC) was significantly upregulated in the wet biofilm and it is involved in electron transport chain maintenance under different stress conditions within the biofilm.

On the other hand, nitrite reductase (nasE) was significantly upregulated in the DSB and plays a major role in energy production under anaerobic/hypoxic conditions. Our study revealed higher

accumulation of cell-wall synthesis associated proteins and Almatroudi et al (2015) study [252] showed thicker EPS in the DSB we suggest that the synthesis of increased cell-wall components is a mechanism to ensure maintenance of a critical level of hydration within the DSB. Wet biofilm is composed of approximately 90% water whilst DSB only has 61% water [556]. Variation in the water content limits the penetration of sufficient solute to the interior of cell clusters. Studies by Stewart (2003), demonstrated that limited water content affects the penetration of oxygen in an adjacent cell cluster due to consumption and diffusion impairment [557]. Therefore, deeper layer of biofilm in a state of oxygen limitation environment in which biofilm requires substrate for oxidation to maintain cell aggregation and stabilisation. Fermentation products such as nitrite, which are present just below the biofilm surface, are able to utilise the oxygen from the surface to maintain cell aggregation and biofilm stabilisation. A very recent study by Graf et al. (2019) reported that, during the oxygen-limited environment, strong positive charge created by fermentation products most likely mediates electrostatic interactions with anionic cell surface components, eDNA, and anionic metabolites leading to strong cell aggregation and biofilm stabilisation [463]. The deeper layers of cells are therefore situated undergrowth-limiting circumstances, with anaerobic or micro anaerobic surroundings. Nitrite reductase could support these cells, confirming their survival without or with low oxygen, and oxygen-limitation has been defined for biofilms of several species including *S. aureus* [126, 342, 463, 476, 535, 536]. In addition, the water availability in the DSB is very low compared to wet biofilm, suggesting DSB cells may also be supported by nasE under limited water content.

Validation of TMT data with qPCR results

The ratios from the qPCR results were obtained by comparing with planktonic in 12dwb and DSB. Individual normalised qPCR results are shown in Appendix 3. Upregulated and downregulated protein expression and gene expression results were expressed in fold change (FC). qPCR results showed that, in DSB, pyc was significantly downregulated in both qPCR and TMT analysis. In 12wb, prs was significantly upregulated in both qPCR and TMT analysis. Between 12dwb and DSB, sspA was significantly downregulated in both qPCR and TMT analysis, indicated a relative consistency for qPCR with the TMT data. However, there was no correlation between qPCR and TMT data for genes (murBC and sdhB) (Table 5.6).

qPCR analysis showed that the levels of gene expression identified were only partially in line with our MS based TMT quantitation analysis. The poor correlation identified between the results from transcriptomics and proteomics analysis could be due to disparities in the half-lives and post-transcription machinery of the samples. Additionally, we found lack of positive correlation between TMT and qPCR results, which we attribute to differences in sample preparation methods such as cell lysis and extraction.

Table 5.6: Relative correlation of selected qPCR gene expression data to TMT protein expression data (significant and common) in 12dwb and DSB compared with planktonic. *FC denotes fold change

			TMT		RT-qPCR	
Accession ID	**Protein Name**	**Gene Name**	**12dwb (FC)***	**DSB (FC)***	**12dwb (FC)***	**DSB (FC)***
AIO21431.1	UDP-N-acetylmuramate--alanine ligase	murC		2.174		0.206
AIO20408.1	UDP-N-acetylenolpyruvoylglucosamine reductase	murB		2.122		0.668
AIO20645.1	glutamyl endopeptidase	sspA	0.149	0.144	0.104	0.083
AIO20163.1	ribose-phosphate pyrophosphokinase	prs	2.814	2.785	3.94	0.632
AIO20712.1	pyruvate carboxylase	pyc		0.448		0.837
AIO20749.1	Succinate dehydrogenase	sdhB	0.283	0.406	3.30	1.313

Conclusions

This is the first report using high throughput TMT-based MS determining proteins in *S. aureus* DSB. Our result showed significant abundance variation compared to planktonic bacteria in wet biofilm and DSB. We observed protein (arg) involved in arginine metabolism, suggested to play pivotal role in biofilm survival in wet biofilm and protein (fabI) involved in fatty acid biosynthesis pathway, suggested to play a vital role in cell survival in DSB. Further pathway analysis revealed that energy metabolism associated proteins (glmS, argG, lacA) were significantly upregulated in the wet biofilm whereas cell-wall synthesis associated proteins (murB, murC) were significantly upregulated in the DSB. In this study, we identified novel regulators of *S. aureus* biofilm formation in DSB. Identified novel regulators (ptaA, murB, murC) play significant role in cell survival and thicker EPS matrix deposition, might lead to one potential mechanism by which DSB increases persistence to biocides. The current study will be helpful in designing advanced, targeted disinfectants and detergents to remove biofilms from dry environments.

Chapter 6: Breast implant capsular contracture reveals changes in the regulation of low-abundance plasma proteins

In this chapter we employed plasma proteome profiling to assess biofilm-related infections of medical implants. The most prevalent complication of implant-based breast augmentation and reconstructive operation is capsular contracture (CC). It is characterised by the tightening and hardening of the tissue capsule around the implant, and as a result can alter the shape and cause pain in the augmented breast. There is wide acceptance that bacterial biofilm infection on the surface of breast implants is associated with the development of CC. However, the mechanisms that lead to CC remain poorly understood.

Therefore, in this chapter we looked at the protein expression profiles in the plasma of biofilm-related breast implant CC patients and compared the results with healthy control patients. Because proteins reflect the physiology of an individual in the circulation system, high-resolution quantitative MS-based proteomics of plasma was used. However, this is challenging because the plasma protein abundance is highly dynamic. Thus, we employed depletion of high-abundance plasma proteins followed by Tandem Mass Tag-based quantitative proteomic approach to better comprehend the underlying mechanisms involved in CC.

Abstract

Capsular contracture (CC) is one of the most common post-operative complications among breast-implant associated infections. However, the mechanisms that lead to CC are still poorly understood. Plasma is an ideal sample for early biomarker discovery in infectious diseases, as it might show specific changes in the absence of direct bacterial evidence. We employed depletion of high-abundance plasma proteins followed by TMT-based quantitative proteomic approach to analyse plasma samples from 10 healthy control patients and 10 breast implant CC patients. A total of 450 proteins were identified from these samples, 43 proteins were significantly ($p < 0.05$) and 16 proteins were differentially expressed in breast implant CC patients as compared to healthy controls. GO enrichment analysis revealed cell, cellular processes, and catalytic activity associated proteins were highest in the cellular component, biological process and molecular function categories, respectively. Further pathway analysis revealed an inflammatory response, focal adhesion, platelet activation, complement and coagulation cascades, as enriched pathways identified in this study. The identified differentially expressed proteins using TMT-based quantitative proteomic approach has the potential to provide important information for future mechanism studies and in the development of breast implant CC biomarker/s.

Keywords: Breast implants, capsular contracture, human plasma, TMT, proteomics

Introduction

Blood and its products (e.g., plasma or serum) are the most desirable source of biomarkers as they comprise some of the secreted proteins and are readily accessible. But, the varying component and wide dynamic variety of protein concentrations (greater than 10 orders of magnitude) pose tremendous challenges in the identification of clinically significant biomarkers among the backdrop of higher-abundance proteins (e.g. albumin, IgG and transferrin) [354]. Therefore, the identification of novel or specific proteins as a biomarker for a particular disease has been hampered by these higher-abundant proteins, even with current high-resolution proteomic approaches, as higher-abundant proteins mask signals from low-abundance proteins.

The depletion of higher-abundant proteins from human plasma/serum has been revealed to advance the detection of relatively low-abundance proteins [354-356].

Because of the greater analytical characteristics, modern high-resolution MS-based proteomics analysis is well-matched for fundamental human disease research and clinical diagnosis. Among the proteomic techniques used to identify biomarkers, 'Tandem Mass Tags' (TMT) has the advantage of being able to achieve multiplexed quantification of up to ten samples simultaneously [334-336], saves instrument time and reduce in complexity with the design of experiments [337], with the ability to identify proteins between samples even in the lower mass zone [357, 358].

Multiple studies have demonstrated that differential regulation of several proteins and identified novel/potential plasma biomarkers for infectious diseases [355, 360-363]. For example, serum proteomics studies by Gouthamchandra *et al.* (2014) reported that retinol-binding protein 4 (RBP4) is a novel regulator in hepatitis C virus (HCV) infection. They confirmed this novel regulator by selecting from highly upregulated candidate followed by further validation using Western blotting and ELISA in two independent cohorts [356]. In addition, they also observed this finding in the JFH1 infectious cell culture system and noticed that the HCV fundamental protein increased RBP4 levels, this indicates that this cellular protein may play a role in regulating HCV infection [356]. Rehman *et al.* (2012) identified the potentially useful serum biomarkers, eukaryotic translation elongation factor 1 alpha 1, which is related with the metastatic progression of human prostate cancer, however, more examination and validation are needed [354]. Moreover, a quantitative proteomic study by Molleken *et al.* (2009) identified increased expression of human microfibril–associated protein-4 (MFAP-4) serum levels in a large number of patients. MFAP-4 has been shown to be a novel biomarker that can predict non-diseased liver versus cirrhosis with high diagnostic accuracy, as well as early versus later stage fibrosis [364].

The aim of this study was to identify the changes in protein expression profiles in the proteome of ten biofilm-related breast implant CC patients and compare the results to those of ten healthy plasma samples using TMT-based MS analysis.

Materials and Methods

In this study, TMT-based high-resolution MS approach was utilised to construct the plasma proteome (following depletion of high-abundance proteins) in healthy controls and patients with biofilm-related breast-implant CC to explore disease-associated alterations of plasma proteins. The experimental workflow is illustrated in Figure 6.1.

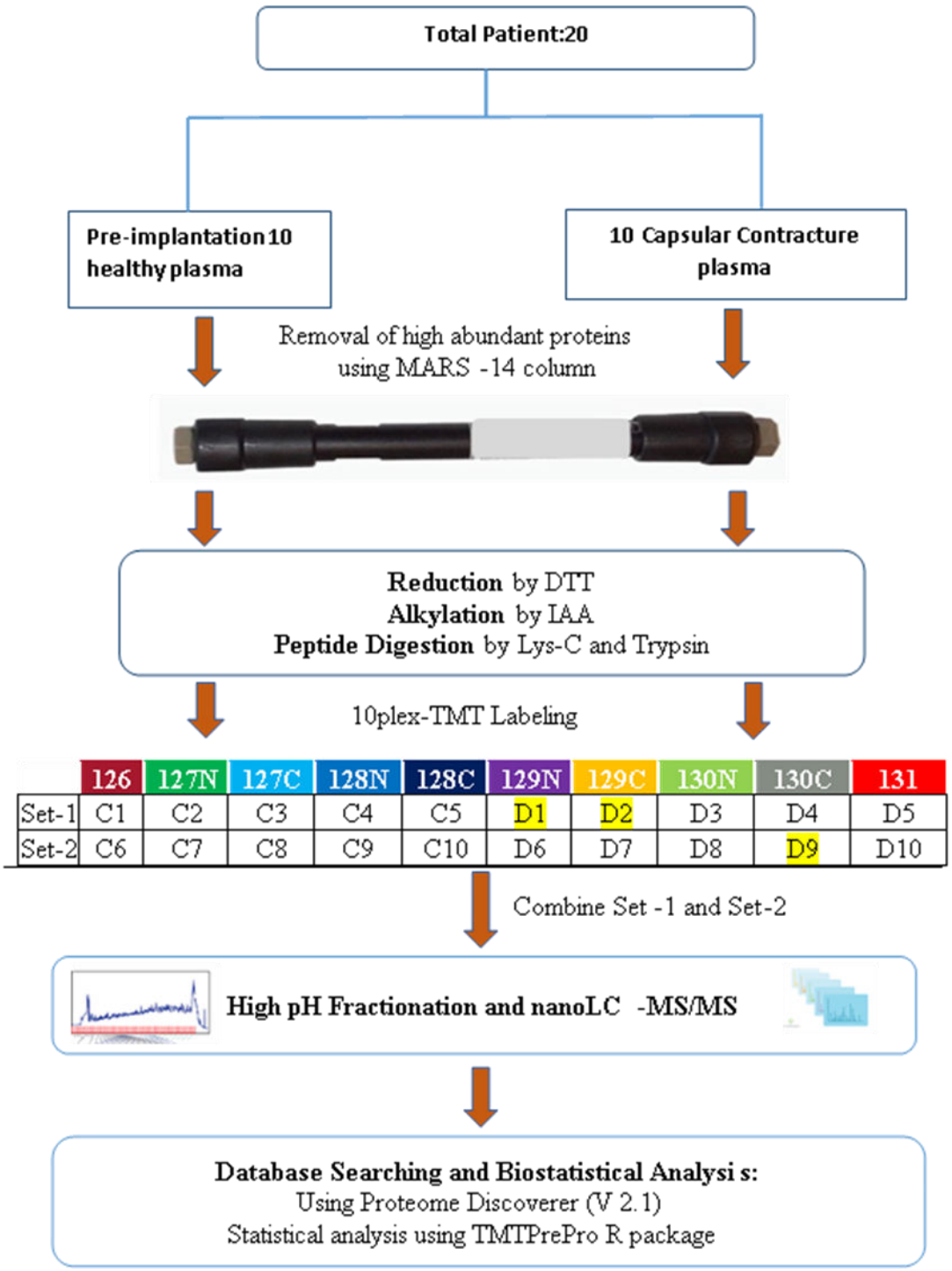

Figure 6.1: Experimental workflow for plasma depletion, TMT labeling and analysis. In this study, we utilized 2xTMT 10-plex reagents. In set 1, 10 samples (C1 to D5) were combined together, subjected to high pH fractionation followed by LC-MS/MS analysis. In set 2, another

10 samples (C6 to D10) were combined together, subjected to high pH fractionation followed by LC-MS/MS analysis. Database search was also performed separately on these two sets. The two sets were combined for analysis using TMTprePro R package.

Patients and ethics

Human ethics approval was obtained from the Macquarie University Human Research Ethics Committee (Reference number 5201600427). Informed consent was sought from study participants (Chapter 2, Appendix 1, 2A, 2B).

Blood was collected from10 healthy patients receiving breast implants for the first time (control patients, C) and from 10 patients with symptomatic contracted capsules surrounding breast implants (D), as described in Chapter 2 (section 2.4, Table 2.5). Clinical data was missing from one control patient but the mean age of the remaining nine control patients was 32 years, range 25 to 39 years. The mean age of the 10 patients with CC was 50±9 years, range 37 to 64.

Collection and processing of human plasma samples

Up to 5ml of blood was collected in ethylenediamintetraacetic acid (EDTA) tubes (BD Biosciences, Australia) and the plasma separated by centrifugation at 800xg for 15 min at RT. Between 2 to 3ml of plasma was removed and transferred in aliquots to 1.5ml microcentrifuge tubes (Axygen; Fisher Biotech, Australia) and centrifuged again at 1600xg for 10 min at RT to remove cellular debris. The plasma was stored in 500µl aliquots at -80°C.

Depletion of human plasma proteins

Plasma from each patient (10 healthy control, 10 capsular contracture) was processed for depletion using a MARS-14 column according to the manufacturer's instructions (Agilent Technologies, USA) as described in Chapter 2, section 2.6. The BCA protein assay (Thermo Fisher Scientific, USA) was performed to measure the final low abundant protein concentration (Chapter 2, section 2.1.6).

Sample Processing for TMT labeling and high pH fractionation

A total of 40µg protein of each sample was processed further for protein reduction, alkylation, and digestion (Chapter 2, section 2.7).

Samples were reconstituted in 100µl of 200mM HEPES (4-(2-Hydroxyethyl) piperazine-1-ethanesulfonic acid), pH 8.8 and labeled with 20µl of TMT for 1hr at RT (Thermo Fisher Scientific, Germany) as described in Chapter 2, section 2.8. A volume of 3.2µl of each labeled sample was then pooled, dried and reconstituted in 10µl of 0.1% formic acid (FA; Merck Ptv Ltd, Finland) and 2% ACN solution (Chapter 2, section 2.8). This was centrifuged for 5min at 14000xg and analysed by MS as described in Chapter 2, section 2.9.

Based on the applied normalisation values from this search result an equal amount of peptides were taken from each sample, pooled and vacuum dried (miVac). The pooled labeled sample was fractionated by high pH RP-HPLC (Agilent Technologies, USA) as described in Chapter 2, section 2.8. The fractionated sample by high pH RP-HPLC was pooled to 17 fractions, dried in vacuum (miVac). Finally, each fraction was resuspended in an appropriate volume of 0.1% FA and 2% ACN for MS analysis.

Nanoflow LC-ESI-MS/MS using Q Exactive

A Q Exactive (Thermo Fisher Scientific, Germany) mass spectrometer equipped with Nano spray source and Easy nLC 1000 (Thermo Fisher Scientific, Denmark) was used for acquiring data as described in Chapter 2, section 2.9. Briefly, each fraction (10µl) was loaded onto a self-packed 100µm x 3.5cm reversed phase peptide trap with Halo® 2.7µm 160 Å ES-C18 desalted with 20µl of loading buffer [0.1% FA] and the peptide trap was then switched on-line with the analytical column. Peptides were eluted with the linear gradients with a flow rate of 300nl/min. Peptides were ionised by electrospray ionisation and data-dependent MS/MS acquisition carried out using a Q Exactive consisting of 1 full MS1 (R=70 K) scan acquisition from 350 to 1850m/z, and 10 HCD type MS2 scans (R=70 K).

Database search, statistical analysis, and bioinformatics

The raw data files were submitted to Proteome Discoverer (PD, version 2.1, Thermo Scientific). The data were processed using Sequest and Mascot (Matrix Science, London, UK) against all bacteria (taxonomy, release date 04/12/2018) and human (taxonomy, release date 04/12/2018) from Uniprot database (Chapter 2, section 2.9). Following the extraction of protein ratios with PD, further processing and statistical analysis was conducted using the TMTPrePro R package

[455]. Differentially expressed proteins were examined using the PANTHER program (http://www.pantherdb.org/). Metabolic pathways of identified proteins were analysed by using Kyoto Encyclopedia of Genes and Genomes (KEGG) mapper (https://www.genome.jp/kegg/tool/map_pathway2.html). The protein–protein interaction (PPI) network of significantly differentially expressed proteins was analysed by the Ingenuity pathway analysis (IPA).

Results

TMT identification

As a result, 539 and 492 proteins were identified in the 10-plex TMT data set 1 and 2, respectively, resulting in a total of 581 proteins identified with the false discovery rate (FDR) <1%. Recent labeling based plasma proteomics studies by employing depletion of high abundance proteins and high pH RP-HPLC pre-fractionation, identified a total of 427 proteins by [360], and 469 proteins by [558]. We identified a total of 581 proteins which indicated that we were able to obtain better proteomic coverage in this study. Of which, 450 non-redundant proteins were commonly identified across all samples by these two TMT experiments. The box plot evaluation revealed that the protein intensity medians of all 20 samples were nearly the same across all the samples, implying no bias towards any samples (Figure 6.2).

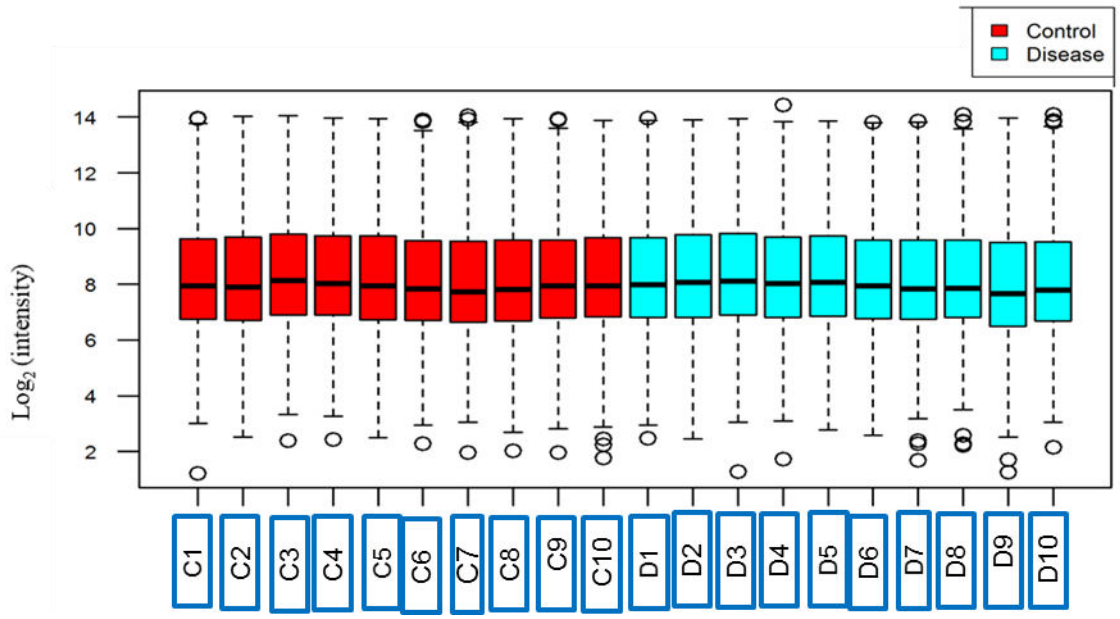

Figure 6.2: Box plots of the average level of log2 protein for each sample.

Filtering the TMT data set using criteria of p-value < 0.05, we identified a total of 43 proteins, in which 16 proteins were differentially expressed (fold change >1.2) in the disease group compared with the control group. The Low number of differentially regulated proteins between patients with contracture and the healthy controls is likely due to the nature of breast implant related contracture, in that these patients are systemically healthy like the control patients. Patients with breast-implant contracture are generally receiving treatment for aesthetic reasons not health reasons.

Among the significantly differentially regulated proteins, five proteins were significantly upregulated whereas 11 proteins were downregulated in the disease patients in comparison with the healthy control patients. A full list of all significantly differentially expressed proteins is given in Table 6.2. Additionally, in our dataset we identified four high confidence bacterial proteins which is mentioned in Table 6.3. To avoid false-positive results identifying bacterial proteins we set high confidence criterion which includes: master proteins, FDR <1%, PSMs (high confidence), > 10 amino acid per protein, and at least 1 unique peptide. Hu et al., (2015), demostrated that biofilm infection of breast implants is multi-species [193]. The presence of

bacterial proteins in healthy control patients is possible as a low grade bacteraemia occurs during teeth cleaning. Therefore, we can speculate that the bacterial proteins reported in this study meet acceptable criteria.

A heatmap analysis of 16 differential proteins using a hierarchical clustering and correlation distance metric was generated to illustrate the alteration of expression levels in disease group versus control group (Figure 6.3). As shown in the dendrogram, an increasing red color indicates increasing levels of protein expression (Figure 6.3). Therefore, in the region where these protein peaks are shown in red, the most notable area of upregulation in the disease group was seen.

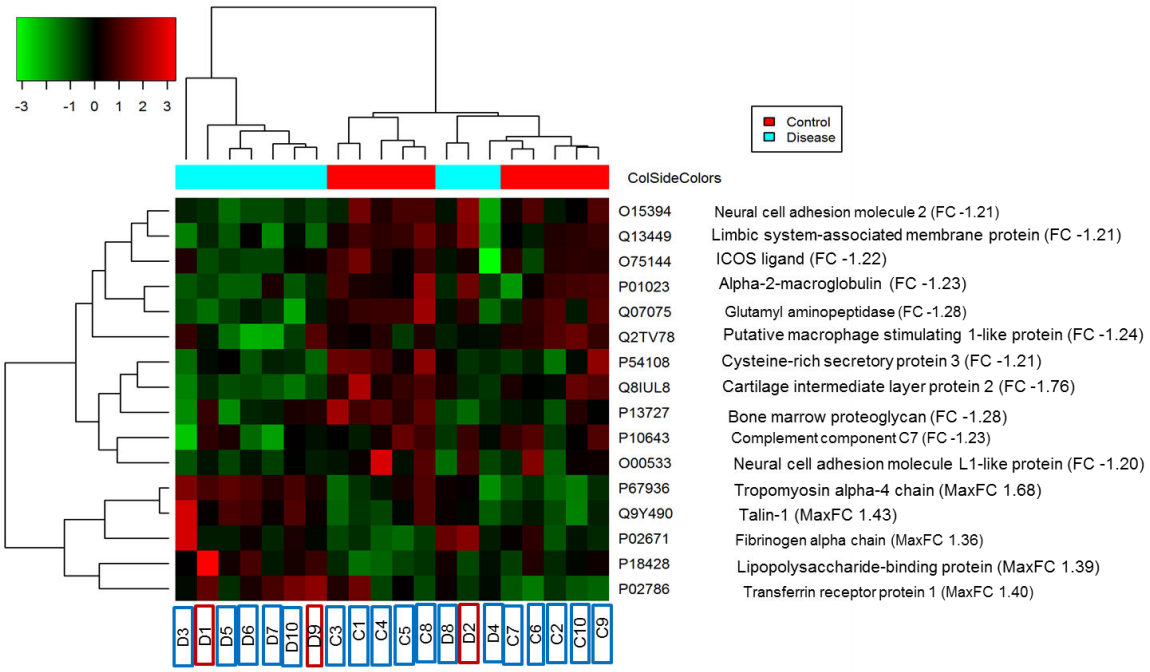

Figure 6.3: Heatmap analysis of the significantly changed proteins. Rows denote proteins and columns denote different samples. Each cell's colour represents a shift in protein expression; red indicates increased and blue indicates decreased relative to the healthy controls. In this study, we performed two set of TMT-based analysis and combined the two sets for analysis by TMT-PrePro R package.

Table 6.2: Functional classification of the significantly differentially expressed proteins in the disease group compared with the control group ($p < 0.05$).

Accession ID	Protein Name	Mean Disease /Mean Control	Fold Change	KEGG Pathways	Subcellular Localisation
Q8IUL8	Cartilage intermediate layer protein 2	0.579	-1.726		Secreted
P67936	Tropomyosin alpha-4 chain	1.687	1.687	Hypertrophic cardiomyopathy, Adrenergic signaling in cardiomyocytes, Dilated cardiomyopathy (DCM), Cardiac muscle contraction	Cytoskeleton /Cytoplasm
Q9Y490	Talin-1 OS=Homo sapiens	1.440	1.440	Rap1 signaling pathway, Human T-cell leukemia virus 1 infection, Platelet activation, Focal adhesion	Cytoskeleton /plasma membrane
P02786	Transferrin receptor protein 1	1.399	1.399	Hematopoietic cell lineage, Endocytosis, HIF-1 signaling pathway, Phagosome, Ferroptosis	Plasma membrane /secreted

P18428	Lipopolysaccharide-binding protein	1.389	1.389	NF-kappa B signaling pathway, Tuberculosis, Toll-like receptor signaling pathway, Salmonella infection	Secreted
P02671	Fibrinogen alpha chain	1.360	1.360	Platelet activation Complement and coagulation cascades	Secreted
P01023	Alpha-2-macroglobulin	0.758	-1.320	Complement and coagulation cascades	Secreted
P13727	Bone marrow proteoglycan	0.780	-1.282	Asthma	Secreted
Q07075	Glutamyl aminopeptidase	0.781	-1.280	Renin-angiotensin system	Plasma membrane
Q2TV78	Putative macrophage stimulating 1-like protein	0.802	-1.246		Secreted
P10643	Complement component C7	0.813	-1.231	Prion diseases Complement and coagulation cascades, Systemic lupus erythematosus	Secreted
O75144	ICOS ligand	0.814	-1.229	Cell adhesion molecules (CAMs), Intestinal immune network for IgA production	Plasma membrane

O15394	Neural cell adhesion molecule 2	0.821	-1.219	Cell adhesion molecules (CAMs), Prion diseases	Plasma membrane
Q13449	Limbic system-associated membrane protein	0.823	-1.215		Plasma membrane
P54108	Cysteine-rich secretory protein 3	0.824	-1.213		Secreted
O00533	Neural cell adhesion molecule L1-like protein	0.827	-1.209		Plasma membrane

Table 6.3: List of bacterial proteins found in this study.

Accession ID	Description	Fold Change	Subcellular Location	KEGG Pathway
P15636	Protease 1 OS=*Achromobacter lyticus*	1.030	Secreted	N/A
P06654	Immunoglobulin G-binding protein G OS=*Streptococcus sp*. group G, GN=spg	1.146	Cell Wall	N/A
Q890U2	Glutamine--fructose-6-phosphate aminotransferase [isomerizing] OS=*Clostridium tetani* (strain Massachusetts / E88), GN=glmS	1.351	Cytoplasm	Alanine, aspartate and glutamate metabolism, Biosynthesis of antibiotics, Metabolic pathways, Amino sugar and nucleotide sugar metabolism
A9MPX1	Zinc transporter ZupT OS=*Salmonella arizonae* (strain ATCC BAA-731 / CDC346-86 / RSK2980), GN=zupT	1.033		N/A

GO analysis of the identified proteins

To understand more about the functions of the proteins significantly identified, we performed Gene Ontology (GO) annotation using PANTHER of the 43 proteins in the cellular component, biological process and molecular function categories. In the cellular component category of GO, the majority of the proteins had a cell (36.4%) and extracellular region (36.4%) followed by membrane (13.6%) (Figure 6.4A).

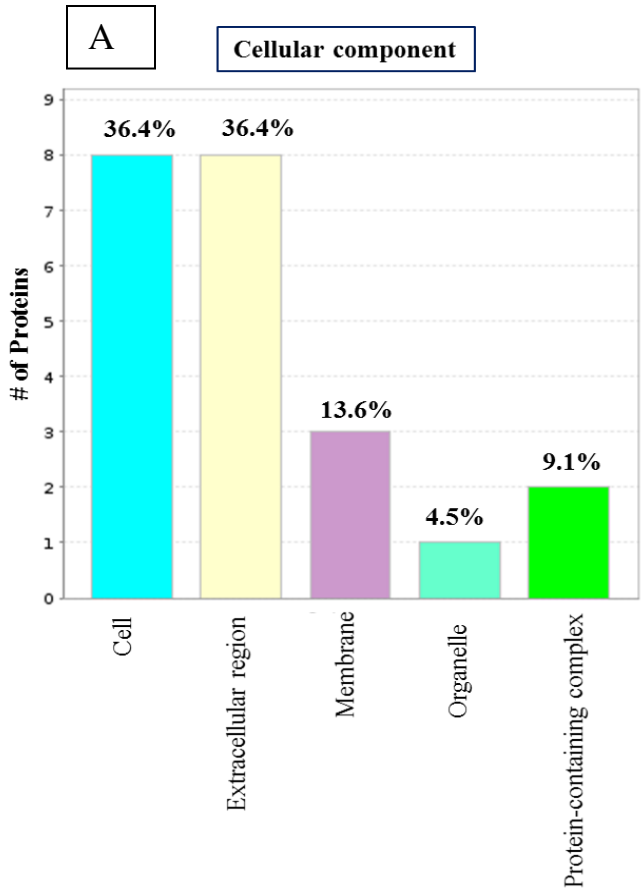

Figure 6.4A: Classification of the significantly identified proteins based on their functional annotations in the cellular component category using GO.

According to the analysis of the biological processes, the primary functions were cellular processes (43.6%) and metabolic processes (20.5%); while others were related to biological regulation, immune system processes, response to stimulus and so on (Figure 6.4B).

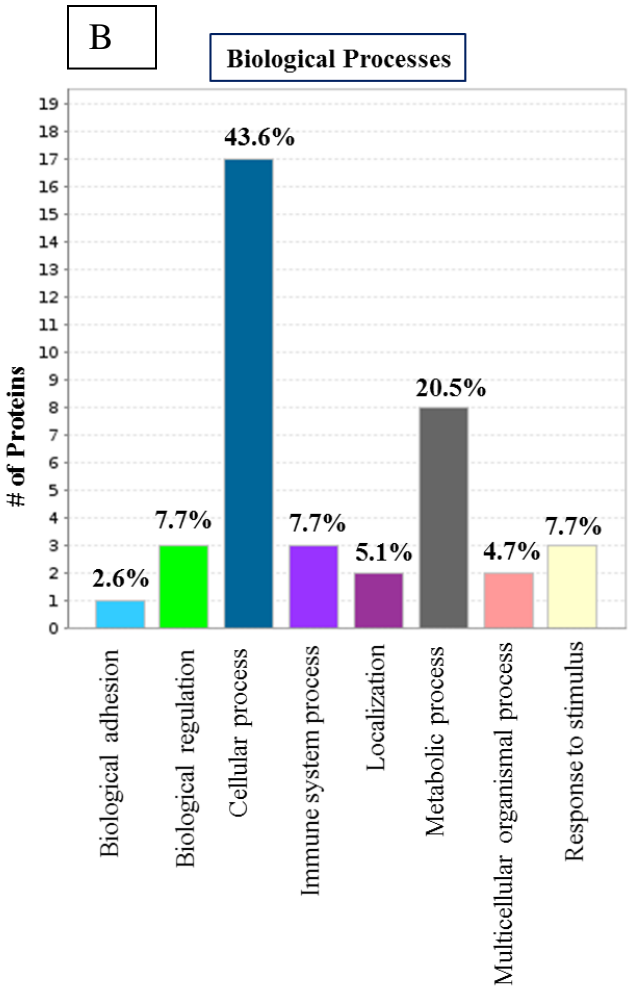

Figure 6.4B: Classification of the significantly identified proteins based on their functional annotations in the biological processes category using GO.

In the molecular function category of GO, the top 2 molecular function terms were catalytic activity (48.4%) and binding (35.5%) followed by molecular function regulator and molecular transducer activity (Figure 6.4C).

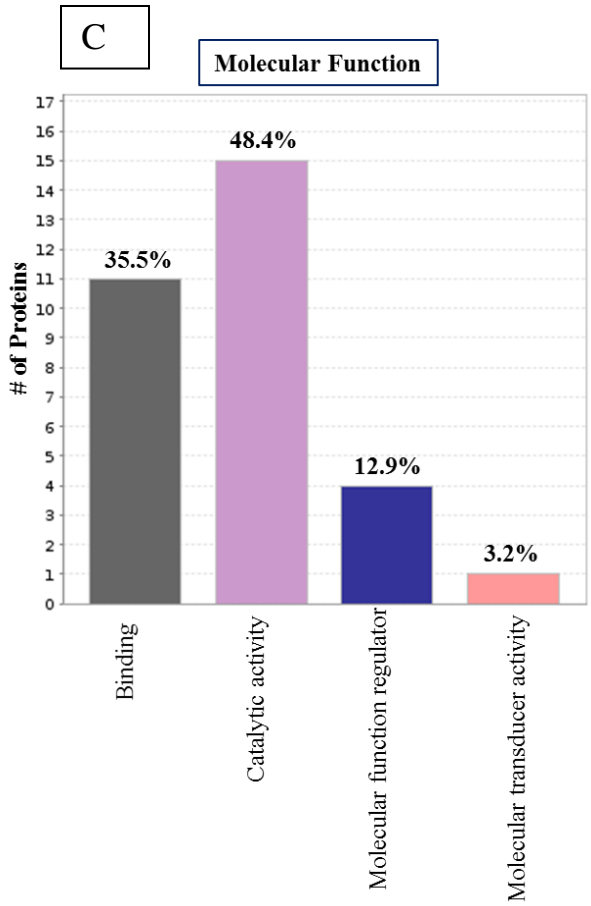

Figure 6.4C: Classification of the significantly identified proteins based on their functional annotations in the molecular function category using GO.

KEGG pathway analysis of the identified proteins

To identify pathways affected by disease groups versus control groups, we analysed the TMT results using KEGG pathways. Among the 16 significantly differentially expressed proteins, 11 proteins were identified in recognised pathways. The 11 unique differentially regulated proteins were mainly involved in platelet activation, focal adhesion, hematopoietic cell lineage, endocytosis, phagosome, ferroptosis, NF-kappa B signaling pathway, toll-like receptor signaling pathway, complement and coagulation cascades, cell adhesion molecules (CAMs) etc. (Table 6.2). Further comprehensive analyses of the roles of the significantly differentially regulated

proteins were carried out by using the Ingenuity pathway analysis (IPA) and searching the existing literature.

Protein-protein interaction analysis of the identified proteins

In order to assess the network of identified proteins to be significantly changed expression in the disease group compared with control group, we generated protein-protein interaction (PPI) networks using the Ingenuity pathway analysis (IPA). PPI analysis of 16 differentially expressed proteins showed a relatively complex network with several distinct biological subgroups that contained highly connected proteins. As depicted in Figure 6.5, proteins involved in platelet activation, complement and coagulation cascades, immune response, inflammatory response, and cell adhesion molecules (CAMs) were highly connected with each other, indicating that functional network of these processes contributes to biofilm-related breast implant CC pathophysiology.

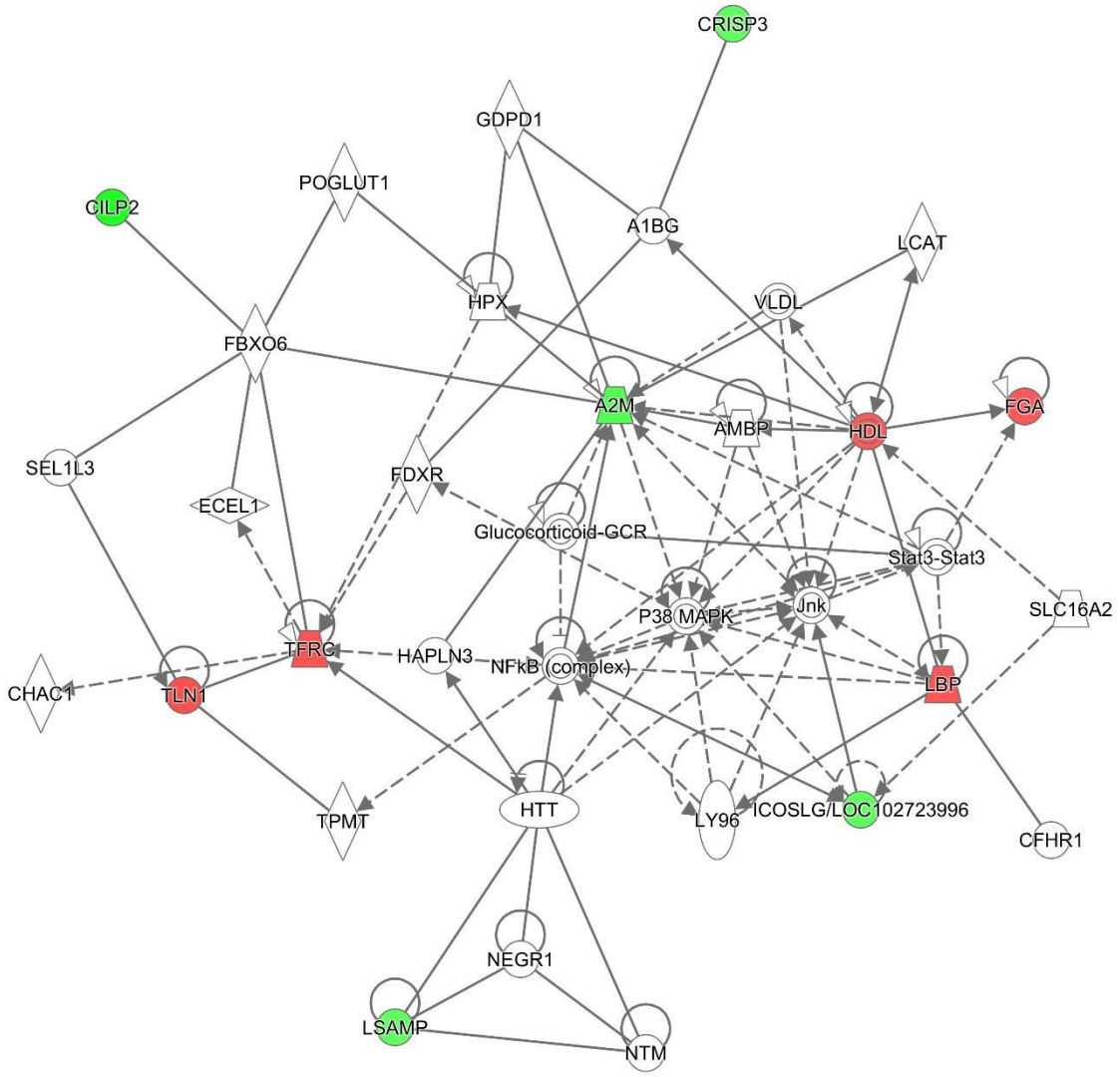

Figure 6.5: PPI network analysis of the significantly differentially regulated proteins in the disease group in comparison with the healthy group using IPA. Interactions between two proteins are indicated with grey lines. Red nodes, denotes upregulated protein and green nodes, denotes downregulated protein.

Discussion

Among the breast implant-associated infections, CC is the most common post-operative complication observed in developing countries including Australia and the mechanisms that lead to CC still remain unclear. There is currently no effective technique for early identification of biofilms and eradication of implant-associated biofilm infection often requires painful and expensive removal or substitute of contaminated devices. Given the vast amount of evidence of the significant correlation between biofilm and CC, it is an unmet demand for potential biomarkers that provide a clue of the existence of bacterial pathogens in plasma and/or host marker proteins in biofilm formation to develop an early stage diagnosis and therapeutic intervention.

In this study, to analyse the alterations in the human plasma proteome due to infection with biofilm-related breast implant CC, we applied a TMT-based high-resolution proteomic strategy for the detection of quantitative differences between proteins derived from the plasma of disease groups versus healthy control groups. With the advancement of labeling based proteomic techniques in the recent times, TMT-based MS is gaining popularity to identify plasma biomarkers for various diseases like cancer, sepsis and infectious diseases [559-562]. The acute phase response associated high-abundance proteins such as C-reactive protein are changed with numerous disease states like myocardial infarction and trauma and rheumatologic diseases [563, 564]. In addition, the wide dynamic range of protein concentrations in plasma samples, depletion of high-abundance plasma proteins improves the detection of relatively lower-abundant proteins which might be clinically important [361]. Therefore, we firstly performed depletion of high-abundant proteins (such as Albumin and IgG) using immune affinity-based depletion method (MARS-14) to improve depth of detection in plasma samples followed by TMT-based MS. As a result, we identified a total of 450 proteins among both disease and healthy groups. Of these, we identified 16 significantly differentially expressed proteins in the biofilm-related breast implant CC compared with healthy controls. Three of the samples obtained from patients with contracture cluster with the control samples. This is probably a reflection on the subclinical progression of the disease.

We identified five significantly upregulated proteins (tropomyosin alpha-4, talin-1, transferrin receptor protein 1, lipopolysaccharide-binding and fibrinogen alpha chain) and 11 downregulated proteins (such as cartilage intermediate layer protein 2, alpha-2-macroglobulin, bone marrow proteoglycan, complement component C7, ICOS ligand, neural cell adhesion molecule 2).

In this study, we observed Fibrinogen alpha chain and Alpha-2-macroglobulin were not depleted by the MARS-14 column. However, the capture efficiency of this targeted proteins might be affected by some of the non-targeted proteins. For example, alpha-2-macroglobulin has strong similarity to nontargeted pregnancy zone protein (a relatively abundant pregnancy-associated plasma protein) which might perhaps lead to the disturbance of targeted protein capture efficiency by pregnancy zone protein. Further, studies by [565], reported that the capture efficiency of Fibrinogen alpha chain was 76% by MARS-14 column, in which we may also expect the presence of this protein with lower abundance variation perhaps due to the untargeted binding of other proteins.

Tropomyosins belong to a multi-isoform family, expressed in muscle as well as in non-muscle cells which include fibroblasts, epithelial cells, serum and platelets. In muscle cells, the function of tropomyosin has been well established where it plays a vital functional role in the contraction of muscle by controlling actin-myosin supportive binding in reaction to the flux of calcium ions. Although, more research required to know the deeper function of tropomyosin in non-muscle cells, however, tropomyosin is an essential component of the cytoskeleton and contributes to cell contraction regulation [566]. Multiple studies reported the upregulation of tropomyosin alpha chain in various diseases such as esophageal carcinogenesis, liver cirrhosis, Behçet's disease, and hepatocellular carcinoma [364, 566-568]. In addition, studies by Biancone *et al.* (1998) observed that the autoimmune responses to tropomyosin in other chronic diseases including ulcerative colitis [569], Alzheimer's disease [570], and autoimmune hepatitis [571]. A proteomic study by Harada *et al.* (2007), showed significant upregulation of tropomyosin alpha-4 in esophageal squamous cell carcinoma and fibroblasts adjacent to cancer cells expressed high levels of tropomyosin alpha 4 chain. This suggested that, in addition to the contribution of tropomyosin alpha 4 chain to morphological change and the cytoskeleton stability of cancer cells, it may be associated with infiltration or metastatic ability [567]. Another interesting proteomic study by

Molleken *et al.*, (2009) using serum of liver cirrhosis patients found significant upregulation of tropomyosin alpha 4 chain, which is probably synthesised by "myofibroblast-like" triggered hepatic stellate cells, and linked with actin filaments of myofibrils and stress fibers. They also suggested that, sources of hepatocellular necrosis associated mediators such as extracellular secretion of free radicals also referred to as oxidant stress, intracellular components, signalling molecules, and these mediators may be circulating, intercellular or act on the same cell [364]. In particular, free radicals (oxidant stress) mediated necrosis may weaken of stellate cell stimulation with increased synthesis of smooth muscle proteins. Taken together, they concluded that it is not entirely surprising that tropomyosin alpha 4 chain can be observed in serum/plasma with significant range from patients with liver cirrhosis and other cirrhosis associated causes [364]. In addition, there is an increase in the cytoskeleton with the increased fibrosis.

Now, interestingly, higher numbers of various types of fibroblasts, including myofibroblasts are observed in CC [175, 176]. Transforming growth factor beta-1 (TGF-β1) and stress associated response plays significant role in the regulation of these molecular factors as well as linked with the repair of wounds [175]. There is a positive correlation between bacterial biofilms and TGF-β1 expression and is consistent with myofibroblast activity and fibrosis [177]. Myofibroblasts are able to produce collagen and a specific form of fibronectin [178] and may contribute to the formation of a contracted capsule around a breast implant [179]. The excessive deposition of collagen and fibronectin may also be exploited by bacteria since several bacterial species generate proteins that binds to collagen and fibronectin which facilitate bacterial adhesion to extracellular matrix molecules [180-183]. Bacteria multiply and form biofilms once they are attached. Hence, it can be speculated that the enhanced count and activity of myofibroblasts may lead to higher production of tropomyosin alpha 4 chain which may lead to the development of biofilm and possibly CC. Therefore, it is not entirely surprising that tropomyosin alpha 4 chain can be observed in higher levels in plasma from patients with biofilm-related breast implant CC.

Talin-1 (TLN1), located at the adhesion complex between cells and their extracellular matrix (ECM), regulates integrin and focal adhesion signalling and is expressed mainly in the liver, kidney, stomach, spleen, lung and vascular smooth muscle. Multiple studies reported that overexpression of talin-1 can promote prostate cancer cell adhesion, migration and invasion [572-

574]. Further studies also reported the upregulation of talin-1 in inflammatory diseases [365-367]. Studies by Khoontawad *et al.*, (2017) reported that the upregulation of talin-1 in the cholangiocarcinoma group, which is associated with the ECM, cell mobility and adhesion, play vital roles in ECM remodelling, attachment and metastasis known to happen during human cholangiocarcinoma [367].

Another upregulated protein, fibrinogen alpha chain is involved in platelet activation, complement and coagulation cascades, and (bacterial) infection/inflammation mechanisms have repeatedly been reported such as vascular wall disease, periprosthetic joint infection, lung and kidney fibrosis [575-577]. Fibrinogen, the precursor of fibrin is a soluble glycoprotein, comprises of three polypeptide chains called Aα, Bβ, and γ, and plays a vital function in triggering and facilitating the inflammation process. Studies by Barr *et al.,* (2018) reported that higher amounts of fibrinogen alpha adhere to the surface of breast implants [578]. ECM proteins (e.g., fibronectin, and fibrinogen) act as ligands to bind cell surface integrin receptors, and the capability of fibronectin to encourage biofilm development is related to the fibrinogen-binding A domain, that facilitates cell to cell attachment via homophilic bonds of low-affinity [577, 578]. If bacteria (such as *S. aureus*), in some cases, may not come into contact directly with the cell, its FnBPs (e.g., fibronectin and fibrinogen) ease binding to host plasma proteins, which can function as linking molecules between the bacteria and the receptors of host cell. FnBPs can cause internalisation via integrin receptors, and internalisation can lead to persistence of infection intracellularly [579].

In our study, increased expression of TLN1 and fibrinogen alpha chain occurred in plasma from patients with biofilm-related breast implant CC compared with healthy controls, which suggests that TLN1 and fibrinogen alpha chain might be a novel candidate of biofilm-related breast implant CC for the diagnosis of breast implant CC. In addition, since the integrin signalling pathway plays a vital role in the pathogenesis of inflammation and the close association of the integrin signalling pathway with TLN1 and fibrinogen alpha chain, we assume that the integrin signalling pathway could be involved in the pathogenesis of breast implant CC.

Transferrin receptor protein 1 (TFRC), the main receptor for cellular iron uptake into cells and is ubiquitously expressed in all tissues, plays a significant role in carrying iron to the host cell

during infection and in inflammation [580-582]. For instance, upregulation of transferrin receptor protein 1 has been observed in animal models of inflammation [583, 584], and in patients with acute respiratory distress syndrome [584]. Further, the upregulation of transferrin receptor protein 1 may decrease the accessibility of vital iron to cause bacterial invasion and is likely to be useful to the host during acute inflammation. Though, iron deposition in tissues is connected with toxicity in chronic inflammation [585] and appears to initiate development of fibrosis and liver disease in the final stages, for example, liver disease or chronic hepatitis C [582].

Another upregulated protein identified in the current study is lipopolysaccharide-binding protein (LBP), which is connected with multiple pathways such as nuclear factor (NF)-kappa B signalling pathway and toll-like receptor signalling. LBP is an acute-phase protein, abundantly synthesised in hepatocytes, responsible for the binding to the lipid A segments of lipopolysaccharide (LPS) and bring on toll-like receptor-4 (TLR-4), cluster of differentiation 14 (CD14), and other signalling pathways in the inflammatory responses [586-588]. Numerous studies stated that, plasma/serum levels of LBP were significantly increased in patients with the disorder associated with systemic inflammatory response, sepsis, and in acute and chronic infections [368-372]. These studies indicate that LBP might be useful as a potential biomarker for inflammatory reactions of both infectious and non-infectious backgrounds.

Among the significantly downregulated proteins, cartilage intermediate layer protein 2 (CILP2) is an extracellular carbohydrate protein that exist in the ECM and is expressed in skin, heart, articular cartilage, adipose tissue, plasma, etc. Numerous set of matrix binding molecules are composition of above tissues which includes collagen types I, III, V and VI. CILP showed significant correlation with TGF-β1 which function as a negative regulator. A study by Lehr *et al.* (2012) conducted in obese men using plasma samples and observed that the downregulation of CILP in the plasma which might be linked with higher TGF-β1 activity and as a consequence an abolition of adipogenesis [589]. In the above study, they observed higher TGF-β1 activity secreted by human adipose tissue in obesity, which is also showed similar trend with myofibroblast activity and fibrosis, and may be linked with the development of a CC around an implant.

Conclusions

In this study, we applied a TMT-based quantitative proteomic approach to construct the plasma proteome in healthy control patients and in patients with biofilm-related breast implant CC to explore disease-associated changes of plasma proteins. We showed that CC has a systemic effect, despite it being subclinical in patients. Moreover, it promotes a non-specific inflammatory response that is measurable in the plasma of patients. Plasma proteomic analysis showed changes in the plasma proteome of disease patients when compared to control patients, although the changes we identified do not appear to be specific for CC. Nevertheless, this study provides new insight into the human plasma proteome of biofilm-related infections and further investigation of the pathways involved are required.

Chapter 7: General Discussion

Recent findings of biofilms on dry hospital surfaces emphasise the failures in current cleaning practices and disinfection and the difficulty in removing these dry surface biofilms (DSB) [239, 245, 247]. DSB have been shown to be principally composed of protein, and thicker extracellular polymeric substances (EPS) [252]. However, so far, no studies have addressed what proteins are in dry surface biofilm on environmental surfaces in healthcare settings. Therefore, *in vitro*, we compared the proteomes of *Staphylococcus aureus* during planktonic, hydrated (wet) biofilms and DSB to bridge the knowledge gap in *S. aureus* cells during planktonic growth and different stages of biofilm lifestyle.

The Gram-positive bacterium *S. aureus* represents a serious public health burden worldwide. It is the most common causes of biofilm-related infections in humans and has been isolated from about 65% of infections related to implantable medical devices. There is presently no effective technique for early identification of biofilms. With the emergence of modern implantable medical devices and surgical techniques, the burden of implant-associated infections has grown. Capsular contracture (CC) is one of the most frequent post-operative problems of breast augmentation and reconstruction worldwide including Australia and reported varying incidence rates of between 19-30% by 10 years post-surgery [146]. However, the mechanisms that lead to CC (that can be very painful and often distort the breast) are still remain unclear. Therefore, there is a dire need for the identification of the involvement of bacteria and/or host marker proteins in biofilm formation to develop an early stage diagnosis and therapeutic regimes. Plasma is one of the most desirable sources of biomarkers since it contains some of the secreted proteins and is readily accessible. In addition, depletion of higher-abundant proteins from human plasma has been revealed to enhance the detection of relatively lower-abundance proteins, as higher-abundant proteins mask signals from lower-abundance proteins. Therefore, *in vivo*, we compared the lower abundant plasma proteome of healthy patients and patients with biofilm-related breast implant capsular contracture (CC). The proteomes were determined using high-resolution Tandem Mass Tag (TMT)-based mass spectrometry.

In the *in vitro* proteomics study, we identified 1636 non-redundant total biofilm extractomes from *S. aureus*. In comparison with planktonic culture with 3-day biofilm (Chapter 3), we identified 273 proteins were significantly differentially regulated (> 2-fold) significant proteins and these proteins could be regarded as possible molecular factors responsible for the difference in the proteome of biofilm compared with planktonic growth. Through GO functional annotation and KEGG pathway analysis, we observed lower metabolic activity in the 3-day biofilm growth mode compared to the planktonic state. Among the significant upregulated proteins in 3-day biofilm compared to planktonic, we identified proteins associated with secondary metabolites, ABC transporters, biosynthesis and metabolism of amino acids, and response to stress. Several ABC transporter proteins (e.g. modB, SACOL0187, potA) significantly upregulated in the 3-day biofilm, play important roles in the delivery of molecules (e.g., metabolic products, proteins, and numerous drugs in different biological processes) with diverse structures and functions [590, 591]. In particular, bacterial ABC transporters are gaining attention as a potential target to better understand of virulence and drug resistance [469], and may be an excellent vaccine candidates as they have been reported to be immunogenic in *S. aureus* infections in humans [440, 477]. Therefore, the unique or significant ABC transporter proteins found in this study may play a vital role in biofilm formation which may lead to potential marker proteins, vaccine and antimicrobial targets for biofilm-related infections.

Early transcriptomic studies by Resch et al. (2005), highlighted that genes associated with formate fermentation, urease activity, and stress response are upregulated in biofilm growth mode which could lead to growth, survival, and persistence in a biofilm state [278].

A recent transcriptomic studies by Efthimiou et al. (2019), reported that genes associated with ion transporters, cell-wall synthesis, autolytic, adhesion proteins, etc. were differentially regulated in *S. aureus* COL biofilm growth mode under varying pH conditions (acidic to alkaline). This study suggested better insight to develop potential treatment and disinfection approaches under such physiological conditions [592].

Furthermore, there have been several studies analysing the transcriptomic profile of *S. aureus* biofilms to test the effect of sublethal concentrations of disinfectants [347], the effect of low concentration drug (Liu et al., 2018), and the role of CymR gene in biofilm formation [349].

In this study (Chapter 3), we identified significant differentially expressed proteins in the biofilm extractomes were extracellular or cell-wall associated proteins, mostly associated with ECM proteins, which are primarily represented by virulence factors. Upregulation of fibrinogen-binding protein observed in this study, emphasises its importance in the *in vitro* and *in vivo* biofilm formation [109, 480], various evasive responses that protect bacteria from the immune system, and binding of *S. aureus* to fibrinogen-binding protein influenced by Rot and Agr mediated regulatory systems [109, 342]. In particular, hyaluronidase (hysA) an extracellular enzyme, was upregulated and is involved in disseminating recognised biofilms by the degradation of hyaluronic acid.

In contrast, proteins associated with virulence factors, translation, and energy metabolisms were significantly downregulated (>2-fold) in the 3-day biofilm, indicating biofilm is slow growing, and has a lower level of metabolic activity. Downregulation of several virulence-related and cell-wall proteins identified in our study, showed that the bacteria adjusted to the diverse biofilm condition by reducing some less essential roles such as adhesion, invasion, and virulence, dispersal and structuring of biofilms. For example, Staphylococcal accessory regulator (SarA) is a positive biofilm regulator through the downregulation of extracellular nuclease (nuc) and proteases [483]. In addition, the regulation of target genes linked with SarA is also facilitated by other regulators which include (e.g. agr, SigB, Rot, or MgrA), RNAIII and icaR, both of them showed antibiofilm activity, and the deactivation of gene expression associated with SarA might be essential to confirm biofilm development [342]. Among them, chitinase (SA0914) an exo-enzyme involved in quorum sensing that prevents the initial stage development of biofilms. Interestingly, hyaluronic acid is the structural constituent of N-acetyl-D-glucosamine which can be hydrolysed by chitinase. Therefore, hysA in conjunction with chitinase may play significant role in the elimination and/or prevention of biofilm development.

We compared the proteome of different stages of biofilm (Chapter 4) and observed a significant range of quantitative proteomic shifts over time. Proteomic analysis across different stages of biofilms highlighted interesting findings on metabolic processes, biosynthetic processes, transport systems (e.g., sugar and ABC transporters), and stress responses involved in *S. aureus* biofilm formation. Further, GO functional annotation and KEGG pathway analysis demonstrated

that the significant variations in the formation of biofilms result from changes in the level of metabolic activity in the different growth mode of biofilms, with a higher level of metabolic activity being observed in the 3dwb. This phenomenon was also supported while we compared the common proteins between 3dwb and 12dwb. We observed, downregulated proteins were higher in the categories of amino acid biosynthesis, energy metabolism, translation, and post-translational modification indicating a lower metabolic activity profile in the 12dwb, thus supporting the overall perspective of biofilms as slow-growing, metabolically lethargic communities. This effect was even more evident in the DSB. Therefore, the changes in metabolic activity could be a key factor of the biofilm formation in *S. aureus*.

Interestingly, we observed five proteins (SA0529, gap, SA2204, vraA, and SA1131) are linked with central metabolism pathways, responsible for energy metabolism and maintaining biofilm growth under diverse environments in the 3dwb. In particular, 2-oxoglutarate ferredoxin oxidoreductase (SA1131) is a key enzyme of the reductive TCA cycle and plays an important role in catalysing the alternative one-step reaction between succinyl-CoA and 2-oxoglutarate bypassing two more subsequent steps. This reaction requires strong reducing power and this enzyme plays a pivotal role in maintaining redox balance, bacterial growth and metabolism of aromatic compounds under anaerobic conditions as well as being utilised as a source for low-potential electron equivalents for carbon dioxide and nitrogen fixation [509, 510]. These interesting findings suggest that, identified proteins involved in the central metabolism pathways showed an alternative metabolic route, and multiple studies have reported that decreased expression of vital enzymes in the TCA cycles increases levels of pathogenic molecular factors [341, 593-595].

On the other hand, we observed interesting findings with sugar transporter systems such as PTS, upregulation of lactose-specific transporter subunits IICB (lacE), galactose-6-phosphate isomerase (lacA) involved in galactose metabolism, and aminoacyltransferase (femX) involved in peptidoglycan biosynthesis in the 12-day old biofilm. These three proteins are linked with energy metabolism and cell-wall synthesis, ensuring cellular viability and thicker EPS matrix deposition. In addition, femX is highly specific to *S. aureus*, and has been shown to catalyse transfer of Gly_1 from glycyl-tRNA to the peptidoglycan precursors independently from the ribosome. FemX has a

unique catalytic mechanism [521, 522] FemX is also essential for expression of β-lactam and vancomycin resistance facilitated by low-affinity penicillin-binding protein family (PBPs) [520]. Taken together, this could be one possible mechanism by which biofilm grown for a longer time biofilm utilise energy consumption, increase cell-wall formation, and due to the unique antibiotic resistance properties of femX provoke extremely persistent to antimicrobials.

A very recent study by Graf et al. (2019), observed proteomic profiling of *S. aureus* biofilm in a flow system. They generated proteomic profiling of extra- and intra-cellular proteins and found a high differential expression of proteins associated with capsular biosynthesis, various virulence factors (such as lipases, hemolysins, and leukotoxins) as a part of the EPS. In addition, they found secreted proteins associated with alkaline virulence factors and ribosomal exhibit a moonlighting/multiple function which contributes to biofilm integrity. Morover, they suggested that during the oxygen-limited environment, strong positive charge created by fermentation products (such as lactate, formate, acetate) most likely mediates electrostatic interactions with anionic cell surface components, eDNA, and anionic metabolites leading to strong cell aggregation and biofilm stabilisation. [463].

In the novel DSB proteomics study (Chapter 5), we took a novel strategy to evaluate the changes in protein expression profiles by comparing the proteomic profiles of *S. aureus* wet and DSB with planktonic culture followed by identifying potential marker proteins in biofilm development.

This study reveals significant abundance variation in wet and DSB compared to planktonic culture. We observed active participation of a specific set of energy metabolism associated proteins (e.g. glmS, argG, lacA) in wet biofilm which is contributes to support normal cell growth and reproduction processes for biofilms.

Interestingly, we observed amino sugar and cell-wall synthesis proteins are highly abundant in the DSB compared to planktonic culture and wet. In addition to the major function of amino acid metabolism in energy metabolism for the biofilm growth, they also initiate an adaptive strategy to nutrient availability, redox balance, and environmental conditions [279, 538]. Further, higher accumulation of amino and nucleotide sugar metabolism, and fermentation pathway associated proteins (such as ptaA, lacG, purD) are also involved in the development of cell wall constituents and the accumulation of EPS matrix molecules. The synthesis of cell wall components and its

associated metabolism is well recognised in *S. aureus*, and we observed significantly higher abundance of peptidoglycan biosynthesis proteins (murC, and murB) in DSB which may lead to the distinctive features of the DSB. These proteins are involved in cell-wall formation and may play a vital role in biofilm formation. These findings suggested that significant upregulation of significant proteins associated with cell-wall synthesis and the link of energy metabolism, and adaptation to diverse environment associated proteins in DSB, keep cells alive and produce thicker EPS matrix leading to increased tolerance to desiccation and biocides. Therefore, these novel findings might be one possible answer to our previous work done by Almatroudi *et al.* (2015), where they reported that DSB is composed of higher amount of proteins and thicker biofilm matrix and is at least partially responsible for the increased tolerance of DSB to detergents and disinfectants. As demonstrated in Figure 7.1, significant dysregulated proteins between wet and DSB based on the synthesis of the proteomic data generated in this study.

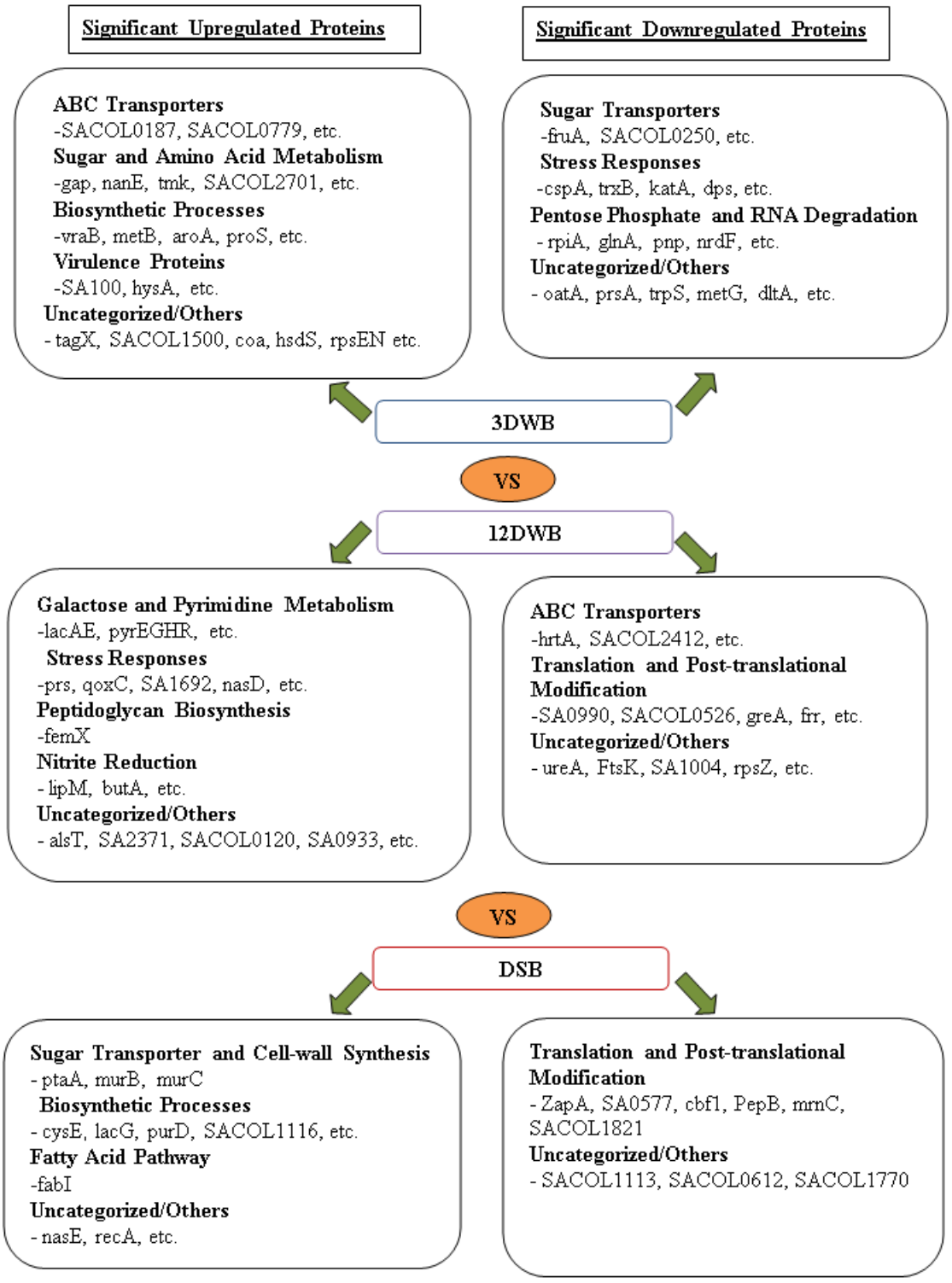

Figure 7.1: A proposed hypothetical model based on the synthesis of the significant proteomic data generated in this study observed between different stages of biofilms.

MurB and murC enzymes are involved in the cytoplasmic biosynthesis steps of peptidoglycan, and simultaneously play a major role in maintaining structural and cellular integrity amongst the surrounding niche against osmotic forces as well as permit the essential fluidity to acclimate to modifications in the shape of microbial cells during different phases of development, division, and infection [540, 541]. However, so far, much of the attention given to bacterial cell-wall surface targeting antimicrobial resistance and the demand to sustain the clinical "upper hand" versus microorganisms, encourage attempts to characterise the less-examined candidates of the pathway and discover novel/potential antimicrobial agents.

Furthermore, a cytoplasmic membrane enzyme fabI plays an important role in completing cycles of the chain elongation process in the essential fatty acid biosynthesis pathway. Significant upregulation of this enzyme involved in fatty acid biosynthesis pathway may be important for biofilm formation in DSB and might be a potential target for biocides to treat biofilm-associated infections. These novel findings might be helpful in designing advanced, targeted disinfectants and detergents to remove biofilms from dry environments.

Our study revealed higher accumulation of cell-wall synthesis associated proteins leading to thicker cell walls and EPS in the DSB compared to planktonic and wet which would result in growth-limiting conditions. It would be expected that oxygen perfusion into biofilm with thicker EPS would also be rate limited. Using next-generation sequencing, Hu *et al.* (2015) showed that clinical DSB are composed of both aerobic and anaerobic organisms. Also, the water availability in the DSB is very low compared to wet biofilm, suggesting DSB cells grow under very adverse environments. The anaerobic or micro anaerobic environment in conjunction with limited water availability in DSB could be supported by nitrite reductase (nasE), which was significantly upregulated in the DSB, ensuring the survivability of cells in the deeper layers of DSB.

More than 80% of proteins have been revealed to function not alone but in complexes [447] and it is crucial to explore the protein complexes together with the circumstances that lead to their development or dissociation in order to fully understand the biological system. Recent advancement in the databases (e.g. STRING) for protein-protein interaction analysis, we can deal with wide-scale protein networks for particular disease with hierarchical functional interactions

under distinct circumstances, in order to uncover secret molecular mechanisms for early diagnosis, prognosis, drug reaction, and biocide effectiveness.

Therefore, in the *in vitro* study, we applied our significant differentially regulated proteins identified in 3dwb, 12dwb, and DSB for PPI network analysis and observed decreased network connections over time and even very fewer connections in DSB. This suggests that, proteins identified in this study showed less number of biological connections in 12dwb and DSB. Since the PPI networks are established on the basis of a combination of high-resolution experiments, genomic context, co-expression, and the common practice of studying *S. aureus* sourced from planktonic mode of growth, the lack of identified related proteins could speculate a generalised lack of significant proteins sourced from biofilm in the database.

In the current study, we specifically focused on only extractomes (extracted supernatant proteins) to explore the proteome changes that exist between different stages of biofilms. We have not considered a large part of precipitated cell pellet fractions and this could be a limitation of this study.

Therefore, this is a proof of concept that, we can observe potential changes between wet and DSB even with comparatively small number of significant proteins. Identified potential marker proteins reported in this study might add valuable information in the global proteome repository, especially novel dry surface biofilm proteome. However, further deep fractionation study might be helpful to explore the large-scale differences between wet and DSB.

In the *in vivo* plasma proteomics study (Chapter 6), TMT-based high-resolution mass spectrometry approach was utilised to construct the plasma proteome, following depletion of high-abundant plasma proteins, in healthy controls and patients with biofilm-related breast-implant CC to explore disease-associated alterations of plasma proteins. The depletion of high-abundant plasma proteins improves the detection of relatively lower-abundant proteins which might be clinically important and more specific for individual clinical conditions. In this study, we have seen clear variations in plasma proteome of biofilm-related breast implant CC patients in comparison to healthy controls and pathway analysis revealed inflammatory response, focal adhesion, platelet activation, complement and coagulation cascades as enriched pathways.

Through this study, we found an interesting correlation with the significant upregulation of tropomyosin alpha-4, increased myofibroblast activity, and the regulatory mechanism by TGF-β which demonstrated a correlation with bacterial biofilms. This finding suggests that increased number and activity of myofibroblasts may lead to higher production of tropomyosin alpha 4 chain which may lead to the biofilm development and probable CC. As a result, higher levels of tropomyosin alpha 4 chain can be detected in plasma from patients with biofilm-related breast-implant CC, which may be considered as a potential diagnostic biomarker for breast-implant CC.

Further, we observed significant upregulation of Talin-1 (TLN1) and fibrinogen alpha chain, which are extracellular matrix (ECM) proteins, and play a key function in activating and mediating the inflammation processes. Studies have demonstrated a higher amount of fibrinogen alpha adhered in the surface of breast implant, and the capability of fibronectin to encourage biofilm development is related to the fibrinogen-binding A domain, that facilitates cell to cell attachment via homophilic bonds of low-affinity [578]. Fibrinogen alpha chain can facilitate binding to host plasma proteins which can function as linking molecules between the bacteria and the receptors of host cell via integrin signalling pathway. Taken together, these findings suggest that, increased expression of TLN1 and fibrinogen alpha chain in plasma from patients with biofilm-related breast-implant CC compared with healthy controls might also be potential candidates for biofilm-related breast-implant CC. In addition, since the integrin signalling pathway plays a vital role in the pathogenesis of inflammation and the close association of the integrin signalling pathway with TLN1 and fibrinogen alpha chain, suggests that the integrin signalling pathway could be involved in the pathogenesis of biofilm-related breast-implant CC.

Furthermore, we also observed increased expression of transferrin receptor protein 1 (TFRC) and lipopolysaccharide (LPS), involved in inflammatory pathways to facilitate inflammatory reactions, and suggesting they might be useful as a potential biomarker for inflammatory reactions of both infectious and non-infectious backgrounds especially breast-implant associated infections.

Future work

In our study, we identified potential enzymes that might work as a potent antibiofilm agents in combination with drugs and/or biocides as well as antibiofilm coating materials for medical devices. Future directions include investigation of potential antibiofilm enzymes from microbial sources and considering cost-effectiveness and green environment, utilisation of bio-industrial waste as a substrate to produce antibiofilm enzymes.

We observed higher abundance of peptidoglycan synthesis associated proteins especially in the DSB. So, it will be interesting to investigate less studied (e.g. murB and murC) cell-wall synthesis proteins to know deeper insight into biofilm biology.

Since we observed the proteome changes in *S. aureus*, it will be a great interest to investigate other DSB species to see the similarities and differences from this species.

Conclusions

In this study, we present the first TMT-based proteomics of *S. aureus*. The current study advances the current *S. aureus* subproteomes and establishes a basis for the identification and study of potential pathways significant to biofilm biology in *S. aureus*. The identification of novel protein targets might be useful in developing novel and/or potential candidates for diagnostic biomarkers, anti-biofilm agents, vaccines, and much needed antimicrobial therapies for *S. aureus* biofilm-associated infections related with implantable medical devices. In addition, these pioneering study with DSB might be helpful in designing advanced, targeted disinfectants and cleaning agents to remove biofilms from dry environments. In the plasma proteomics study, we have seen clear variations in plasma proteome of biofilm-related breast implant CC patients in comparison to healthy controls. These novel findings promote further research to verify outcomes in large groups of patients and various clinical backgrounds which might shed new possibilities to develop universal biomarker(s) for biofilm-related implant diseases.

References

[1] V.O. Adetunji, T.O. Isola, Crystal violet binding assay for assessment of biofilm formation by *Listeria monocytogenes* and Listeria spp on wood, steel and glass surfaces, Global Veterinaria 6(1) (2011) 6-10.

[2] M.R. Parsek, P.K. Singh, Bacterial biofilms: an emerging link to disease pathogenesis, Annual Reviews in Microbiology 57(1) (2003) 677-701.

[3] M.R. Kiedrowski, A.R. Horswill, New approaches for treating staphylococcal biofilm infections, Annals of the New York Academy of Sciences 1241(1) (2011) 104-121.

[4] L. Barrett, B. Atkins, The clinical presentation of prosthetic joint infection, Journal of Antimicrobial Chemotherapy 69(suppl_1) (2014) i25-i27.

[5] S. Chatterjee, P. Maiti, R. Dey, A. Kundu, R. Dey, Biofilms on indwelling urologic devices: microbes and antimicrobial management prospect, Annals of medical and health sciences research 4(1) (2014) 100-104.

[6] D. Ajdic, Y. Zoghbi, D. Gerth, Z.J. Panthaki, S. Thaller, The relationship of bacterial biofilms and capsular contracture in breast implants, Aesthetic surgery journal 36(3) (2016) 297-309.

[7] A. Pajkos, A.K. Deva, K. Vickery, C. Cope, Detection of Subclinical Infection in Significant Breast Implant Capsules, Plastic and reconstructive surgery (2003).

[8] M.R. Rasouli, B. Zmistowski, J. Parvizi, Diagnosis of periprosthetic joint infection, Current Orthopaedic Practice 24(1) (2013) 92-97.

[9] J. Parvizi, I.M. Pawasarat, K.A. Azzam, A. Joshi, E.N. Hansen, K.J. Bozic, Periprosthetic joint infection: the economic impact of methicillin-resistant infections, The Journal of arthroplasty 25(6) (2010) 103-107.

[10] X. Song, E. Perencevich, J. Campos, B.L. Short, N. Singh, Clinical and economic impact of methicillin-resistant *Staphylococcus aureus* colonization or infection on neonates in intensive care units, Infection Control & Hospital Epidemiology 31(2) (2010) 177-182.

[11] A.S. Collins, Preventing health care–associated infections, (2008).

[12] M. Haque, M. Sartelli, J. McKimm, M.A. Bakar, Health care-associated infections–an overview, Infection and drug resistance 11 (2018) 2321.

[13] T.A. Brennan, L.L. Leape, N.M. Laird, L. Hebert, A.R. Localio, A.G. Lawthers, J.P. Newhouse, P.C. Weiler, H.H. Hiatt, Incidence of adverse events and negligence in hospitalized patients: results of the Harvard Medical Practice Study I, New England journal of medicine 324(6) (1991) 370-376.

[14] L.L. Leape, T.A. Brennan, N. Laird, A.G. Lawthers, A.R. Localio, B.A. Barnes, L. Hebert, J.P. Newhouse, P.C. Weiler, H. Hiatt, The nature of adverse events in hospitalized patients: results of the Harvard Medical Practice Study II, New England journal of medicine 324(6) (1991) 377-384.

[15] M. Garrouste-Orgeas, F. Philippart, C. Bruel, A. Max, N. Lau, B. Misset, Overview of medical errors and adverse events, Annals of intensive care 2(1) (2012) 2.

[16] N.P. Nair, L. Chalmers, G.M. Peterson, B.J. Bereznicki, R.L. Castelino, L.R. Bereznicki, Hospitalization in older patients due to adverse drug reactions–the need for a prediction tool, Clinical interventions in aging 11 (2016) 497.

[17] K. Henriksen, J.B. Battles, E.S. Marks, D.I. Lewin, Advances in Patient Safety: From Research to Implementation (Volume 3: Implementation Issues), (2005).

[18] A. Huttner, S. Harbarth, J. Carlet, S. Cosgrove, H. Goossens, A. Holmes, V. Jarlier, A. Voss, D. Pittet, Antimicrobial resistance: a global view from the 2013 World Healthcare-Associated Infections Forum, Antimicrobial resistance and infection control 2(1) (2013) 31.

[19] P. Garling, Hospital Acquired Infections. Final Report of the Special Commission of Inquiry Acute Care Services in NSW Public Hospitals: Overview, NSW Government, 2008, pp. 581-703.

[20] M. Cruickshank, C. Murphy, Reducing harm to patients from healthcare associated infections: An Australian infection prevention and control model for acute hospitals, Sydney: Australian Commission on Safety and Quality in Health Care (2009).

[21] S.S. Magill, W. Hellinger, J. Cohen, R. Kay, C. Bailey, B. Boland, D. Carey, J. de Guzman, K. Dominguez, J. Edwards, Prevalence of healthcare-associated infections in acute care hospitals in Jacksonville, Florida, Infection Control & Hospital Epidemiology 33(3) (2012) 283-291.

[22] FSHHSP, French Society for Hospital Hygiene Surveillance and Prevention of healthcare associated infections, (2010).

[23] A.F. Messina, D.M. Berman, S.R. Ghazarian, R. Patel, J. Neustadt, G. Hahn, E.M. Sibinga, The management and outcome of spinal implant-related infections in pediatric patients: a retrospective review, The Pediatric infectious disease journal 33(7) (2014) 720-723.

[24] X. Nuvials, M. Palomar, F. Alvarez-Lerma, P. Olaechea, S. Otero, S. Uriona, M. Catalán, R. Gimeno, M. Gracia, I. Seijas, Health-care associated infections. Patient characteristics and influence on the clinical outcome of patients admitted to icu. envin-helics registry data, Intensive care medicine experimental 3(S1) (2015) A82.

[25] E.C.f.D. Prevention, Control, Annual Epidemiological Report 2013: Reporting on 2011 surveillance data and 2012 epidemic intelligence data, Stockholm: ECDC (2013) 215-216.

[26] E.T. Martin, K.S. Kaye, C. Knott, H. Nguyen, M. Santarossa, R. Evans, E. Bertran, L. Jaber, Diabetes and risk of surgical site infection: a systematic review and meta-analysis, infection control & hospital epidemiology 37(1) (2016) 88-99.

[27] T.C. Horan, R.P. Gaynes, W.J. Martone, W.R. Jarvis, T.G. Emori, CDC definitions of nosocomial surgical site infections, 1992: a modification of CDC definitions of surgical wound infections, Infection Control & Hospital Epidemiology 13(10) (1992) 606-608.

[28] Y. Maehara, K. Shirabe, S. Kohnoe, Y. Emi, E. Oki, Y. Kakeji, H. Baba, M. Ikeda, M. Kobayashi, T. Takayama, Impact of intra-abdominal absorbable sutures on surgical site infection in gastrointestinal and hepato-biliary-pancreatic surgery: results of a multicenter, randomized, prospective, phase II clinical trial, Surgery today 47(9) (2017) 1060-1071.

[29] F.A. Al-Mulhim, M.A. Baragbah, M. Sadat-Ali, A.S. Alomran, M.Q. Azam, Prevalence of surgical site infection in orthopedic surgery: a 5-year analysis, International surgery 99(3) (2014) 264-268.

[30] V.M. Jodra, L.S. de los Terreros Soler, C.D.-A. Perez, C.M.S. Requejo, N.P. Farrás, Excess length of stay attributable to surgical site infection following hip replacement: a nested case-control study, Infection Control & Hospital Epidemiology 27(12) (2006) 1299-1303.

[31] S. Kusachi, N. Kashimura, T. Konishi, J. Shimizu, M. Kusunoki, M. Oka, T. Wakatsuki, J. Kobayashi, Y. Sawa, H. Imoto, Length of stay and cost for surgical site infection after abdominal and cardiac surgery in Japanese hospitals: multi-center surveillance, Surgical infections 13(4) (2012) 257-265.

[32] D.M. Tsai, E.J. Caterson, Current preventive measures for health-care associated surgical site infections: a review, Patient safety in surgery 8(1) (2014) 42.

[33] J. Allen, T. Rey-Conde, J. North, P. Kruger, W. Babidge, A. Wysocki, R. Ware, J. Veerman, G. Maddern, Processes of care in surgical patients who died with hospital-acquired infections in Australian hospitals, Journal of Hospital Infection 99(1) (2018) 17-23.

[34] C. Owens, K. Stoessel, Surgical site infections: epidemiology, microbiology and prevention, Journal of Hospital Infection 70 (2008) 3-10.

[35] B. Duerden, C. Fry, A.P. Johnson, M.H. Wilcox, The control of methicillin-resistant *Staphylococcus aureus* blood stream infections in England, Open forum infectious diseases, Oxford University Press, 2015, p. ofv035.

[36] K.-Y. Lin, A. Cheng, Y.-C. Chang, M.-C. Hung, J.-T. Wang, W.-H. Sheng, P.-R. Hseuh, Y.-C. Chen, S.-C. Chang, Central line-associated bloodstream infections among critically-ill patients in the era of bundle care, Journal of Microbiology, Immunology and Infection 50(3) (2017) 339-348.

[37] M. Cruickshank, J. Ferguson, A. Bull, Reducing harm to patients from health care associated infection: the role of surveillance. Chapter 3: Surgical site infection–an abridged version, Healthcare Infection 14(3) (2009) 109-114.

[38] R.P. Wenzel, M.B. Edmond, The impact of hospital-acquired bloodstream infections, Emerging infectious diseases 7(2) (2001) 174.

[39] A.G. Barnett, K. Page, M. Campbell, E. Martin, R. Rashleigh-Rolls, K. Halton, D.L. Paterson, L. Hall, N. Jimmieson, K. White, The increased risks of death and extra lengths of hospital and ICU stay from hospital-acquired bloodstream infections: a case–control study, BMJ open 3(10) (2013) e003587.

[40] K.B. Laupland, Incidence of bloodstream infection: a review of population-based studies, Clinical microbiology and infection 19(6) (2013) 492-500.

[41] E. Zimlichman, D. Henderson, O. Tamir, C. Franz, P. Song, C.K. Yamin, C. Keohane, C.R. Denham, D.W. Bates, Health care–associated infections: a meta-analysis of costs and financial impact on the US health care system, JAMA internal medicine 173(22) (2013) 2039-2046.

[42] S.I. Blot, P. Depuydt, L. Annemans, D. Benoit, E. Hoste, J.J. De Waele, J. Decruyenaere, D. Vogelaers, F. Colardyn, K.H. Vandewoude, Clinical and economic outcomes in critically ill patients with nosocomial catheter-related bloodstream infections, Clinical Infectious Diseases 41(11) (2005) 1591-1598.

[43] S. Saint, D.L. Veenstra, B.A. Lipsky, The clinical and economic consequences of nosocomial central venous catheter-related infection: are antimicrobial catheters useful?, Infection Control & Hospital Epidemiology 21(6) (2000) 375-380.

[44] D.P. Calfee, Crisis in hospital-acquired, healthcare-associated infections, Annual review of medicine 63 (2012) 359-371.

[45] R.P. Jordan, S. Malic, M.G.J. Waters, D.J. Stickler, D.W. Williams, Development of an antimicrobial urinary catheter to inhibit urinary catheter encrustation, Microbiology Discovery 3(1) (2015).

[46] S.á. Jacobsen, D. Stickler, H. Mobley, M. Shirtliff, Complicated catheter-associated urinary tract infections due to *Escherichia coli* and Proteus mirabilis, Clinical microbiology reviews 21(1) (2008) 26-59.

[47] B. Foxman, Epidemiology of urinary tract infections: incidence, morbidity, and economic costs, Disease-a-month 49(2) (2003) 53-70.

[48] P. Tenke, T. Mezei, I. Bőde, B. Köves, Catheter-associated urinary tract infections, European Urology Supplements 16(4) (2017) 138-143.

[49] R.M. Klevens, J.R. Edwards, C.L. Richards Jr, T.C. Horan, R.P. Gaynes, D.A. Pollock, D.M. Cardo, Estimating health care-associated infections and deaths in US hospitals, 2002, Public health reports 122(2) (2007) 160-166.

[50] Y.J. Cortese, V.E. Wagner, M. Tierney, D. Devine, A. Fogarty, Review of Catheter-Associated Urinary Tract Infections and In Vitro Urinary Tract Models, Journal of healthcare engineering 2018 (2018).

[51] R.M. Donlan, Biofilms and device-associated infections, Emerging infectious diseases 7(2) (2001) 277.

[52] L.E. Nicolle, Catheter associated urinary tract infections, Antimicrobial resistance and infection control 3(1) (2014) 23.

[53] B.G. Mitchell, J.K. Ferguson, M. Anderson, J. Sear, A. Barnett, Length of stay and mortality associated with healthcare-associated urinary tract infections: a multi-state model, Journal of Hospital Infection 93(1) (2016) 92-99.

[54] V.D. Rosenthal, D.G. Maki, A. Mehta, C. Álvarez-Moreno, H. Leblebicioglu, F. Higuera, L.E. Cuellar, N. Madani, Z. Mitrev, L. Dueñas, International nosocomial infection control consortium report, data summary for 2002-2007, issued January 2008, American journal of infection control 36(9) (2008) 627-637.

[55] V.D. Rosenthal, H.M. Al-Abdely, A.A. El-Kholy, S.A.A. AlKhawaja, H. Leblebicioglu, Y. Mehta, V. Rai, N.V. Hung, S.S. Kanj, M.F. Salama, International Nosocomial Infection Control Consortium report, data summary of 50 countries for 2010-2015: Device-associated module, American journal of infection control 44(12) (2016) 1495-1504.

[56] A. Torres, M.S. Niederman, J. Chastre, S. Ewig, P. Fernandez-Vandellos, H. Hanberger, M. Kollef, G.L. Bassi, C.M. Luna, I. Martin-Loeches, International ERS/ESICM/ESCMID/ALAT

guidelines for the management of hospital-acquired pneumonia and ventilator-associated pneumonia: Guidelines for the management of hospital-acquired pneumonia (HAP)/ventilator-associated pneumonia (VAP) of the European Respiratory Society (ERS), European Society of Intensive Care Medicine (ESICM), European Society of Clinical Microbiology and Infectious Diseases (ESCMID) and Asociación Latinoamericana del Tórax (ALAT), European Respiratory Journal 50(3) (2017) 1700582.

[57] J. Chastre, J.-Y. Fagon, Ventilator-associated pneumonia, American journal of respiratory and critical care medicine 165(7) (2002) 867-903.

[58] D.K. Warren, S.J. Shukla, M.A. Olsen, M.H. Kollef, C.S. Hollenbeak, M.J. Cox, M.M. Cohen, V.J. Fraser, Outcome and attributable cost of ventilator-associated pneumonia among intensive care unit patients in a suburban medical center, Critical care medicine 31(5) (2003) 1312-1317.

[59] M.H. Kollef, C.W. Hamilton, F.R. Ernst, Economic impact of ventilator-associated pneumonia in a large matched cohort, Infection Control & Hospital Epidemiology 33(3) (2012) 250-256.

[60] E. Alp, G. Kalin, R. Coskun, M. Sungur, M. Guven, M. Doganay, Economic burden of ventilator-associated pneumonia in a developing country, Journal of Hospital Infection 81(2) (2012) 128-130.

[61] W.G. Melsen, M.M. Rovers, R.H. Groenwold, D.C. Bergmans, C. Camus, T.T. Bauer, E.W. Hanisch, B. Klarin, M. Koeman, W.A. Krueger, Attributable mortality of ventilator-associated pneumonia: a meta-analysis of individual patient data from randomised prevention studies, The Lancet infectious diseases 13(8) (2013) 665-671.

[62] V. Rosenthal, F. Udwadia, H. Munoz, N. Erben, F. Higuera, K. Abidi, E. Medeiros, E.F. Maldonado, S. Kanj, A. Gikas, Time-dependent analysis of extra length of stay and mortality due to ventilator-associated pneumonia in intensive-care units of ten limited-resources countries: findings of the International Nosocomial Infection Control Consortium (INICC), Epidemiology & Infection 139(11) (2011) 1757-1763.

[63] D.R. Park, The microbiology of ventilator-associated pneumonia, Respiratory care 50(6) (2005) 742-765.

[64] S.Y. Chi, T.O. Kim, C.W. Park, J.Y. Yu, B. Lee, H.S. Lee, Y.I. Kim, S.C. Lim, Y.S. Kwon, Bacterial pathogens of ventilator associated pneumonia in a tertiary referral hospital, Tuberculosis and respiratory diseases 73(1) (2012) 32-37.

[65] F. Barbier, A. Andremont, M. Wolff, L. Bouadma, Hospital-acquired pneumonia and ventilator-associated pneumonia: recent advances in epidemiology and management, Current opinion in pulmonary medicine 19(3) (2013) 216-228.

[66] A. Bonell, R. Azarrafiy, V.T.L. Huong, T.L. Viet, V.D. Phu, V.Q. Dat, H. Wertheim, H.R. van Doorn, S. Lewycka, B. Nadjm, A systematic review and meta-analysis of ventilator-associated pneumonia in adults in Asia: an analysis of national income level on incidence and etiology, Clinical Infectious Diseases 68(3) (2018) 511-518.

[67] J.D. Hunter, Ventilator associated pneumonia, Bmj 344 (2012) e3325.

[68] D. McDougald, S.A. Rice, N. Barraud, P.D. Steinberg, S. Kjelleberg, Should we stay or should we go: mechanisms and ecological consequences for biofilm dispersal, Nature Reviews Microbiology 10(1) (2012) 39-50.

[69] R.M. Donlan, Biofilms: microbial life on surfaces, Emerging infectious diseases 8(9) (2002) 881.

[70] H. Heukelekian, A. Heller, Relation between food concentration and surface for bacterial growth, Journal of bacteriology 40(4) (1940) 547.

[71] C.E. Zobell, The effect of solid surfaces upon bacterial activity, Journal of bacteriology 46(1) (1943) 39.

[72] J.W. Costerton, G. Geesey, K.-J. Cheng, How bacteria stick, Scientific American 238(1) (1978) 86-95.

[73] W.G. Characklis, K.C. Marshall, Biofilms, (1990).

[74] J.W. Costerton, K. Cheng, G.G. Geesey, T.I. Ladd, J.C. Nickel, M. Dasgupta, T.J. Marrie, Bacterial biofilms in nature and disease, Annual Reviews in Microbiology 41(1) (1987) 435-464.

[75] J.W. Costerton, Z. Lewandowski, D.E. Caldwell, D.R. Korber, H.M. Lappin-Scott, Microbial biofilms, Annual Reviews in Microbiology 49(1) (1995) 711-745.

[76] D. Davies, G. Geesey, Regulation of the alginate biosynthesis gene algC in *Pseudomonas aeruginosa* during biofilm development in continuous culture, Applied and environmental microbiology 61(3) (1995) 860-867.

[77] J.W. Costerton, P.S. Stewart, E.P. Greenberg, Bacterial biofilms: a common cause of persistent infections, science 284(5418) (1999) 1318-1322.

[78] R.M. Donlan, J.W. Costerton, Biofilms: survival mechanisms of clinically relevant microorganisms, Clinical microbiology reviews 15(2) (2002) 167-193.

[79] D. Dufour, V. Leung, C.M. Lévesque, Bacterial biofilm: structure, function, and antimicrobial resistance, Endodontic Topics 1(22) (2012) 2-16.

[80] I.B. Beech, J.A. Sunner, K. Hiraoka, Microbe-surface interactions in biofouling and biocorrosion processes, Int Microbiol 8(3) (2005) 157-68.

[81] S. Srey, I.K. Jahid, S.-D. Ha, Biofilm formation in food industries: a food safety concern, Food Control 31(2) (2013) 572-585.

[82] USNIH, US National Institute of Health, (2019).

[83] N.K. Archer, M.J. Mazaitis, J.W. Costerton, J.G. Leid, M.E. Powers, M.E. Shirtliff, *Staphylococcus aureus* biofilms: properties, regulation, and roles in human disease, Virulence 2(5) (2011) 445-459.

[84] S.D. Stowe, J.J. Richards, A.T. Tucker, R. Thompson, C. Melander, J. Cavanagh, Anti-biofilm compounds derived from marine sponges, Marine drugs 9(10) (2011) 2010-2035.

[85] G. Ramage, M.M. Tunney, S. Patrick, S.P. Gorman, J.R. Nixon, Formation of *Propionibacterium acnes* biofilms on orthopaedic biomaterials and their susceptibility to antimicrobials, Biomaterials 24(19) (2003) 3221-3227.

[86] E. Drenkard, F.M. Ausubel, Pseudomonas biofilm formation and antibiotic resistance are linked to phenotypic variation, Nature 416(6882) (2002) 740-743.

[87] C. Fux, J.W. Costerton, P.S. Stewart, P. Stoodley, Survival strategies of infectious biofilms, Trends in microbiology 13(1) (2005) 34-40.

[88] M. Jamal, U. Tasneem, T. Hussain, S. Andleeb, Bacterial biofilm: its composition, formation and role in human infections, RRJMB 4 (2015) 1-14.

[89] H.-C. Flemming, J. Wingender, The biofilm matrix, Nature Reviews Microbiology 8(9) (2010) 623.

[90] J.W. Costerton, Z. Lewandowski, D.E. Caldwell, D.R. Korber, H.M. Lappin-Scott, Microbial biofilms, Annual review of microbiology 49(1) (1995) 711-745.

[91] S.S. Branda, Å. Vik, L. Friedman, R. Kolter, Biofilms: the matrix revisited, Trends in microbiology 13(1) (2005) 20-26.

[92] P. Speziale, L. Visai, S. Rindi, G. Pietrocola, G. Provenza, M. Provenzano, Prevention and treatment of *Staphylococcus* biofilms, Current medicinal chemistry 15(30) (2008) 3185-3195.

[93] S. Sugimoto, K.-i. Okuda, R. Miyakawa, M. Sato, K.-i. Arita-Morioka, A. Chiba, K. Yamanaka, T. Ogura, Y. Mizunoe, C. Sato, Imaging of bacterial multicellular behaviour in biofilms in liquid by atmospheric scanning electron microscopy, Scientific reports 6 (2016) 25889.

[94] A. Chiba, S. Sugimoto, F. Sato, S. Hori, Y. Mizunoe, A refined technique for extraction of extracellular matrices from bacterial biofilms and its applicability, Microbial biotechnology 8(3) (2015) 392-403.

[95] C.R. Arciola, D. Campoccia, P. Speziale, L. Montanaro, J.W. Costerton, Biofilm formation in Staphylococcus implant infections. A review of molecular mechanisms and implications for biofilm-resistant materials, Biomaterials 33(26) (2012) 5967-82.

[96] S.E. Cramton, C. Gerke, N.F. Schnell, W.W. Nichols, F. Götz, The intercellular adhesion (ica) locus is present in *Staphylococcus aureus* and is required for biofilm formation, Infection and immunity 67(10) (1999) 5427-5433.

[97] S.E. Cramton, M. Ulrich, F. Götz, G. Döring, Anaerobic conditions induce expression of polysaccharide intercellular adhesin in *Staphylococcus aureus* and *Staphylococcus epidermidis*, Infection and immunity 69(6) (2001) 4079-4085.

[98] J.P. O'Gara, ica and beyond: biofilm mechanisms and regulation in *Staphylococcus epidermidis* and *Staphylococcus aureus*, FEMS microbiology letters 270(2) (2007) 179-188.

[99] P. Houston, S.E. Rowe, C. Pozzi, E.M. Waters, J.P. O'Gara, Essential role for the major autolysin in the fibronectin-binding protein-mediated *Staphylococcus aureus* biofilm phenotype, Infection and immunity 79(3) (2011) 1153-1165.

[100] S. Hennig, S.N. Wai, W. Ziebuhr, Spontaneous switch to PIA-independent biofilm formation in an ica-positive *Staphylococcus epidermidis* isolate, International journal of medical microbiology 297(2) (2007) 117-122.

[101] H. Rohde, E.C. Burandt, N. Siemssen, L. Frommelt, C. Burdelski, S. Wurster, S. Scherpe, A.P. Davies, L.G. Harris, M.A. Horstkotte, Polysaccharide intercellular adhesin or protein factors in biofilm accumulation of *Staphylococcus epidermidis* and *Staphylococcus aureus* isolated from prosthetic hip and knee joint infections, Biomaterials 28(9) (2007) 1711-1720.

[102] M.A. Tormo, E. Knecht, F. Götz, I. Lasa, J.R. Penades, Bap-dependent biofilm formation by pathogenic species of *Staphylococcus*: evidence of horizontal gene transfer?, Microbiology 151(7) (2005) 2465-2475.

[103] K. Smith, A. Perez, G. Ramage, D. Lappin, C.G. Gemmell, S. Lang, Biofilm formation by Scottish clinical isolates of *Staphylococcus aureus*, Journal of medical microbiology 57(8) (2008) 1018-1023.

[104] L. Hall-Stoodley, J.W. Costerton, P. Stoodley, Bacterial biofilms: from the natural environment to infectious diseases, Nature reviews microbiology 2(2) (2004) 95-108.

[105] R.D. Monds, G.A. O'Toole, The developmental model of microbial biofilms: ten years of a paradigm up for review, Trends in microbiology 17(2) (2009) 73-87.

[106] B.R. Boles, A.R. Horswill, Agr-mediated dispersal of *Staphylococcus aureus* biofilms, PLoS pathogens 4(4) (2008) e1000052.

[107] K.J. Lauderdale, C.L. Malone, B.R. Boles, J. Morcuende, A.R. Horswill, Biofilm dispersal of community-associated methicillin-resistant *Staphylococcus aureus* on orthopedic implant material, Journal of Orthopaedic Research 28(1) (2010) 55-61.

[108] D.E. Moormeier, J.L. Bose, A.R. Horswill, K.W. Bayles, Temporal and stochastic control of *Staphylococcus aureus* biofilm development, MBio 5(5) (2014) e01341-14.

[109] A.E. Paharik, A.R. Horswill, The Staphylococcal Biofilm: Adhesins, Regulation, and Host Response, Microbiology Spectrum 4(2) (2016).

[110] T.J. Foster, M. Höök, Surface protein adhesins of *Staphylococcus aureus*, Trends in microbiology 6(12) (1998) 484-488.

[111] J.M. Patti, B.L. Allen, M.J. McGavin, M. Hook, MSCRAMM-mediated adherence of microorganisms to host tissues, Annual Reviews in Microbiology 48(1) (1994) 585-617.

[112] A. Peschel, C. Vuong, M. Otto, F. Götz, The d-Alanine Residues of*Staphylococcus aureus* Teichoic Acids Alter the Susceptibility to Vancomycin and the Activity of Autolytic Enzymes, Antimicrobial agents and chemotherapy 44(10) (2000) 2845-2847.

[113] M.G. Bowden, L. Visai, C.M. Longshaw, K.T. Holland, P. Speziale, M. Höök, Is the GehD lipase from *Staphylococcus epidermidis* a collagen binding adhesin?, Journal of Biological Chemistry 277(45) (2002) 43017-43023.

[114] G. McKay, D. Nguyen, Antibiotic resistance and tolerance in bacterial biofilms, Handbook of antimicrobial resistance (2014) 1-24.

[115] M. Souli, H. Giamarellou, Effects of slime produced by clinical isolates of coagulase-negative staphylococci on activities of various antimicrobial agents, Antimicrobial agents and chemotherapy 42(4) (1998) 939-941.

[116] K.K. Jefferson, D.A. Goldmann, G.B. Pier, Use of confocal microscopy to analyze the rate of vancomycin penetration through *Staphylococcus aureus* biofilms, Antimicrobial agents and chemotherapy 49(6) (2005) 2467-2473.

[117] R. Singh, P. Ray, A. Das, M. Sharma, Penetration of antibiotics through *Staphylococcus aureus* and *Staphylococcus epidermidis* biofilms, Journal of antimicrobial chemotherapy 65(9) (2010) 1955-1958.

[118] O. Habimana, K. Steenkeste, M.-P. Fontaine-Aupart, M.-N. Bellon-Fontaine, S. Kulakauskas, R. Briandet, Diffusion of nanoparticles in biofilms is altered by bacterial cell wall hydrophobicity, Applied and environmental microbiology 77(1) (2011) 367-368.

[119] P.S. Stewart, J. Rayner, F. Roe, W. Rees, Biofilm penetration and disinfection efficacy of alkaline hypochlorite and chlorosulfamates, Journal of applied microbiology 91(3) (2001) 525-532.

[120] C. Campanac, L. Pineau, A. Payard, G. Baziard-Mouysset, C. Roques, Interactions between biocide cationic agents and bacterial biofilms, Antimicrobial agents and chemotherapy 46(5) (2002) 1469-1474.

[121] J.N. Anderl, M.J. Franklin, P.S. Stewart, Role of antibiotic penetration limitation in Klebsiella pneumoniae biofilm resistance to ampicillin and ciprofloxacin, Antimicrobial agents and chemotherapy 44(7) (2000) 1818-1824.

[122] K.S. Thomson, E.S. Moland, Version 2000: the new β-lactamases of Gram-negative bacteria at the dawn of the new millennium, Microbes and Infection 2(10) (2000) 1225-1235.

[123] S. Garneau-Tsodikova, K.J. Labby, Mechanisms of resistance to aminoglycoside antibiotics: overview and perspectives, MedChemComm 7(1) (2016) 11-27.

[124] P.S. Stewart, T. Zhang, R. Xu, B. Pitts, M.C. Walters, F. Roe, J. Kikhney, A. Moter, Reaction–diffusion theory explains hypoxia and heterogeneous growth within microbial biofilms associated with chronic infections, npj Biofilms and Microbiomes 2 (2016) 16012.

[125] M.C. Walters, F. Roe, A. Bugnicourt, M.J. Franklin, P.S. Stewart, Contributions of antibiotic penetration, oxygen limitation, and low metabolic activity to tolerance of *Pseudomonas aeruginosa* biofilms to ciprofloxacin and tobramycin, Antimicrobial agents and chemotherapy 47(1) (2003) 317-323.

[126] G. Borriello, E. Werner, F. Roe, A.M. Kim, G.D. Ehrlich, P.S. Stewart, Oxygen limitation contributes to antibiotic tolerance of *Pseudomonas aeruginosa* in biofilms, Antimicrobial agents and chemotherapy 48(7) (2004) 2659-2664.

[127] C. Sternberg, B.B. Christensen, T. Johansen, A.T. Nielsen, J.B. Andersen, M. Givskov, S. Molin, Distribution of bacterial growth activity in flow-chamber biofilms, Applied and environmental microbiology 65(9) (1999) 4108-4117.

[128] Z. Zheng, P.S. Stewart, Growth limitation of *Staphylococcus epidermidis* in biofilms contributes to rifampin tolerance, Biofilms 1(1) (2004) 31-35.

[129] R. Eng, F. Padberg, S. Smith, E. Tan, C. Cherubin, Bactericidal effects of antibiotics on slowly growing and nongrowing bacteria, Antimicrobial agents and chemotherapy 35(9) (1991) 1824-1828.

[130] D. Evans, D. Allison, M. Brown, P. Gilbert, Susceptibility of *Pseudomonas aeruginosa* and *Escherichia coli* biofilms towards ciprofloxacin: effect of specific growth rate, Journal of Antimicrobial Chemotherapy 27(2) (1991) 177-184.

[131] J.P. Folsom, L. Richards, B. Pitts, F. Roe, G.D. Ehrlich, A. Parker, A. Mazurie, P.S. Stewart, Physiology of *Pseudomonas aeruginosa* in biofilms as revealed by transcriptome analysis, BMC microbiology 10(1) (2010) 294.

[132] D. Hogan, R. Kolter, Why are bacteria refractory to antimicrobials?, Current opinion in microbiology 5(5) (2002) 472-477.

[133] S.-J. Liaw, Y.-L. Lee, P.-R. Hsueh, Multidrug resistance in clinical isolates of *Stenotrophomonas maltophilia*: roles of integrons, efflux pumps, phosphoglucomutase (SpgM), and melanin and biofilm formation, International journal of antimicrobial agents 35(2) (2010) 126-130.

[134] K. Poole, Efflux pumps as antimicrobial resistance mechanisms, Annals of medicine 39(3) (2007) 162-176.

[135] P.N. Markham, A.A. Neyfakh, Efflux-mediated drug resistance in Gram-positive bacteria, Current opinion in microbiology 4(5) (2001) 509-514.

[136] A. Kumar, H.P. Schweizer, Bacterial resistance to antibiotics: active efflux and reduced uptake, Advanced drug delivery reviews 57(10) (2005) 1486-1513.

[137] K. Poole, Efflux-mediated antimicrobial resistance, Journal of Antimicrobial Chemotherapy 56(1) (2005) 20-51.

[138] T.R. De Kievit, M.D. Parkins, R.J. Gillis, R. Srikumar, H. Ceri, K. Poole, B.H. Iglewski, D.G. Storey, Multidrug efflux pumps: expression patterns and contribution to antibiotic resistance in *Pseudomonas aeruginosa* biofilms, Antimicrobial agents and chemotherapy 45(6) (2001) 1761-1770.

[139] L. Zhang, T.-F. Mah, Involvement of a novel efflux system in biofilm-specific resistance to antibiotics, Journal of bacteriology 190(13) (2008) 4447-4452.

[140] S.J. Pamp, M. Gjermansen, H.K. Johansen, T. Tolker-Nielsen, Tolerance to the antimicrobial peptide colistin in *Pseudomonas aeruginosa* biofilms is linked to metabolically active cells, and depends on the pmr and mexAB-oprM genes, Molecular microbiology 68(1) (2008) 223-240.

[141] W.-C. Chiang, S.J. Pamp, M. Nilsson, M. Givskov, T. Tolker-Nielsen, The metabolically active subpopulation in *Pseudomonas aeruginosa* biofilms survives exposure to membrane-targeting antimicrobials via distinct molecular mechanisms, FEMS Immunology & Medical Microbiology 65(2) (2012) 245-256.

[142] B.R. Boles, P.K. Singh, Endogenous oxidative stress produces diversity and adaptability in biofilm communities, Proceedings of the National Academy of Sciences (2008).

[143] D. Lebeaux, J.-M. Ghigo, C. Beloin, Biofilm-related infections: bridging the gap between clinical management and fundamental aspects of recalcitrance toward antibiotics, Microbiology and Molecular Biology Reviews 78(3) (2014) 510-543.

[144] K. Driffield, K. Miller, J. Bostock, A. O'neill, I. Chopra, Increased mutability of *Pseudomonas aeruginosa* in biofilms, Journal of Antimicrobial Chemotherapy 61(5) (2008) 1053-1056.

[145] V.J. Ryder, I. Chopra, A.J. O'Neill, Increased mutability of Staphylococci in biofilms as a consequence of oxidative stress, PLoS One 7(10) (2012) e47695.

[146] FDA, Breast Implant-Associated Anaplastic Large Cell Lymphoma (BIA-ALCL), (2018).

[147] R.O. Darouiche, Treatment of infections associated with surgical implants, New England Journal of Medicine 350(14) (2004) 1422-1429.

[148] R. Kuehl, P.S. Brunetto, A.-K. Woischnig, M. Varisco, Z. Rajacic, J. Vosbeck, L. Terracciano, K.M. Fromm, N. Khanna, Preventing implant-associated infections by silver coating, Antimicrobial agents and chemotherapy 60(4) (2016) 2467-2475.

[149] Z. Khatoon, C.D. McTiernan, E.J. Suuronen, T.-F. Mah, E.I. Alarcon, Bacterial biofilm formation on implantable devices and approaches to its treatment and prevention, Heliyon 4(12) (2018) e01067.

[150] M. Ribeiro, F.J. Monteiro, M.P. Ferraz, Infection of orthopedic implants with emphasis on bacterial adhesion process and techniques used in studying bacterial-material interactions, Biomatter 2(4) (2012) 176-194.

[151] ASPS, ASPS Plastic Surgery Statistics Report, (2018).

[152] S.E. Gabriel, J.E. Woods, W.M. O'fallon, C.M. Beard, L.T. Kurland, L.J. Melton, Complications leading to surgery after breast implantation, New England Journal of Medicine 336(10) (1997) 677-682.

[153] W.P. Adams Jr, J.L. Rios, S.J. Smith, Enhancing patient outcomes in aesthetic and reconstructive breast surgery using triple antibiotic breast irrigation: six-year prospective clinical study, Plastic and reconstructive surgery 117(1) (2006) 30-36.

[154] A. Araco, G. Gravante, F. Araco, D. Delogu, V. Cervelli, Capsular contracture: results of 3002 patients with aesthetic breast augmentation, Plastic and reconstructive surgery 118(6) (2006) 1499-1500.

[155] Y. El-Sheikh, R. Tutino, C. Knight, F. Farrokhyar, N. Hynes, Incidence of capsular contracture in silicone versus saline cosmetic augmentation mammoplasty: A meta-analysis, Canadian Journal of Plastic Surgery 16(4) (2008) 211-215.

[156] B. Cunningham, The Mentor study on contour profile gel silicone MemoryGel breast implants, Plastic and reconstructive surgery 120(7) (2007) 33S-39S.

[157] S.L. Spear, D.K. Murphy, A. Slicton, P.S. Walker, I.S.B.I.U.S. Group, Inamed silicone breast implant core study results at 6 years, Plastic and reconstructive surgery 120(7) (2007) 8S-16S.

[158] O. Asplund, L. Gylbert, G. Jurell, C. Ward, Textured or smooth implants for submuscular breast augmentation: a controlled study, Plastic and reconstructive surgery 97(6) (1996) 1200-1206.

[159] C.-H. Wong, M. Samuel, B.-K. Tan, C. Song, Capsular contracture in subglandular breast augmentation with textured versus smooth breast implants: a systematic review, Plastic and reconstructive surgery 118(5) (2006) 1224-1236.

[160] TGA, Breast implants and anaplastic large-cell lymphoma. , (2019).

[161] I. Hopper, E. Parker, B. Pelligrini, C. Mulvany, M. Pase, S. Ahem, A. Earnest, J. McNeil, The Australian Breast Device Registry 2016 Report, Monash University: Melbourne, Australia (2018).

[162] M.P. Conte, F. Superti, M. Moio, M.G. Ammendolia, C. Longhi, M. Aleandri, M. Marazzato, P. Goldoni, P. Parisi, Z. Borab, Bacterial biofilm associated with a case of capsular contracture, The new microbiologica 41(2) (2018).

[163] S.L. Spear, J.J. Baker, Classification of capsular contracture after prosthetic breast reconstruction, Plastic and reconstructive surgery 96(5) (1995) 1119-23; discussion 1124.

[164] W.P. Adams Jr, Capsular contracture: what is it? What causes it? How can it be prevented and managed?, Clinics in plastic surgery 36(1) (2009) 119-126.

[165] J.A. McCurdy, Capsular contracture following augmentation mammaplasty: Etiology and pathogenesis, Breast augmentation, Springer2009, pp. 525-540.

[166] A. Araco, R. Caruso, F. Araco, J. Overton, G. Gravante, Capsular contractures: a systematic review, Plastic and reconstructive surgery 124(6) (2009) 1808-1819.

[167] N.V. Tran, J.L. Del Pozo, P.M. Petty, C.H. Johnson, M.F. Walsh, U. Bite, R.P. Clay, J.N. Mandrekar, K.E. Piper, J.M. Steckelberg, Bacteria on breast implants are associated with capsular contracture, Plastic and reconstructive surgery 124(4S) (2009) 38-39.

[168] L. Snell, M. Brown, Breast implant capsules and subclinical infection, Plastic and reconstructive surgery 124(4S) (2009) 38.

[169] N. Handel, T. Cordray, J. Gutierrez, J.A. Jensen, A long-term study of outcomes, complications, and patient satisfaction with breast implants, Plastic and reconstructive surgery 117(3) (2006) 757-767.

[170] A. Pajkos, A.K. Deva, K. Vickery, C. Cope, L. Chang, Y.E. Cossart, Detection of subclinical infection in significant breast implant capsules, Plastic and reconstructive surgery 111(5) (2003) 1605-1611.

[171] H. Tamboto, K. Vickery, A.K. Deva, Subclinical (biofilm) infection causes capsular contracture in a porcine model following augmentation mammaplasty, Plastic and reconstructive surgery 126(3) (2010) 835-842.

[172] U. Rieger, J. Mesina, D. Kalbermatten, M. Haug, H. Frey, R. Pico, R. Frei, G. Pierer, N. Lüscher, A. Trampuz, Bacterial biofilms and capsular contracture in patients with breast implants, British Journal of Surgery 100(6) (2013) 768-774.

[173] G. Zhao, M.L. Usui, S.I. Lippman, G.A. James, P.S. Stewart, P. Fleckman, J.E. Olerud, Biofilms and Inflammation in Chronic Wounds, Advances in wound care 2(7) (2013) 389-399.

[174] J.D. Bryers, Medical biofilms, Biotechnology and bioengineering 100(1) (2008) 1-18.

[175] L. Van De Water, S. Varney, J.J. Tomasek, Mechanoregulation of the myofibroblast in wound contraction, scarring, and fibrosis: opportunities for new therapeutic intervention, Advances in wound care 2(4) (2013) 122-141.

[176] Y. Rinkevich, G.G. Walmsley, M.S. Hu, Z.N. Maan, A.M. Newman, M. Drukker, M. Januszyk, G.W. Krampitz, G.C. Gurtner, H.P. Lorenz, Identification and isolation of a dermal lineage with intrinsic fibrogenic potential, Science 348(6232) (2015) aaa2151.

[177] K. Mazhar, M. Gunawardana, P. Webster, C. Hochstim, J. Koempel, N. Kokot, U. Sinha, D. Rice, M. Baum, Bacterial biofilms and increased bacterial counts are associated with airway stenosis, Otolaryngology--Head and Neck Surgery 150(5) (2014) 834-840.

[178] N. Vedrenne, B. Coulomb, A. Danigo, F. Bonté, A. Desmoulière, The complex dialogue between (myo) fibroblasts and the extracellular matrix during skin repair processes and ageing, Pathologie Biologie 60(1) (2012) 20-27.

[179] K. Hwang, H.B. Sim, F. Huan, D.J. Kim, Myofibroblasts and capsular tissue tension in breast capsular contracture, Aesthetic plastic surgery 34(6) (2010) 716-721.

[180] L.M. Switalski, J.M. Patti, W. Butcher, A.G. Gristina, P. Speziale, M. Höök, A collagen receptor on *Staphylococcus aureus* strains isolated from patients with septic arthritis mediates adhesion to cartilage, Molecular microbiology 7(1) (1993) 99-107.

[181] B. Kreikemeyer, M. Nakata, S. Oehmcke, C. Gschwendtner, J. Normann, A. Podbielski, Streptococcus pyogenes Collagen Type I-binding Cpa Surface Protein Expression profile, binding characteristics, biological functions, and potential clinical impact, Journal of Biological Chemistry 280(39) (2005) 33228-33239.

[182] B.E. Menzies, The role of fibronectin binding proteins in the pathogenesis of *Staphylococcus aureus* infections, Current opinion in infectious diseases 16(3) (2003) 225-229.

[183] S.R. Talay, P. Valentin-Weigand, P. Jerlström, K. Timmis, G. Chhatwal, Fibronectin-binding protein of *Streptococcus pyogenes*: sequence of the binding domain involved in adherence of streptococci to epithelial cells, Infection and immunity 60(9) (1992) 3837-3844.

[184] M. Thomas, J.A. D'Silva, A.J. Borole, R.M. Chilgar, Periprosthetic atypical mycobaterial infection in breast implants: a new kid on the block!, Journal of Plastic, Reconstructive & Aesthetic Surgery 66(1) (2013) e16-e19.

[185] E.M. Feldman, D.P. Kontoyiannis, S.E. Sharabi, E. Lee, Y. Kaufman, L. Heller, Breast implant infections: is cefazolin enough?, Plastic and reconstructive surgery 126(3) (2010) 779-785.

[186] J.J. Baker, M.L. Chandler, R.R. LeVier, Occurrence and activity of myofibroblasts in human capsular tissue surrounding mammary implants, Plastic and reconstructive surgery 68(6) (1981) 905-912.

[187] R.A. Mladick, Significance of *Staphylococcus epidermidis* causing subclinical infection, Plastic and reconstructive surgery 115(5) (2005) 1426-1427.

[188] B. Pittet, D. Montandon, D. Pittet, Infection in breast implants, The Lancet infectious diseases 5(2) (2005) 94-106.

[189] T.A. Rouault, Pathogenic bacteria prefer heme, Science 305(5690) (2004) 1577-1578.

[190] Z. Shah, J.J. Lehman, J. Tan, Does infection play a role in breast capsular contracture?, Plastic and reconstructive surgery 68(1) (1981) 34-42.

[191] N. Kossovsky, J.P. Heggers, R.W. Parsons, M.C. Robson, Acceleration of capsule formation around silicone implants by infection in a guinea pig model, Plastic and reconstructive surgery 73(1) (1984) 91-98.

[192] U.M. Rieger, G. Pierer, N.J. Luscher, A. Trampuz, Sonication of removed breast implants for improved detection of subclinical infection, Aesthetic plastic surgery 33(3) (2009) 404-8.

[193] H. Hu, A. Jacombs, K. Vickery, S.L. Merten, D.G. Pennington, A.K. Deva, Chronic biofilm infection in breast implants is associated with an increased T-cell lymphocytic infiltrate:

implications for breast implant–associated lymphoma, Plastic and reconstructive surgery 135(2) (2015) 319-329.

[194] D. Chessa, G. Ganau, L. Spiga, A. Bulla, V. Mazzarello, G.V. Campus, S. Rubino, *Staphylococcus aureus* and *Staphylococcus epidermidis* Virulence Strains as Causative Agents of Persistent Infections in Breast Implants, PloS one 11(1) (2016) e0146668.

[195] L.A. Poultsides, L.L. Liaropoulos, K.N. Malizos, The socioeconomic impact of musculoskeletal infections, JBJS 92(11) (2010) e13.

[196] S.M. Kurtz, K.L. Ong, J. Schmier, F. Mowat, K. Saleh, E. Dybvik, J. Kärrholm, G. Garellick, L.I. Havelin, O. Furnes, Future clinical and economic impact of revision total hip and knee arthroplasty, JBJS 89(suppl_3) (2007) 144-151.

[197] K.J. Bozic, S.M. Kurtz, E. Lau, K. Ong, T.P. Vail, D.J. Berry, The epidemiology of revision total hip arthroplasty in the United States, JBJS 91(1) (2009) 128-133.

[198] H.O. Gbejuade, A.M. Lovering, J.C. Webb, The role of microbial biofilms in prosthetic joint infections: a review, Acta orthopaedica 86(2) (2015) 147-158.

[199] A.G. Gristina, J. Costerton, Bacterial adherence to biomaterials and tissue. The significance of its role in clinical sepsis, JBJS 67(2) (1985) 264-273.

[200] A.G. Gristina, Biomaterial-centered infection: microbial adhesion versus tissue integration, Science 237(4822) (1987) 1588-1595.

[201] E. Rochford, R. Richards, T. Moriarty, Influence of material on the development of device-associated infections, Clinical Microbiology and Infection 18(12) (2012) 1162-1167.

[202] J. Barberan, Management of infections of osteoarticular prosthesis, Clinical Microbiology and Infection 12 (2006) 93-101.

[203] R.R. Laffer, P. Graber, P.E. Ochsner, W. Zimmerli, Outcome of prosthetic knee-associated infection: evaluation of 40 consecutive episodes at a single centre, Clin Microbiol Infect 12(5) (2006) 433-9.

[204] L. Montanaro, P. Speziale, D. Campoccia, S. Ravaioli, I. Cangini, G. Pietrocola, S. Giannini, C.R. Arciola, Scenery of Staphylococcus implant infections in orthopedics, Future microbiology 6(11) (2011) 1329-49.

[205] S.A. Kristian, T. Golda, F. Ferracin, S.E. Cramton, B. Neumeister, A. Peschel, F. Gotz, R. Landmann, The ability of biofilm formation does not influence virulence of *Staphylococcus aureus* and host response in a mouse tissue cage infection model, Microb Pathog 36(5) (2004) 237-45.

[206] M.E. Olson, K.L. Garvin, P.D. Fey, M.E. Rupp, Adherence of *Staphylococcus epidermidis* to biomaterials is augmented by PIA, Clinical orthopaedics and related research 451 (2006) 21-4.

[207] A. Ahlberg, A.S. Carlsson, L. Lindberg, Hematogenous infection in total joint replacement, Clinical orthopaedics and related research (137) (1978) 69-75.

[208] M.K. Glynn, J.M. Sheehan, An analysis of the causes of deep infection after hip and knee arthroplasties, Clinical orthopaedics and related research (178) (1983) 202-6.

[209] O.M. Lidwell, E.J. Lowbury, W. Whyte, R. Blowers, S.J. Stanley, D. Lowe, Bacteria isolated from deep joint sepsis after operation for total hip or knee replacement and the sources of the infections with *Staphylococcus aureus*, The Journal of hospital infection 4(1) (1983) 19-29.

[210] S. Corvec, M.E. Portillo, B.M. Pasticci, O. Borens, A. Trampuz, Epidemiology and new developments in the diagnosis of prosthetic joint infection, The International journal of artificial organs 35(10) (2012) 923-34.

[211] N. Høiby, T. Bjarnsholt, C. Moser, G.L. Bassi, T. Coenye, G. Donelli, L. Hall-Stoodley, V. Holá, C. Imbert, K. Kirketerp-Møller, D. Lebeaux, A. Oliver, A.J. Ullmann, C. Williams, ESCMID∗ guideline for the diagnosis and treatment of biofilm infections 2014, Clinical Microbiology and Infection 21, Supplement 1 (2015) S1-S25.

[212] J. Parvizi, O.F. Erkocak, C.J. Della Valle, Culture-negative periprosthetic joint infection, J Bone Joint Surg Am 96(5) (2014) 430-6.

[213] P. Stoodley, S. Kathju, F.Z. Hu, G. Erdos, J.E. Levenson, N. Mehta, B. Dice, S. Johnson, L. Hall-Stoodley, L. Nistico, N. Sotereanos, J. Sewecke, J.C. Post, G.D. Ehrlich, Molecular and imaging techniques for bacterial biofilms in joint arthroplasty infections, Clinical orthopaedics and related research (437) (2005) 31-40.

[214] J.W. Costerton, Biofilm Theory Can Guide the Treatment of Device-Related Orthopaedic Infections, Clinical Orthopaedics and Related Research® 437 (2005) 7-11.

[215] K.E. Dempsey, M.P. Riggio, A. Lennon, V.E. Hannah, G. Ramage, D. Allan, J. Bagg, Identification of bacteria on the surface of clinically infected and non-infected prosthetic hip joints removed during revision arthroplasties by 16S rRNA gene sequencing and by microbiological culture, Arthritis Research & Therapy 9(3) (2007) R46.

[216] L. Hall-Stoodley, P. Stoodley, S. Kathju, C. Moser, N. Høiby, T. Bjarnsholt, J. William Costerton, A. Moter, Towards diagnostic guidelines for biofilm-associated infections, FEMS Immunology & Medical Microbiology 65(2) (2012) 127-145.

[217] W. Vongpatanasin, L.D. Hillis, R.A. Lange, Prosthetic heart valves, New England Journal of Medicine 335(6) (1996) 407-416.

[218] G.M. Viola, R.O. Darouiche, Cardiovascular implantable device infections, Current infectious disease reports 13(4) (2011) 333-342.

[219] M. Ramasamy, J. Lee, Recent nanotechnology approaches for prevention and treatment of biofilm-associated infections on medical devices, BioMed research international 2016 (2016).

[220] M.C. Chifiriuc, O. Banu, C. Bleotu, V. Lazăr, Interaction of bacteria isolated from clinical biofilms with cardiovascular prosthetic devices and eukaryotic cells, Anaerobe 17(6) (2011) 419-421.

[221] E. Braunwald, Valvular heart disease In: Braunwald E, ed, Heart Disease, WB Saunders, Philadelphia (1980) p1149.

[222] S. Bosio, S. Leekha, S.I. Gamb, A.J. Wright, C.L. Terrell, D.V. Miller, Mycobacterium fortuitum prosthetic valve endocarditis: a case for the pathogenetic role of biofilms, Cardiovascular Pathology 21(4) (2012) 361-364.

[223] D.J. Stickler, Bacterial biofilms in patients with indwelling urinary catheters, Nature Reviews Urology 5(11) (2008) 598.

[224] D. Stickler, Bacterial biofilms and the encrustation of urethral catheters, Biofouling 9(4) (1996) 293-305.

[225] K. Murugan, K. Selvanayaki, S. Al-Sohaibani, Urinary catheter indwelling clinical pathogen biofilm formation, exopolysaccharide characterization and their growth influencing parameters, Saudi journal of biological sciences 23(1) (2016) 150-159.

[226] S. Neethirajan, M.A. Clond, A. Vogt, Medical biofilms—nanotechnology approaches, Journal of biomedical nanotechnology 10(10) (2014) 2806-2827.

[227] S.L. Percival, N.A. Sabbuba, P. Kite, D.J. Stickler, The effect of EDTA instillations on the rate of development of encrustation and biofilms in Foley catheters, Urological research 37(4) (2009) 205-209.

[228] M.T. Hessen, D. Kaye, J.M. Zuckerman, Infections associated with foreign bodies in the urinary tract, Infections Associated with Indwelling Medical Devices, Third Edition, American Society of Microbiology2000, pp. 325-344.

[229] D. Stickler, S. Morgan, Observations on the development of the crystalline bacterial biofilms that encrust and block Foley catheters, Journal of Hospital Infection 69(4) (2008) 350-360.

[230] S.S. Talsma, Biofilms on medical devices, Home Healthcare Now 25(9) (2007) 589-594.

[231] J.M. Boyce, Environmental contamination makes an important contribution to hospital infection, Journal of Hospital Infection 65 Suppl 2 (2007) 50-4.

[232] M.J. Brady, C.M. Lisay, A.V. Yurkovetskiy, S.P. Sawan, Persistent silver disinfectant for the environmental control of pathogenic bacteria, American journal of infection control 31(4) (2003) 208-214.

[233] W.A. Rutala, S.L. Barbee, N.C. Aguiar, M.D. Sobsey, D.J. Weber, Antimicrobial activity of home disinfectants and natural products against potential human pathogens, Infection Control & Hospital Epidemiology 21(1) (2000) 33-38.

[234] D.J. Weber, W.A. Rutala, M.B. Miller, K. Huslage, E. Sickbert-Bennett, Role of hospital surfaces in the transmission of emerging health care-associated pathogens: norovirus, Clostridium difficile, and Acinetobacter species, American journal of infection control 38(5) (2010) S25-S33.

[235] D. Chowdhury, S. Tahir, M. Legge, H. Hu, T. Prvan, K. Johani, G.S. Whiteley, T. Glasbey, A.K. Deva, K. Vickery, Transfer of dry surface biofilm in the healthcare environment: the role of healthcare workers' hands as vehicles, Journal of Hospital Infection 100(3) (2018) e85-e90.

[236] D. Lindsay, A. Von Holy, Bacterial biofilms within the clinical setting: what healthcare professionals should know, Journal of Hospital Infection 64(4) (2006) 313-325.

[237] L. Hall-Stoodley, P. Stoodley, Biofilm formation and dispersal and the transmission of human pathogens, Trends in Microbiology 13(1) (2005) 7-10.

[238] L.M. Feazel, L.K. Baumgartner, K.L. Peterson, D.N. Frank, J.K. Harris, N.R. Pace, Opportunistic pathogens enriched in showerhead biofilms, Proceedings of the National Academy of Sciences 106(38) (2009) 16393-16399.

[239] H. Hu, K. Johani, I.B. Gosbell, A.S. Jacombs, A. Almatroudi, G.S. Whiteley, A.K. Deva, S. Jensen, K. Vickery, Intensive care unit environmental surfaces are contaminated by multidrug-resistant bacteria in biofilms: combined results of conventional culture, pyrosequencing, scanning electron microscopy, and confocal laser microscopy, J Hosp Infect 91(1) (2015) 35-44.

[240] K. Vickery, H. Hu, A.S. Jacombs, D.A. Bradshaw, A.K. Deva, A review of bacterial biofilms and their role in device-associated infection, Healthcare Infection 18(2) (2013) 61-66.

[241] B.G. Mitchell, S. Dancer, M. Anderson, E. Dehn, Risk of organism acquisition from prior room occupants: a systematic review and meta-analysis, Journal of Hospital Infection 91(3) (2015) 211-217.

[242] K. Marion-Ferey, M. Pasmore, P. Stoodley, S. Wilson, G. Husson, J.W. Costerton, Biofilm removal from silicone tubing: an assessment of the efficacy of dialysis machine decontamination procedures using an in vitro model, Journal of Hospital Infection 53(1) (2003) 64-71.

[243] G. O'Toole, H.B. Kaplan, R. Kolter, Biofilm formation as microbial development, Annual Reviews in Microbiology 54(1) (2000) 49-79.

[244] A. Almatroudi, I.B. Gosbell, H. Hu, S.O. Jensen, B. Espedido, S. Tahir, T. Glasbey, P. Legge, G. Whiteley, A. Deva, *Staphylococcus aureus* dry-surface biofilms are not killed by

sodium hypochlorite: implications for infection control, Journal of Hospital Infection 93(3) (2016) 263-270.

[245] D. Chowdhury, A. Rahman, H. Hu, S.O. Jensen, A.K. Deva, K. Vickery, Effect of disinfectant formulation and organic soil on the efficacy of oxidizing disinfectants against biofilms, Journal of Hospital Infection (2018).

[246] K. Vickery, Q.-D. Ngo, J. Zou, Y.E. Cossart, The effect of multiple cycles of contamination, detergent washing, and disinfection on the development of biofilm in endoscope tubing, American journal of infection control 37(6) (2009) 470-475.

[247] S. Yezli, J. Otter, Does the discovery of biofilms on dry hospital environmental surfaces change the way we think about hospital disinfection?, Journal of Hospital Infection 81(4) (2012) 293-294.

[248] A.C. Abreu, R.R. Tavares, A. Borges, F. Mergulhão, M. Simões, Current and emergent strategies for disinfection of hospital environments, Journal of Antimicrobial Chemotherapy 68(12) (2013) 2718-2732.

[249] K. Vickery, A. Deva, A. Jacombs, J. Allan, P. Valente, I.B. Gosbell, Presence of biofilm containing viable multiresistant organisms despite terminal cleaning on clinical surfaces in an intensive care unit, Journal of Hospital Infection 80(1) (2012) 52-55.

[250] J. Otter, K. Vickery, J.d. Walker, E. deLancey Pulcini, P. Stoodley, S. Goldenberg, J. Salkeld, J. Chewins, S. Yezli, J. Edgeworth, Surface-attached cells, biofilms and biocide susceptibility: implications for hospital cleaning and disinfection, Journal of Hospital Infection 89(1) (2015) 16-27.

[251] K. Ledwoch, S. Dancer, J. Otter, K. Kerr, D. Roposte, L. Rushton, R. Weiser, E. Mahenthiralingam, D. Muir, J.-Y. Maillard, Beware biofilm! Dry biofilms containing bacterial

pathogens on multiple healthcare surfaces; a multi-centre study, Journal of Hospital Infection 100(3) (2018) e47-e56.

[252] A. Almatroudi, H. Hu, A. Deva, I.B. Gosbell, A. Jacombs, S.O. Jensen, G. Whiteley, T. Glasbey, K. Vickery, A new dry-surface biofilm model: an essential tool for efficacy testing of hospital surface decontamination procedures, Journal of microbiological methods 117 (2015) 171-176.

[253] L. Sehulster, R.Y. Chinn, M.J. Arduino, J. Carpenter, R. Donlan, D. Ashford, R. Besser, B. Fields, M. McNeil, C. Whitney, Guidelines for environmental infection control in health-care facilities, Morbidity and mortality weekly report recommendations and reports RR 52(10) (2003).

[254] H.F. Wertheim, D.C. Melles, M.C. Vos, W. van Leeuwen, A. van Belkum, H.A. Verbrugh, J.L. Nouwen, The role of nasal carriage in *Staphylococcus aureus* infections, The Lancet infectious diseases 5(12) (2005) 751-762.

[255] J.-A. Hennekinne, M.-L. De Buyser, S. Dragacci, *Staphylococcus aureus* and its food poisoning toxins: characterization and outbreak investigation, FEMS microbiology reviews 36(4) (2012) 815-836.

[256] J. Schelin, N. Wallin-Carlquist, M. Thorup Cohn, R. Lindqvist, G.C. Barker, The formation of *Staphylococcus aureus* enterotoxin in food environments and advances in risk assessment, Virulence 2(6) (2011) 580-592.

[257] F.R. DeLeo, B.A. Diep, M. Otto, Host defense and pathogenesis in *Staphylococcus aureus* infections, Infectious disease clinics of North America 23(1) (2009) 17-34.

[258] M.M. Dinges, P.M. Orwin, P.M. Schlievert, Exotoxins of *Staphylococcus aureus*, Clinical microbiology reviews 13(1) (2000) 16-34.

[259] H.F. Chambers, F.R. DeLeo, Waves of resistance: *Staphylococcus aureus* in the antibiotic era, Nature Reviews Microbiology 7(9) (2009) 629-641.

[260] F.D. Lowy, *Staphylococcus aureus* infections, New England journal of medicine 339(8) (1998) 520-532.

[261] P. Moreillon, Y.-A. Que, Infective endocarditis, The Lancet 363(9403) (2004) 139-149.

[262] A. Van Belkum, D.C. Melles, Not all *Staphylococcus aureus* strains are equally pathogenic, Discovery medicine 5(26) (2009) 148-152.

[263] J. Bien, O. Sokolova, P. Bozko, Characterization of virulence factors of *Staphylococcus aureus*: novel function of known virulence factors that are implicated in activation of airway epithelial proinflammatory response, Journal of pathogens 2011 (2011).

[264] A.L. Cheung, A.S. Bayer, G. Zhang, H. Gresham, Y.-Q. Xiong, Regulation of virulence determinants in vitro and in vivo in *Staphylococcus aureus*, FEMS Immunology & Medical Microbiology 40(1) (2004) 1-9.

[265] C. Garzoni, W.L. Kelley, *Staphylococcus aureus*: new evidence for intracellular persistence, Trends in microbiology 17(2) (2009) 59-65.

[266] D.V. Sánchez, Assessment of control strategies against *Staphylococcus aureus* biofilms potentially present in the fishery industry, Universidade de Vigo, 2014.

[267] M.I. Bokarewa, T. Jin, A. Tarkowski, *Staphylococcus aureus*: staphylokinase, The international journal of biochemistry & cell biology 38(4) (2006) 504-509.

[268] C.J. de Haas, K.E. Veldkamp, A. Peschel, F. Weerkamp, W.J. Van Wamel, E.C. Heezius, M.J. Poppelier, K.P. Van Kessel, J.A. van Strijp, Chemotaxis inhibitory protein of *Staphylococcus aureus*, a bacterial antiinflammatory agent, Journal of Experimental Medicine 199(5) (2004) 687-695.

[269] A. Haggar, C. Ehrnfelt, J. Holgersson, J.-I. Flock, The extracellular adherence protein from *Staphylococcus aureus* inhibits neutrophil binding to endothelial cells, Infection and immunity 72(10) (2004) 6164-6167.

[270] I. Jongerius, J. Köhl, M.K. Pandey, M. Ruyken, K.P. van Kessel, J.A. van Strijp, S.H. Rooijakkers, Staphylococcal complement evasion by various convertase-blocking molecules, Journal of Experimental Medicine 204(10) (2007) 2461-2471.

[271] I. Jongerius, M. Puister, J. Wu, M. Ruyken, J.A. van Strijp, S.H. Rooijakkers, Staphylococcal complement inhibitor modulates phagocyte responses by dimerization of convertases, The journal of immunology 184(1) (2010) 420-425.

[272] K. O'Riordan, J.C. Lee, *Staphylococcus aureus* capsular polysaccharides, Clinical microbiology reviews 17(1) (2004) 218-234.

[273] C. Prat, J. Bestebroer, C.J. de Haas, J.A. van Strijp, K.P. van Kessel, A new staphylococcal anti-inflammatory protein that antagonizes the formyl peptide receptor-like 1, The Journal of Immunology 177(11) (2006) 8017-8026.

[274] M.K. Sandel, J.L. McKillip, Virulence and recovery of *Staphylococcus aureus* relevant to the food industry using improvements on traditional approaches, Food Control 15(1) (2004) 5-10.

[275] A.L. Cheung, V.A. Fischetti, The role of fibrinogen in staphylococcal adherence to catheters in vitro, Journal of Infectious Diseases 161(6) (1990) 1177-1186.

[276] P. François, P. Vaudaux, T.J. Foster, D.P. Lew, Host-bacteria interactions in foreign body infections, Infection Control & Hospital Epidemiology 17(8) (1996) 514-520.

[277] R. Arya, S.A. Princy, Exploration of modulated genetic circuits governing virulence determinants in *Staphylococcus aureus*, Indian journal of microbiology 56(1) (2016) 19-27.

[278] A. Resch, R. Rosenstein, C. Nerz, F. Götz, Differential gene expression profiling of *Staphylococcus aureus* cultivated under biofilm and planktonic conditions, Applied and environmental microbiology 71(5) (2005) 2663-2676.

[279] M.C.B. Ammons, B.P. Tripet, R.P. Carlson, K.R. Kirker, M.A. Gross, J.J. Stanisich, V.r. Copié, Quantitative NMR metabolite profiling of methicillin-resistant and methicillin-susceptible *Staphylococcus aureus* discriminates between biofilm and planktonic phenotypes, Journal of proteome research 13(6) (2014) 2973-2985.

[280] B. Zhang, R. Powers, Analysis of bacterial biofilms using NMR-based metabolomics, Future medicinal chemistry 4(10) (2012) 1273-1306.

[281] S. Rachid, K. Ohlsen, U. Wallner, J. Hacker, M. Hecker, W. Ziebuhr, Alternative Transcription Factor ϛB Is Involved in Regulation of Biofilm Expression in a *Staphylococcus aureus*Mucosal Isolate, Journal of bacteriology 182(23) (2000) 6824-6826.

[282] J.M. Yarwood, D.J. Bartels, E.M. Volper, E.P. Greenberg, Quorum sensing in *Staphylococcus aureus* biofilms, Journal of bacteriology 186(6) (2004) 1838-1850.

[283] Y. Zhu, E.C. Weiss, M. Otto, P.D. Fey, M.S. Smeltzer, G.A. Somerville, *Staphylococcus aureus* biofilm metabolism and the influence of arginine on polysaccharide intercellular adhesin synthesis, biofilm formation, and pathogenesis, Infection and immunity 75(9) (2007) 4219-4226.

[284] D.R. Cue, M.G. Lei, C. Lee, Genetic regulation of the intercellular adhesion locus in staphylococci, Frontiers in cellular and infection microbiology 2 (2012) 38.

[285] D. Cue, M.G. Lei, T.T. Luong, L. Kuechenmeister, P.M. Dunman, S. O'Donnell, S. Rowe, J.P. O'Gara, C.Y. Lee, Rbf promotes biofilm formation by *Staphylococcus aureus* via repression of icaR, a negative regulator of icaADBC, Journal of bacteriology 191(20) (2009) 6363-6373.

[286] Y. Lim, M. Jana, T.T. Luong, C.Y. Lee, Control of glucose-and NaCl-induced biofilm formation by rbf in *Staphylococcus aureus*, Journal of bacteriology 186(3) (2004) 722-729.

[287] G. Ji, R. Beavis, R.P. Novick, Bacterial interference caused by autoinducing peptide variants, Science 276(5321) (1997) 2027-2030.

[288] B.R. Boles, A.R. Horswill, Agr-mediated dispersal of *Staphylococcus aureus* biofilms, PLoS Pathog 4(4) (2008) e1000052.

[289] R.L. Koenig, J.L. Ray, S.J. Maleki, M.S. Smeltzer, B.K. Hurlburt, *Staphylococcus aureus* AgrA binding to the RNAIII-agr regulatory region, Journal of bacteriology 186(22) (2004) 7549-7555.

[290] E. Geisinger, R.P. Adhikari, R. Jin, H.F. Ross, R.P. Novick, Inhibition of rot translation by RNAIII, a key feature of agr function, Molecular microbiology 61(4) (2006) 1038-1048.

[291] P.á. Dunman, E. Murphy, S. Haney, D. Palacios, G. Tucker-Kellogg, S. Wu, E. Brown, R. Zagursky, D. Shlaes, S. Projan, Transcription Profiling-Based Identification of*Staphylococcus aureus* Genes Regulated by the agrand/or sarA Loci, Journal of bacteriology 183(24) (2001) 7341-7353.

[292] S. Periasamy, H.-S. Joo, A.C. Duong, T.-H.L. Bach, V.Y. Tan, S.S. Chatterjee, G.Y. Cheung, M. Otto, How *Staphylococcus aureus* biofilms develop their characteristic structure, Proceedings of the National Academy of Sciences 109(4) (2012) 1281-1286.

[293] J.M. Mootz, C.L. Malone, L.N. Shaw, A.R. Horswill, Staphopains modulate *Staphylococcus aureus* biofilm integrity, Infection and immunity (2013) IAI. 00377-13.

[294] J.M. Mootz, M.A. Benson, C.E. Heim, H.A. Crosby, J.S. Kavanaugh, P.M. Dunman, T. Kielian, V.J. Torres, A.R. Horswill, R ot is a key regulator of *Staphylococcus aureus* biofilm formation, Molecular microbiology 96(2) (2015) 388-404.

[295] H.-Y. Hsieh, C.W. Tseng, G.C. Stewart, Regulation of Rot expression in *Staphylococcus aureus*, Journal of bacteriology 190(2) (2008) 546-554.

[296] L.B. Regassa, R.P. Novick, M.J. Betley, Glucose and nonmaintained pH decrease expression of the accessory gene regulator (agr) in *Staphylococcus aureus*, Infection and immunity 60(8) (1992) 3381-3388.

[297] J.M. Yarwood, J.K. McCormick, M.L. Paustian, V. Kapur, P.M. Schlievert, Repression of the *Staphylococcus aureus* accessory gene regulator in serum and in vivo, Journal of bacteriology 184(4) (2002) 1095-1101.

[298] P.R. Hall, B.O. Elmore, C.H. Spang, S.M. Alexander, B.C. Manifold-Wheeler, M.J. Castleman, S.M. Daly, M.M. Peterson, E.K. Sully, J.K. Femling, Nox2 modification of LDL is essential for optimal apolipoprotein B-mediated control of agr type III *Staphylococcus aureus* quorum-sensing, PLoS pathogens 9(2) (2013) e1003166.

[299] M.M. Peterson, J.L. Mack, P.R. Hall, A.A. Alsup, S.M. Alexander, E.K. Sully, Y.S. Sawires, A.L. Cheung, M. Otto, H.D. Gresham, Apolipoprotein B is an innate barrier against invasive *Staphylococcus aureus* infection, Cell host & microbe 4(6) (2008) 555-566.

[300] M. Pynnonen, R.E. Stephenson, K. Schwartz, M. Hernandez, B.R. Boles, Hemoglobin promotes *Staphylococcus aureus* nasal colonization, PLoS pathogens 7(7) (2011) e1002104.

[301] A.K. Syed, S. Ghosh, N.G. Love, B.R. Boles, Triclosan promotes *Staphylococcus aureus* nasal colonization, MBio 5(2) (2014) e01015-13.

[302] C. Goerke, S. Campana, M.G. Bayer, G. Döring, K. Botzenhart, C. Wolz, Direct Quantitative Transcript Analysis of theagr Regulon of *Staphylococcus aureus* during Human Infection in Comparison to the Expression Profile In Vitro, Infection and immunity 68(3) (2000) 1304-1311.

[303] C. Goerke, C. Wolz, Regulatory and genomic plasticity of *Staphylococcus aureus* during persistent colonization and infection, International journal of medical microbiology 294(2-3) (2004) 195-202.

[304] C. Goerke, C. Wolz, Adaptation of *Staphylococcus aureus* to the cystic fibrosis lung, International Journal of Medical Microbiology 300(8) (2010) 520-525.

[305] S.M. Daly, B.O. Elmore, J.S. Kavanaugh, K.D. Triplett, M. Figueroa, H.A. Raja, T. El-Elimat, H.A. Crosby, J.K. Femling, N.B. Cech, ω-Hydroxyemodin limits *Staphylococcus aureus* quorum sensing-mediated pathogenesis and inflammation, Antimicrobial agents and chemotherapy (2015) AAC. 04564-14.

[306] E.K. Sully, N. Malachowa, B.O. Elmore, S.M. Alexander, J.K. Femling, B.M. Gray, F.R. DeLeo, M. Otto, A.L. Cheung, B.S. Edwards, Selective chemical inhibition of agr quorum sensing in *Staphylococcus aureus* promotes host defense with minimal impact on resistance, PLoS pathogens 10(6) (2014) e1004174.

[307] N.B. Cech, A.R. Horswill, Small-molecule quorum quenchers to prevent *Staphylococcus aureus* infection, Future microbiology 8(12) (2013) 1511-1514.

[308] A.K. Zielinska, K.E. Beenken, L.N. Mrak, H.J. Spencer, G.R. Post, R.A. Skinner, A.J. Tackett, A.R. Horswill, M.S. Smeltzer, sarA-mediated repression of protease production plays a key role in the pathogenesis of *Staphylococcus aureus* USA 300 isolates, Molecular microbiology 86(5) (2012) 1183-1196.

[309] K.E. Beenken, J.S. Blevins, M.S. Smeltzer, Mutation of sarA in *Staphylococcus aureus* limits biofilm formation, Infection and immunity 71(7) (2003) 4206-4211.

[310] J. Valle, A. Toledo-Arana, C. Berasain, J.M. Ghigo, B. Amorena, J.R. Penadés, I. Lasa, SarA and not σB is essential for biofilm development by *Staphylococcus aureus*, Molecular microbiology 48(4) (2003) 1075-1087.

[311] J.N. Snowden, M. Beaver, K. Beenken, M. Smeltzer, A.R. Horswill, T. Kielian, *Staphylococcus aureus* sarA regulates inflammation and colonization during central nervous system biofilm formation, PloS one 8(12) (2013) e84089.

[312] M.P. Trotonda, A.C. Manna, A.L. Cheung, I. Lasa, J.R. Penadés, SarA positively controls bap-dependent biofilm formation in *Staphylococcus aureus*, Journal of bacteriology 187(16) (2005) 5790-5798.

[313] W.C. Chan, B.J. Coyle, P. Williams, Virulence Regulation and Quorum Sensing in Staphylococcal Infections: Competitive AgrC Antagonists as Quorum Sensing Inhibitors §, Journal of medicinal chemistry 47(19) (2004) 4633-4641.

[314] A.F. Gillaspy, C.Y. Lee, S. Sau, A.L. Cheung, M.S. Smeltzer, Factors Affecting the Collagen Binding Capacity of *Staphylococcus aureus*, Infection and immunity 66(7) (1998) 3170-3178.

[315] J.S. Blevins, A.F. Gillaspy, T.M. Rechtin, B.K. Hurlburt, M.S. Smeltzer, The staphylococcal accessory regulator (sar) represses transcription of the *Staphylococcus aureus* collagen adhesin gene (cna) in an agr-independent manner, Molecular microbiology 33(2) (1999) 317-326.

[316] I. Kullik, P. Giachino, The alternative sigma factor σB in *Staphylococcus aureus*: regulation of the sigB operon in response to growth phase and heat shock, Archives of microbiology 167(2-3) (1997) 151-159.

[317] J. Pané-Farré, B. Jonas, K. Förstner, S. Engelmann, M. Hecker, The σ B regulon in *Staphylococcus aureus* and its regulation, International journal of medical microbiology 296(4) (2006) 237-258.

[318] K.M. Conlon, H. Humphreys, J.P. O'Gara, icaR encodes a transcriptional repressor involved in environmental regulation of ica operon expression and biofilm formation in *Staphylococcus epidermidis*, Journal of bacteriology 184(16) (2002) 4400-4408.

[319] J.K.-M. Knobloch, S. Jäger, M.A. Horstkotte, H. Rohde, D. Mack, RsbU-dependent regulation of *Staphylococcus epidermidis* biofilm formation is mediated via the alternative sigma factor σB by repression of the negative regulator gene icaR, Infection and immunity 72(7) (2004) 3838-3848.

[320] S.P. Nair, M. Bischoff, M.M. Senn, B. Berger-Bächi, The σB regulon influences internalization of *Staphylococcus aureus* by osteoblasts, Infection and immunity 71(7) (2003) 4167-4170.

[321] R. Nicholas, T. Li, D. McDevitt, A. Marra, S. Sucoloski, P. Demarsh, D. Gentry, Isolation and Characterization of a sigBDeletion Mutant of *Staphylococcus aureus*, Infection and immunity 67(7) (1999) 3667-3669.

[322] J.L. Lister, A.R. Horswill, *Staphylococcus aureus* biofilms: recent developments in biofilm dispersal, Frontiers in cellular and infection microbiology 4 (2014) 178.

[323] A. Khemiri, T. Jouenne, P. Cosette, Proteomics dedicated to biofilmology: what have we learned from a decade of research?, Medical microbiology and immunology 205(1) (2016) 1-19.

[324] A. Rani, S. Babu, Environmental proteomic studies: closer step to understand bacterial biofilms, World Journal of Microbiology and Biotechnology 34(8) (2018) 120.

[325] A. Resch, S. Leicht, M. Saric, L. Pásztor, A. Jakob, F. Götz, A. Nordheim, Comparative proteome analysis of *Staphylococcus aureus* biofilm and planktonic cells and correlation with transcriptome profiling, Proteomics 6(6) (2006) 1867-1877.

[326] J. Chew, P.S. Zilm, J.M. Fuss, N.J. Gully, A proteomic investigation of *Fusobacterium nucleatum* alkaline-induced biofilms, BMC Microbiology 12(1) (2012) 189.

[327] S.S. Atshan, M.N. Shamsudin, Z. Sekawi, L.T.T. Lung, F. Barantalab, Y.K. Liew, M.A. Alreshidi, S.A. Abduljaleel, R.A. Hamat, Comparative proteomic analysis of extracellular proteins expressed by various clonal types of *Staphylococcus aureus* and during planktonic growth and biofilm development, Frontiers in microbiology 6 (2015).

[328] A. Collet, P. Cosette, C. Beloin, J.-M. Ghigo, C. Rihouey, P. Lerouge, G.-A. Junter, T. Jouenne, Impact of rpoS deletion on the proteome of *Escherichia coli* grown planktonically and as biofilm, Journal of proteome research 7(11) (2008) 4659-4669.

[329] A. Lourenço, A. de Las Heras, M. Scortti, J. Vazquez-Boland, J.F. Frank, L. Brito, Comparison of Listeria monocytogenes exoproteomes from biofilm and planktonic state: Lmo2504, a protein associated with biofilms, Appl. Environ. Microbiol. 79(19) (2013) 6075-6082.

[330] Y. Wang, L. Yi, Z. Wu, J. Shao, G. Liu, H. Fan, W. Zhang, C. Lu, Comparative proteomic analysis of Streptococcus suis biofilms and planktonic cells that identified biofilm infection-related immunogenic proteins, PLoS One 7(4) (2012) e33371.

[331] T. van Alen, H. Claus, R.P. Zahedi, J. Groh, H. Blazyca, M. Lappann, A. Sickmann, U. Vogel, Comparative proteomic analysis of biofilm and planktonic cells of *Neisseria meningitidis*, Proteomics 10(24) (2010) 4512-4521.

[332] M.S. Silva, A.A. De Souza, M.A. Takita, C.A. Labate, M.A. Machado, Analysis of the biofilm proteome of *Xylella fastidiosa*, Proteome science 9(1) (2011) 58.

[333] M.E. Clark, Z. He, A.M. Redding, M.P. Joachimiak, J.D. Keasling, J.Z. Zhou, A.P. Arkin, A. Mukhopadhyay, M.W. Fields, Transcriptomic and proteomic analyses of Desulfovibrio vulgaris biofilms: carbon and energy flow contribute to the distinct biofilm growth state, BMC genomics 13(1) (2012) 138.

[334] W.M. da Silva, J. Bei, N. Amigo, P. Valacco, A.F. Amadio, Q. Zhang, X. Wu, M. Larzábal, Z. Chen, A. Cataldi, Quantification of Enterohemorrhagic *Escherichia coli* O157: H7 proteome using TMT-Based Analysis, bioRxiv (2018) 312652.

[335] J.A. Paulo, J.D. O'Connell, R.A. Everley, J. O'Brien, M.A. Gygi, S.P. Gygi, Quantitative mass spectrometry-based multiplexing compares the abundance of 5000 S. cerevisiae proteins across 10 carbon sources, Journal of proteomics 148 (2016) 85-93.

[336] S.J. Emery, M. Mirzaei, D. Vuong, D. Pascovici, J.M. Chick, E. Lacey, P.A. Haynes, Induction of virulence factors in Giardia duodenalis independent of host attachment, Scientific reports 6 (2016) 20765.

[337] Z. Li, R.M. Adams, K. Chourey, G.B. Hurst, R.L. Hettich, C. Pan, Systematic comparison of label-free, metabolic labeling, and isobaric chemical labeling for quantitative proteomics on LTQ Orbitrap Velos, Journal of proteome research 11(3) (2012) 1582-1590.

[338] J.A. Paulo, M.P. Jedrychowski, E.T. Chouchani, L. Kazak, S.P. Gygi, Multiplexed isobaric tag-based profiling of seven murine tissues following in vivo nicotine treatment using a minimalistic proteomics strategy, Proteomics 18(10) (2018) 1700326.

[339] N.C. Soares, G. Bou, J.M. Blackburn, Editorial: Proteomics of Microbial Human Pathogens, Frontiers in Microbiology 7(1742) (2016).

[340] A. Otto, J.M. van Dijl, M. Hecker, D. Becher, The *Staphylococcus aureus* proteome, International Journal of Medical Microbiology 304(2) (2014) 110-120.

[341] N. Islam, Y. Kim, J.M. Ross, M.R. Marten, Proteomic analysis of *Staphylococcus aureus* biofilm cells grown under physiologically relevant fluid shear stress conditions, Proteome science 12(1) (2014) 21.

[342] M. Moche, R. Schlüter, J.r. Bernhardt, K. Plate, K. Riedel, M. Hecker, D.r. Becher, Time-resolved analysis of cytosolic and surface-associated proteins of *Staphylococcus aureus* HG001 under planktonic and biofilm conditions, Journal of proteome research 14(9) (2015) 3804-3822.

[343] P. Ymele-Leki, J.M. Ross, Erosion from *Staphylococcus aureus* biofilms grown under physiologically relevant fluid shear forces yields bacterial cells with reduced avidity to collagen, Applied and environmental microbiology 73(6) (2007) 1834-1841.

[344] L. Foulston, A.K. Elsholz, A.S. DeFrancesco, R. Losick, The extracellular matrix of *Staphylococcus aureus* biofilms comprises cytoplasmic proteins that associate with the cell surface in response to decreasing pH, MBio 5(5) (2014) e01667-14.

[345] M.G. Lei, R.K. Gupta, C.Y. Lee, Proteomics of *Staphylococcus aureus* biofilm matrix in a rat model of orthopedic implant-associated infection, PloS one 12(11) (2017) e0187981.

[346] P. Turner, A. McLennan, A. Bates, M. White, Molecular Biology (Third Edition), Taylor & Francis Group, UK, 2005.

[347] M. Slany, J. Oppelt, L. Cincarova, Formation of *Staphylococcus aureus* biofilm in the presence of sub-lethal concentrations of disinfectants: a transcriptomic analysis using RNA-seq, Applied and environmental microbiology (2017) AEM. 01643-17.

[348] J. Liu, L. Yang, Y. Hou, T. Soteyome, B. Zeng, J. Su, L. Li, B. Li, D. Chen, Y. Li, Transcriptomics study on *Staphylococcus aureus* biofilm under low concentration of ampicillin, Frontiers in microbiology 9 (2018).

[349] O. Soutourina, O. Poupel, J.Y. Coppée, A. Danchin, T. Msadek, I. Martin-Verstraete, CymR, the master regulator of cysteine metabolism in *Staphylococcus aureus*, controls host sulphur source utilization and plays a role in biofilm formation, Molecular microbiology 73(2) (2009) 194-211.

[350] S.P. Tse, M. Beauchemin, D. Morse, S.C. Lo, Refining Transcriptome Gene Catalogs by MS-Validation of Expressed Proteins, Proteomics 18(1) (2018) 1700271.

[351] M. Pernemalm, J. Lehtiö, Mass spectrometry-based plasma proteomics: state of the art and future outlook, Expert review of proteomics 11(4) (2014) 431-448.

[352] M. Harel, P. Oren-Giladi, O. Kaidar-Person, Y. Shaked, T. Geiger, Proteomics of microparticles with SILAC Quantification (PROMIS-Quan): a novel proteomic method for plasma biomarker quantification, Molecular & Cellular Proteomics 14(4) (2015) 1127-1136.

[353] S. Lv, L. Wei, J.-h. Wang, J.-y. Wang, F. Liu, Identification of novel molecular candidates for acute liver failure in plasma of BALB/c murine model, Journal of proteome research 6(7) (2007) 2746-2752.

[354] I. Rehman, C.A. Evans, A. Glen, S.S. Cross, C.L. Eaton, J. Down, G. Pesce, J.T. Phillips, O.S. Yen, G.N. Thalmann, iTRAQ identification of candidate serum biomarkers associated with metastatic progression of human prostate cancer, PloS one 7(2) (2012) e30885.

[355] S. Ray, S.K. Patel, V. Kumar, J. Damahe, S. Srivastava, Differential expression of serum/plasma proteins in various infectious diseases: specific or nonspecific signatures, PROTEOMICS–Clinical Applications 8(1-2) (2014) 53-72.

[356] K. Gouthamchandra, A. Kumar, S. Shwetha, A. Mukherjee, M. Chandra, B. Ravishankar, M. Khaja, P.C. Sadhukhan, S. Das, Serum proteomics of hepatitis C virus infection reveals retinol-binding protein 4 as a novel regulator, Journal of General Virology 95(8) (2014) 1654-1667.

[357] T. Köcher, P. Pichler, M. Schutzbier, C. Stingl, A. Kaul, N. Teucher, G. Hasenfuss, J.M. Penninger, K. Mechtler, High precision quantitative proteomics using iTRAQ on an LTQ Orbitrap: a new mass spectrometric method combining the benefits of all, Journal of proteome research 8(10) (2009) 4743-4752.

[358] P. Pichler, T. Köcher, J. Holzmann, T. Möhring, G. Ammerer, K. Mechtler, Improved precision of iTRAQ and TMT quantification by an axial extraction field in an Orbitrap HCD cell, Analytical chemistry 83(4) (2011) 1469-1474.

[359] A. Venkatesh, C. Gil, M. Fuentes, J. LaBaer, S. Srivastava, A Perspective on Proteomics of Infectious Diseases, PROTEOMICS–Clinical Applications 12(4) (2018) 1700139.

[360] N. Zhou, K. Wang, S. Fang, X. Zhao, T. Huang, H. Chen, F. Yan, Y. Tang, H. Zhou, J. Zhu, Discovery of a potential plasma protein biomarker panel for acute-on-chronic liver failure induced by Hepatitis B Virus, Frontiers in physiology 8 (2017) 1009.

[361] P. Kuusela, M. Saraswat, S. Joenväärä, J. Kaartinen, A. Järvinen, R. Renkonen, Changes in plasma protein levels as an early indication of a bloodstream infection, PloS one 12(2) (2017) e0172987.

[362] J. Li, L. Sun, F. Xu, J. Xiao, W. Jiao, H. Qi, C. Shen, A. Shen, Characterization of plasma proteins in children of different Mycobacterium tuberculosis infection status using label-free quantitative proteomics, Oncotarget 8(61) (2017) 103290.

[363] A. Kumar, S. Singh, S.K. Ahirwar, G. Nath, Proteomics-based identification of plasma proteins and their association with the host–pathogen interaction in chronic typhoid carriers, International Journal of Infectious Diseases 19 (2014) 59-66.

[364] C. Mölleken, B. Sitek, C. Henkel, G. Poschmann, B. Sipos, S. Wiese, B. Warscheid, C. Broelsch, M. Reiser, S.L. Friedman, Detection of novel biomarkers of liver cirrhosis by proteomic analysis, Hepatology 49(4) (2009) 1257-1266.

[365] T. Li, B. Zheng, Z. Huang, H. Lu, Q. Lin, Z. Liao, Z. Lin, L. Zhao, X. Wang, J. Gu, Over-expression of talin 1 and integrin-linked kinase in PBMCs of patients with ankylosing spondylitis: a proteomic study, Clinical and Experimental Rheumatology-Incl Supplements 28(6) (2010) 828.

[366] M.M. Youns, W. Abdel, H.A. Abdel, Z.A. Hassan, M.S. Attia, Serum talin-1 is a potential novel biomarker for diagnosis of hepatocellular carcinoma in Egyptian patients, Asian Pacific journal of cancer prevention 14(6) (2013) 3819-3823.

[367] J. Khoontawad, C. Pairojkul, R. Rucksaken, P. Pinlaor, C. Wongkham, P. Yongvanit, A. Pugkhem, A. Jones, J. Plieskatt, J. Potriquet, Differential protein expression marks the transition from infection with Opisthorchis viverrini to cholangiocarcinoma, Molecular & Cellular Proteomics 16(5) (2017) 911-923.

[368] M. Prucha, I. Herold, R. Zazula, L. Dubska, M. Dostal, T. Hildebrand, J. Hyanek, Significance of lipopolysaccharide-binding protein (an acute phase protein) in monitoring critically ill patients, Critical Care 7(6) (2003) R154.

[369] J. Zweigner, H.-J. Gramm, O.C. Singer, K. Wegscheider, R.R. Schumann, High concentrations of lipopolysaccharide-binding protein in serum of patients with severe sepsis or

septic shock inhibit the lipopolysaccharide response in human monocytes, Blood 98(13) (2001) 3800-3808.

[370] H.-C. Nien, S.-J. Hsu, T.-H. Su, P.-J. Yang, J.-C. Sheu, J.-T. Wang, L.-P. Chow, C.-L. Chen, J.-H. Kao, W.-S. Yang, High serum lipopolysaccharide-binding protein level in chronic hepatitis C viral infection is reduced by anti-viral treatments, PloS one 12(1) (2017) e0170028.

[371] S.M. Opal, P.J. Scannon, J.-L. Vincent, M. White, S.F. Carroll, J.E. Palardy, N.A. Parejo, J.P. Pribble, J.H. Lemke, Relationship between plasma levels of lipopolysaccharide (LPS) and LPS-binding protein in patients with severe sepsis and septic shock, The Journal of infectious diseases 180(5) (1999) 1584-1589.

[372] C. Brănescu, D. Şerban, C. Şavlovschi, A. Dascălu, A. Kraft, Lipopolysaccharide binding protein (LBP)–an inflammatory marker of prognosis in the acute appendicitis, Journal of medicine and life 5(3) (2012) 342.

[373] B. Aslam, M. Basit, M.A. Nisar, M. Khurshid, M.H. Rasool, Proteomics: technologies and their applications, Journal of chromatographic science 55(2) (2017) 182-196.

[374] C. Bruce, K. Stone, E. Gulcicek, K. Williams, Proteomics and the analysis of proteomic data: 2013 overview of current protein-profiling technologies, Current protocols in bioinformatics 41(1) (2013) 13.21. 1-13.21. 17.

[375] A. Doerr, Mass spectrometry–based targeted proteomics, Nature methods 10(1) (2012) 23.

[376] J.P. Savaryn, A.D. Catherman, P.M. Thomas, M.M. Abecassis, N.L. Kelleher, The emergence of top-down proteomics in clinical research, Genome medicine 5(6) (2013) 53.

[377] N.A. Kulak, G. Pichler, I. Paron, N. Nagaraj, M. Mann, Minimal, encapsulated proteomic-sample processing applied to copy-number estimation in eukaryotic cells, Nature methods 11(3) (2014) 319.

[378] S.-E. Ong, L.J. Foster, M. Mann, Mass spectrometric-based approaches in quantitative proteomics, Methods 29(2) (2003) 124-130.

[379] T. Glatter, C. Ludwig, E. Ahrné, R. Aebersold, A.J. Heck, A. Schmidt, Large-scale quantitative assessment of different in-solution protein digestion protocols reveals superior cleavage efficiency of tandem Lys-C/trypsin proteolysis over trypsin digestion, Journal of proteome research 11(11) (2012) 5145-5156.

[380] D.L. Swaney, C.D. Wenger, J.J. Coon, Value of using multiple proteases for large-scale mass spectrometry-based proteomics, Journal of proteome research 9(3) (2010) 1323-1329.

[381] E. Mostovenko, C. Hassan, J. Rattke, A.M. Deelder, P.A. van Veelen, M. Palmblad, Comparison of peptide and protein fractionation methods in proteomics, EuPA Open Proteomics 1 (2013) 30-37.

[382] T.M. Annesley, Ion suppression in mass spectrometry, Clinical chemistry 49(7) (2003) 1041-1044.

[383] R. Matthiesen, J. Bunkenborg, Introduction to mass spectrometry-based proteomics, Mass spectrometry data analysis in proteomics, Springer2013, pp. 1-45.

[384] C. Choudhary, M. Mann, Decoding signalling networks by mass spectrometry-based proteomics, Nature reviews Molecular cell biology 11(6) (2010) 427-439.

[385] M.J. Schroeder, J. Shabanowitz, J.C. Schwartz, D.F. Hunt, J.J. Coon, A neutral loss activation method for improved phosphopeptide sequence analysis by quadrupole ion trap mass spectrometry, Analytical chemistry 76(13) (2004) 3590-3598.

[386] L.M. Mikesh, B. Ueberheide, A. Chi, J.J. Coon, J.E. Syka, J. Shabanowitz, D.F. Hunt, The utility of ETD mass spectrometry in proteomic analysis, Biochimica et Biophysica Acta (BBA)-Proteins and Proteomics 1764(12) (2006) 1811-1822.

[387] R.A. Zubarev, D.M. Horn, E.K. Fridriksson, N.L. Kelleher, N.A. Kruger, M.A. Lewis, B.K. Carpenter, F.W. McLafferty, Electron capture dissociation for structural characterization of multiply charged protein cations, Analytical chemistry 72(3) (2000) 563-573.

[388] J.E. Syka, J.A. Marto, D.L. Bai, S. Horning, M.W. Senko, J.C. Schwartz, B. Ueberheide, B. Garcia, S. Busby, T. Muratore, Novel linear quadrupole ion trap/FT mass spectrometer: performance characterization and use in the comparative analysis of histone H3 post-translational modifications, Journal of proteome research 3(3) (2004) 621-626.

[389] J.V. Olsen, B. Macek, O. Lange, A. Makarov, S. Horning, M. Mann, Higher-energy C-trap dissociation for peptide modification analysis, Nature methods 4(9) (2007) 709-712.

[390] T. Pekar Second, J.D. Blethrow, J.C. Schwartz, G.E. Merrihew, M.J. MacCoss, D.L. Swaney, J.D. Russell, J.J. Coon, V. Zabrouskov, Dual-pressure linear ion trap mass spectrometer improving the analysis of complex protein mixtures, Analytical chemistry 81(18) (2009) 7757-7765.

[391] L.R. Snyder, J.J. Kirkland, J.W. Dolan, Introduction to modern liquid chromatography, John Wiley & Sons2011.

[392] A.B. Kanu, P. Dwivedi, M. Tam, L. Matz, H.H. Hill Jr, Ion mobility–mass spectrometry, Journal of mass spectrometry 43(1) (2008) 1-22.

[393] A. Michalski, E. Damoc, J.-P. Hauschild, O. Lange, A. Wieghaus, A. Makarov, N. Nagaraj, J. Cox, M. Mann, S. Horning, Mass spectrometry-based proteomics using Q Exactive, a high-performance benchtop quadrupole Orbitrap mass spectrometer, Molecular & Cellular Proteomics 10(9) (2011).

[394] M. Hardman, A.A. Makarov, Interfacing the orbitrap mass analyzer to an electrospray ion source, Analytical chemistry 75(7) (2003) 1699-1705.

[395] M. Scigelova, A. Makarov, Orbitrap mass analyzer–overview and applications in proteomics, Proteomics 6(S2) (2006) 16-21.

[396] A. Makarov, Electrostatic axially harmonic orbital trapping: a high-performance technique of mass analysis, Analytical chemistry 72(6) (2000) 1156-1162.

[397] A. Makarov, E. Denisov, A. Kholomeev, W. Balschun, O. Lange, K. Strupat, S. Horning, Performance evaluation of a hybrid linear ion trap/orbitrap mass spectrometer, Analytical chemistry 78(7) (2006) 2113-2120.

[398] J.V. Olsen, J.C. Schwartz, J. Griep-Raming, M.L. Nielsen, E. Damoc, E. Denisov, O. Lange, P. Remes, D. Taylor, M. Splendore, A dual pressure linear ion trap Orbitrap instrument with very high sequencing speed, Molecular & cellular proteomics 8(12) (2009) 2759-2769.

[399] P. Sinitcyn, J.D. Rudolph, J. Cox, Computational methods for understanding mass spectrometry–based shotgun proteomics data, Annual Review of Biomedical Data Science 1 (2018) 207-234.

[400] M.M. Savitski, M. Wilhelm, H. Hahne, B. Kuster, M. Bantscheff, A scalable approach for protein false discovery rate estimation in large proteomic data sets, Molecular & Cellular Proteomics 14(9) (2015) 2394-2404.

[401] D.N. Perkins, D.J. Pappin, D.M. Creasy, J.S. Cottrell, Probability-based protein identification by searching sequence databases using mass spectrometry data, ELECTROPHORESIS: An International Journal 20(18) (1999) 3551-3567.

[402] J.K. Eng, A.L. McCormack, J.R. Yates, An approach to correlate tandem mass spectral data of peptides with amino acid sequences in a protein database, Journal of the american society for mass spectrometry 5(11) (1994) 976-989.

[403] R. Craig, R.C. Beavis, TANDEM: matching proteins with tandem mass spectra, Bioinformatics 20(9) (2004) 1466-1467.

[404] J. Cox, N. Neuhauser, A. Michalski, R.A. Scheltema, J.V. Olsen, M. Mann, Andromeda: a peptide search engine integrated into the MaxQuant environment, Journal of proteome research 10(4) (2011) 1794-1805.

[405] A.I. Nesvizhskii, R. Aebersold, Interpretation of shotgun proteomic data: the protein inference problem, Molecular & cellular proteomics 4(10) (2005) 1419-1440.

[406] T. Huang, J. Wang, W. Yu, Z. He, Protein inference: a review, Briefings in bioinformatics 13(5) (2012) 586-614.

[407] L. Reiter, M. Claassen, S.P. Schrimpf, M. Jovanovic, A. Schmidt, J.M. Buhmann, M.O. Hengartner, R. Aebersold, Protein identification false discovery rates for very large proteomics data sets generated by tandem mass spectrometry, Molecular & Cellular Proteomics 8(11) (2009) 2405-2417.

[408] N. Rauniyar, J.R. Yates III, Isobaric labeling-based relative quantification in shotgun proteomics, Journal of proteome research 13(12) (2014) 5293-5309.

[409] A.J. Heck, J. Krijgsveld, Mass spectrometry-based quantitative proteomics, Expert review of proteomics 1(3) (2004) 317-326.

[410] S.-E. Ong, M. Mann, Mass spectrometry–based proteomics turns quantitative, Nature chemical biology 1(5) (2005) 252-262.

[411] S. Wiese, K.A. Reidegeld, H.E. Meyer, B. Warscheid, Protein labeling by iTRAQ: a new tool for quantitative mass spectrometry in proteome research, Proteomics 7(3) (2007) 340-350.

[412] A. Thompson, J. Schäfer, K. Kuhn, S. Kienle, J. Schwarz, G. Schmidt, T. Neumann, C. Hamon, Tandem mass tags: a novel quantification strategy for comparative analysis of complex protein mixtures by MS/MS, Analytical chemistry 75(8) (2003) 1895-1904.

[413] P.J. Boersema, R. Raijmakers, S. Lemeer, S. Mohammed, A.J. Heck, Multiplex peptide stable isotope dimethyl labeling for quantitative proteomics, Nature protocols 4(4) (2009) 484.

[414] S.-E. Ong, B. Blagoev, I. Kratchmarova, D.B. Kristensen, H. Steen, A. Pandey, M. Mann, Stable isotope labeling by amino acids in cell culture, SILAC, as a simple and accurate approach to expression proteomics, Molecular & cellular proteomics 1(5) (2002) 376-386.

[415] T. Werner, I. Becher, G. Sweetman, C. Doce, M.M. Savitski, M. Bantscheff, High-resolution enabled TMT 8-plexing, Analytical chemistry 84(16) (2012) 7188-7194.

[416] A.M. Altelaar, C.K. Frese, C. Preisinger, M.L. Hennrich, A.W. Schram, H.T.M. Timmers, A.J. Heck, S. Mohammed, Benchmarking stable isotope labeling based quantitative proteomics, Journal of proteomics 88 (2013) 14-26.

[417] S.Y. Ow, M. Salim, J. Noirel, C. Evans, P.C. Wright, Minimising iTRAQ ratio compression through understanding LC-MS elution dependence and high-resolution HILIC fractionation, Proteomics 11(11) (2011) 2341-2346.

[418] L.V. DeSouza, J. Grigull, S. Ghanny, V. Dubé, A.D. Romaschin, T.J. Colgan, K.M. Siu, Endometrial carcinoma biomarker discovery and verification using differentially tagged clinical samples with multidimensional liquid chromatography and tandem mass spectrometry, Molecular & cellular proteomics 6(7) (2007) 1170-1182.

[419] Y. Ma, T. Xiao, Q. Xu, X. Shao, H. Wang, iTRAQ-based quantitative analysis of cancer-derived secretory proteome reveals TPM2 as a potential diagnostic biomarker of colorectal cancer, Frontiers of medicine 10(3) (2016) 278-285.

[420] Q.-L. Xin, C.-L. Deng, X. Chen, J. Wang, S.-B. Wang, W. Wang, F. Deng, B. Zhang, G. Xiao, L.-K. Zhang, Quantitative proteomic analysis of mosquito C6/36 cells reveals host proteins involved in Zika virus infection, Journal of virology (2017) JVI. 00554-17.

[421] G.C. McAlister, E.L. Huttlin, W. Haas, L. Ting, M.P. Jedrychowski, J.C. Rogers, K. Kuhn, I. Pike, R.A. Grothe, J.D. Blethrow, Increasing the multiplexing capacity of TMTs using reporter ion isotopologues with isobaric masses, Analytical chemistry 84(17) (2012) 7469-7478.

[422] E. Rodríguez-Suárez, A.D. Whetton, The application of quantification techniques in proteomics for biomedical research, Mass spectrometry reviews 32(1) (2013) 1-26.

[423] C.A. Smith, E.J. Want, G. O'Maille, R. Abagyan, G. Siuzdak, XCMS: processing mass spectrometry data for metabolite profiling using nonlinear peak alignment, matching, and identification, Analytical chemistry 78(3) (2006) 779-787.

[424] R.A. Scheltema, A. Jankevics, R.C. Jansen, M.A. Swertz, R. Breitling, PeakML/mzMatch: a file format, Java library, R library, and tool-chain for mass spectrometry data analysis, Analytical chemistry 83(7) (2011) 2786-2793.

[425] A. Schmidt, I. Forne, A. Imhof, Bioinformatic analysis of proteomics data, BMC systems biology 8(2) (2014) S3.

[426] S.P. Wein, R.G. Coˆte, M. Dumousseau, F. Reisinger, H. Hermjakob, J.A. Vizcaíno, Improvements in the protein identifier cross-reference service, Nucleic acids research 40(W1) (2012) W276-W280.

[427] B. Waegele, I. Dunger-Kaltenbach, G. Fobo, C. Montrone, H.-W. Mewes, A. Ruepp, CRONOS: the cross-reference navigation server, Bioinformatics 25(1) (2009) 141-143.

[428] M. Ashburner, C.A. Ball, J.A. Blake, D. Botstein, H. Butler, J.M. Cherry, A.P. Davis, K. Dolinski, S.S. Dwight, J.T. Eppig, Gene ontology: tool for the unification of biology, Nature genetics 25(1) (2000) 25-29.

[429] J. Cox, M. Mann, MaxQuant enables high peptide identification rates, individualized ppb-range mass accuracies and proteome-wide protein quantification, Nature biotechnology 26(12) (2008) 1367-1372.

[430] A. Conesa, S. Götz, J.M. García-Gómez, J. Terol, M. Talón, M. Robles, Blast2GO: a universal tool for annotation, visualization and analysis in functional genomics research, Bioinformatics 21(18) (2005) 3674-3676.

[431] R. Malik, K. Dulla, E.A. Nigg, R. Körner, From proteome lists to biological impact–tools and strategies for the analysis of large MS data sets, Proteomics 10(6) (2010) 1270-1283.

[432] H. Tipney, L. Hunter, An introduction to effective use of enrichment analysis software, Human genomics 4(3) (2010) 202.

[433] M.A. Peabody, M.R. Laird, C. Vlasschaert, R. Lo, F.S. Brinkman, PSORTdb: expanding the bacteria and archaea protein subcellular localization database to better reflect diversity in cell envelope structures, Nucleic acids research 44(D1) (2015) D663-D668.

[434] J.D. Bendtsen, H. Nielsen, G. von Heijne, S. Brunak, Improved prediction of signal peptides: SignalP 3.0, Journal of molecular biology 340(4) (2004) 783-795.

[435] J.D. Bendtsen, L. Kiemer, A. Fausbøll, S. Brunak, Non-classical protein secretion in bacteria, BMC microbiology 5(1) (2005) 58.

[436] O. Emanuelsson, H. Nielsen, S. Brunak, G. Von Heijne, Predicting subcellular localization of proteins based on their N-terminal amino acid sequence, Journal of molecular biology 300(4) (2000) 1005-1016.

[437] C.S. Yu, Y.C. Chen, C.H. Lu, J.K. Hwang, Prediction of protein subcellular localization, Proteins: Structure, Function, and Bioinformatics 64(3) (2006) 643-651.

[438] N. Islam, J.M. Ross, M.R. Marten, Proteome analyses of *Staphylococcus aureus* biofilm at elevated levels of NaCl, Clinical microbiology (Los Angeles, Calif.) 4(5) (2015).

[439] T. Busche, M. Hillion, V. Van Loi, D. Berg, B. Walther, T. Semmler, B. Strommenger, W. Witte, C. Cuny, A. Mellmann, Comparative Secretome Analyses of Human and Zoonotic *Staphylococcus aureus* Isolates CC8, CC22, and CC398, Molecular & Cellular Proteomics 17(12) (2018) 2412-2433.

[440] R.A. Brady, J.G. Leid, A.K. Camper, J.W. Costerton, M.E. Shirtliff, Identification of *Staphylococcus aureus* proteins recognized by the antibody-mediated immune response to a biofilm infection, Infection and immunity 74(6) (2006) 3415-3426.

[441] G. MacBeath, Protein microarrays and proteomics, Nature genetics 32(4s) (2002) 526.

[442] P. Khatri, M. Sirota, A.J. Butte, Ten years of pathway analysis: current approaches and outstanding challenges, PLoS computational biology 8(2) (2012) e1002375.

[443] M. Kanehisa, S. Goto, KEGG: kyoto encyclopedia of genes and genomes, Nucleic acids research 28(1) (2000) 27-30.

[444] S.R. Chowbina, X. Wu, F. Zhang, P.M. Li, R. Pandey, H.N. Kasamsetty, J.Y. Chen, HPD: an online integrated human pathway database enabling systems biology studies, BMC bioinformatics, BioMed Central, 2009, p. S5.

[445] D. Nishimura, BioCarta, Biotech Software & Internet Report: The Computer Software Journal for Scient 2(3) (2001) 117-120.

[446] L. Matthews, G. Gopinath, M. Gillespie, M. Caudy, D. Croft, B. de Bono, P. Garapati, J. Hemish, H. Hermjakob, B. Jassal, Reactome knowledgebase of human biological pathways and processes, Nucleic acids research 37(suppl_1) (2008) D619-D622.

[447] T. Berggård, S. Linse, P. James, Methods for the detection and analysis of protein–protein interactions, Proteomics 7(16) (2007) 2833-2842.

[448] D. Szklarczyk, A. Franceschini, S. Wyder, K. Forslund, D. Heller, J. Huerta-Cepas, M. Simonovic, A. Roth, A. Santos, K.P. Tsafou, STRING v10: protein–protein interaction networks, integrated over the tree of life, Nucleic acids research 43(D1) (2014) D447-D452.

[449] A. Chatr-Aryamontri, B.-J. Breitkreutz, S. Heinicke, L. Boucher, A. Winter, C. Stark, J. Nixon, L. Ramage, N. Kolas, L. O'donnell, The BioGRID interaction database: 2013 update, Nucleic acids research 41(D1) (2012) D816-D823.

[450] S. Kerrien, B. Aranda, L. Breuza, A. Bridge, F. Broackes-Carter, C. Chen, M. Duesbury, M. Dumousseau, M. Feuermann, U. Hinz, The IntAct molecular interaction database in 2012, Nucleic acids research 40(D1) (2011) D841-D846.

[451] A. Chatr-Aryamontri, A. Ceol, L.M. Palazzi, G. Nardelli, M.V. Schneider, L. Castagnoli, G. Cesareni, MINT: the Molecular INTeraction database, Nucleic acids research 35(suppl_1) (2006) D572-D574.

[452] T. Keshava Prasad, R. Goel, K. Kandasamy, S. Keerthikumar, S. Kumar, S. Mathivanan, D. Telikicherla, R. Raju, B. Shafreen, A. Venugopal, Human protein reference database—2009 update, Nucleic acids research 37(suppl_1) (2008) D767-D772.

[453] E. Glaab, A. Baudot, N. Krasnogor, R. Schneider, A. Valencia, EnrichNet: network-based gene set enrichment analysis, Bioinformatics 28(18) (2012) i451-i457.

[454] I. Sadovskaya, E. Vinogradov, S. Flahaut, G. Kogan, S. Jabbouri, Extracellular carbohydrate-containing polymers of a model biofilm-producing strain, *Staphylococcus epidermidis* RP62A, Infection and immunity 73(5) (2005) 3007-3017.

[455] M. Mirzaei, D. Pascovici, J.X. Wu, J. Chick, Y. Wu, B. Cooke, P. Haynes, M.P. Molloy, TMT One-Stop Shop: From Reliable Sample Preparation to Computational Analysis Platform, in: S. Keerthikumar, S. Mathivanan (Eds.), Proteome Bioinformatics, Springer New York, New York, NY, 2017, pp. 45-66.

[456] N.Y. Yu, J.R. Wagner, M.R. Laird, G. Melli, S. Rey, R. Lo, P. Dao, S.C. Sahinalp, M. Ester, L.J. Foster, F.S.L. Brinkman, PSORTb 3.0: improved protein subcellular localization prediction with refined localization subcategories and predictive capabilities for all prokaryotes, Bioinformatics 26(13) (2010) 1608-1615.

[457] D. Szklarczyk, A. Franceschini, S. Wyder, K. Forslund, D. Heller, J. Huerta-Cepas, M. Simonovic, A. Roth, A. Santos, K.P. Tsafou, M. Kuhn, P. Bork, L.J. Jensen, C. von Mering, STRING v10: protein–protein interaction networks, integrated over the tree of life, Nucleic Acids Research 43(D1) (2015) D447-D452.

[458] T.J. Treangen, R.A. Maybank, S. Enke, M.B. Friss, L.F. Diviak, D.K. Karaolis, S. Koren, B. Ondov, A.M. Phillippy, N.H. Bergman, Complete genome sequence of the quality control strain *Staphylococcus aureus* subsp. aureus ATCC 25923, Genome Announc. 2(6) (2014) e01110-14.

[459] M.W. Pfaffl, A new mathematical model for relative quantification in real-time RT–PCR, Nucleic acids research 29(9) (2001) e45-e45.

[460] N. Solis, J.A. Cain, S.J. Cordwell, Comparative analysis of *Staphylococcus epidermidis* strains utilizing quantitative and cell surface shaving proteomics, Journal of proteomics 130 (2016) 190-199.

[461] M. Bukowski, B. Wladyka, G. Dubin, Exfoliative toxins of *Staphylococcus aureus*, Toxins 2(5) (2010) 1148-1165.

[462] R.J. Gordon, F.D. Lowy, Pathogenesis of methicillin-resistant *Staphylococcus aureus* infection, Clinical infectious diseases 46(Supplement_5) (2008) S350-S359.

[463] A.C. Graf, A. Leonard, M. Schäuble, L.M. Rieckmann, J. Hoyer, S. Maaß, M. Lalk, D. Becher, J. Pané-Farré, K. Riedel, Virulence factors produced by *Staphylococcus aureus* biofilms have a moonlighting function contributing to biofilm integrity, Molecular & Cellular Proteomics (2019) mcp. RA118. 001120.

[464] G. Cheng, R. Karunakaran, A.K. East, P.S. Poole, Multiplicity of sulfate and molybdate transporters and their role in nitrogen fixation in Rhizobium leguminosarum bv. viciae Rlv3841, Molecular Plant-Microbe Interactions 29(2) (2016) 143-152.

[465] J. Verdon, N. Girardin, C. Lacombe, J.-M. Berjeaud, Y. Héchard, δ-hemolysin, an update on a membrane-interacting peptide, Peptides 30(4) (2009) 817-823.

[466] P. Shah, E. Swiatlo, A multifaceted role for polyamines in bacterial pathogens, Molecular microbiology 68(1) (2008) 4-16.

[467] F. Antognoni, S. Del Duca, A. Kuraishi, E. Kawabe, T. Fukuchi-Shimogori, K. Kashiwagi, K. Igarashi, Transcriptional inhibition of the operon for the spermidine uptake system by the substrate-binding protein PotD, Journal of Biological Chemistry 274(4) (1999) 1942-1948.

[468] S.S. Atshan, M.N. Shamsudin, T. Lung, L. Than, Z. Sekawi, E. Ghaznavi-Rad, C. Pei Pei, Comparative characterisation of genotypically different clones of MRSA in the production of biofilms, BioMed Research International 2012 (2012).

[469] F.L. Theodoulou, I.D. Kerr, ABC transporter research: going strong 40 years on, Biochem Soc Trans 43(5) (2015) 1033-40.

[470] J. Yang, Y. He, J. Jiang, W. Chen, Q. Gao, L. Pan, C. Shi, Comparative proteomic analysis by iTRAQ-2DLC-MS/MS provides insight into the key proteins involved in Cronobacter sp. biofilm formation, Food Control 63 (2016) 93-100.

[471] S.S. Branda, J.E. González-Pastor, E. Dervyn, S.D. Ehrlich, R. Losick, R. Kolter, Genes involved in formation of structured multicellular communities by Bacillus subtilis, Journal of bacteriology 186(12) (2004) 3970-3979.

[472] R. Crowley, J. Leigh, P. Ward, H. Lappin-Scott, L. Bowler, Differential protein expression in Streptococcus uberis under planktonic and biofilm growth conditions, Appl. Environ. Microbiol. 77(1) (2011) 382-384.

[473] S.M. Hinsa, M. Espinosa-Urgel, J.L. Ramos, G.A. O'toole, Transition from reversible to irreversible attachment during biofilm formation by Pseudomonas fluorescens WCS365 requires an ABC transporter and a large secreted protein, Molecular microbiology 49(4) (2003) 905-918.

[474] E.M. Vanderlinde, J.J. Harrison, A. Muszyński, R.W. Carlson, R.J. Turner, C.K. Yost, Identification of a novel ABC transporter required for desiccation tolerance, and biofilm formation in Rhizobium leguminosarum bv. viciae 3841, FEMS microbiology ecology 71(3) (2010) 327-340.

[475] X. Zhu, F. Long, Y. Chen, S. Knøchel, Q. She, X. Shi, A putative ABC transporter is involved in negative regulation of biofilm formation by Listeria monocytogenes, Appl. Environ. Microbiol. 74(24) (2008) 7675-7683.

[476] K.E. Beenken, P.M. Dunman, F. McAleese, D. Macapagal, E. Murphy, S.J. Projan, J.S. Blevins, M.S. Smeltzer, Global gene expression in *Staphylococcus aureus* biofilms, J Bacteriol 186(14) (2004) 4665-84.

[477] O. Vytvytska, E. Nagy, M. Blüggel, H.E. Meyer, R. Kurzbauer, L.A. Huber, C.S. Klade, Identification of vaccine candidate antigens of *Staphylococcus aureus* by serological proteome analysis, Proteomics 2(5) (2002) 580-590.

[478] R.M. Corrigan, H. Miajlovic, T.J. Foster, Surface proteins that promote adherence of *Staphylococcus aureus* to human desquamated nasal epithelial cells, BMC microbiology 9(1) (2009) 22.

[479] B. Hofbauer, J. Vomacka, M. Stahl, V.S. Korotkov, M.C. Jennings, W.M. Wuest, S.A. Sieber, Dual Inhibitor of *Staphylococcus aureus* Virulence and Biofilm Attenuates Expression of Major Toxins and Adhesins, Biochemistry 57(11) (2018) 1814-1820.

[480] B. Kot, H. Sytykiewicz, I. Sprawka, Expression of the Biofilm-Associated Genes in Methicillin-Resistant *Staphylococcus aureus* in Biofilm and Planktonic Conditions, International journal of molecular sciences 19(11) (2018) 3487.

[481] C.B. Ibberson, C.P. Parlet, J. Kwiecinski, H.A. Crosby, D.K. Meyerholz, A.R. Horswill, Hyaluronan modulation impacts *Staphylococcus aureus* biofilm infection, Infection and immunity 84(6) (2016) 1917-1929.

[482] M.A. Rahman, Y.H. Choi, G. Pradeep, J.C. Yoo, An ammonium sulfate sensitive chitinase from Streptomyces sp. CS501, Archives of pharmacal research 37(12) (2014) 1522-1529.

[483] L.H. Tsang, J.E. Cassat, L.N. Shaw, K.E. Beenken, M.S. Smeltzer, Factors contributing to the biofilm-deficient phenotype of *Staphylococcus aureus* sarA mutants, PloS one 3(10) (2008) e3361.

[484] T. Kantyka, K. Plaza, J. Koziel, D. Florczyk, H.R. Stennicke, I.B. Thogersen, J.J. Enghild, G.A. Silverman, S.C. Pak, J. Potempa, Inhibition of *Staphylococcus aureus* cysteine proteases by human serpin potentially limits staphylococcal virulence, Biological chemistry 392(5) (2011) 483-489.

[485] X. Chen, H. Wu, Y. Cao, X. Yao, L. Zhao, T. Wang, Y. Yang, D. Lv, Y. Chai, Y. Cao, Ion-pairing chromatography on a porous graphitic carbon column coupled with time-of-flight mass spectrometry for targeted and untargeted profiling of amino acid biomarkers involved in Candida albicans biofilm formation, Molecular BioSystems 10(1) (2014) 74-85.

[486] E.A. Wall, J.H. Caufield, C.E. Lyons, K.A. Manning, T. Dokland, G.E. Christie, Specific N-terminal cleavage of ribosomal protein L 27 in S taphylococcus aureus and related bacteria, Molecular microbiology 95(2) (2015) 258-269.

[487] A. Weiss, B.D. Moore, M.H. Tremblay, D. Chaput, A. Kremer, L.N. Shaw, The ω subunit governs RNA polymerase stability and transcriptional specificity in *Staphylococcus aureus*, Journal of bacteriology 199(2) (2017) e00459-16.

[488] S. Li, H. Li, T. Qi, X. Yan, B. Wang, J. Guan, Y. Li, Comparative transcriptomics analyses of the different growth states of multidrug-resistant Acinetobacter baumannii, Biomedicine & Pharmacotherapy 85 (2017) 564-574.

[489] K.D. Xu, M.J. Franklin, C.-H. Park, G.A. McFeters, P.S. Stewart, Gene expression and protein levels of the stationary phase sigma factor, RpoS, in continuously-fed *Pseudomonas aeruginosa* biofilms, FEMS microbiology letters 199(1) (2001) 67-71.

[490] W. Li, Z. Yao, L. Sun, W. Hu, J. Cao, W. Lin, X. Lin, Proteomics analysis reveals a potential antibiotic cocktail therapy strategy for Aeromonas hydrophila infection in biofilm, Journal of proteome research 15(6) (2016) 1810-1820.

[491] H. Weber, S. Engelmann, D. Becher, M. Hecker, Oxidative stress triggers thiol oxidation in the glyceraldehyde-3-phosphate dehydrogenase of *Staphylococcus aureus*, Molecular microbiology 52(1) (2004) 133-140.

[492] L. Oliveira, P. Madureira, E.B. Andrade, A. Bouaboud, E. Morello, P. Ferreira, C. Poyart, P. Trieu-Cuot, S. Dramsi, Group B streptococcus GAPDH is released upon cell lysis, associates with bacterial surface, and induces apoptosis in murine macrophages, PloS one 7(1) (2012) e29963.

[493] C. Gil, C. Solano, S. Burgui, C. Latasa, B. García, A. Toledo-Arana, I. Lasa, J. Valle, Biofilm Matrix Exoproteins Induce a Protective Immune Response against *Staphylococcus aureus* Biofilm Infection, Infection and Immunity 82(3) (2014) 1017-1029.

[494] K. Sauer, A.K. Camper, G.D. Ehrlich, J.W. Costerton, D.G. Davies, *Pseudomonas aeruginosa* displays multiple phenotypes during development as a biofilm, Journal of bacteriology 184(4) (2002) 1140-1154.

[495] S. Planchon, M. Desvaux, I. Chafsey, C. Chambon, S. Leroy, M. Hébraud, R. Talon, Comparative subproteome analyses of planktonic and sessile Staphylococcus xylosus C2a: new insight in cell physiology of a coagulase-negative Staphylococcus in biofilm, Journal of proteome research 8(4) (2009) 1797-1809.

[496] M. Eschbach, K. Schreiber, K. Trunk, J. Buer, D. Jahn, M. Schobert, Long-term anaerobic survival of the opportunistic pathogen *Pseudomonas aeruginosa* via pyruvate fermentation, Journal of bacteriology 186(14) (2004) 4596-4604.

[497] K. Sambanthamoorthy, A. Schwartz, V. Nagarajan, M.O. Elasri, The role of msa in *Staphylococcus aureus* biofilm formation, BMC microbiology 8(1) (2008) 221.

[498] M.I. Klein, J. Xiao, B. Lu, C.M. Delahunty, J.R. Yates, III, H. Koo, Streptococcus mutans Protein Synthesis during Mixed-Species Biofilm Development by High-Throughput Quantitative Proteomics, PLOS ONE 7(9) (2012) e45795.

[499] R.A. Brady, G.A. May, J.G. Leid, M.L. Prior, J.W. Costerton, M.E. Shirtliff, Resolution of *Staphylococcus aureus* Biofilm Infection Using Vaccination and Antibiotic Treatment, Infection and Immunity 79(4) (2011) 1797.

[500] G. Borriello, L. Richards, G.D. Ehrlich, P.S. Stewart, Arginine or nitrate enhances antibiotic susceptibility of *Pseudomonas aeruginosa* in biofilms, Antimicrobial agents and chemotherapy 50(1) (2006) 382-384.

[501] A. Bridier, R. Briandet, V. Thomas, F. Dubois-Brissonnet, Resistance of bacterial biofilms to disinfectants: a review, Biofouling 27(9) (2011) 1017-1032.

[502] M.E. Falagas, A.M. Kapaskelis, V.D. Kouranos, O.K. Kakisi, Z. Athanassa, D.E. Karageorgopoulos, Outcome of antimicrobial therapy in documented biofilm-associated infections: a review of the available clinical evidence, Drugs 69(10) (2009) 1351-61.

[503] H. Van Acker, P. Van Dijck, T. Coenye, Molecular mechanisms of antimicrobial tolerance and resistance in bacterial and fungal biofilms, Trends in microbiology 22(6) (2014) 326-333.

[504] M.H. Cardoso, K.C. de Almeida, E.d.S. Cândido, A.M. Murad, S.C. Dias, O.L. Franco, Comparative NanoUPLC-MS E analysis between magainin I-susceptible and-resistant *Escherichia coli* strains, Scientific reports 7(1) (2017) 4197.

[505] L. Shi, B.P. Tu, Acetyl-CoA and the regulation of metabolism: mechanisms and consequences, Current opinion in cell biology 33 (2015) 125-131.

[506] N.J. Phillips, C.T. Steichen, B. Schilling, D.M. Post, R.K. Niles, T.B. Bair, M.L. Falsetta, M.A. Apicella, B.W. Gibson, Proteomic analysis of Neisseria gonorrhoeae biofilms shows shift to anaerobic respiration and changes in nutrient transport and outermembrane proteins, PloS one 7(6) (2012) e38303.

[507] J. Herschend, Z.B. Damholt, A.M. Marquard, B. Svensson, S.J. Sørensen, P. Hägglund, M. Burmølle, A meta-proteomics approach to study the interspecies interactions affecting microbial biofilm development in a model community, Scientific reports 7(1) (2017) 16483.

[508] R. Khairon, N.M. Zin, M. Abdul Rahman, D.F. Basri, Comparative proteomic analysis of differential proteins in response to aqueous extract of quercus infectoria gall in methicillin-resistant *Staphylococcus aureus*, International journal of proteomics 2016 (2016).

[509] M. Yamamoto, H. Arai, M. Ishii, Y. Igarashi, Role of two 2-oxoglutarate: ferredoxin oxidoreductases in Hydrogenobacter thermophilus under aerobic and anaerobic conditions, FEMS microbiology letters 263(2) (2006) 189-193.

[510] E. Dörner, M. Boll, Properties of 2-oxoglutarate: ferredoxin oxidoreductase from Thauera aromatica and its role in enzymatic reduction of the aromatic ring, Journal of bacteriology 184(14) (2002) 3975-3983.

[511] Y. Zhu, R. Nandakumar, M.R. Sadykov, N. Madayiputhiya, T.T. Luong, R. Gaupp, C.Y. Lee, G.A. Somerville, RpiR homologues may link *Staphylococcus aureus* RNAIII synthesis and pentose phosphate pathway regulation, Journal of bacteriology 193(22) (2011) 6187-6196.

[512] I. Grimm, J. Dumke, J. Dreier, C. Knabbe, T. Vollmer, Biofilm formation and transcriptome analysis of Streptococcus gallolyticus subsp. gallolyticus in response to lysozyme, PloS one 13(1) (2018) e0191705.

[513] M. Chen, Q. Yu, H. Sun, Novel strategies for the prevention and treatment of biofilm related infections, International journal of molecular sciences 14(9) (2013) 18488-18501.

[514] K. Johani, H. Hu, L. Santos, S. Schiller, A. Deva, G. Whiteley, A. Almatroudi, K. Vickery, Determination of bacterial species present in biofilm contaminating the channels of clinical endoscopes, Infection, Disease & Health 23(4) (2018) 189-196.

[515] M.A. Priestman, T. Funke, I.M. Singh, S.S. Crupper, E. Schönbrunn, 5-Enolpyruvylshikimate-3-phosphate synthase from *Staphylococcus aureus* is insensitive to glyphosate, FEBS letters 579(3) (2005) 728-732.

[516] H.S. Karki, J.H. Ham, The roles of the shikimate pathway genes, aroA and aroB, in virulence, growth and UV tolerance of B urkholderia glumae strain 411gr-6, Molecular plant pathology 15(9) (2014) 940-947.

[517] T. Suriyanarayanan, L. Qingsong, L.T. Kwang, L.Y. Mun, T. Truong, C.J. Seneviratne, Correction: Quantitative proteomics of strong and weak biofilm formers of Enterococcus faecalis reveals novel regulators of biofilm formation, Molecular & Cellular Proteomics 17(10) (2018) 2081-2081.

[518] S. Giannouli, M. Labrou, A. Kyritsis, A. Ikonomidis, S. Pournaras, C. Stathopoulos, A. Tsakris, Detection of mutations in the FemXAB protein family in oxacillin-susceptible mecA-positive *Staphylococcus aureus* clinical isolates, Journal of Antimicrobial Chemotherapy 65(4) (2010) 626-633.

[519] J.-L. Mainardi, R. Villet, T.D. Bugg, C. Mayer, M. Arthur, Evolution of peptidoglycan biosynthesis under the selective pressure of antibiotics in Gram-positive bacteria, FEMS microbiology reviews 32(2) (2008) 386-408.

[520] M. Fonvielle, M. Chemama, R. Villet, M. Lecerf, A. Bouhss, J.-M. Valery, M. Etheve-Quelquejeu, M. Arthur, Aminoacyl-tRNA recognition by the FemX Wv transferase for bacterial cell wall synthesis, Nucleic acids research 37(5) (2009) 1589-1601.

[521] S.S. Hegde, J.S. Blanchard, Kinetic and mechanistic characterization of recombinant Lactobacillus viridescens FemX (UDP-N-acetylmuramoyl pentapeptide-lysine N6-alanyltransferase), Journal of Biological Chemistry 278(25) (2003) 22861-22867.

[522] S.S. Hegde, T.E. Shrader, FemABX family members are novel nonribosomal peptidyltransferases and important pathogen-specific drug targets, Journal of Biological Chemistry 276(10) (2001) 6998-7003.

[523] M. Kok, G. Bron, B. Erni, S. Mukhija, Effect of enzyme I of the bacterial phosphoenolpyruvate: sugar phosphotransferase system (PTS) on virulence in a murine model, Microbiology 149(9) (2003) 2645-2652.

[524] B. Suo, H. Yang, Y. Wang, H. Lv, Z. Li, C. Xu, Z. Ai, Comparative proteomic and morphological change analyses of *Staphylococcus aureus* during resuscitation from prolonged freezing, Frontiers in microbiology 9 (2018).

[525] R.N. Allan, P. Skipp, J. Jefferies, S.C. Clarke, S.N. Faust, L. Hall-Stoodley, J. Webb, Pronounced metabolic changes in adaptation to biofilm growth by Streptococcus pneumoniae, PLoS One 9(9) (2014) e107015.

[526] A. Fischer, S.-J. Yang, A.S. Bayer, A.R. Vaezzadeh, S. Herzig, L. Stenz, M. Girard, G. Sakoulas, A. Scherl, M.R. Yeaman, Daptomycin resistance mechanisms in clinically derived *Staphylococcus aureus* strains assessed by a combined transcriptomics and proteomics approach, Journal of antimicrobial chemotherapy 66(8) (2011) 1696-1711.

[527] L.A. Bøhle, E.M. Færgestad, E. Veiseth-Kent, H. Steinmoen, I.F. Nes, V.G. Eijsink, G. Mathiesen, Identification of proteins related to the stress response in Enterococcus faecalis V583 caused by bovine bile, Proteome science 8(1) (2010) 37.

[528] A. Hiron, B. Posteraro, M. Carrière, L. Remy, C. Delporte, M. La Sorda, M. Sanguinetti, V. Juillard, E. Borezée-Durant, A nickel ABC-transporter of *Staphylococcus aureus* is involved in urinary tract infection, Molecular microbiology 77(5) (2010) 1246-1260.

[529] M.D. Kiran, D.E. Akiyoshi, A. Giacometti, O. Cirioni, G. Scalise, N. Balaban, OpuC–an ABC transporter that is associated with *Staphylococcus aureus* pathogenesis, The International journal of artificial organs 32(9) (2009) 600-610.

[530] K.J. Tanaka, S. Song, K. Mason, H.W. Pinkett, Selective substrate uptake: the role of ATP-binding cassette (ABC) importers in pathogenesis, Biochimica et Biophysica Acta (BBA)-Biomembranes 1860(4) (2018) 868-877.

[531] M. Otto, F. Götz, ABC transporters of staphylococci, Research in microbiology 152(3-4) (2001) 351-356.

[532] N.D. Hammer, E.P. Skaar, Molecular mechanisms of *Staphylococcus aureus* iron acquisition, Annual review of microbiology 65 (2011) 129-147.

[533] L.K. Jensen, H.E. Jensen, J. Koch, T. Bjarnsholt, S. Eickhardt, M. Shirtliff, Specific antibodies to *Staphylococcus aureus* biofilm are present in serum from pigs with osteomyelitis, in vivo 29(5) (2015) 555-560.

[534] M. Jonsson, J.T. Juuti, P. François, R. AlMajidi, M. Pietiäinen, M. Girard, C. Lindholm, M.J. Saller, A.J. Driessen, P. Kuusela, Inactivation of the Ecs ABC transporter of *Staphylococcus aureus* attenuates virulence by altering composition and function of bacterial wall, PloS one 5(12) (2010) e14209.

[535] A.F. Junka, S. Deja, D. Smutnicka, P. Szymczyk, G. Ziółkowski, M. Bartoszewicz, P. Młynarz, Differences in metabolic profiles of planktonic and biofilm cells in *Staphylococcus aureus*-(1) H Nuclear Magnetic Resonance search for candidate biomarkers, Acta Biochimica Polonica 60(4) (2013).

[536] L.l. Santi, W.O. Beys-da-Silva, M. Berger, D. Calzolari, J.A. Guimarães, J.J. Moresco, J.R. Yates III, Proteomic profile of Cryptococcus neoformans biofilm reveals changes in metabolic processes, Journal of proteome research 13(3) (2014) 1545-1559.

[537] A. Pajkos, K. Vickery, Y. Cossart, Is biofilm accumulation on endoscope tubing a contributor to the failure of cleaning and decontamination?, The Journal of hospital infection 58(3) (2004) 224-9.

[538] Y. Zhu, E.C. Weiss, M. Otto, P.D. Fey, M.S. Smeltzer, G.A. Somerville, *Staphylococcus aureus* Biofilm Metabolism and the Influence of Arginine on Polysaccharide Intercellular Adhesin Synthesis, Biofilm Formation, and Pathogenesis, Infection and Immunity 75(9) (2007) 4219-4226.

[539] X.-H. Wu, H.-L. Yu, Z.-Y. Ba, J.-Y. Chen, H.-G. Sun, B.-Z. Han, Sampling methods for NMR-based metabolomics of *Staphylococcus aureus*, Biotechnology Journal 5(1) (2010) 75-84.

[540] W.W. Navarre, O. Schneewind, Surface proteins of gram-positive bacteria and mechanisms of their targeting to the cell wall envelope, Microbiol. Mol. Biol. Rev. 63(1) (1999) 174-229.

[541] A.L. Lovering, S.S. Safadi, N.C. Strynadka, Structural perspective of peptidoglycan biosynthesis and assembly, Annual review of biochemistry 81 (2012) 451-478.

[542] Y.-H. Huang, J.-S. Lin, J.-C. Ma, H.-H. Wang, Functional characterization of triclosan-resistant enoyl-acyl-carrier protein reductase (FabV) in *Pseudomonas aeruginosa*, Frontiers in microbiology 7 (2016) 1903.

[543] L.M. McMurry, M. Oethinger, S.B. Levy, Triclosan targets lipid synthesis, Nature 394(6693) (1998) 531.

[544] R.J. Heath, Y.-T. Yu, M.A. Shapiro, E. Olson, C.O. Rock, Broad spectrum antimicrobial biocides target the FabI component of fatty acid synthesis, Journal of Biological Chemistry 273(46) (1998) 30316-30320.

[545] E. Jungermann, Soap bacteriostats, Journal of the American Oil Chemists' Society 45(5) (1968) 345-350.

[546] R.J. Heath, J. Li, G.E. Roland, C.O. Rock, Inhibition of the *Staphylococcus aureus*NADPH-dependent enoyl-acyl carrier protein reductase by triclosan and hexachlorophene, Journal of Biological Chemistry 275(7) (2000) 4654-4659.

[547] J. Latimer, S. Forbes, A.J. McBain, Attenuated virulence and biofilm formation in *Staphylococcus aureus* following sublethal exposure to triclosan, Antimicrobial agents and chemotherapy 56(6) (2012) 3092-3100.

[548] L. Yang, Y. Liu, C. Sternberg, S. Molin, Evaluation of enoyl-acyl carrier protein reductase inhibitors as *Pseudomonas aeruginosa* quorum-quenching reagents, Molecules 15(2) (2010) 780-792.

[549] P. Gilbert, A. McBain, P. Sreenivasan, Common therapeutic approaches for the control of oral biofilms: microbiological safety and efficacy, Clinical microbiology and infection 13 (2007) 17-24.

[550] M.T. Ferreira, A.S. Manso, P. Gaspar, M.G. Pinho, A.R. Neves, Effect of oxygen on glucose metabolism: utilization of lactate in *Staphylococcus aureus* as revealed by in vivo NMR studies, PLoS One 8(3) (2013) e58277.

[551] S. Kolbeck, J. Behr, R.F. Vogel, C. Ludwig, M.A. Ehrmann, Acid stress response of Staphylococcus xylosus elicits changes in the proteome and cellular membrane, Journal of applied microbiology (2019).

[552] M. Pagels, S. Fuchs, J. Pané-Farré, C. Kohler, L. Menschner, M. Hecker, P.J. McNamarra, M.C. Bauer, C. Von Wachenfeldt, M. Liebeke, Redox sensing by a Rex-family repressor is involved in the regulation of anaerobic gene expression in *Staphylococcus aureus*, Molecular microbiology 76(5) (2010) 1142-1161.

[553] K.-C. Chiu, C.-J. Lin, G.-C. Shaw, Transcriptional regulation of the L-lactate permease gene lutP by the LutR repressor of Bacillus subtilis RO-NN-1, Microbiology 160(10) (2014) 2178-2189.

[554] Y. Chai, R. Kolter, R. Losick, A widely conserved gene cluster required for lactate utilization in Bacillus subtilis and its involvement in biofilm formation, Journal of bacteriology 191(8) (2009) 2423-2430.

[555] M.D. Morrison, W.L. Nicholson, Meta-analysis of data from spaceflight transcriptome experiments does not support the idea of a common bacterial “spaceflight response”, Scientific reports 8(1) (2018) 14403.

[556] A. Almatroudi, S. Tahir, H. Hu, D. Chowdhury, I.B. Gosbell, S.O. Jensen, G.S. Whiteley, A.K. Deva, T. Glasbey, K. Vickery, *Staphylococcus aureus* dry-surface biofilms are more resistant to heat treatment than traditional hydrated biofilms, Journal of Hospital Infection 98(2) (2018) 161-167.

[557] P.S. Stewart, Diffusion in biofilms, Journal of bacteriology 185(5) (2003) 1485-1491.

[558] N. Sahebekhtiari, M. Saraswat, S. Joenväärä, R. Jokinen, A. Lovric, S. Kaye, A. Mardinoglu, A. Rissanen, J. Kaprio, R. Renkonen, Plasma Proteomics Analysis Reveals

Dysregulation of Complement Proteins and Inflammation in Acquired Obesity—A Study on Rare BMI-Discordant Monozygotic Twin Pairs, PROTEOMICS–Clinical Applications 13(4) (2019) 1800173.

[559] R. Moulder, S.D. Bhosale, D.R. Goodlett, R. Lahesmaa, Analysis of the plasma proteome using iTRAQ and TMT-based Isobaric labeling, Mass spectrometry reviews 37(5) (2018) 583-606.

[560] Y. Chen, A. Huang, W. Ao, Z. Wang, J. Yuan, Q. Song, D. Wei, H. Ye, Proteomic analysis of serum proteins from HIV/AIDS patients with Talaromyces marneffei infection by TMT labeling-based quantitative proteomics, Clinical Proteomics 15(1) (2018) 40.

[561] P.E. Geyer, L.M. Holdt, D. Teupser, M. Mann, Revisiting biomarker discovery by plasma proteomics, Molecular systems biology 13(9) (2017) 942.

[562] G. Pimienta, D.M. Heithoff, A. Rosa-Campos, M. Tran, J.D. Esko, M.J. Mahan, J.D. Marth, J.W. Smith, Plasma Proteome Signature of Sepsis: a Functionally Connected Protein Network, Proteomics 19(5) (2019) 1800389.

[563] O. Eberhard, M. Haubitz, F. Brunkhorst, V. Kliem, K. Koch, R. Brunkhorst, Usefulness of procalcitonin for differentiation between activity of systemic autoimmune disease (systemic lupus erythematosus/systemic antineutrophil cytoplasmic antibody-associated vasculitis) and invasive bacterial infection, Arthritis & Rheumatism 40(7) (1997) 1250-1256.

[564] M. Nikfardjam, M. Müllner, W. Schreiber, E. Oschatz, M. Exner, H. Domanovits, A. Laggner, K. Huber, The association between C-reactive protein on admission and mortality in patients with acute myocardial infarction, Journal of internal medicine 247(3) (2000) 341-345.

[565] C. Tu, P.A. Rudnick, M.Y. Martinez, K.L. Cheek, S.E. Stein, R.J. Slebos, D.C. Liebler, Depletion of abundant plasma proteins and limitations of plasma proteomics, Journal of proteome research 9(10) (2010) 4982-4991.

[566] S. Mahesh, Z. Li, R. Buggage, F. Mor, I. Cohen, E. Chew, R. Nussenblatt, Alpha tropomyosin as a self-antigen in patients with Behçet's disease, Clinical & Experimental Immunology 140(2) (2005) 368-375.

[567] T. Harada, Y. Kuramitsu, A. Makino, M. Fujimoto, N. Iizuka, Y. Hoshii, M. Takashima, M. Tamesa, T. Nishimura, S. Takeda, Expression of tropomyosin alpha 4 chain is increased in esophageal squamous cell carcinoma as evidenced by proteomic profiling by two-dimensional electrophoresis and liquid chromatography-mass spectrometry/mass spectrometry, PROTEOMICS–Clinical Applications 1(2) (2007) 215-223.

[568] C.Y. Lam, C.W. Yip, T.C. Poon, C.K. Cheng, E.W. Ng, N.C. Wong, P.F. Cheung, P.B. Lai, I.O. Ng, S.T. Fan, Identification and characterization of tropomyosin 3 associated with granulin-epithelin precursor in human hepatocellular carcinoma, PLoS One 7(7) (2012) e40324.

[569] L. Biancone, G. Monteleone, R. Marasco, F. Pallone, Autoimmunity to tropomyosin isoforms in ulcerative colitis (UC) patients and unaffected relatives, Clinical and experimental immunology 113(2) (1998) 198.

[570] P. Galloway, P. Mulvihill, S. Siedlak, M. Mijares, M. Kawai, H. Padget, R. Kim, G. Perry, Immunochemical demonstration of tropomyosin in the neurofibrillary pathology of Alzheimer's disease, The American journal of pathology 137(2) (1990) 291.

[571] G. Dighiero, P. Lymberi, C. Monot, N. Abuaf, Sera with high levels of anti-smooth muscle and anti-mitochondrial antibodies frequently bind to cytoskeleton proteins, Clinical & Experimental Immunology 82(1) (1990) 52-56.

[572] M. Tsujioka, K. Yoshida, K. Inouye, Talin B is required for force transmission in morphogenesis of Dictyostelium, The EMBO journal 23(11) (2004) 2216-2225.

[573] N. Xu, H.-J. Chen, S.-H. Chen, X.-Y. Xue, H. Chen, Q.-S. Zheng, Y. Wei, X.-D. Li, J.-B. Huang, H. Cai, Upregulation of Talin-1 expression associates with advanced pathological features and predicts lymph node metastases and biochemical recurrence of prostate cancer, Medicine 95(29) (2016).

[574] M.A. Senetar, R.O. McCann, Gene duplication and functional divergence during evolution of the cytoskeletal linker protein talin, Gene 362 (2005) 141-152.

[575] S. Klim, F. Amerstorfer, G. Gruber, G. Bernhardt, R. Radl, L. Leitner, A. Leithner, M. Glehr, Fibrinogen–A Practical and Cost Efficient Biomarker for Detecting Periprosthetic Joint Infection, Scientific reports 8(1) (2018) 8802.

[576] S. Marfà, W. Jimenez, Fibrinogen α-Chain as a Serum Marker of Liver Disease, Biomarkers in Liver Disease (2016) 1-20.

[577] Y.-P. Ko, M.J. Flick, Fibrinogen is at the interface of host defense and pathogen virulence in *Staphylococcus aureus* infection, Seminars in thrombosis and hemostasis, Thieme Medical Publishers, 2016, pp. 408-421.

[578] S.P. Barr, E.W. Hill, A. Bayat, Novel proteomic assay of breast implants reveals proteins with significant binding differences: implications for surface coating and biocompatibility, Aesthetic surgery journal 38(9) (2018) 962-969.

[579] N. Kavanagh, E.J. Ryan, A. Widaa, G. Sexton, J. Fennell, S. O'Rourke, K.C. Cahill, C.J. Kearney, F.J. O'Brien, S.W. Kerrigan, Staphylococcal osteomyelitis: disease progression, treatment challenges, and future directions, Clinical microbiology reviews 31(2) (2018) e00084-17.

[580] D.N. Martin, S.L. Uprichard, Identification of transferrin receptor 1 as a hepatitis C virus entry factor, Proceedings of the National Academy of Sciences 110(26) (2013) 10777-10782.

[581] X. Pan, B. Tamilselvam, E.J. Hansen, S. Daefler, Modulation of iron homeostasis in macrophages by bacterial intracellular pathogens, BMC microbiology 10(1) (2010) 64.

[582] B. Andriopoulos, S. Hegedüsch, J. Mangin, H.-D. Riedel, U. Hebling, J. Wang, K. Pantopoulos, S. Mueller, Sustained hydrogen peroxide induces iron uptake by transferrin receptor-1 independent of the iron regulatory protein/iron-responsive element network, Journal of Biological Chemistry 282(28) (2007) 20301-20308.

[583] M. Hirayama, Y. Kohgo, H. Kondo, N. Shintani, K. Fujikawa, K. Sasaki, J. Kato, Y. Nhtsu, Regulation of iron metabolism in HepG2 cells: a possible role for cytokines in the hepatic deposition of iron, Hepatology 18(4) (1993) 874-880.

[584] R. Upton, Y. Chen, S. Mumby, J. Gutteridge, P. Anning, A. Nicholson, T. Evans, G. Quinlan, Variable tissue expression of transferrin receptors: relevance to acute respiratory distress syndrome, European Respiratory Journal 22(2) (2003) 335-341.

[585] S. Mueller, N.H. Afdhal, D. Schuppan, Iron, HCV, and liver cancer: hard metal setting the pace?, Gastroenterology 130(7) (2006) 2229-2234.

[586] J. Weiss, Bactericidal/permeability-increasing protein (BPI) and lipopolysaccharide-binding protein (LBP): structure, function and regulation in host defence against Gram-negative bacteria, Portland Press Limited, 2003.

[587] M. Manco, L. Putignani, G.F. Bottazzo, Gut microbiota, lipopolysaccharides, and innate immunity in the pathogenesis of obesity and cardiovascular risk, Endocrine reviews 31(6) (2010) 817-844.

[588] I.L. Ahrén, A. Bjartell, A. Egesten, K. Riesbeck, Lipopolysaccharide-Binding Protein Increases Toll-like Receptor 4–Dependent Activation by Nontypeable Haemophilus influenzae, The Journal of infectious diseases 184(7) (2001) 926-930.

[589] S. Lehr, S. Hartwig, D. Lamers, S. Famulla, S. Müller, F.-G. Hanisch, C. Cuvelier, J. Ruige, K. Eckardt, D.M. Ouwens, Identification and validation of novel adipokines released from primary human adipocytes, Molecular & cellular proteomics 11(1) (2012) M111. 010504.

[590] A.L. Davidson, E. Dassa, C. Orelle, J. Chen, Structure, function, and evolution of bacterial ATP-binding cassette systems, Microbiol Mol Biol Rev 72(2) (2008) 317-64, table of contents.

[591] L. Cuthbertson, V. Kos, C. Whitfield, ABC transporters involved in export of cell surface glycoconjugates, Microbiology and Molecular Biology Reviews 74(3) (2010) 341-362.

[592] G. Efthimiou, G. Tsiamis, M.A. Typas, K.M. Pappas, Transcriptomic adjustments of *Staphylococcus aureus* COL (MRSA) forming biofilms under acidic and alkaline conditions, Frontiers in microbiology 10 (2019) 2393.

[593] M.R. Sadykov, M.E. Olson, S. Halouska, Y. Zhu, P.D. Fey, R. Powers, G.A. Somerville, Tricarboxylic acid cycle-dependent regulation of *Staphylococcus epidermidis* polysaccharide intercellular adhesin synthesis, Journal of bacteriology 190(23) (2008) 7621-7632.

[594] G.A. Somerville, R.A. Proctor, At the crossroads of bacterial metabolism and virulence factor synthesis in Staphylococci, Microbiol. Mol. Biol. Rev. 73(2) (2009) 233-248.

[595] C. Vuong, J.B. Kidder, E.R. Jacobson, M. Otto, R.A. Proctor, G.A. Somerville, *Staphylococcus epidermidis* polysaccharide intercellular adhesin production significantly increases during tricarboxylic acid cycle stress, Journal of bacteriology 187(9) (2005) 2967-2973.

Appendices

Appendix 1. **Human ethics approval**

Appendix 2A. and 2B. **Participant information and consent forms**

Appendix 3. Validation of selected genes from *S. aureus* proteomic results using qPCR

Appendix 4. Functional classification of the significantly upregulated common proteins between 3dwb and 12dwb compared with planktonic culture

Appendix 5. Functional classification of the significantly downregulated common proteins between 3dwb and 12dwb compared with planktonic culture

Appendix 6. Functional classification of the significantly upregulated common proteins between 12dwb and DSB compared with planktonic culture

Appendix 7. Functional classification of the significantly downregulated common proteins between 12dwb and DSB compared with planktonic culture

Appendix 8. Copyright permission for figures

Office of the Deputy Vice-Chancellor
(Research)

Research Office
Research Hub, Building C5C East
Macquarie University
NSW 2109 Australia
T: +61 (2) 9850 4459
http://www.research.mq.edu.au/
ABN 90 952 801 237

MACQUARIE University
SYDNEY·AUSTRALIA

1 September 2016

Dear Professor Deva

Reference No: 5201600427

Title: *Breast implant related infection, biofilm, capsular contracture, cancer*

Thank you for submitting the above application for ethical and scientific review. Your application was considered by the Macquarie University Human Research Ethics Committee (HREC (Medical Sciences)).

I am pleased to advise that ethical and scientific approval has been granted for this project to be conducted at:

- Macquarie University

This research meets the requirements set out in the *National Statement on Ethical Conduct in Human Research* (2007 – Updated May 2015) (the *National Statement*).

Standard Conditions of Approval:

1. Continuing compliance with the requirements of the *National Statement,* which is available at the following website:

http://www.nhmrc.gov.au/book/national-statement-ethical-conduct-human-research

2. This approval is valid for five (5) years, subject to the submission of annual reports. Please submit your reports on the anniversary of the approval for this protocol.

3. All adverse events, including events which might affect the continued ethical and scientific acceptability of the project, must be reported to the HREC within 72 hours.

4. Proposed changes to the protocol and associated documents must be submitted to the Committee for approval before implementation.

It is the responsibility of the Chief investigator to retain a copy of all documentation related to

this project and to forward a copy of this approval letter to all personnel listed on the project.

Should you have any queries regarding your project, please contact the Ethics Secretariat on 9850 4194 or by email ethics.secretariat@mq.edu.au

The HREC (Medical Sciences) Terms of Reference and Standard Operating Procedures are available from the Research Office website at:

http://www.research.mq.edu.au/for/researchers/how_to_obtain_ethics_approval/human_research_ethics

The HREC (Medical Sciences) wishes you every success in your research.

Yours sincerely

Professor Tony Eyers
Chair, Macquarie University Human Research Ethics Committee (Medical Sciences)

This HREC is constituted and operates in accordance with the National Health and Medical Research Council's (NHMRC) *National Statement on Ethical Conduct in Human Research*

Details of this approval are as follows:
Approval Date: 25 August 2016
The following documentation has been reviewed and approved by the HREC (Medical Sciences):

***If the document has no version date listed one will be created for you. Please ensure the footer of these documents are updated to include this version date to ensure ongoing version control.**

Department of Biomedical Sciences
Faculty of Medicine and Health Sciences
MACQUARIE UNIVERSITY NSW 2109

Phone: +61 (0)98502773
Fax: +61 (0)98123610
Email: karen.vickery@ mq.edu.au
Email: anand.deva@ mq.edu.au

MACQUARIE University
SYDNEY·AUSTRALIA

Chief Investigator's / Supervisor's Name & Title: **A/Professor Karen Vickery and A/Professor Anand Deva**

Participant Information and Consent Form

Name of Project: Breast implant related infection, biofilm, capsular contracture and cancer

You are invited to participate in a study of the biological and immunological causes associated with breast implant capsular contracture (constriction of tissue around the breast implant) and cancer. The purpose of the study is to better understand the causes of these complications.

The study is being conducted by Associate Professor Karen Vickery and Associate Professor Anand Deva of the Faculty of Medicine and Health Sciences. Contact either Karen Vickery on Ph 98502773, email karen.vickery@mq.edu.au or Anand Deva on Ph 98123890, email anand.deva@mq.edu.au.

If you decide to participate, you will be donating part of the tissue capsule around the breast implant that is to be removed at the time of your surgery. If you are patient with breast cancer, or patient with breast augmentation, 5 ml of peripheral blood maybe taken at the time of surgery when you have IV access, so no additional harm or discomfort should be experienced. Blood samples will be used to look at lymphocytes, proteins and other immunological characteristics.

We will look for evidence of bacteria or the chemicals and cells involved in the immune response to the breast contraction or cancer. There will be no surgery or procedure additional to the operation that has been recommended by your surgeon. Also there will be no additional cost to you. This tissue is normally removed and would be thrown away.

We will be collecting your general medical information and age for comparison between patients and for data analysis. Any information or personal details gathered in the course of the study are confidential. No individual will be identified in any publication of the results. All the data will be kept securely in a locked filing cabinet in a locked room at Faculty of Medicine and Health Sciences, Macquarie University. Only study personnel will have access to the data. A summary of the results of the data can be made available to you on request by contacting either Associate Professor Karen Vickery or Associate Professor Anand Deva, Faculty of Medicine and Health Sciences, 2 Technology Place, Macquarie University 2109.
Participation in this study is entirely voluntary: you are not obliged to participate and if you decide to participate, you are free to withdraw at any time without having to give a reason and without consequence.

I, *(participant's name)* have read *(or, where appropriate, have had read to me)* and understand the information above and any questions I have asked have been answered to my satisfaction. I agree to participate in this research, knowing that I can withdraw from further participation in the research at any time without consequence. I have been given a copy of this form to keep.

Participant's Name:_____
(Block letters)

Participant's Signature:_____ Date:_____

Investigator's Name:_____
(Block letters)

Investigator's Signature: _____ __ Date:_____

The ethical aspects of this study have been approved by the Macquarie University Human Research Ethics Committee. If you have any complaints or reservations about any ethical aspect of your participation in this research, you may contact the Committee through the Director, Research Ethics & Integrity (telephone (02) 9850 7854; email ethics@mq.edu.au). Any complaint you make will be treated in confidence and investigated, and you will be informed of the outcome.

(INVESTIGATOR'S [OR PARTICIPANT'S] COPY)

Department of Biomedical Sciences
Faculty of Medicine and Health Sciences
MACQUARIE UNIVERSITY NSW 2109

Phone: +61 (0)98502773
Fax: +61 (0)98123610
Email: karen.vickery@ mq.edu.au
Email: anand.deva@ mq.edu.au

Chief Investigator's / Supervisor's Name & Title: **A/Professor Karen Vickery and A/Professor Anand Deva**

Participant Information and Consent Form

Name of Project: Breast implant related infection, biofilm, capsular contracture and cancer

We would like to invite you as a healthy person receiving breast implants to participate in an investigation into breast augmentation complications by donating a small amount of blood. As a patient without any complications we will compare the proteins and cells in your blood against the proteins and cells in blood obtained from patients with breast implant related complications. Your blood will act as a normal control. In this way we hope to better understand the biological and immunological causes associated with breast implant capsular contracture (constriction of tissue around the breast implant) and cancer.

The study is being conducted by Associate Professor Karen Vickery and Associate Professor Anand Deva of the Faculty of Medicine and Health Sciences. Contact either Karen Vickery on Ph 98502773, email karen.vickery@mq.edu.au or Anand Deva on Ph 98123890, email anand.deva@mq.edu.au.

If you decide to participate, you will be donating 5ml of peripheral blood at the time of surgery when you have IV access, so no additional harm or discomfort should be experienced. There will be no surgery or procedure additional to the operation that has been recommended by your surgeon. Also there will be no additional cost to you.

We will be collecting your general medical information and age for comparison between patients and data analysis. Any information or personal details gathered in the course of the study are confidential. No individual will be identified in any publication of the results. All the data will be kept securely in a locked filing cabinet in a locked room at Faculty of Medicine and Health Sciences, Macquarie University. Only study personnel will have access to the data. A summary of the results of the data can be made available to you on request by contacting either Associate Professor Karen Vickery or Associate Professor Anand Deva, Faculty of Medicine and Health Sciences, 2 Technology Place, Macquarie University 2109.

Participation in this study is entirely voluntary: you are not obliged to participate and if you decide to participate, you are free to withdraw at any time without having to give a reason and without consequence.

I, *(participant's name)* have read *(or, where appropriate, have had read to me)* and understand the information above and any questions I have asked have been answered to my satisfaction. I agree to participate in this research, knowing that I can withdraw from further participation in the research at any time without consequence. I have been given a copy of this form to keep.

Participant's Name:_____
(Block letters)

Participant's Signature:_____ Date:_____

Investigator's Name:_____
(Block letters)

Investigator's Signature: _____ __ Date:_____

The ethical aspects of this study have been approved by the Macquarie University Human Research Ethics Committee. If you have any complaints or reservations about any ethical aspect of your participation in this research, you may contact the Committee through the Director, Research Ethics & Integrity (telephone (02) 9850 7854; email ethics@mq.edu.au). Any complaint you make will be treated in confidence and investigated, and you will be informed of the outcome.

(INVESTIGATOR'S [OR PARTICIPANT'S] COPY)

Appendix 3: Validation of selected genes from *S. aureus* proteomic results using qPCR. Reverse transcription quantitative PCR relative expression normalised to 16s rRNA gene.

	Genes								
Samples	**murB**	**murC**	**pyc**	**sdhB**	**HysA**	**SA0914**	**sspA**	**femX**	**prs**
DSB1	0.0096	0.0439	0.0414	0.1535	0.0008	0.3892	0.0204	0.1331	0.0652
DSB2	0.0106	0.0485	0.0375	0.1697	0.0009	0.3522	0.0199	0.1471	0.0590
DSB average	0.0101	0.0462	0.0394	0.1616	0.0009	0.3707	0.0201	0.1401	0.0621
12dwb1	0.0016	0.0694	0.0114	0.6641	0.0055	0.1406	0.0176	0.1220	0.3513
12dwb2	0.0021	0.0107	0.0107	0.1487	0.0085	0.0376	0.0143	0.0426	0.4232
12dwb average	0.0018	0.0400	0.0111	0.4064	0.0070	0.0891	0.0160	0.0823	0.3872
3dwb1	0.0017	0.0090	0.0236	0.2237	0.0018	0.1712	0.0012	0.0363	0.2186
3dwb2	0.0007	0.0027	0.0136	0.0469	0.0011	0.1306	0.0027	0.0358	0.0798
3dwb average	0.0012	0.0058	0.0186	0.1353	0.0015	0.1509	0.0019	0.0361	0.1492
Planktonic 1	0.0942	0.1162	0.0803	0.2125	0.0572	0.1594	0.3787	0.2069	0.1202
Planktonic 2	0.0049	0.0221	0.0146	0.0336	0.0049	0.0380	0.0061	0.0477	0.0762
Planktonic average	0.0496	0.0692	0.0474	0.1230	0.0311	0.0987	0.1924	0.1273	0.0982
Comparison between the samples									
DSB/12dwb	5.4875	1.1547	3.5606	0.3977	0.1218	4.1596	1.2605	1.7029	0.1604
DSB/3dwb	8.3944	7.9089	2.1232	1.1945	0.5821	2.4567	10.3820	3.8836	0.4165
DSB/Planktonic	0.2036	0.6685	0.8317	1.3137	0.0274	3.7557	0.1046	1.1004	0.6326
12dwb/3dwb	1.5297	6.8493	0.5963	3.0037	4.7784	0.5906	8.2365	2.2806	2.5962
12dwb/Planktonic	0.0371	0.5789	0.2336	3.3034	0.2247	0.9029	0.0830	0.6462	3.9430
3dwb/Planktonic	0.0243	0.0845	0.3917	1.0998	0.0470	1.5288	0.0101	0.2833	1.5188

Appendix 4. Functional classification of the significantly upregulated common proteins between 3dwb and 12dwb compared with planktonic culture (p <0.05). *FC denotes fold change; ** CM denotes Cytoplasmic Membrane.

Accession ID	Protein Name	Gene Name	3dwb (FC)*	12dwb (FC)*	Protein Pathways	Subcellular Localisation
AIO20486.1	hypothetical protein KQ76_04110	SA0772	5.09	2.36		Unknown
AIO21910.1	molybdenum ABC transporter permease	modB	4.68	2.57	ABC transporters	CM**
AIO20812.1	DNA-directed RNA polymerase subunit omega	rpoZ SA1053	4.52	3.74	Metabolic pathways, Pyrimidine metabolism, RNA polymerase, Purine metabolism	Unknown
AIO19852.1	branched-chain amino acid transporter II carrier protein	SA0180	4.04	3.81		CM
AIO21307.1	hypothetical protein KQ76_08425	SA1443	3.57	2.10		Cytoplasmic
AIO21316.1	hypothetical protein KQ76_08470	SAS049	3.38	2.21		Unknown
AIO21773.1	membrane protein	SA1937	3.32	3.20		CM
AIO21982.1	hypothetical protein KQ76_12230	SACOL2344	3.30	2.32		Cytoplasmic
AIO21211.1	2-oxoisovalerate dehydrogenase	bfmBAA	3.19	2.12	Metabolic pathways, Biosynthesis of secondary metabolites, Biosynthesis of antibiotics, Propanoate metabolism, Valine, leucine and isoleucine degradation	Cytoplasmic
AIO21660.1	DNA-binding protein		3.12	2.97		Cytoplasmic
AIO22226.1	fructosamine kinase	SA2374	2.97	2.71		Cytoplasmic

AIO21786.1	lytic regulatory protein	truncated-SA	2.89	2.02		CM
AIO22040.1	formate/nitrite transporter	SACOL2401	2.84	2.56		CM
AIO22234.1	pantoate--beta-alanine ligase	panC SACOL2614	2.82	2.91	Metabolic pathways, Biosynthesis of secondary metabolites, beta-Alanine metabolism, Pantothenate and CoA biosynthesis	Cytoplasmic
AIO20178.1	dihydropteroate synthase	folP SA0472	2.76	3.28	Metabolic pathways, Folate biosynthesis	Cytoplasmic
AIO20787.1	cell division protein FtsA	ftsA SA1028	2.74	2.94		Cytoplasmic
AIO20718.1	glycerophosphodiester phosphodiesterase	SA0969	2.72	2.38	Glycerophospholipid metabolism	Cytoplasmic
AIO21337.1	50S ribosomal protein L27	rpmA SA1471	2.64	2.64	Ribosome	Cytoplasmic
AIO21727.1	membrane protein	yidC SA1893	2.53	2.46	Quorum sensing, Protein export, Bacterial secretion system	CM
AIO21819.1	hypothetical protein KQ76_11385	SA1986	2.52	3.27		CM
AIO22003.1	L-lactate permease	SACOL2363	2.47	2.50		CM
AIO21769.1	hypothetical protein KQ76_11075	SA1933	2.47	2.10		Cytoplasmic
AIO20806.1	orotidine 5'-phosphate decarboxylase	pyrF SA1047	2.42	2.54	Metabolic pathways, Pyrimidine metabolism	Cytoplasmic
AIO20697.1	spermidine/putrescine ABC transporter ATP-binding protein	potA SA0950	2.39	2.30	ABC transporters	CM

AIO21790.1	glucosamine--fructose-6-phosphate aminotransferase	glmS SACOL2145	2.37	2.13	Metabolic pathways, Amino sugar and nucleotide sugar metabolism, Alanine, aspartate and glutamate metabolism, Biosynthesis of antibiotics	Cytoplasmic
AIO20817.1	peptide deformylase	SA1058	2.35	2.10		Cytoplasmic
AIO21826.1	PTS system lactose-specific transporter subunit IIA	lacF SA1993	2.34	2.36	Metabolic pathways, Galactose metabolism, Phosphotransferase system (PTS)	Cytoplasmic
AIO21333.1	ATP-dependent DNA helicase RuvB	ruvB SACOL1696	2.33	2.55	Homologous recombination	Cytoplasmic
AIO20958.1	guanosine 5'-monophosphate oxidoreductase	guaC SACOL1371	2.28	3.28	Purine metabolism	Cytoplasmic
AIO20949.1	threonine synthase	thrC SACOL1363	2.27	2.00	Metabolic pathways, Biosynthesis of secondary metabolites, Microbial metabolism in diverse environments, Vitamin B6 metabolism, Glycine, serine and threonine metabolism, Biosynthesis of amino acids	Cytoplasmic
AIO19973.1	5'-nucleotidase	SA0295	2.23	2.77		Unknown

AIO20535.1	argininosuccinate lyase	argH SA0821	2.21	2.43	Metabolic pathways, Biosynthesis of secondary metabolites, Biosynthesis of antibiotics, Biosynthesis of amino acids, Alanine, aspartate and glutamate metabolism, Arginine biosynthesis	Cytoplasmic
AIO20535.1	argininosuccinate lyase	argH SA0821	2.21	2.43	Metabolic pathways, Biosynthesis of secondary metabolites, Biosynthesis of antibiotics, Biosynthesis of amino acids, Alanine, aspartate and glutamate metabolism, Arginine biosynthesis	Cytoplasmic
AIO21768.1	pantothenate kinase	coaW SA1932	2.17	2.01	Metabolic pathways, Pantothenate and CoA biosynthesis	Unknown
AIO21133.1	capsid protein		2.17	2.03		Extracellular
AIO20536.1	argininosuccinate synthase	argG SA0822	2.15	2.01	Metabolic pathways, Biosynthesis of secondary metabolites, Biosynthesis of antibiotics, Biosynthesis of amino acids, Alanine, aspartate and glutamate metabolism, Arginine biosynthesis	Cytoplasmic
AIO20205.1	50S ribosomal protein L10	rplJ SA0497	2.15	2.16	Ribosome	Cytoplasmic
AIO22278.1	amino acid APC transporter	arcD	2.10	2.23		CM
AIO20778.1	hypothetical protein KQ76_05635	SA1019	2.09	2.41		Unknown

AIO20985.1	LytR family transcriptional regulator	msrR SA1195	2.08	2.13		CM
OOC90965.1	glutamine ABC transporter ATP-binding protein	SA1674	2.05	2.83		CM
AIO19823.1	UDP-N-acetylglucosamine 2-epimerase	capG	2.02	2.09	Metabolic pathways, Amino sugar and nucleotide sugar metabolism	Cytoplasmic

Appendix 5. Functional classification of the significantly downregulated common proteins between 3dwb and 12dwb compared with planktonic culture (p <0.05). *FC denotes fold change; ** CM denotes Cytoplasmic Membrane.

Accession ID	Protein Name	Gene Name	3dwb (FC)*	12dwb (FC)*	Protein Pathways	Subcellular Localisation
AIO21667.1	delta-hemolysin	hld SA1841.1 SAS065	0.03	0.03	Quorum sensing	Cytoplasmic
AIO20700.1	spermidine/putrescine ABC transporter substrate-binding protein	potD	0.05	0.08	ABC transporters	Unknown
AIO20763.1	alpha-hemolysin	SA1007	0.07	0.06		Extracellular
AIO22369.1	phosphodiesterase	hlb SACOL2003	0.08	0.12		Extracellular
OOC90902.1	calcium-binding protein	SACOL1846	0.08	0.05		Unknown
AIO20644.1	cysteine protease	sspB SACOL1056	0.09	0.11		Extracellular
AIO22207.1	transglycosylase	isaA SACOL2584	0.10	0.11		Extracellular
AIO20556.1	hypothetical protein KQ76_04470	SA0841	0.11	0.08		CM**
AIO19942.1	peptidase M23	lytM SACOL0263	0.11	0.12		Extracellular
AIO20056.1	hypothetical protein KQ76_01725		0.12	0.10		CM
AIO20660.1	chitinase	SA0914	0.12	0.09		Extracellular
AIO19947.1	staphyloxanthin biosynthesis protein	SACOL0270	0.13	0.13		Extracellular
AIO21349.1	DNA-3-methyladenine glycosylase	tag	0.14	0.40	Base excision repair	Unknown
AIO21509.1	serine protease	splC SACOL1867	0.14	0.28		Extracellular
AIO20463.1	thermonuclease	nuc SACOL0860	0.14	0.16		Extracellular
AIO20332.1	peptidase M23B	SA0620	0.15	0.14		Cellwall
AIO20645.1	glutamyl endopeptidase	sspA SACOL1057	0.15	0.15	Quorum sensing	Extracellular

AIO20716.1	SCP-like extracellular protein	SA0967	0.15	0.17		Unknown
AIO19770.1	1-phosphatidylinositol phosphodiesterase	plc	0.17	0.19	Inositol phosphate metabolism	Extracellular
AIO20387.1	glycerol phosphate lipoteichoic acid synthase	ltaS SA0674	0.17	0.15	Metabolic pathways, Glycerolipid metabolism	CM
AIO22290.1	N-acetylmuramoyl-L-alanine amidase	SACOL2666	0.17	0.14		Extracellular
AIO21492.1	hypothetical protein KQ76_09365	SACOL1852	0.19	0.16		Unknown
AIO21221.1	acetyl-CoA carboxylase	accB	0.19	0.23	Metabolic pathways, Microbial metabolism in diverse environments, Biosynthesis of secondary metabolites, Biosynthesis of antibiotics, Pyruvate metabolism, Carbon metabolism, Fatty acid metabolism, Propanoate metabolism, Fatty acid biosynthesis	Cytoplasmic
AIO19779.1	peptidoglycan-binding protein LysM	spa SACOL0095	0.21	0.16	*Staphylococcus aureus* infection	Cell wall
AIO20739.1	ribonuclease HIII	rnhC SACOL1150	0.22	0.22	DNA replication	Unknown
AIO20228.1	hydrolase	sdrD SA0520	0.22	0.22	*Staphylococcus aureus* infection	Cell wall
AIO20126.1	N-acetylmuramoyl-L-alanine amidase	sle1 aaa SA0423	0.23	0.29		Cell wall
AIO20637.1	acetyltransferase	SA0893	0.23	0.17		Cytoplasmic

AIO21273.1	molecular chaperone DnaJ	dnaJ SA1408	0.24	0.21		Cytoplasmic
AIO20577.1	competence negative regulator MecA	mecA SA0857	0.24	0.31		Cytoplasmic
AIO20418.1	ABC transporter	SACOL0811	0.24	0.27		Cytoplasmic
AIO21353.1	delta-aminolevulinic acid dehydratase	hemB SA1492	0.24	0.27	Metabolic pathways, Microbial metabolism in diverse environments, Biosynthesis of secondary metabolites, Porphyrin and chlorophyll metabolism	Cytoplasmic
AIO21508.1	serine protease	splE SACOL1865	0.24	0.40	Quorum sensing	Extracellular
AIO19987.1	lipase	lip2 geh SA0309	0.24	0.14	Metabolic pathways, Glycerolipid metabolism	Extracellular
AIO20651.1	mannosyl-glycoprotein endo-beta-N-acetylglucosamidase	atl nag SACOL1062	0.25	0.24		Extracellular
AIO21549.1	Fur family transcriptional regulator	perR SACOL1919	0.25	0.48		Cytoplasmic
AIO22042.1	glutathione S-transferase	SACOL2402	0.25	0.29		Unknown
AIO21406.1	Free methionine-(R)-sulfoxide reductase	SACOL1768	0.26	0.26	Cysteine and methionine metabolism	Cytoplasmic
AIO20229.1	bis(5'-nucleosyl)-tetraphosphatase	sdrE SACOL0610	0.26	0.26	*Staphylococcus aureus* infection	Cellwall
AIO22060.1	gamma-hemolysin subunit A	hlgC SA2208	0.26	0.35	*Staphylococcus aureus* infection	Extracellular
AIO20738.1	phenylalanyl-tRNA synthase subunit beta	pheT SA0986	0.27	0.38	Aminoacyl-tRNA biosynthesis	Cytoplasmic
AIO21601.1	cysteine protease	sspP scpA SA1725	0.27	0.23		Extracellular
AIO20874.1	50S ribosomal protein L7	SA1111	0.27	0.34		Unknown

AIO21505.1	serine protease	splF SA1627	0.27	0.25	Quorum sensing	Extracellular
AIO22081.1	sodium:proton antiporter	SA2228	0.27	0.21		CM
AIO20884.1	zinc protease	SA1121	0.27	0.29		Cytoplasmic
AIO20093.1	superantigen-like protein	set11	0.28	0.33	*Staphylococcus aureus* infection	Extracellular
AIO21182.1	transcriptional regulator	srrA SA1323	0.28	0.33	Two-component system	Cytoplasmic
AIO20960.1	secretion protein	SACOL1373	0.28	0.47		Unknown
AIO22350.1	peptidase		0.28	0.13		Extracellular
AIO21805.1	uridylyltransferase	SA1974	0.28	0.36		Cytoplasmic
AIO21160.1	single-stranded DNA-binding protein	ssb	0.28	0.39	Homologous recombination, Mismatch repair, DNA replication	Unknown
AIO22099.1	peptidase M28	SA2244	0.29	0.32		Cytoplasmic
AIO22349.1	hypothetical protein	KQ76_14165	0.29	0.30		Unknown
AIO20756.1	formyl peptide receptor-like 1 inhibitory protein	flr SA1001	0.30	0.35	*Staphylococcus aureus* infection	Unknown
AIO20951.1	HAD family hydrolase	SA1167	0.30	0.43		Cytoplasmic
AIO22292.1	adhesin	sasF SACOL2668	0.30	0.43		Cellwall
AIO19988.1	alpha/beta hydrolase	SACOL0391	0.31	0.32		Cytoplasmic
AIO20737.1	phenylalanine--tRNA ligase	pheS SA0985	0.31	0.35	Aminoacyl-tRNA biosynthesis	Cytoplasmic
AIO21246.1	penicillin-binding protein	pbp3	0.31	0.36	Metabolic pathways, beta-Lactam resistance, Peptidoglycan biosynthesis	CM
OOC94232.1	aureolysin	aur SACOL2659	0.31	0.32	*Staphylococcus aureus* infection, Cationic antimicrobial peptide (CAMP) resistance	Extracellular

AIO21853.1	50S ribosomal protein L17	rplQ SA2022	0.31	0.44	Ribosome	Cytoplasmic
AIO21842.1	toxin	SACOL2197	0.32	0.40		CM
AIO21565.1	hypothetical protein KQ76_09970	SAS054	0.32	0.37		Cytoplasmic
AIO22160.1	lactate dehydrogenase	ldhD ddh SACOL2535	0.33	0.29	Pyruvate metabolism, Microbial metabolism in diverse environments	Cytoplasmic
AIO20515.1	hypothetical protein KQ76_04260	SACOL0943	0.33	0.50		Cytoplasmic
AIO20442.1	hypothetical protein KQ76_03870	SACOL0835	0.33	0.32		Cytoplasmic
OOC94758.1	alpha/beta hydrolase	SA1990	0.34	0.33		Unknown
AIO22074.1	glycerate kinase	SA2220	0.34	0.24	Metabolic pathways, Microbial metabolism in diverse environments, Biosynthesis of antibiotics, Glycerolipid metabolism, Glyoxylate and dicarboxylate metabolism, Glycine, serine and threonine metabolism	Cytoplasmic
AIO21275.1	heat shock protein GrpE	grpE SA1410	0.34	0.36		Cytoplasmic
AIO22275.1	clumping factor B	clfB SA2423	0.34	0.33	*Staphylococcus aureus* infection	Cellwall
AIO20071.1	NADPH-dependent oxidoreductase	nfrA SACOL0453	0.34	0.26	Metabolic pathways, Riboflavin metabolism	Cytoplasmic
AIO22317.1	lipase	lip1 SA2463	0.35	0.20	Metabolic pathways, Glycerolipid metabolism	Extracellular

AIO19780.1	MarR family transcriptional regulator	sarS sarH1 SA0108	0.35	0.45		Cytoplasmic
AIO20100.1	hypothetical protein KQ76_01960	SA0395	0.35	0.14		Unknown
AIO20863.1	elongation factor Ts	tsf SACOL1276	0.35	0.36		Cytoplasmic
OOC93971.1	phosphoglucomutase	pgcA SA2279	0.36	0.41	Metabolic pathways, Microbial metabolism in diverse environments, Biosynthesis of secondary metabolites, Biosynthesis of antibiotics, Purine metabolism, Amino sugar and nucleotide sugar metabolism, Starch and sucrose metabolism, Streptomycin biosynthesis, Glycolysis / Gluconeogenesis, Pentose phosphate pathway, Galactose metabolism	Cytoplasmic
AIO21506.1	serine protease	splE SACOL1865	0.36	0.36		Extracellular
AIO20279.1	hypothetical protein KQ76_03005	SA0570	0.36	0.48		Unknown
AIO21343.1	membrane protein	SA1476	0.36	0.30		Unknown
AIO22338.1	adhesin		0.46	0.37		Cellwall
AIO20534.1	glycerophosphodiester phosphodiesterase	glpQ	0.37	0.22	Glycerophospholipid metabolism	Cellwall
AIO21274.1	molecular chaperone DnaK	dnaK SA1409	0.37	0.43	RNA degradation	Cytoplasmic

AIO21449.1	leucyl-tRNA synthetase	leuS SA1579	0.37	0.36	Aminoacyl-tRNA biosynthesis	Cytoplasmic
AIO21282.1	competence protein ComE	comEB	0.37	0.41	Metabolic pathways, Pyrimidine metabolism	Cytoplasmic
AIO20170.1	hypothetical protein KQ76_02355	SA0464	0.38	0.43		Cytoplasmic
AIO21073.1	hypothetical protein KQ76_07205	SACOL1491	0.38	0.51		Unknown
AIO21788.1	HAD family hydrolase	SA1957	0.38	0.30		Cytoplasmic
AIO22136.1	fibronectin-binding protein	fnbA SA2291	0.39	0.23	Bacterial invasion of epithelial cells	Cellwall
OOC92415.1	sphingomyelin phosphodiesterase	hlb SACOL2003	0.39	0.33	Quorum sensing, Metabolic pathways, Inositol phosphate metabolism, Glycerophospholipid metabolism, Biosynthesis of secondary metabolites	Extracellular
AIO21298.1	acetyl-CoA carboxylase biotin carboxylase subunit	SA1434	0.40	0.41	Metabolic pathways, Microbial metabolism in diverse environments, Biosynthesis of secondary metabolites, Biosynthesis of antibiotics, Pyruvate metabolism, Carbon metabolism, Fatty acid metabolism, Propanoate metabolism, Fatty acid biosynthesis	Cytoplasmic

AIO22387.1	replication-associated protein (plasmid)	SAP031	0.40	0.41		Unknown
AIO20202.1	antitermination protein NusG	nusG SA0494	0.40	0.46		Cytoplasmic
AIO21033.1	hypothetical protein KQ76_06965	SA1242	0.41	0.46		Unknown
AIO20885.1	zinc protease	SACOL1298	0.42	0.46		Unknown
AIO21583.1	ferritin	ftnA SA1709	0.42	0.44		Cytoplasmic
AIO20406.1	iron ABC transporter substrate-binding protein	SA0691	0.42	0.35	ABC transporters	CM
AIO20712.1	pyruvate carboxylase	pyc SACOL1123	0.43	0.50	Metabolic pathways, Pyruvate metabolism, Microbial metabolism in diverse environments, Biosynthesis of amino acids, Carbon metabolism, Citrate cycle (TCA cycle)	Cytoplasmic
AIO20704.1	hypothetical protein KQ76_05255	SA0957	0.43	0.49		Cytoplasmic
AIO21607.1	nitric oxide synthase	nos SA1730	0.43	0.44	Metabolic pathways, Biosynthesis of secondary metabolites, Arginine biosynthesis, Arginine and proline metabolism	Cytoplasmic
AIO22191.1	TetR family transcriptional regulator	SA2340	0.43	0.51		Cytoplasmic
AIO20225.1	HAD family hydrolase	SA0517	0.43	0.42		Cytoplasmic
AIO22285.1	hypothetical protein KQ76_13835	SACOL2661	0.43	0.37		Extracellular

AIO19949.1	type VII secretion protein EsaA	esaA SA0272	0.44	0.43		CM
AIO21157.1	replication protein		0.44	0.31		Cytoplasmic
AIO22336.1	pyrrolidone-carboxylate peptidase	pcp SACOL2714	0.44	0.32		Cytoplasmic
AIO20749.1	succinate dehydrogenase	sdhB	0.45	0.28	Metabolic pathways, Microbial metabolism in diverse environments, Biosynthesis of secondary metabolites, Biosynthesis of antibiotics, Carbon metabolism, Citrate cycle (TCA cycle), Oxidative phosphorylation, Butanoate metabolism	Cytoplasmic
AIO20783.1	penicillin-binding protein	pbpA	0.46	0.39	Metabolic pathways, beta-Lactam resistance, Peptidoglycan biosynthesis	CM
AIO19900.1	nitric oxide dioxygenase	SA0231	0.47	0.34		Cytoplasmic
AIO21223.1	peptidase M24	SACOL1588	0.47	0.50		Cytoplasmic
AIO20194.1	glutamyl-tRNA synthetase	gltX SA0486	0.47	0.39	Metabolic pathways, Aminoacyl-tRNA biosynthesis	Cytoplasmic
AIO20273.1	arginine--tRNA ligase	argS SACOL0663	0.47	0.48	Aminoacyl-tRNA biosynthesis	Cytoplasmic
AIO20259.1	dihydrolipoamide dehydrogenase	SA0551	0.48	0.42		Cytoplasmic
AIO20623.1	conjugal transfer protein	SACOL1582	0.48	0.42		Unknown

AIO22143.1	hypothetical protein KQ76_13105	SACOL2519	0.48	0.30		Cytoplasmic
AIO21116.1	gamma-hemolysin subunit A	hlgC SA2208	0.48	0.35		Extracellular
AIO21194.1	ribonuclease Z	rnz SACOL1548	0.49	0.47		Cytoplasmic
AIO20555.1	phosphatidylethanolamine-binding protein	SACOL0984	0.49	0.49		Unknown
AIO20584.1	GTP pyrophosphokinase	SA0864	0.49	0.50	Purine metabolism	Cytoplasmic
AIO20455.1	hypothetical protein KQ76_03935	SACOL0851	0.49	0.42		Unknown
AIO20687.1	hypothetical protein KQ76_05170	SA0941	0.49	0.50		Cytoplasmic
AIO20838.1	cell division protein FtsY	ftsY SACOL1251	0.49	0.49	Quorum sensing, Protein export, Bacterial secretion system	CM
OOC91307.1	hypothetical protein BWO94_08325	SA1008	0.50	0.50		Unknown
AIO20835.1	acyl carrier protein	acpP hmrB SA1075	0.50	0.47		Cytoplasmic
AIO20196.1	cysteinyl-tRNA synthetase	cysS SACOL0576	0.50	0.41	Aminoacyl-tRNA biosynthesis	Cytoplasmic
AIO19963.1	QueA protein	SACOL0282	0.50	0.49		Cytoplasmic
AIO22017.1	hypothetical protein KQ76_12415	SA2168	0.50	0.39		Unknown
AIO20583.1	hypothetical protein KQ76_04610	SACOL1009	0.51	0.46		CM

Appendix 6. Functional classification of the significantly upregulated common proteins between 12dwb and DSB compared with planktonic culture (p <0.05). *FC denotes fold change; ** CM denotes Cytoplasmic Membrane.

Accession ID	Protein Name	Gene Name	12dwb (FC)*	DSB (FC)*	Protein Pathways	Subcellular Localisation
AIO22223.1	type II secretion protein	SA2371	3.59	2.46		Unknown
AIO21382.1	isocitrate dehydrogenase	icd citC SA1517	3.06	2.17	Metabolic pathways, Biosynthesis of secondary metabolites, Biosynthesis of amino acids, Biosynthesis of antibiotics, Microbial metabolism in diverse environments, Carbon metabolism, 2-Oxocarboxylic acid metabolism, Glutathione metabolism, Citrate cycle (TCA cycle)	Cytoplasmic
AIO20590.1	membrane protein	SA0870	2.62	2.04		CM**
AIO22305.1	hypothetical protein KQ76_13935	SA2451	5.52	4.40		Unknown
OOC90965.1	glutamine ABC transporter ATP-binding protein	SA1674	2.83	2.30		CM
AIO20668.1	phosphoribosylformylglycin amidine synthase	purL SACOL1078	2.45	2.03	Metabolic pathways, Biosynthesis of secondary metabolites, Purine metabolism, Biosynthesis of antibiotics	Cytoplasmic

AIO20812.1	DNA-directed RNA polymerase subunit omega	rpoZ SA1053	3.74	3.16	Metabolic pathways, Pyrimidine metabolism, Purine metabolism, RNA polymerase,	Cytoplasmic
AIO20535.1	argininosuccinate lyase	argH SA0821	2.43	2.06	Metabolic pathways, Biosynthesis of secondary metabolites, Biosynthesis of amino acids, Biosynthesis of antibiotics, Alanine, aspartate and glutamate metabolism, Arginine biosynthesis	Cytoplasmic
AIO20780.1	cell division protein MraZ	mraZ SA1021	2.58	2.21		Cytoplasmic
AIO19852.1	branched-chain amino acid transporter II carrier protein	SA0180	3.81	3.27		CM
AIO20178.1	dihydropteroate synthase	folP SA0472	3.28	2.81	Metabolic pathways, Folate biosynthesis	CM
AIO20178.1	dihydropteroate synthase	folP SA0472	3.28	2.81	Metabolic pathways, Folate biosynthesis	Cytoplasmic
AIO21773.1	membrane protein	SA1937	3.20	2.82		CM
AIO21226.1	octanoyltransferase	lipM SA1363	2.68	2.38	Metabolic pathways, Lipoic acid metabolism	Cytoplasmic
AIO20979.1	sodium:alanine symporter	alsT	2.67	2.42		CM
AIO20958.1	guanosine 5'-monophosphate oxidoreductase	guaC SACOL1371	3.28	2.97	Purine metabolism	Cytoplasmic
AIO21819.1	hypothetical protein KQ76_11385	SA1986	3.27	2.96		CM

AIO22040.1	formate/nitrite transporter	SACOL2401	2.56	2.33		CM
AIO21727.1	membrane protein	yidC SA1893	2.46	2.27	Protein export, Bacterial secretion system, Quorum sensing	CM
AIO21864.1	50S ribosomal protein L18	rplR SA2032	2.33	2.19	Ribosome	Cytoplasmic
AIO19795.1	acetoin reductase	butA SA0122	2.49	2.35	Butanoate metabolism	Cytoplasmic
AIO22226.1	fructosamine kinase	SA2374	2.71	2.55		Cytoplasmic
AIO21765.1	CTP synthetase	pyrG ctrA SA1929	2.32	2.24	Metabolic pathways, Pyrimidine metabolism	Cytoplasmic
AIO21934.1	octopine dehydrogenase	SA2095	2.20	2.13		Cytoplasmic
AIO20806.1	orotidine 5'-phosphate decarboxylase	pyrF SA1047	2.54	2.49	Metabolic pathways, Pyrimidine metabolism	Cytoplasmic
AIO21333.1	ATP-dependent DNA helicase RuvB	ruvB SACOL1696	2.55	2.50	Homologous recombination	Cytoplasmic 9.98

AIO21826.1	PTS system lactose-specific transporter subunit IIA	lacF SA1993	2.36	2.32	Metabolic pathways, Galactose metabolism, Phosphotransferase system (PTS)	Cytoplasmic 10.01
AIO20163.1	ribose-phosphate pyrophosphokinase	prs SA0458	2.81	2.79	Metabolic pathways, Biosynthesis of secondary metabolites, Biosynthesis of amino acids, Biosynthesis of antibiotics, Purine metabolism, Microbial metabolism in diverse environments, Carbon metabolism, Pentose phosphate pathway	Cytoplasmic
AIO21316.1	hypothetical protein KQ76_08470	SAS049	2.21	2.21		Unknown
AIO21860.1	preprotein translocase subunit SecY	secY SA2028	2.15	2.16	Protein export, Bacterial secretion system, Quorum sensing	CM
AIO21768.1	pantothenate kinase	coaW SA1932	2.01	2.03	Metabolic pathways, Pantothenate and CoA biosynthesis	Unknown
AIO20718.1	glycerophosphodiester phosphodiesterase	SA0969	2.38	2.45	Glycerophospholipid metabolism	Cytoplasmic
AIO21539.1	pseudouridine synthase	SA1668	2.50	2.58		Cytoplasmic
AIO20864.1	uridylate kinase	pyrH smbA SA1101	2.07	2.20	Metabolic pathways, Pyrimidine metabolism	Cytoplasmic

AIO20697.1	spermidine/putrescine ABC transporter ATP-binding protein	potA SA0950	2.30	2.46	ABC transporters	CM
AIO21307.1	hypothetical protein KQ76_08425	SA1443	2.10	2.26		Cytoplasmic
AIO21769.1	hypothetical protein KQ76_11075	SA1933	2.10	2.26		Cytoplasmic
AIO20807.1	orotate phosphoribosyltransferase	pyrE SA1048	2.13	2.30	Metabolic pathways, Pyrimidine metabolism	Cytoplasmic
AIO21210.1	2-oxoisovalerate dehydrogenase	SACOL1561	3.11	3.36	Metabolic pathways, Biosynthesis of secondary metabolites, Biosynthesis of antibiotics, Propanoate metabolism, Valine, leucine and isoleucine degradation	Cytoplasmic
AIO21335.1	ACT domain-containing protein	SA1469	3.27	3.59	Metabolic pathways, Biosynthesis of secondary metabolites, Biosynthesis of amino acids, Biosynthesis of antibiotics, Phenylalanine, tyrosine and tryptophan biosynthesis	Cytoplasmic
AIO22278.1	amino acid APC transporter	arcD	2.23	2.47		CM
AIO20787.1	cell division protein FtsA	ftsA SA1028	2.94	3.29		Cytoplasmic
AIO21825.1	PTS system lactose-specific transporter subunits IICB	lacE SACOL2181	2.27	2.54	Metabolic pathways, Phosphotransferase system (PTS), Galactose metabolism	CM

AIO21878.1	50S ribosomal protein L23	rplW SA2045	2.15	2.41	Ribosome	Cytoplasmic
AIO20778.1	hypothetical protein KQ76_05635	SA1019	2.41	2.71		Unknown
AIO21910.1	molybdenum ABC transporter permease	modB	2.57	2.93	ABC transporters	CM
AIO21879.1	50S ribosomal protein L4	rplD SA2046	2.03	2.33	Ribosome	Unknown
AIO20968.1	exonuclease	sbcD SA1180	2.36	2.73		Cytoplasmic
AIO22176.1	PTS system glucose-specific transporter subunit IICBA	glcB SACOL2552	2.07	2.40	Phosphotransferase system (PTS), Amino sugar and nucleotide sugar metabolism, Glycolysis / Gluconeogenesis	CM
AIO22234.1	pantoate--beta-alanine ligase	panC SACOL2614	2.91	3.42	Metabolic pathways, Biosynthesis of secondary metabolites, Pantothenate and CoA biosynthesis, beta-Alanine metabolism	Cytoplasmic
AIO21337.1	50S ribosomal protein L27	rpmA SA1471	2.64	3.12	Ribosome	Cytoplasmic
AIO20205.1	50S ribosomal protein L10	rplJ SA0497	2.16	2.69	Ribosome	Cytoplasmic
AIO20817.1	peptide deformylase	SA1058	2.10	2.66		Cytoplasmic
AIO19749.1	hypothetical protein KQ76_00135		2.73	3.48		Cytoplasmic
AIO20985.1	LytR family transcriptional regulator	msrR SA1195	2.13	2.75		CM
AIO21707.1	4'-phosphopantetheinyl transferase	acpS dpj SA1875	2.37	3.18	Pantothenate and CoA biosynthesis	

OOC94735.1	hypothetical protein BWO94_01050		3.63	4.91		Unknown
AIO20937.1	hypothetical protein KQ76_06475	SAS040	2.84	3.94		Unknown
AIO20620.1	hypothetical protein KQ76_04815	SACOL1585	2.20	3.15		Unknown
AIO20395.1	lipid kinase	SACOL0787	2.05	3.03		Unknown
AIO21848.1	50S ribosomal protein L13	rplM SA2017	2.14	3.28	Ribosome	Unknown

Appendix 7. Functional classification of the significantly downregulated common proteins between 12dwb and DSB compared with planktonic culture (p <0.05). *FC denotes fold change; ** CM denotes Cytoplasmic Membrane.

Accession ID	Protein Name	Gene Name	12dwb (FC)*	DSB (FC)*	Protein Pathways	Subcellular Localisation
AIO20700.1	spermidine/putrescine ABC transporter substrate-binding protein	potD	0.08	0.04	ABC transporters	Unknown
AIO22060.1	gamma-hemolysin subunit A	hlgC SA2208	0.35	0.22	*Staphylococcus aureus* infection	Extracellular
AIO20660.1	chitinase	SA0914	0.09	0.06		Unknown
AIO20463.1	thermonuclease	nuc SACOL0860	0.16	0.12		Extracellular
AIO21509.1	serine protease	splC SACOL1867	0.28	0.20		Extracellular
AIO20279.1	hypothetical protein KQ76_03005	SA0570	0.48	0.36		Unknown
AIO19987.1	lipase	lip2 geh SA0309	0.14	0.10	Metabolic pathways, Glycerolipid metabolism	Extracellular
AIO20583.1	hypothetical protein KQ76_04610	SACOL1009	0.46	0.35		CM**
AIO20651.1	mannosyl-glycoprotein endo-beta-N-acetylglucosamidase	atl nag SACOL1062	0.24	0.18		Extracellular

AIO21353.1	delta-aminolevulinic acid dehydratase	hemB SA1492	0.27	0.21	Metabolic pathways, Microbial metabolism in diverse environments, Biosynthesis of secondary metabolites, Porphyrin and chlorophyll metabolism	Cytoplasmic
AIO20960.1	secretion protein	SACOL1373	0.47	0.37		Unknown
AIO21128.1	hypothetical protein KQ76_07495		0.35	0.28		Cytoplasmic
OOC94758.1	alpha/beta hydrolase	SA1990	0.33	0.26		Unknown
AIO20644.1	cysteine protease	sspB SACOL1056	0.11	0.09		Extracellular
AIO19870.1	peptidase M23	SA0205	0.19	0.16		Extracellular
AIO20093.1	superantigen-like protein	set11	0.33	0.28	*Staphylococcus aureus* infection	Extracellular
AIO20534.1	glycerophosphodiester phosphodiesterase	glpQ	0.22	0.18		Unknown
AIO20738.1	phenylalanyl-tRNA synthase subunit beta	pheT SA0986	0.38	0.33	Aminoacyl-tRNA biosynthesis	Cytoplasmic
AIO22292.1	adhesin	sasF SACOL2668	0.43	0.37		Cellwall
AIO21549.1	Fur family transcriptional regulator	perR SACOL1919	0.48	0.42		Cytoplasmic
AIO21667.1	delta-hemolysin	hld SA1841.1 SAS065	0.03	0.03	Quorum sensing	Unknown
AIO20100.1	hypothetical protein KQ76_01960	SA0395	0.14	0.12		Unknown
AIO20951.1	HAD family hydrolase	SA1167	0.43	0.37		Cytoplasmic
AIO20623.1	conjugal transfer protein	SACOL1582	0.42	0.37		Unknown

AIO22349.1	hypothetical protein KQ76_14165		0.30	0.27		Unknown
AIO20056.1	hypothetical protein KQ76_01725		0.10	0.09		CM
AIO21298.1	acetyl-CoA carboxylase biotin carboxylase subunit	SA1434	0.41	0.36	Metabolic pathways, Microbial metabolism in diverse environments, Biosynthesis of secondary metabolites, Biosynthesis of antibiotics, Carbon metabolism, Fatty acid metabolism, Propanoate metabolism, Pyruvate metabolism, Fatty acid biosynthesis	Cytoplasmic
AIO19780.1	MarR family transcriptional regulator	sarS sarH1 SA0108	0.45	0.40		Cytoplasmic
AIO20712.1	pyruvate carboxylase	pyc SACOL1123	0.50	0.45	Metabolic pathways, Pyruvate metabolism, Microbial metabolism in diverse environments, Biosynthesis of amino acids, Citrate cycle (TCA cycle), Carbon metabolism	Cytoplasmic
AIO19770.1	1-phosphatidylinositol phosphodiesterase	plc	0.19	0.17	Inositol phosphate metabolism	Extracellular
AIO22290.1	N-acetylmuramoyl-L-alanine amidase	SACOL2666	0.14	0.12		Extracellular
AIO20332.1	peptidase M23B	SA0620	0.14	0.13		Cell wall

AIO20756.1	formyl peptide receptor-like 1 inhibitory protein	flr SA1001	0.35	0.32	*Staphylococcus aureus* infection	Unknown
AIO21349.1	DNA-3-methyladenine glycosylase	tag	0.40	0.36	Base excision repair	Unknown
AIO21997.1	LytTR family transcriptional regulator	SA2153	0.43	0.40		Unknown
AIO21607.1	nitric oxide synthase	nos SA1730	0.44	0.40	Metabolic pathways, Biosynthesis of secondary metabolites, Arginine biosynthesis, Arginine and proline metabolism	Cytoplasmic
AIO20419.1	DegV domain-containing protein	SACOL0812	0.49	0.45		Cytoplasmic
AIO21983.1	esterase	SA2140	0.48	0.44		Cytoplasmic
AIO22180.1	LysR family transcriptional regulator	SA2330	0.34	0.32		Cytoplasmic
AIO20126.1	N-acetylmuramoyl-L-alanine amidase	sle1 aaa SA0423	0.29	0.27		Cellwall
AIO21449.1	leucyl-tRNA synthetase	leuS SA1579	0.36	0.34	Aminoacyl-tRNA biosynthesis	Cytoplasmic
AIO20739.1	ribonuclease HIII	rnhC SACOL1150	0.22	0.20	DNA replication	Unknown
AIO20704.1	hypothetical protein KQ76_05255	SA0957	0.49	0.46		Cytoplasmic
AIO20387.1	glycerol phosphate lipoteichoic acid synthase	ltaS SA0674	0.15	0.14	Metabolic pathways, Glycerolipid metabolism	CM
OOC91307.1	hypothetical protein BWO94_08325	SA1008	0.50	0.47		Unknown
AIO21583.1	ferritin	ftnA SA1709	0.44	0.42		Cytoplasmic
AIO21618.1	hypothetical protein KQ76_10250	SAS056	0.46	0.44		

AIO19947.1	staphyloxanthin biosynthesis protein	SACOL0270	0.13	0.12		Extracellular
AIO21246.1	penicillin-binding protein	pbp3	0.36	0.35	Metabolic pathways, beta-Lactam resistance, Peptidoglycan biosynthesis	CM
AIO20202.1	antitermination protein NusG	nusG SA0494	0.46	0.44		Cytoplasmic
OOC94232.1	aureolysin	aur SACOL2659	0.32	0.30	*Staphylococcus aureus* infection, Cationic antimicrobial peptide (CAMP) resistance	Extracellular
AIO19779.1	peptigoglycan-binding protein LysM	spa SACOL0095	0.16	0.15	*Staphylococcus aureus* infection	Cellwall
AIO20863.1	elongation factor Ts	tsf SACOL1276	0.36	0.35		Cytoplasmic
AIO22317.1	lipase	lip1 SA2463	0.20	0.19	Metabolic pathways, Glycerolipid metabolism	Extracellular
AIO22350.1	peptidase		0.13	0.12		Extracellular
AIO20885.1	zinc protease	SACOL1298	0.46	0.44		Unknown
AIO20273.1	arginine-tRNA ligase	argS SACOL0663	0.48	0.47	Aminoacyl-tRNA biosynthesis	Cytoplasmic
AIO21182.1	transcriptional regulator	srrA SA1323	0.33	0.32	Two-component system	Cytoplasmic
AIO20196.1	cysteinyl-tRNA synthetase	cysS SACOL0576	0.41	0.40	Aminoacyl-tRNA biosynthesis	Cytoplasmic
AIO20645.1	glutamyl endopeptidase	sspA SACOL1057	0.15	0.15	Quorum sensing	Extracellular
AIO20455.1	hypothetical protein KQ76_03935	SACOL0851	0.42	0.41		Unknown

AIO22160.1	lactate dehydrogenase	ldhD ddh SACOL2535	0.29	0.29	Pyruvate metabolism, Microbial metabolism in diverse environments	Cytoplasmic
AIO21406.1	Free methionine-(R)-sulfoxide reductase	SACOL1768	0.26	0.25	Cysteine and methionine metabolism	Cytoplasmic
AIO22099.1	peptidase M28	SA2244	0.32	0.31		Cytoplasmic
AIO20194.1	glutamyl-tRNA synthetase	gltX SA0486	0.39	0.39	Metabolic pathways, Aminoacyl-tRNA biosynthesis	Cytoplasmic
AIO22275.1	clumping factor B	clfB SA2423	0.33	0.33	*Staphylococcus aureus* infection	Cellwall
AIO21805.1	uridylyltransferase	SA1974	0.36	0.36		Cytoplasmic
OOC93971.1	phosphoglucomutase	pgcA SA2279	0.41	0.41	Metabolic pathways, Microbial metabolism in diverse environments, Biosynthesis of secondary metabolites, Biosynthesis of antibiotics, Purine metabolism, Galactose metabolism, Glycolysis / Gluconeogenesis, Glycerophospholipid metabolism, Pentose phosphate pathway, Amino sugar and nucleotide sugar metabolism, Streptomycin biosynthesis, Starch and sucrose metabolism	Cytoplasmic
OOC94101.1	DUF2648 domain-containing protein	SACOL2649	0.50	0.51		Unknown
AIO19942.1	peptidase M23	lytM SACOL0263	0.12	0.12		Extracellular

AIO21492.1	hypothetical protein KQ76_09365	SACOL1852	0.16	0.16		Unknown
AIO19900.1	nitric oxide dioxygenase	SA0231	0.34	0.35		Cytoplasmic
AIO21508.1	serine protease	splE SACOL1865	0.40	0.41		Extracellular
AIO20228.1	hydrolase	sdrD SA0520	0.22	0.22	*Staphylococcus aureus* infection	Cellwall
AIO20556.1	hypothetical protein KQ76_04470	SA0841	0.08	0.08		CM
AIO22338.1	adhesin		0.46	0.47		Cellwall
OOC90902.1	calcium-binding protein	SACOL1846	0.05	0.05		Unknown
AAX11326.1	enterotoxin type Gv precursor	entG seg SA1642	0.40	0.41	*Staphylococcus aureus* infection	Extracellular
AIO22285.1	hypothetical protein KQ76_13835	SACOL2661	0.37	0.39		Extracellular
AIO20759.1	fibrinogen-binding protein	SA1004	0.47	0.50	*Staphylococcus aureus* infection	Unknown
AIO22081.1	sodium:proton antiporter	SA2228	0.21	0.22		CM
AIO22369.1	phosphodiesterase	hlb SACOL2003	0.12	0.12	Metabolic pathways, Quorum sensing, Biosynthesis of secondary metabolites	Extracellular
AIO22017.1	hypothetical protein KQ76_12415	SA2168	0.39	0.42		Unknown
AIO21033.1	hypothetical protein KQ76_06965	SA1242	0.46	0.49		Unknown
AIO20783.1	penicillin-binding protein	pbpA	0.39	0.42	Metabolic pathways, beta-Lactam resistance, Peptidoglycan biosynthesis	CM

AIO21282.1	competence protein ComE	comEB	0.41	0.44	Metabolic pathways, Pyrimidine metabolism	Cytoplasmic
AIO20229.1	bis(5'-nucleosyl)-tetraphosphatase	sdrE SACOL0610	0.26	0.28	*Staphylococcus aureus* infection	Cellwall
AIO21274.1	molecular chaperone DnaK	dnaK SA1409	0.43	0.47	RNA degradation	Cytoplasmic
AIO22174.1	thioredoxin	SA2324	0.42	0.47		Cytoplasmic
AIO20145.1	DNA polymerase III subunit delta'	SACOL0526	0.31	0.34	Metabolic pathways, DNA replication, Pyrimidine metabolism, Purine metabolism, Homologous recombination, Mismatch repair	Cytoplasmic
AIO20763.1	alpha-hemolysin	SA1007	0.06	0.06		Extracellular
AIO20737.1	phenylalanine--tRNA ligase	pheS SA0985	0.35	0.39	Aminoacyl-tRNA biosynthesis	Cytoplasmic
AIO21788.1	HAD family hydrolase	SA1957	0.30	0.34		Cytoplasmic
AIO20874.1	50S ribosomal protein L7	SA1111	0.34	0.38		Unknown
AIO21867.1	30S ribosomal protein S14	rpsZ rpsN1 SA2034.1 SAS079	0.26	0.29	Ribosome	Cytoplasmic
AIO20189.1	excinuclease ABC subunit B	SA0481	0.36	0.40		Cytoplasmic
OOC92415.1	sphingomyelin phosphodiesterase	hlb SACOL2003	0.33	0.37	Glycerophospholipid metabolism, Inositol phosphate metabolism	Extracellular
AIO21275.1	heat shock protein GrpE	grpE SA1410	0.36	0.41		Cytoplasmic
AIO20225.1	HAD family hydrolase	SA0517	0.42	0.48		Cytoplasmic
AIO20637.1	acetyltransferase	SA0893	0.17	0.20		Cytoplasmic

AIO22130.1	DNA mismatch repair protein MutT	SACOL2500	0.41	0.47		Unknown
AIO20418.1	ABC transporter	SACOL0811	0.27	0.31		Cytoplasmic
AIO21842.1	toxin	SACOL2197	0.40	0.46		CM
AIO22387.1	replication-associated protein (plasmid)	SAP031	0.41	0.48		Unknown
AIO20884.1	zinc protease	SA1121	0.29	0.34		Cytoplasmic
AIO22136.1	fibronectin-binding protein	fnbA SA2291	0.23	0.26	Bacterial invasion of epithelial cells	Cellwall
AIO20222.1	deoxycytidine kinase	SA0514	0.43	0.50	Metabolic pathways, Purine metabolism, Pyrimidine metabolism	Cytoplasmic
AIO21273.1	molecular chaperone DnaJ	dnaJ SA1408	0.21	0.24		Cytoplasmic
AIO22207.1	transglycosylase	isaA SACOL2584	0.11	0.14		Extracellular
AIO19907.1	PTS sugar transporter subunit IIA	SA0236	0.24	0.29	Metabolic pathways, Galactose metabolism, Phosphotransferase system (PTS)	Cytoplasmic
AIO20259.1	dihydrolipoamide dehydrogenase	SA0551	0.42	0.51		Cytoplasmic
AIO21343.1	membrane protein	SA1476	0.30	0.37		Unknown
AIO20071.1	NADPH-dependent oxidoreductase	nfrA SACOL0453	0.26	0.32	Metabolic pathways, Riboflavin metabolism	Cytoplasmic

AIO21601.1	cysteine protease	sspP scpA SA1725	0.23	0.29		Extracellular
AIO20406.1	iron ABC transporter substrate-binding protein	SA0691	0.35	0.44	ABC transporters	CM
AIO20716.1	SCP-like extracellular protein	SA0967	0.17	0.22		Unknown
AIO21889.1	hypothetical protein KQ76_11750	SAS081	0.34	0.44		Cytoplasmic
AIO21919.1	urease subunit gamma	ureA SA2082	0.35	0.45	Metabolic pathways, Microbial metabolism in diverse environments, Purine metabolism, Arginine biosynthesis	Cytoplasmic
AIO19988.1	alpha/beta hydrolase	SACOL0391	0.32	0.42		Cytoplasmic
AIO22336.1	pyrrolidone-carboxylate peptidase	pcp SACOL2714	0.32	0.41		Cytoplasmic
AIO22042.1	glutathione S-transferase	SACOL2402	0.29	0.40		Unknown
AIO21116.1	gamma-hemolysin subunit A	hlgC SA2208	0.35	0.48		Extracellular
AIO22074.1	glycerate kinase	SA2220	0.24	0.34	Metabolic pathways, Microbial metabolism in diverse environments, Biosynthesis of antibiotics, Glycerolipid metabolism, lyoxylate and dicarboxylate metabolism, Glycine, serine and threonine metabolism	Cytoplasmic
AIO21505.1	serine protease	splF SA1627	0.25	0.35	Quorum sensing	Extracellular

AIO20749.1	succinate dehydrogenase	sdhB	0.28	0.41	Metabolic pathways, Microbial metabolism in diverse environments, Biosynthesis of secondary metabolites, Biosynthesis of antibiotics, Carbon metabolism, Citrate cycle (TCA cycle), Butanoate metabolism, Oxidative phosphorylation	Cytoplasmic
AIO21157.1	replication protein		0.31	0.47		Cytoplasmic
AIO21221.1	acetyl-CoA carboxylase	accB	0.23	0.40	Metabolic pathways, Microbial metabolism in diverse environments, Biosynthesis of secondary metabolites, Biosynthesis of antibiotics, Carbon metabolism, Fatty acid metabolism, Propanoate metabolism, Pyruvate metabolism, Fatty acid biosynthesis	Cytoplasmic

Appendix 8 (Copyright permission for figures) of this thesis has been removed as it may contain sensitive/ confidential content